

**DEVELOPMENT OF SMALL MOLECULE REPLICATION INHIBITORS
AGAINST WESTERN EQUINE ENCEPHALITIS VIRUS**

by

Janice A. Sindac

A dissertation submitted in partial fulfillment
of the requirements for the degree of
Doctor of Philosophy
(Medicinal Chemistry)
in The University of Michigan
2014

Doctoral Committee:

Research Professor Scott D. Larsen, Co-Chair
Assistant Professor David J. Miller, Co-Chair
Professor Henry I. Mosberg
Professor Richard Neubig, Michigan State University

DEDICATION

To my mother, father, and loyal puppy Lucy-Goose

ACKNOWLEDGEMENT

Graduate school and obtaining my doctorate have been the most challenging experience I have endured. I would not have been able to achieve this goal without the support of many individuals. First, I express the greatest love and gratitude to my mother and father. Both have given me endless encouragement throughout the years. They have demonstrated the value of diligence, perseverance, professionalism, and kindness towards others. I thank my loyal pup, Lucy, who has accompanied me throughout this journey for the last several years. She has provided the smiles, laughs, and distractions at the end of very long days.

Several terrific women have given their encouragement from afar. Both Andiliy Lai and Katrina “clam” Chan have battled the cold to make annual visits. I am very fortunate to have met Cameron Milbrandt, Cassandra Ann Burdyshaw, and Sarah Burnworth 13 years ago at the University of California, San Diego. Between the dinners, wildfires, marriages and children, we have managed to become the best of friends and cheerleaders.

My scientific career started long before the University of Michigan. I am thankful to Dr. Yoshihisa Kobayashi, Erin Olsen-Jansenn, Dr. Thong Nguyen, and Dr. Hitesh Patel. Dr. Kobayashi, Erin Olsen and Dr. Nguyen were great mentors during my undergraduate research and they helped lay down the foundations for my synthetic research to this day. To Dr. Hitesh Patel, I am endlessly grateful for giving me the

chance to work at Ambit, Inc. To this day, he gives me endless support and encouragement as he did when I first walked into Ambit, bright-eyed and curious.

It has been a privilege to work in the Larsen Lab. The staff chemists, Michael Wilson, Kim Hutchings, and Walajapet Rajeswaran have been a wealth of knowledge, support, and encouragement for the past four years. I would like to thank Dr. Jessica Bell for being a wonderful “coffee-buddy” for the first three years in the lab. Also, thank you to Dr. Bryan Yestrepky for sharing his home brews. To the new members: Brandt Huddle, Jeffery Zwicker, and Helen Waldschmidt for injecting new life and humor into the lab. To Scotty Barraza, the WEEV project would not be the same without him as a teammate and friend. Finally, I am excessively grateful to have the opportunity to work for Dr. Scott Larsen. He has been a great source of knowledge and support throughout the years.

Words cannot express the gratitude that I have for the people I have mentioned above.

- Janice A. Sindac

TABLE OF CONTENTS

DEDICATION	ii
ACKNOWLEDGEMENT	iii
LIST OF FIGURES	ix
LIST OF SCHEMES.....	xi
LIST OF TABLES	xii
ABSTRACT.....	xiii
CHAPTER I. INTRODUCTION.....	1
Alphavirus transmission and infection.....	1
Pathology	2
Bioterrorism	3
Therapeutics	3
Genomic Structure	4
Viral Replication.....	5
High-throughput screen (HTS)	7
Preliminary SAR.....	10
CHAPTER II. FIRST GENERATION INDOLE-2-CARBOXAMIDE DERIVATIVES	14
Rationale	14
Synthesis	15
Carboxamide position and initial SAR	16

Chirality	17
<i>In Vitro</i> antiviral activity.....	20
Neuroadaptive Sindbis virus (NSV) <i>in vivo</i> study.....	21
Physicochemical properties	24
N1-indole derivatives synthesis and SAR development.....	28
5-hydroxy indole synthesis	31
Conclusions.....	37
CHAPTER III. SECOND GENERATION INDOLE-2-CARBOXAMIDE ANALOGS	39
Rationale	39
SAR development	39
Chirality	40
Antiviral activity	40
Physicochemical properties	44
Conclusions.....	45
CHAPTER IV. THIRD GENERATION INDOLE-2-CARBOXAMIDE ANALOGS....	46
Rationale	46
SAR development	46
Hydrogen bonding substitutions	48
Hydrogen bonding substitution SAR development	49
Physicochemical Properties	54
<i>In vitro</i> antiviral and viability studies	57
<i>In vivo</i> WEEV infection study	58

Conclusions.....	59
CHAPTER V. INDOLE SUBSTITUTION.....	60
Rationale.....	60
Synthesis.....	61
Antiviral activity.....	68
Physicochemical Properties.....	69
WEEV <i>in vivo</i> infection study.....	72
Pharmacokinetic experiments.....	73
Conclusions.....	74
CHAPTER VI. TARGET IDENTIFICATION.....	75
Rationale.....	75
Biological target identification and Mode of Action.....	75
Tag-free photoaffinity probes.....	80
Synthesis.....	85
SAR development.....	90
Current status of target identification.....	92
Conclusions.....	94
CHAPTER VII. FUTURE DIRECTION.....	97
Photoprobes.....	97
<i>In vivo</i> Survival Studies with Neuroprotective Agents.....	98
Chikungunya Virus.....	98
CHAPTER VIII. EXPERIMENTALS.....	99

Carboxamide Derivatives.....	100
N1-indole derivatives.....	138
5-hydroxy indole derivatives	151
Indole replacement derivatives	168
Photoaffinity probes.....	191
Biological experiments	213
REFERENCES	214

LIST OF FIGURES

Figure 1: Alphavirus genome.....	4
Figure 2: WEEV replication.	7
Figure 3: WEEV replicon plasmid.....	8
Figure 4: Key preliminary SAR.....	13
Figure 5: (A) Physical properties of marketed CNS drugs (B) Three points of diversity	15
Figure 6: Chirality effect.....	19
Figure 7: WEEV and NSV antiviral studies.	21
Figure 8: NSV infection studies CCG 203927 (11) and CCG 203926 (12).	22
Figure 9: Fluorojade staining of hippocampus neuronal cells post NSV infection	23
Figure 10: MDR recognition and PAMPA-BBB measurements.....	27
Figure 11: Viral Titer and Viability results for 32 and 31	42
Figure 12: Select metabolic stability.....	44
Figure 13: Select metabolic stability.....	54
Figure 14: Pgp recognition and passive permeability for pyridylethyl carboxamide analogs	56
Figure 15: FMV antiviral viral results for compound 50 analogs	57
Figure 16: <i>In vivo</i> WEEV infection treatment with compound 50	58
Figure 17: Indole replacement antiviral results	68
Figure 18: Metabolic stability of indole substituents.....	70

Figure 19: MDR recognition and PAMPA-BBB measurements	71
Figure 20: <i>In vivo</i> WEEV infection treatment with compound 110	72
Figure 21: Plasma and brain concentration for 12, 50, and 140	73
Figure 22: Broad spectrum activity against of compound 50 and 140	76
Figure 23: fLuc-encoding reporter plasmids.....	78
Figure 24: Representative tag free photoaffinity probe sequence with 126	83
Figure 25: (A) azide (B) diazirine (C) benzophenone photoprobes protein labeling mechanism.	84
Figure 26: Pilot target identification experiment with photoprobe 126.....	94
Figure 27: Fluorinated photoprobes.....	97

LIST OF SCHEMES

Scheme 1: Representative synthesis for thienopyrrole synthesis	12
Scheme 2: Benzylamide derivative synthesis	15
Scheme 3: N1 indole analog synthesis.....	28
Scheme 4: Initial 5-hydroxy indole analogs	32
Scheme 5: Synthesis of synthon 167	33
Scheme 6: Synthesis of inhibitors 102, 103, and 104.....	34
Scheme 7: Synthesis of compound 101	36
Scheme 8: Synthesis of synthon 190	61
Scheme 9: Synthesis of analogs 112 and 117	62
Scheme 10: Synthesis of analog 110, 111, 113, 114, 116	63
Scheme 11: Synthesis of analog 115 and 118.....	64
Scheme 12: Synthesis of analog 120	85
Scheme 13: Synthesis of analog 121	86
Scheme 14: Synthesis of analog 122	86
Scheme 15: Synthesis of analog 123	87
Scheme 16: Synthesis of analog 124	88
Scheme 17: Synthesis of photoprobe 125.....	89
Scheme 18: Synthesis of photoprobe 126.....	90

LIST OF TABLES

Table 1: Initial HTS hit selection.....	10
Table 2: Initial indole carboxamide analogs	18
Table 3: N1-indole derivatives.....	30
Table 4: 5-hydroxy indole SAR.....	37
Table 5: CCG 203929 (22) analogs	43
Table 6: Inhibitor 50 derivatives.....	51
Table 7: CCG 205432 hydrogen bonding exploration.....	53
Table 8: Indole Substitution.....	66
Table 9: Photoaffinity probes.....	95

ABSTRACT

Arboviruses such as western equine encephalitis virus (WEEV) are capable of causing a wide range of diseases in humans. The CDC and NIAID consider WEEV as a potential bioterrorism weapon due to several factors: potential for aerosol transmission, lack of effective countermeasures, and ease of genetic manipulation to increase virulence and high levels of death. A series of thieno[3,2-*b*]pyrrole-based inhibitors were discovered to be active against WEEV following a high-throughput screen (HTS). This dissertation discusses the development of novel indole-2-carboxamide RNA replication inhibitors with improved *in vitro* and *in vivo* activity and the development of tag-free photoaffinity probes for target identification. A first-generation indole, CCG 203926 (**12**), with modestly improved potency and metabolic stability over the original screening lead CCG 32091, achieved efficacy in a preliminary *in vivo* study against neuroadapted Sindbis virus. Second-generation inhibitor, CCG 205432 (**50**), was the first inhibitor with submicromolar activity and further improved half-life compared to CCG-203926. In a WEEV-infected mouse model, in which CCG 203926 was inactive, it increased survival and decreased disease severity. Even though a related third generation inhibitor, CCG 209023 (**110**), was less potent than **50**, it had a significantly improved half-life, lower recognition by Pgp and equal efficacy to CCG-205432 at improving survival. It was determined that **50** and related indole-2-carboxamide inhibitors have a wide range of activity against other RNA viruses and elicit their antiviral activity by targeting host factors instead of viral enzymatic proteins. One of the two photoaffinity probes, **126**, is

equipotent to lead indole **50** and is currently being used for preliminary target identification studies. Compound **110** is also being studied as a combination therapy with neuroprotective agents. The lack of clinical therapeutics against alphaviruses emphasizes the significance of this work, as there is a critical need to develop potent antivirals against these pathogens.

CHAPTER I. INTRODUCTION

Alphavirus transmission and infection

Arboviruses (arthropod-borne virus) are viruses that are transmitted through arthropod vectors such as mosquitoes, mites, and ticks.¹ The viral family *Togarividae* is an example of such viruses. *Togarividae* contains four genera: *Alphavirus*, *Rubivirus*, *Pestivirus*, and *Arterivirus*.² *Alphaviruses* include Venezuelan, eastern, and western equine encephalitis viruses (VEEV, EEEV, and WEEV, respectively). WEEV is considered as a recombinant virus where its structural glycoproteins are from the Sindbis virus (SV) and the rest of its genome is derived from EEEV.³ Virus propagation relies heavily on the continuous transmission cycle between host and vector. Viruses with birds as their primary hosts, such as WEE, have wider distributions.⁴ However, once introduced, it becomes a localized strain and distinguishable from a virus at a different geographical area.^{4,5} WEEV is enzootic to the western United States, Canada, and South America.⁶ WEEV utilizes rodents and passerine birds as hosts and *Culex tarsalis* as its vector mosquito.⁷ Epizootic events are due to the infection of a bridging mosquito and transmission of the disease to non-traditional hosts such as equines and humans. Humans are considered “dead-end” hosts because the viremia is not prolonged or high-titered enough for efficient transmission to the mosquito vector.^{8,9}

Encephalitic alphaviruses infect the central nervous system (CNS) and induce neuronal cell death via two pathways: direct viral infection or indirect excitotoxicity due

to an overactive glutamate pathway.¹⁰⁻¹² Glutamate stimulates AMPA (α -amino-3-hydroxy-5-methyl-4-isoxazole propionic acid), NMDA (N-methyl-D-aspartate), and kainite receptors.¹⁰ Glutamate activation of these receptors results in the influx of Ca^{+2} , Na^{+} and Zn^{+2} ions into the cell resulting in cell depolarization. NMDA receptors are highly permeable to Ca^{+2} ions while AMPA is more resistant to Ca^{+2} influx. However, during infection, AMPA receptors may have an increased permeability to Ca^{+2} .^{13, 14} This excess Ca^{+2} ion due to glutamate receptor activation results in neuronal excitotoxicity.¹⁰ Studies have shown that administration of NMDA or AMPA receptor antagonists during viral infection decreased neuronal death without affecting virus titers and levels of apoptosis.^{10, 15} However, in Sindbis virus models, only AMPA antagonists protected mice from severe paralysis.^{10, 16} In addition, glial cells participate in removal of excess glutamate in the synapse. Insufficient maintenance of glutamate levels results in excitotoxicity and triggers cell lysis of both infected and normal cells.¹⁶ Factors that determine the cells' susceptibility include: cellular maturity, levels of cellular regulatory systems, level of viral infection and neurovirulence.¹⁶⁻¹⁸ The dual pathway in which these viruses attack the CNS emphasizes the need for antivirals to prevent viral replication and neuroprotective agents to maintain neuronal homeostasis.^{10, 19, 20}

Pathology

Because WEEV is transmitted through a mosquito bite, initial infection occurs outside of the CNS. Pathogen release begins in the bloodstream and enters the CNS.²¹⁻²³ WEEV causes a wide range of ailments from minor rashes to encephalitis. It has a short incubation period of 2-7 days, which may be asymptomatic.⁸ Between 1964 and 2005,

there have only been 639 confirmed human cases with a fatality rate of 3-7%.⁸ During epidemics, the case fatality rate may reach 15%.² Death is higher among children and the elderly.²⁴⁻²⁶ Survivors may experience severe neurological sequelae that may last weeks or a lifetime.²⁷

Neuroadaptive Sindbis virus (NSV), a representative alphavirus, showed that neuronal injury was prominent in the hippocampus, brainstem, cortex, and spinal cord.^{10, 28, 29} After NSV infection, mice were shown to suffer from encephalomyelitis and hindlimb paralysis.^{20, 30-32} WEEV infections manifest themselves in the CNS as vasculitis and focal hemorrhages in the basal ganglia and thalamus.³³

Bioterrorism

Some arboviruses have been recognized by the National Institute for Allergy and Infectious Diseases (NIAID) and the Center for Disease Control (CDC) as potential biological weapons.^{34, 35} In the 1960s, the US military weaponized and stored VEEV. The viruses were later destroyed.^{36, 37} Even though alphaviruses are naturally transmitted through mosquitoes, the equine encephalitis viruses remain highly infectious in an aerosol form.^{37, 38} Several factors contribute to their consideration as a biological threat: stability in aerosol form, ease of large-scale production, lack of effective countermeasures, and possible genetic manipulation to increase virulence that may lead to high mortality rates.^{37, 39, 40}

Therapeutics

A host's immune response plays a critical role in minimizing and recovering from an alphavirus infection. Early in the infection, the host's innate immune response

triggers the production of interferon (IFN).^{41,42} IFN may limit virus replication until the host's adaptive immune system develops where antibody response aids in viral clearance and recovery.⁴³ In addition, antibodies have been shown to confer protection against glycoproteins E1 and E2, both of which are necessary for virus infection.^{42,44} When used therapeutically, synthetic IFN, such as interferon alfacon-1, showed protective qualities when administered before WEEV infection.⁴⁵ However, interferon alfacon-1 has a short lifetime and requires multiple doses.⁴² Vaccines against the equine encephalitic viruses have been developed and approved for veterinary use. Live, attenuated virus (TC-83) vaccine against VEEV has high reactogenicity, requires frequent booster shots, has low efficacy and is restricted to researchers.^{37,46-48} Formalin-inactivated vaccines for EEEV and WEEV (PE-6 and CM-4884, respectively) are available to laboratory researchers; however, they have low efficacy.^{42,47,49} Currently, there are no effective clinical treatments available for alphavirus infections.

Genomic Structure

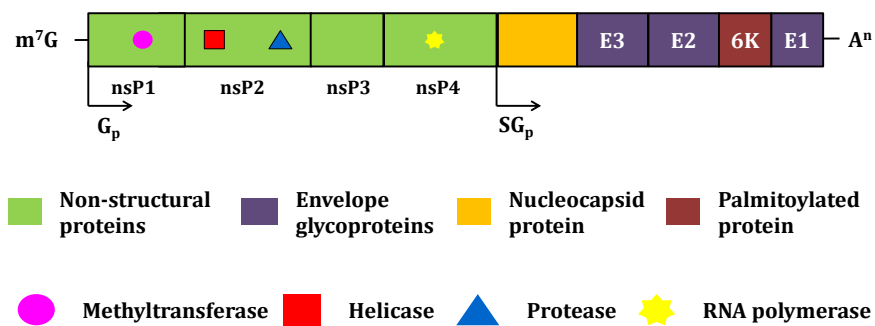


Figure 1: Alphavirus genome

WEEV is an enveloped virus and its genome is expressed by a single strand, positive polarity RNA sequence that serves as a direct template for replication. It contains a 5'-cap and a 3'-polyadenylated tail. In addition, it has a subgenomic RNA sequence that encodes for structural proteins produced during viral RNA replication. The genome also encodes non-structural proteins (nsP) with various enzymatic activities.

Nonstructural protein 1 (nsP1) is required for initiating the synthesis of a negative strand RNA. It caps both genomic and subgenomic RNA.⁵⁰ It functions as a methyltransferase and a guanylyltransferase.^{51, 52} The second non-structural protein (nsP2) serves as both helicase and protease. The C-terminal of nsP2 is a cysteine protease responsible for the processing of nonstructural polyprotein.^{51, 53} Elimination of the C-terminal domain resulted in a loss of enzymatic activity.⁵¹ The function of the nsP3 is not well understood. Nonstructural protein (nsP4) expresses the RNA dependent-RNA polymerase (RdRp). This protein synthesizes both negative- and positive-strand RNAs.⁷

Viral Replication

Alphavirus infection begins with the attachment of the virus to the cell followed by internalization. Membrane fusion between host and virus is facilitated by the E1-E2 heterodimer.⁵⁴ The acidic environment in the endosomes initiates the exposure of E1 fusion domain and the virus and endosomal membrane fuses.^{55, 56} During early infection, the association of the nucleocapsid with ribosomes triggers the disassembly of the viral core.⁵⁷ However, newly generated nucleocapsids become stable during late stages of infection. These differences in stability may be due to the different sizes between mature and new nucleocapsids. Also, changes in the sodium and potassium ion concentrations

allow increased nucleocapsid stability and the low pH in the endosomes initiates capsid degradation.⁵¹ During infection, host protein synthesis stops shortly after infection. It was previously shown that a decrease in potassium cations resulted in the decrease in translation of host mRNA; however, viral mRNA was insensitive to the change.^{58,59} In addition, it may also be attributed to the viral mRNA having a higher affinity for initiation factors such as eIF-4B compared to host mRNA.⁵¹ Early in the infection, both plus-strand and minus-strand RNA are rapidly synthesized. However, the synthesis of minus-strand RNA stops while plus-strand RNA synthesis continues throughout the infection.⁵¹ The minus-strand RNA serves as a template for both the synthesis of genomic RNA and a capped, polyadenylated subgenomic mRNA. Translation of the subgenomic RNA results in the formation of a structural protein polypeptide (Figure 1).^{49,60} The nucleocapsid autocleaves itself from the nascent structural polypeptide. Once the capsid is released, glycoprotein E3 binds to the membrane of the rough endoplasmic reticulum. During the synthesis of E3 and E2 various oligosaccharides and fatty acids are added.⁶⁰ Segments of E2 remain exposed to the cytoplasm after hydrophobic domains of E2 anchor the polypeptide to the endoplasmic reticulum. A peptide sequence following the anchoring sequence in E2, referred to as 6K, signals the insertion of the glycoprotein E1 and is cleaved from E1 and E2.⁶¹ The polypeptide containing E2 and E3 translocates to the Golgi apparatus where it is further cleaved to the mature E2 and E1. The glycoproteins are released from the Golgi apparatus.⁶²⁻⁶⁴ New virus packaging mainly occurs through budding from the host plasma membrane (Figure 2).⁶⁵

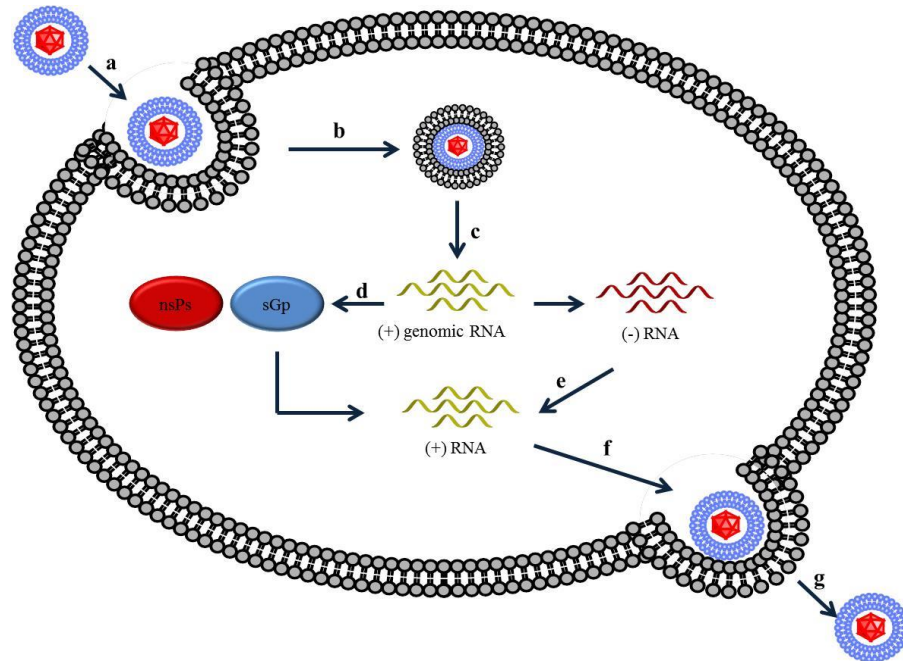


Figure 2: WEEV replication.

(a) binding (b) endocytosis (c) fusion and RNA release (d) genomic RNA translation (e) transcription (f) packaging and budding (g) cell lyse and virus release

High-throughput screen (HTS)

The laboratory of David Miller and the University of Michigan Center for Chemical Genomics (CCG) collaborated to run a high-throughput screen of 55,000 compounds. A replicon (pWR-Luc) based primary screen utilized a modified WEEV plasmid transfected into BSR-T7/5 cells. BSR-T7/5 cells are BHK cells that express a T7 RNA polymerase.⁶⁶ As previously discussed, viral replication may induce the production of type I interferons in order to combat infection. BHK cells are incapable of producing IFN; therefore, reduction in replication may be due to the presence of inhibitors.⁶⁶⁻⁶⁹ As seen in studies using SV replicon, translation of the subgenomic RNA is enhanced by the presence of a 27 nucleotide sequence preceding a characteristic hairpin structure. Alphaviruses do not necessarily have high homology, but they all have a 27-29

nucleotide distance between the promoter and the hairpin structure. Therefore, the first 27 amino acids of the subgenomic RNA were preserved.^{66, 70} Since the structural genes encoded in the subgenomic region are unnecessary for genome replication, they were replaced with the firefly luciferase gene (Figure 3).^{66, 71} The hepatitis δ virus ribozyme δ Rz/T7_T terminator was placed downstream of the polyadenylation region to ensure the proper formation of a 3' end.⁶⁶ Furthermore, because of the absence of structural nucleocapsids and envelope proteins (discussed in page 5), which are necessary for viral entry into host cells, secondary infections do not occur.^{72, 73} Therefore, these replicon systems can be handled in a lower safety level than those required by WEEV. Because of the constitutive T7 promoter, the luciferase gene is expressed resulting in a baseline luminescent signal. However, addition of an effective inhibitor decreased luminescence indicating that replication was interrupted.

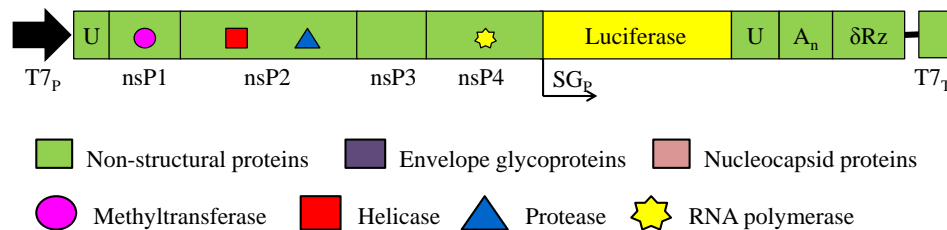


Figure 3: WEEV replicon plasmid.

T7p (T7 polymerase promoter), T7_T (hepatitis δ virus ribozyme δ Rz/T7t terminator), SG_p (subgenomic promoter), A_n (polyadenylated tail), U (untranslated region).

Image adapted from Ref. 66

The compound testing funnel consisted of a battery of screens and validations (Table 1). Potential inhibitors were tested at 10 μ M and were chosen from the HTS if they showed greater than 90% activity compared to the positive control, Ribarivin or if they showed greater than two standard deviations compared to the vehicle (DMSO). Using the same replicon system, inhibitors were confirmed by dose response testing at

concentrations ranging from 100 $\mu\text{mol/L}$ to 10 nmol/L . In order to eliminate compounds that were potential luciferase inhibitors, compounds previously active on luciferase-based assays were eliminated. Seventy seven out of 114 compounds from the previous category had an $\text{IC}_{50} < 100 \mu\text{M}$. The compounds were taken into another replicon assay utilizing a construct that is derived from EEEV and VEEV. Instead of having a firefly luciferase gene as an indicator, it utilizes a secreted alkaline phosphatase (SEAP) reporter gene. Similar to the luciferase replicon, the SEAP replicon monitors the level of genome replication within the cell. The SEAP assay further eliminates any compounds that were luciferase inhibitors. In addition, it indicated whether an inhibitor may have activity against other alphaviruses.⁶⁶ Finally, active compounds were subjected to another dose-response assay using the pWR-Luc replicon and an MTT assays to directly compare activity and toxicity, respectively. Compounds with a selectivity index ($\text{CC}_{50}/\text{IC}_{50}$) of > 5 were considered for further development (Table 1). Four compounds were initially identified; however, CCG 32091 (**1**) exhibited a selectivity index of >20 and an IC_{50} of 24 μM , which is comparable to ribavirin in the same assay with selectivity index of 19 and an IC_{50} of 16 μM (Figure 4).⁶⁶

Table 1: Initial HTS hit selection.

	Experiment	Criterion	Number of Compounds
	CCG chemical library		51,028
HTS	pWR-Luc replicon & BSR-T7/5 cells	(1) fLUC activity > 2 SD/plate below negative control, DMSO OR (2) > 90% per plate of level obtained by positive control, Ribavirin	196
HTS triage	pWR-Luc replicon & BSR-T7/5 cells	Inactive in previous CCG Luciferase based assays	114
HTS confirmation	pWR-Luc replicon & BSR-T7/5 cells	IC ₅₀ < 100 μM	77
Secondary screen	EEEV/VEEV-SEAP replicon bearing BHK cells	IC ₅₀ < 100 μM	11
Tertiary screen	pWR-Luc replicon & BSR-T7/5 cells	Selectivity index > 5	4

Table source: Ref. 66; CCG: University of Michigan Center for Chemical Genomics, IC₅₀: inhibitory concentration at 50%; CC₅₀: cytotoxicity concentration at 50%; fLUC: firefly luciferase; Selectivity index: CC₅₀/IC₅₀

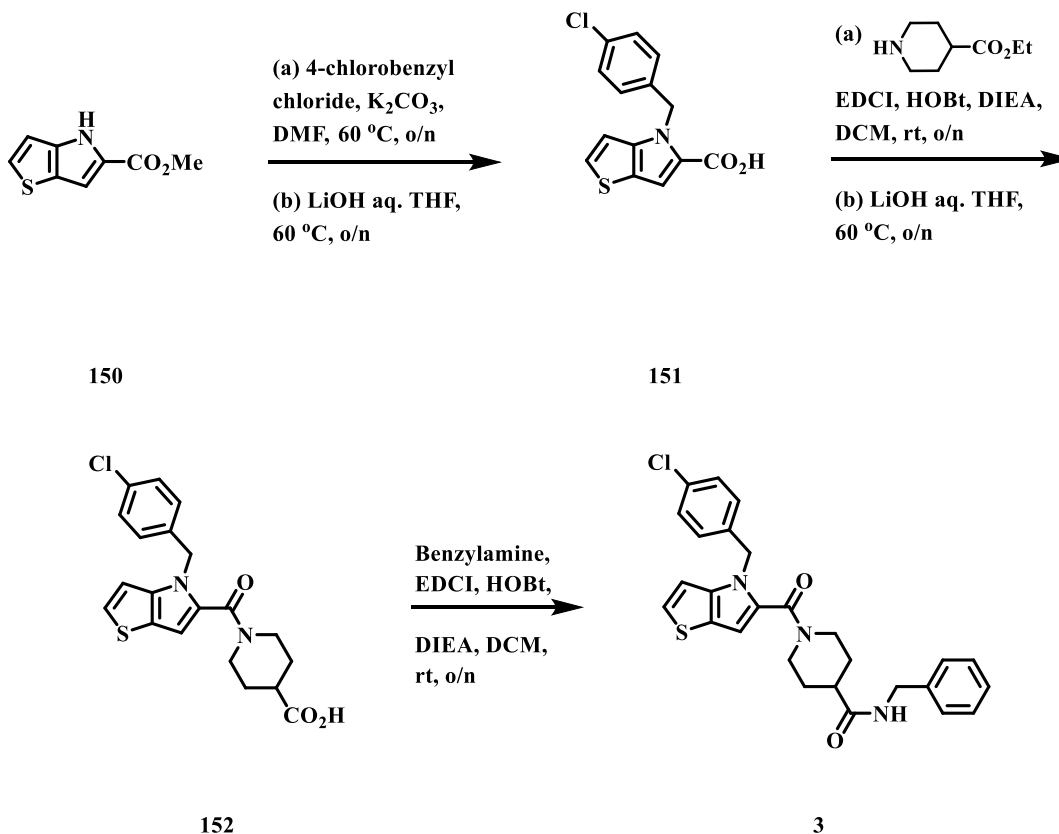
Preliminary SAR

Metabolic stability is an important aspect of drug discovery. Metabolism occurs in two phases. These two phases generate polar molecules that facilitate clearance of endogenous and exogenous compounds. Molecules do not necessarily need to proceed through both phases of metabolism to be cleared from the body.

Phase I involves oxidations, hydrolyses and dealkylations. Phase II involves conjugations.⁷⁴ Phase I metabolism occurs via oxidative enzymes such as the family of cytochrome P450 (CYP450) enzymes and flavin mono-oxygenase (FMO).⁷⁵ CYP450 enzymes are primarily responsible for the majority of the oxidative hydroxylations of compounds.^{74, 76, 77} The mechanism proceeds through a heme-NAPDH mediated

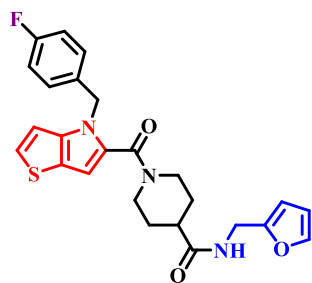
oxygenation of molecules using molecular oxygen.⁷⁷ If a molecule is sufficiently polar to be excreted, it can bypass Phase II metabolism. If not, Phase II metabolism involves the addition of moieties such as glucuronic acid, sulfate, and glutathione.⁷⁴ Even though the main objective of metabolism is to increase clearance rate of compounds from the body, this process can generate reactive species that may interact with macromolecules in cells (DNA, RNA, etc.). These intermediates may lead to toxicity and other side effects. In drug development, metabolism affects bioavailability, exposure and clearance.⁷⁸ Therefore, it is necessary that all active compounds be evaluated for metabolic stability before considering compounds for *in vivo* studies.

Figure 4 shows key compounds that led to the transformation of the original thienopyrrole HTS hit (**1**) to the indole lead compound CCG 102516 (**10**). Anticipating possible metabolic liabilities due to the thienopyrrole and the furanyl carboxamide via CYP450 oxidation, the two functionalities were replaced with bioisosteres. Bioisosteres are functional groups that have similar chemical and physical properties, but also elicit the same biological activity.^{79, 80} The thienopyrrole and furanyl carboxamide were replaced with the indole and the benzyl carboxamide, respectively. A representative synthetic route, developed by Dr. Bryan Yestrepky, used to generate thienopyrrole inhibitors is shown in Scheme 1. Methyl 4*H*-thieno[3,2-*b*]pyrrole-5-carboxylate (**150**) was alkylated with 4-chlorobenzyl chloride in the presence of potassium carbonate. Subsequently, the resulting ester was saponified to carboxylic acid **151** using lithium hydroxide. Amide bond formation followed by hydrolysis resulted in acid **152**. Peptide coupling with benzylamine resulted in inhibitor **3**.

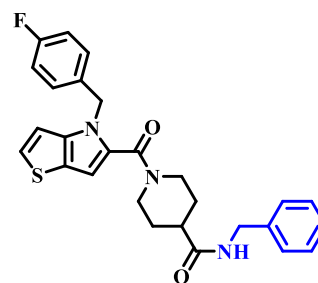


Scheme 1: Representative synthesis for thienopyrrole synthesis
 *synthetic route developed by Dr. Bryan Yestrepky

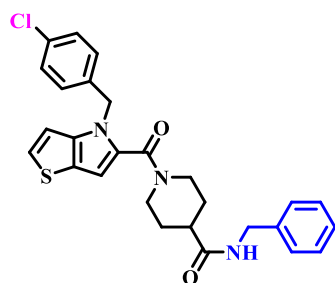
Replacement of the furanyl carboxamide in **1** with the benzyl carboxamide (**2**) resulted in equipotent compounds. Exchanging the fluorine with a chlorine (**3**) improved potency. Finally, replacing the thienopyrrole with an indole generated the first generation indole lead, CCG 102516 (**10**). The similar potencies of **1** and **10** indicated that both the benzyl carboxamide and indole were valid bioisosteric replacements for the furanyl carboxamide and thienopyrrole, respectively.⁸¹



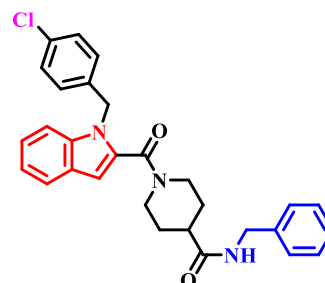
CCG 32091[#] (1)
IC₅₀ = 23.7 ± 6.9 μM
CC₅₀ > 100 μM



CCG 32088[#] (2)
IC₅₀ = 25.4 ± 7.3 μM
CC₅₀ > 100 μM



CCG 203881 (3)
IC₅₀ = 10.1 ± 2.8 μM
CC₅₀ > 100 μM



CCG 102516* (10)
IC₅₀ = 15.6 ± 5.2 μM
CC₅₀ > 100 μM

Figure 4: Key preliminary SAR
synthesized by Dr. Bryan Yestrepky, * synthesized by Dr. Kyle Buldoc

In order to evaluate the original metabolic liability hypothesis, a microsomal stability experiment was performed by Scott J. Barraza. Inhibitors (1.0 μM in DMSO) were incubated in mouse liver microsomes (MLM) for 15 minutes. The percentage of the parent compound was measured over time via LC/MS.⁸¹ Compounds **3** and **10** had a half lives of approximately 1.7 and 7.3 minutes, respectively. This experiment demonstrated an increase in metabolic stability, validating the indole and benzyl carboxamide as bioisosteric replacements.

CHAPTER II. FIRST GENERATION INDOLE-2-CARBOXAMIDE DERIVATIVES

Rationale

SAR development around compound **10** focused on optimizing potency while minimizing toxicity in order to achieve *in vivo* activity. Figure 5B identifies the three points of diversifications that were pursued in the SAR studies. Concurrently, the general characteristics of a successful CNS drug had to be taken into consideration for analog design since we were targeting a neurotropic alphavirus. The calculated physical properties exhibited by marketed CNS drugs versus compound **10** are shown in Figure 5A.^{82, 83} It is apparent from this comparison that during our SAR optimization we would need to reduce the molecular weight (MW) and/or topological polar surface area (TPSA) in order to maximize potential for CNS penetration.

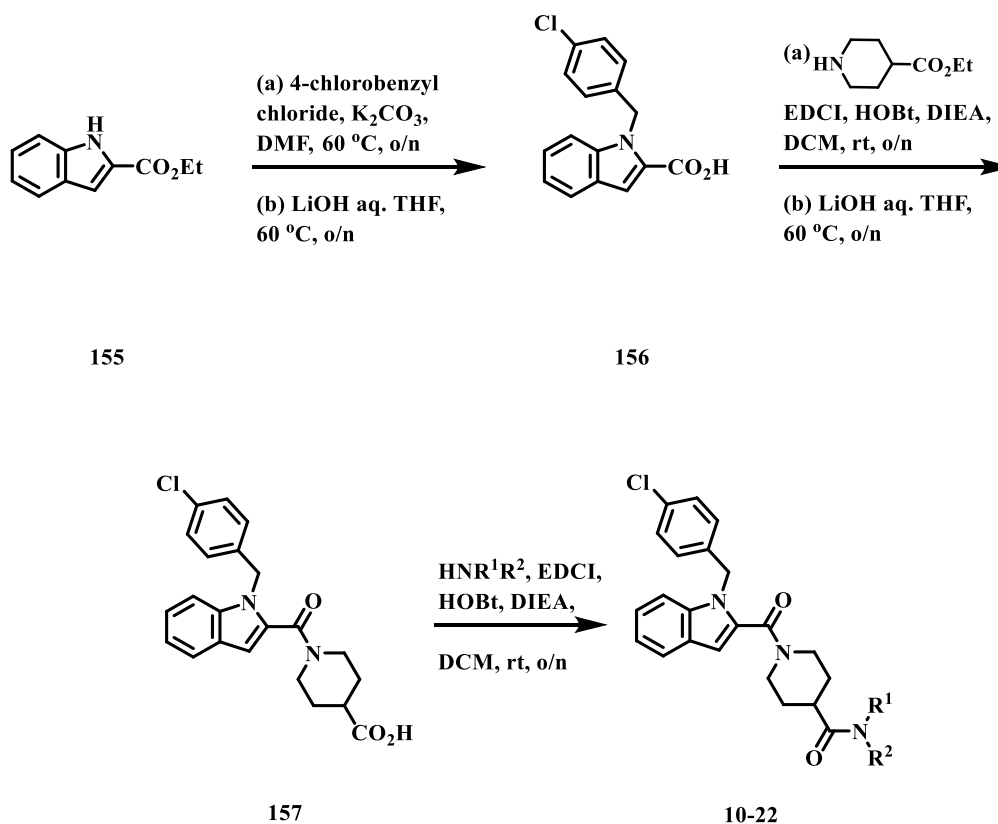
Because our lead was identified in a phenotypic replicon screen, we had no knowledge of the actual molecular target. Thus, we also planned to use SAR to provide information regarding which areas of the molecule were interacting most strongly with the unknown target. Molecular modifications leading to an increase or decrease in potency would suggest an important interaction between the functional groups being altered and the protein target. On the contrary, changes that did not affect potency would imply that the functional group was in a position not interacting strongly with the binding site, possibly a solvent exposed portion of the molecule. We considered that this

information would be important in designing effective affinity probes (Chapter VI) by identifying areas that could be modified without compromising activity along with areas of the molecule that were in close proximity to the binding site.

A	Property	Marketed CNS drugs	Compound 10	B
	MW (g/mol)	319	486	
	HBD & HBA	4.41	5	
	TPSA (Å)	40.5	52.6	
	cLogP	3.43	4.55	

Figure 5: (A) Physical properties of marketed CNS drugs (B) Three points of diversity

Synthesis



Scheme 2: Benzylamide derivative synthesis

Carboxamide derivatives were synthesized according to Scheme 2. Ethyl 1*H*-indole-2-carboxylate was alkylated with 4-chlorobenzyl chloride in the presence of potassium carbonate. The resulting ester was hydrolyzed using lithium hydroxide to generate acid **156**. A peptide coupling with ethyl isonipecotate followed by another saponification resulted in compound **157**. Amide coupling with various amines generated carboxamide inhibitors **10 - 22**.

Carboxamide position and initial SAR

All new analogs were tested for activity in the WEEV replicon assay previously described in Chapter I. Table 2 summarizes the WEEV replicon activity of the initial indole derivatives. SAR indicated that replacement of benzyl carboxamide in **10** with a phenyl carboxamide **17** is detrimental to the activity. In contrast, lengthening to a phenethyl carboxamide (**56**, Table 6) produced an inhibitor equipotent to **10**. This suggested the possibility of a potential hydrophobic binding pocket that might be exploited to increase activity due to a favorable π - π stacking interaction. The position of the carboxamide in relation to the indole core was also examined. The analogous piperidine-3-carboxamide (**24**) resulted in a diminishment of activity. Therefore future indole inhibitors were designed to retain the piperidine-4-carboxamide substitution pattern.

Increasing lipophilicity by adding a methyl or halogens to the benzyl aromatic ring (**13-15**) did not improve potency. Interestingly, small aliphatic analogs (**19, 20, 23**) had similar potencies to **10**, suggesting that the benzyl amide is not making optimum interactions with the binding site. Addition of polarity such as a prolinol (**18**) or 4-

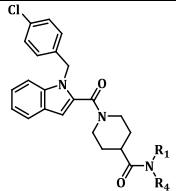
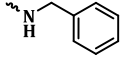
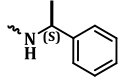
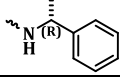
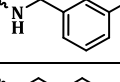
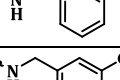
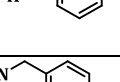
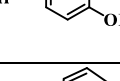
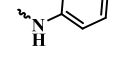
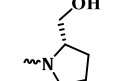
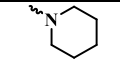
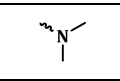
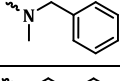
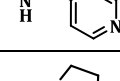
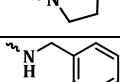
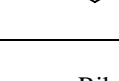
methoxybenzyl (**16**) resulted in a reduction or complete loss of potency. N-methylation of the benzylamide (**21**) resulted in an equipotent inhibitor.

Significantly, replacement of the phenyl ring of **10** with pyridine (**22**) provided an improvement in potency ($IC_{50} = 6.8 \mu\text{M}$) without increasing cytotoxicity. This finding was our first indication that a distal hydrogen bonding motif might be capable of interacting with the binding site. This hypothesis was further investigated as described in Chapters III and IV.

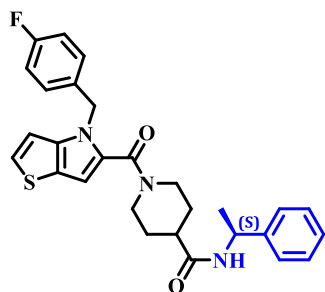
Chirality

The thienopyrrole series mentioned in Chapter I demonstrated that chirality has a marked effect on activity (Figure 6). Taking a similar approach, both the (*S*) and (*R*)- α -methylbenzyl carboxamide (**11** and **12**) derivatives were synthesized for the indole series. Of the two enantiomers, only the *R*-isomer showed activity. The high level of enantioselectivity signifies that the inhibitors are interacting with a chiral macromolecule instead of an achiral structure such as a cellular membrane. We viewed this pair of enantiomers as ideal probes with which to establish that replicon activity is correlated with antiviral activity, both *in vitro* and *in vivo*. The two analogs have identical physical properties except for their chirality, and thus any subsequent differences in their antiviral and *in vivo* activity could be directly correlated with the replicon assay, rather than any differences in their physicochemical properties.

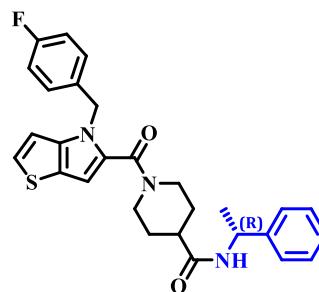
Table 2: Initial indole carboxamide analogs

	CCG Number	NR ₁ R ₄	IC ₅₀ (μM) ^a	CC ₅₀ (μM) ^b
10*	102516		15.5 ± 5.6	>100
11	203927		>100	>100
12	203926		6.5 ± 1.5	89.9
13	204042		75.1 ± 43.8	>100
14	206399		>50	>50
15	204043		15.3 ± 9.0	>100
16	204025		>50	ND
17	206334		>50	ND
18	204021		30.6 ± 4.5	98.9
19	203928		9.2 ± 2.8	51.7
20	204022		10.5 ± 2.1	>100
21	203930		16.9 ± 4.4	87.0
22	203929		6.8 ± 1.7	>100
23	102514		22.2 ± 4.3	65.6
24**	205483		30.6 ± 7.3	>100

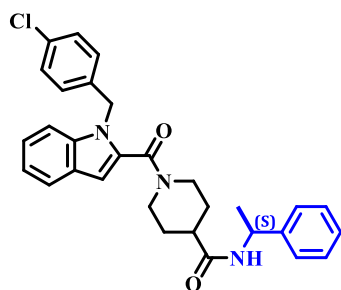
^aInhibition of luciferase expression in WEEV replicon assay. Ribavirin as positive control has an IC₅₀ in the assay of 16 μM. Values are mean of at least n=3 independent experiments ± SE. ^bCell viability determined by inhibition of mitochondrial reduction of MTT. Values are mean of at least n=3 independent experiments. Provided by Dr. David Miller. *synthesized by Dr. Kyle Buldoc; **synthesized using ethyl nipecotate



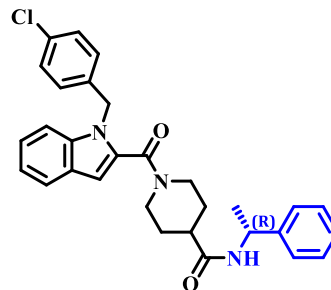
CCG 203045# (4)
 $IC_{50} > 100 \mu M$
 $CC_{50} > 100 \mu M$



CCG 203047# (5)
 $IC_{50} = 8.3 \pm 1.4 \mu M$
 $CC_{50} > 100 \mu M$



CCG 203927 (11)
 $IC_{50} > 100 \mu M$
 $CC_{50} > 100 \mu M$



CCG 203926 (12)
 $IC_{50} = 6.5 \pm 1.5 \mu M$
 $CC_{50} = 89.9 \pm 20.3 \mu M$

Figure 6: Chirality effect
#synthesized by Dr. Bryan Yestrepky

***In Vitro* antiviral activity**

In order to determine whether the inhibitor activities in the replicon assay will translate to antiviral activity, the cytopathic effect (CPE) and viral titer reduction were measured. CPE plaque assays measure the level of morphological changes caused by a virus infection. These changes include: rounding of infected cells, fusion with adjacent cells, and pyknosis.⁸⁴ It was previously shown that WEEV causes the rounding of cells and forms pyknotic cells.⁸⁵ Post-infection viability was measured using an MTT assay, similar to that used in the HTS. Human BE(2)-C neuronal cells were infected with either NSV or WEEV. Due to the rapid rate of viral replication and production, both WEEV and NSV are highly virulent in cultured cells. Cells were incubated with 25 μ M of inhibitor for 24 hours before the viral titer and cellular viability were measured.⁸¹ The negative and positive controls were DMSO and ribavirin (Rib), respectively. The initial experiment compared the thienopyrrole core (**3**), the achiral indole core (**10**) and (*R*) versus (*S*) enantiomers (**12** and **11**) for their different antiviral effects.

Figure 7 shows that compounds that were active in the replicon assay (Rib, **3**, **10**, and **12**) increased neuronal survival and decreased viral titer, while the inactive enantiomer (**11**) was unchanged from negative control DMSO in both assays. These antiviral effects of the active analogs were observed regardless of the virus. This experiment firmly established a correlation between the replicon assay and antiviral activity, suggesting that the observed antiviral effects may be due to inhibition of RNA replication.

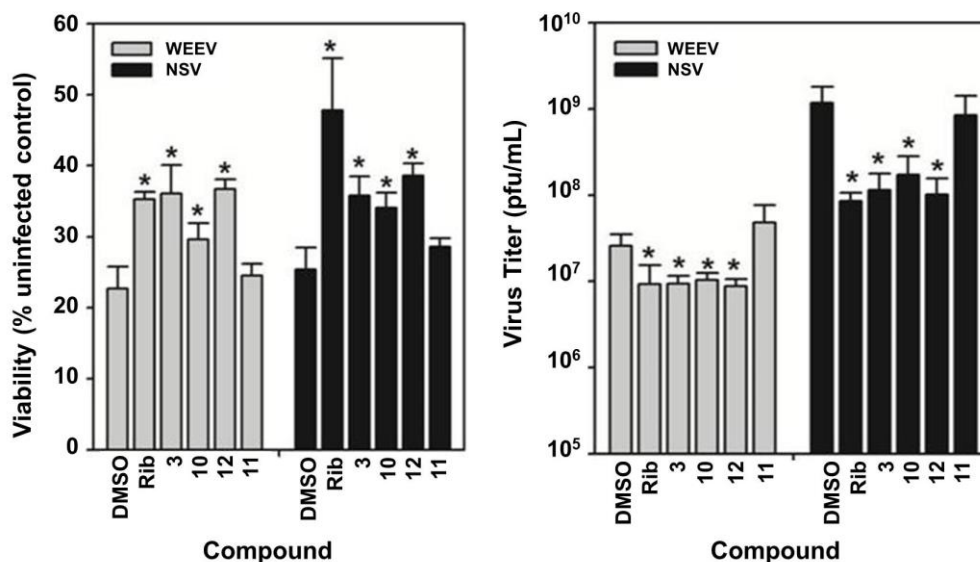


Figure 7: WEEV and NSV antiviral studies. Human BE(2)-C neuronal cells were infected with WEEV or NSV and incubated with inhibitors at 25 μ M. Cell viability and viral titers were measured 24 h post infection via MTT and plaque assays. Ribavirin(Rib) as positive control; DMSO negative. $P < 0.05$ Graph courtesy of Dr. David Miller

Neuroadaptive Sindbis virus (NSV) *in vivo* study

Dr. David Irani and Pennelope Blakely conducted an *in vivo* study comparing **11** and **12**. The experiment utilized NSV infection because of its lower biosafety level containment (BSL2) requirement than WEEV (BSL3). Direct intracranial infection with NSV causes lethal infection in mice within 7-10 days.^{31,32} It infects the brain and spinal cord leading to hind leg paralysis in weanling mice.^{31,32,86} The Irani lab utilized inbred C57BL/6 mice 5-6 weeks of age. Mice were inoculated with 10³ plaque forming units (pfu) of NSV via direct intracranial injection. Six groups of mice (5 mice/group) were treated via intraperitoneal injection with either **11** or **12** at 10 mg/kg or 30 mg/kg, vehicle or untreated. Treatment started 12 hours post-infection until day seven. Dosing was stopped at day 7 because viral titers peak in 7 days in the CNS. After this point, viral

titer decreases indicating that a full host immune response has been reached. Each mouse was given a clinical score according to the following categories: (1) normal (2) partial paralysis (some weakness in hind legs) (3) moderate paralysis (weakness in both hind legs) (4) severe paralysis (complete paralysis in hind legs) and (5) dead.⁸¹ Mice were observed for another seven days, at which point they were euthanized.

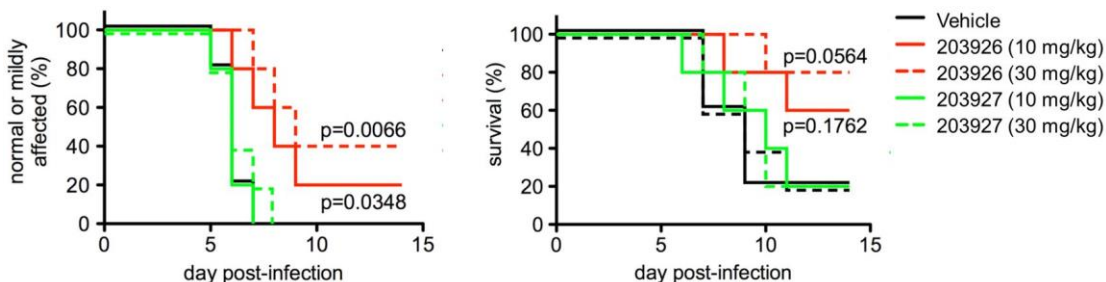


Figure 8: NSV infection studies CCG 203927 (**11**) and CCG 203926 (**12**). Six groups of C57BL/6 mice (n=5/group) infected with 10^3 pfu/mL of NSV were treated with **11** or **12** using 10 mg/kg or 30 mg/kg/dose, vehicle or left untreated. Animals were treated via intraperitoneal injection every 12 hours beginning 12 hours after virus challenge until day 7. (A) Disease severity (B) Survival Graph courtesy of Dr. David Irani and Penelope Blakely

Figure 8 shows that the more active enantiomer (**12**) offered protection against the disease and increased survival compared to vehicle while the inactive enantiomer (**11**) was indistinguishable from vehicle. The observed protection was also dose-dependent, with the higher dose achieving greater statistical significance. It is worth noting that despite the increased survival, the mice were impacted severely by the infection. This is also reflected in the pathology results described below.⁸¹

As previously described in Chapter I, alphavirus infection may also cause neuronal cell death through excitotoxicity and microglial system. This pathway affects both infected and normal cells.^{10, 16} Therefore, it is important for developed inhibitors to offer some neuroprotection. In addition to the survival experiment, the Irani lab determined the extent to which neuronal cells were degenerating. Degenerating cells can

be identified with fluorojade staining.⁸⁷ After the mice were sacrificed, tissue sections were harvested and labeled. Figure 9, a representative staining slide identifies neuronal cells from the hippocampus, a prominent location in the CNS infected by NSV.¹⁰ The Nissl Red stain (red) labeled all neurons while fluorojade staining labeled only degenerating neurons (green with arrows). The graph shows the percentage of neurons degenerated. Once again, the active (*R*)-enantiomer conferred protection while its counterpart and the vehicle were ineffective.

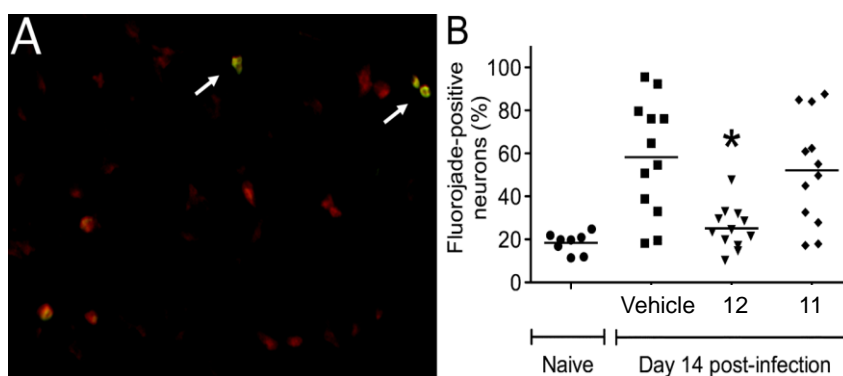


Figure 9: Fluorojade staining of hippocampus neuronal cells post NSV infection. Neuronal cells from the hippocampus, a site of heavy NSV infection, were chosen for further study. (A) Fluorojade staining of damaged hippocampal neurons in the brains of NSV-infected mice. NisslRed was first used to label neurons in sections through the hippocampus, while fluorojade staining (arrows) was then performed to identify those cells undergoing active degeneration. (B) The proportion of fluorojade-positive hippocampal neurons was determined in quadruplicate slides prepared from 3 mice in each group. * $p < 0.05$. Figure provided by Dr. David Irani and Penelope Blakely

Both the *in vitro* and *in vivo* experiments described above demonstrated that compound **12** was able to modulate both antiviral and neuroprotective activities, indicating the feasibility of eliciting a pharmacological response that increases survival and decreases disease severity. However, it was imperative to explore other regions of the indole core in order to further improve potency, maintain minimal toxicity, and modify physicochemical properties to optimize potential for CNS activity (Figure 5).

Physicochemical properties

It has been estimated that more than 98% of drug candidates targeting the CNS do not make it into the market.^{88, 89} Neurotherapeutic candidates face both a structural and biochemical barrier. The blood brain barrier (BBB) isolates the CNS from the circulatory system and maintains a microenvironment.⁹⁰ Structurally, the BBB is composed of tight junctions (TJs) that limit the permeability of therapeutics and polar solutes into the brain.⁹¹⁻⁹³ In addition, BBB has few pinocytotic vesicles and lacks fenestrations.⁸² This barrier limits the rate of diffusion from the periphery into the CNS. In general small molecules enter the CNS through diffusion and it is inversely proportional to molecular weight, and directly proportional to lipophilicity.⁹² However, many molecules do not abide by these rules because there is another obstacle therapeutics encounter.

Biochemically, macromolecules encounter the P-glycoprotein (Pgp) efflux transporter. It is a transmembrane protein that has a broad range of substrates and is expressed in high population in the CNS.⁹⁴ Even though CNS entry is aided with higher lipophilicity, it may be counter-productive.⁹⁵ Pgp recognition generally increases with lipophilicity facilitating the efflux of lipophilic xenobiotics from the CNS.^{91, 96}

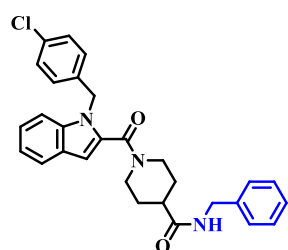
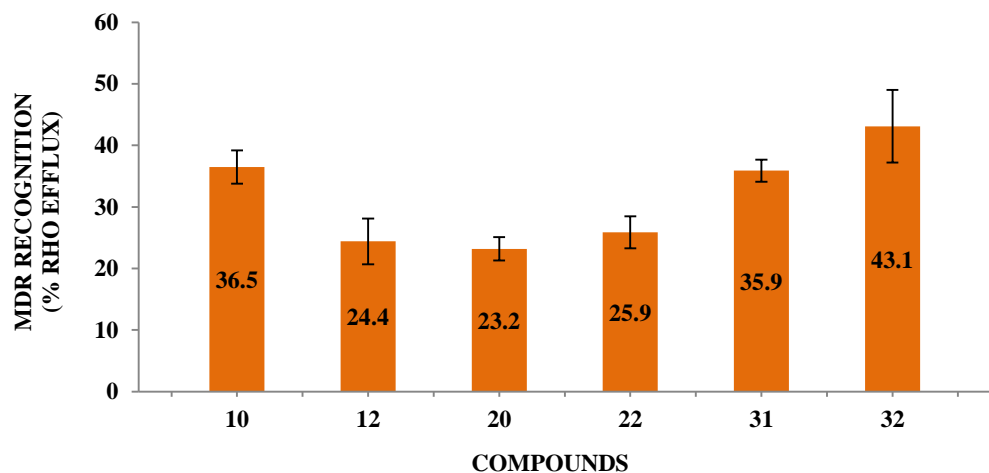
In order for our inhibitors to elicit the greatest efficacy, it is necessary for them to have high passive permeability, low Pgp recognition, and high metabolic stability. The level to which Pgp interacts with these inhibitors was determined by measuring Rhodamine 123 (Rho 123) uptake into MDCK cells transfected with human Pgp (MDR1-MDCKII).⁹⁷ Rho 123 is a known Pgp substrate and is readily effluxed.⁹⁵ In this assay, tariquidar, a known Pgp inhibitor, is included as a control. This takes into account the natural variation of Pgp expression in the cells. In the presence of a Pgp inhibitor or a

competitive substrate for Pgp, there will be an increase in intracellular concentration of Rho 123.⁹⁸ The results for a test compound are expressed as a percent of the effect that tariquidar has on Rho123 uptake in the same assay. A higher number indicates higher recognition by Pgp. Results for selected compounds are presented in Figure 10.

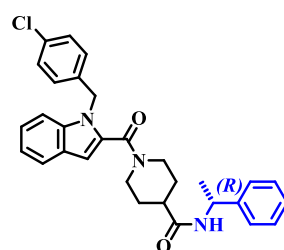
Another factor that determines CNS penetration is the passive permeability of these compounds through the BBB. An *in vitro* experiment that estimates passive permeability across the BBB is parallel artificial membrane permeability assay (PAMPA). Select inhibitors were tested using the PAMPA Explorer program from pION using a PAMPA-BBB lipid mixture.^{99,100} PAMPA involves a “sandwich” of two 96-well plates. This is formed by a donor plate and an acceptor plate separated by an artificial lipid membrane. The donor plates contain a DMSO stock solution of inhibitors diluted with a proprietary pION, Inc. system solution. Inhibitors passively diffuse through the artificial membrane into the acceptor plate. The difference in UV absorbance after a 4 hour incubation between the donor and acceptor plate determines the extent to which a molecule is permeable.⁹⁹⁻¹⁰¹ Due to the low solubility of these compounds, a 20% acetonitrile co-solvent was used in the donor wells.¹⁰² In PAMPA-BBB experiments, a $\log P_{\text{eff}} > -4$ are considered highly permeable while those that have a $\log P_{\text{eff}}$ of ≤ -6.0 are considered to have low permeability.⁹⁹

As shown by Figure 10, select compounds from the initial indole derivatives have medium to low passive permeability. The active (*R*)-isomer (**12**) was recognized less by Pgp than the indole lead (**10**). However, decreasing molecular weight and lipophilicity with the dimethyl carboxamide (**20**) and 4-pyridylmethyl carboxamide (**22**) did not aid in decreasing Pgp interaction compared to **12**.

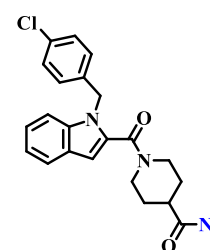
Even though it would be expected that an overall increase in lipophilicity in compound **12** (cLogP 5.07) compared to **10** (cLogP 4.75), which is known to increase metabolic susceptibility to CYP450 oxidation, would lead to reduced metabolic stability, the presence of an α -methylbenzyl carboxamide (MLM $T_{1/2}$ = 31 min, **12**) actually increased metabolic stability.¹⁰³ This suggested that the addition of a methyl group blocks a major site of metabolism in **10** (MLM $T_{1/2}$ = 7.3 min).



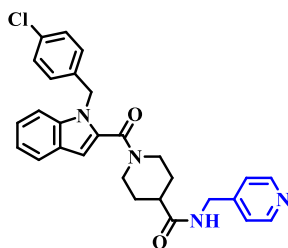
Compound 10



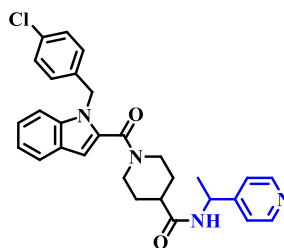
Compound 12
log P_{eff} = -6.52 ± 3.14



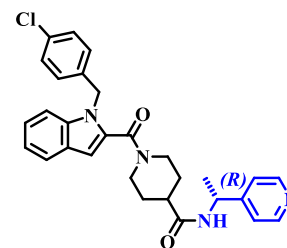
Compound 20
log P_{eff} = -4.19 ± 0.03



Compound 22
log P_{eff} = -4.16 ± 0.12



Compound 32
log P_{eff} = -3.99 ± 0.01

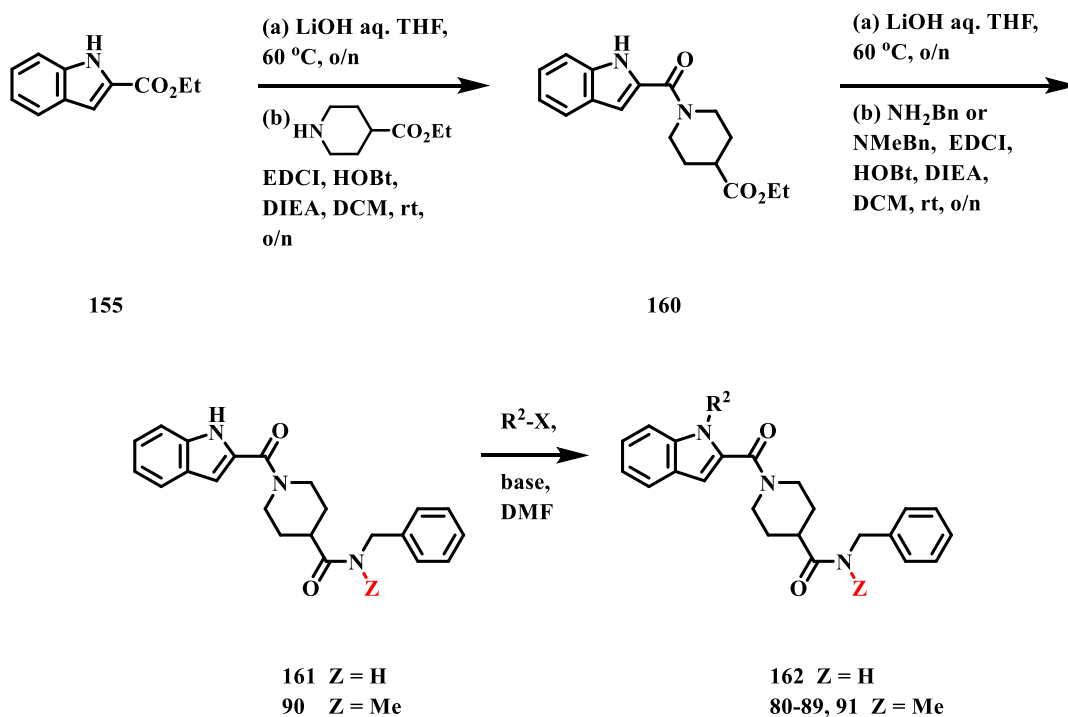


Compound 31
log P_{eff} = -4.02 ± 0.03

Figure 10: MDR recognition and PAMPA-BBB measurements

Rhodamine 123 (Rho 123) uptake was measured in MDR1-MDCKII cells utilizing Glomax Multi Detection System (Promega). 'MDR1 recognition' was assessed by measuring uptake in the presence of MDR inhibitor, tariquidar (5 μ M), and either 30 μ M of anti-viral or vehicle, and calculating: % Rho 123_{eff} = $(C_{av} - C_{veh}) * 100 / (C_{tar} - C_{veh})$, where C_{av} = concentration of Rho 123 in the presence of anti-viral, C_{veh} = concentration in the presence of vehicle, C_{tar} = concentration of Rho 123 in the presence of tariquidar. In the presence of tariquidar, Rho 123 uptake was $1123 \pm 54\%$ of vehicle controls (n=44). MDR recognition provided by Dr. Richard Keep and Jianming Xiang

N1-indole derivatives synthesis and SAR development



Scheme 3: N1 indole analog synthesis

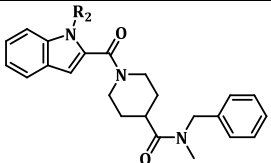
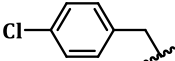
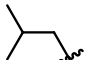
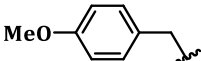
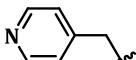
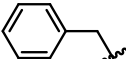
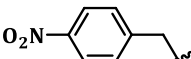
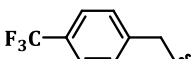
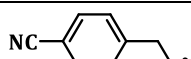
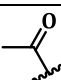
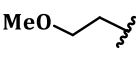
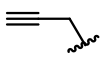
Another region explored was the N1-indole position (R^2 , Figure 5). The N1 indole analogs were originally designed to contain the benzyl carboxamide seen in compound **10**. The synthetic route used to generate N1-indole inhibitors is shown in Scheme 3. Ethyl-2-indole carboxylate was hydrolyzed in the presence of lithium hydroxide. Subsequent EDCI coupling with ethyl isonipecotate provided ester **160**. Compound **160** was saponified and coupled with either benzylamide or *N*-methylbenzyl amide resulting in advanced intermediates **161** or **90**, respectively.

The original synthetic route using intermediate **161** posed several synthetic difficulties due to the similar acidities of the N1-indole proton and the carboxamide

proton ($pK_a = 12.3$ and 15.5 , respectively) present on **161**.¹⁰⁴ The use of strong bases such as potassium tert-butoxide and sodium hydride resulted in a mixture of N-alkylation products being obtained. These included the desired N1-analogs, along with bisalkylation at the N-1 and carboxamide NH, and mono-alkylation at the carboxamide position N-H. However, bases such as cesium carbonate resulted in decomposition possibly due to the required prolonged reaction times in the presence of heat. According to Table 2, the presence of an *N*-methylbenzyl carboxamide (**21**) did not compromise activity compared to **10**; therefore, indicating that *N*-methyl benzylamine could serve as a valid substitute for benzylamine during our initial survey of N1-indole SAR. Preparation of N1-indole inhibitors thus proceeded through advanced intermediate **90**. Alkylation resulted in inhibitors **80-89** and **91** (Table 3).

Table 3 shows that modifications on the N1-indole position resulted in minimal change or decreased activity. Due to the lack of improvement in potency, both the first and second generation carboxamide analogs contained the original 4-chlorobenzyl motif at the N1-indole position. Furthermore, this lack of SAR suggested that the indole substituent is not likely to be making strong interactions with the molecular target.

Table 3: N1-indole derivatives

	CCG Number	R ₂	IC ₅₀ (μM) ^a	CC ₅₀ (μM) ^b
21	203930		16.9 ± 4.4	87.0
80	206332		27.9 ± 3.6	58.2
81	205477		16.5 ± 0.8	99.2
82	208789		24.2 ± 3.6	80.3
83	205404		17.0 ± 1.1	64.8
84	205484		61.3 ± 35.5	>100
85	208917		35.1 ± 43.5	90.3
86	206330		95.9 ± 7.0	>100
87	206333		35.1 ± 43.5	90.3
88	206331		>50	>50
89	206401		>50	>50
90	205400	H	27.7 ± 3.9	>100
91	205428	Me	>50	>50

^aInhibition of luciferase expression in WEEV replicon assay. Ribavirin as positive control has an IC₅₀ in the assay of 16 μM. Values are mean of at least n=3 independent experiments ± SE. ^bCell viability determined by inhibition of mitochondrial reduction of MTT. Values are mean of at least n=3 independent experiments. Provided by Dr. David Miller and Craig Dobry.

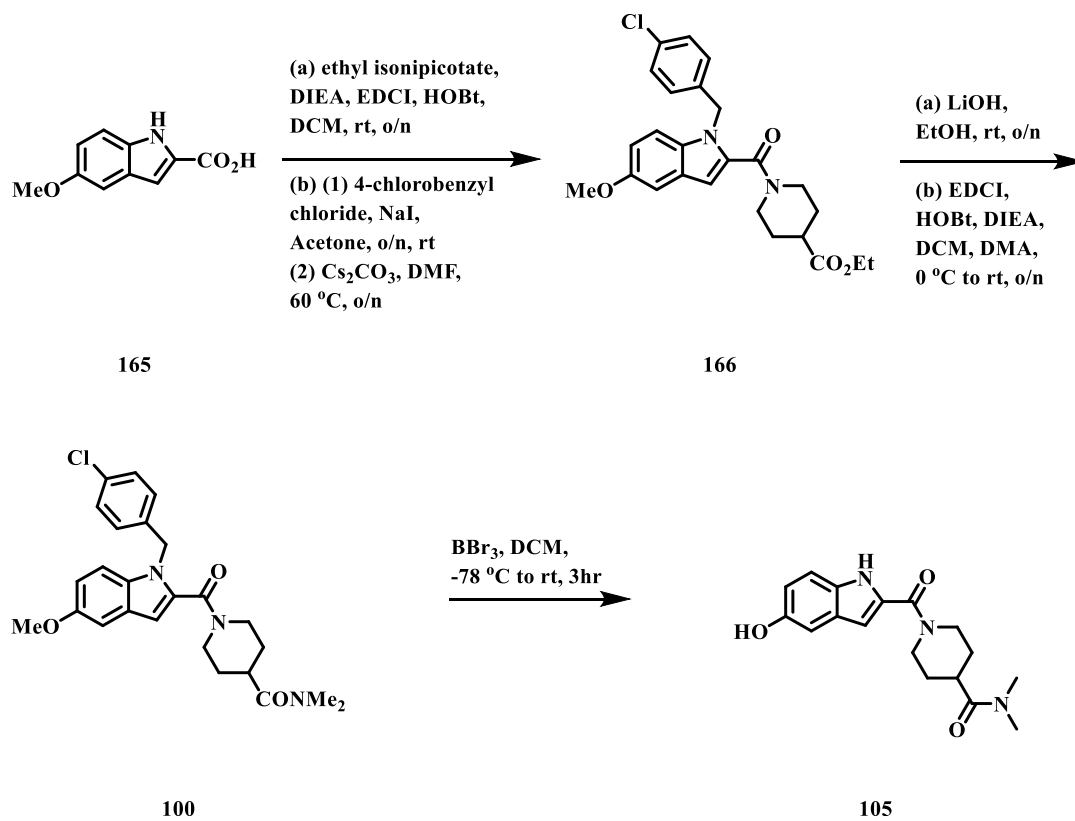
5-hydroxy indole synthesis

Another area we elected to explore was the 5-position of the indole ring, using an ether linker to facilitate diversity introduction (Figure 5B). Scheme 4 shows the initial synthesis of the 5-hydroxy indole analogs. The synthesis began with the peptide coupling between 5-methoxy-1H-indole-2-carboxylic acid and ethyl isonipecotate. The N1-indole alkylation occurred in a two-step process. It began with a Finkelstein reaction with 4-chlorobenzyl chloride and sodium iodide. The resulting iodide was used to alkylate the N1-indole position to generate intermediate **166**. Saponification using lithium hydroxide followed by another amide bond coupling using dimethyl amine resulted in **100**. However, attempted O-demethylation using boron tribromide resulted in both demethylation and debenzylation of intermediate **100**, giving low yield of inhibitor **105**.

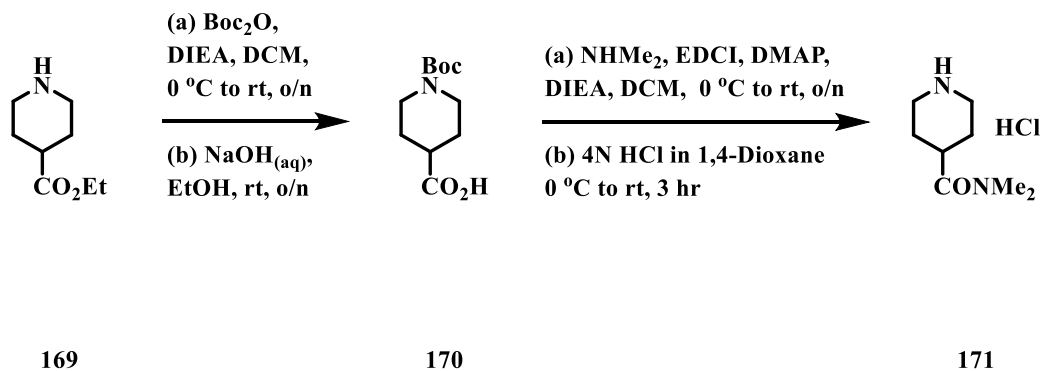
To avoid the lack of chemoselective demethylation, a second synthetic route towards the 5-hydroxy indole analogs was undertaken beginning with the Boc protection of ethyl isonipecotate followed by basic saponification to generate **170**. Peptide coupling with dimethyl amine and subsequent deprotection using hydrochloric acid resulted in synthon **171** (Scheme 5).

In parallel, 5-methoxy-1H-indole-2-carboxylic acid was esterified in the presence of hydrochloric acid and ethanol. Demethylation using boron tribromide resulted in **172**.¹⁰⁵ The resulting phenol was protected with tert-butyldimethylsilyl chloride.¹⁰⁶ However, subsequent alkylation using 4-chlorobenzyl chloride provided the desired intermediate **173** along with bisalkylated product **174**, indicating that premature desilylation of the 5-OH was occurring. Compounds **173** and **174** were isolated in a 3:1 ratio, respectively. Bisalkylation may be due to the susceptibility of the TBS group to

cleavage by the newly generated chloride anion during the alkylation. The inseparable mixture was taken directly to the next step. Silyl deprotection using tetrabutylammonium fluoride allowed isolation of intermediate **175**. Alkylation with various alkyl bromide followed by hydrolysis resulted in intermediates **176-178**. Subsequent amide coupling with synthon **171** resulted in analogs **102-104** (Scheme 6).

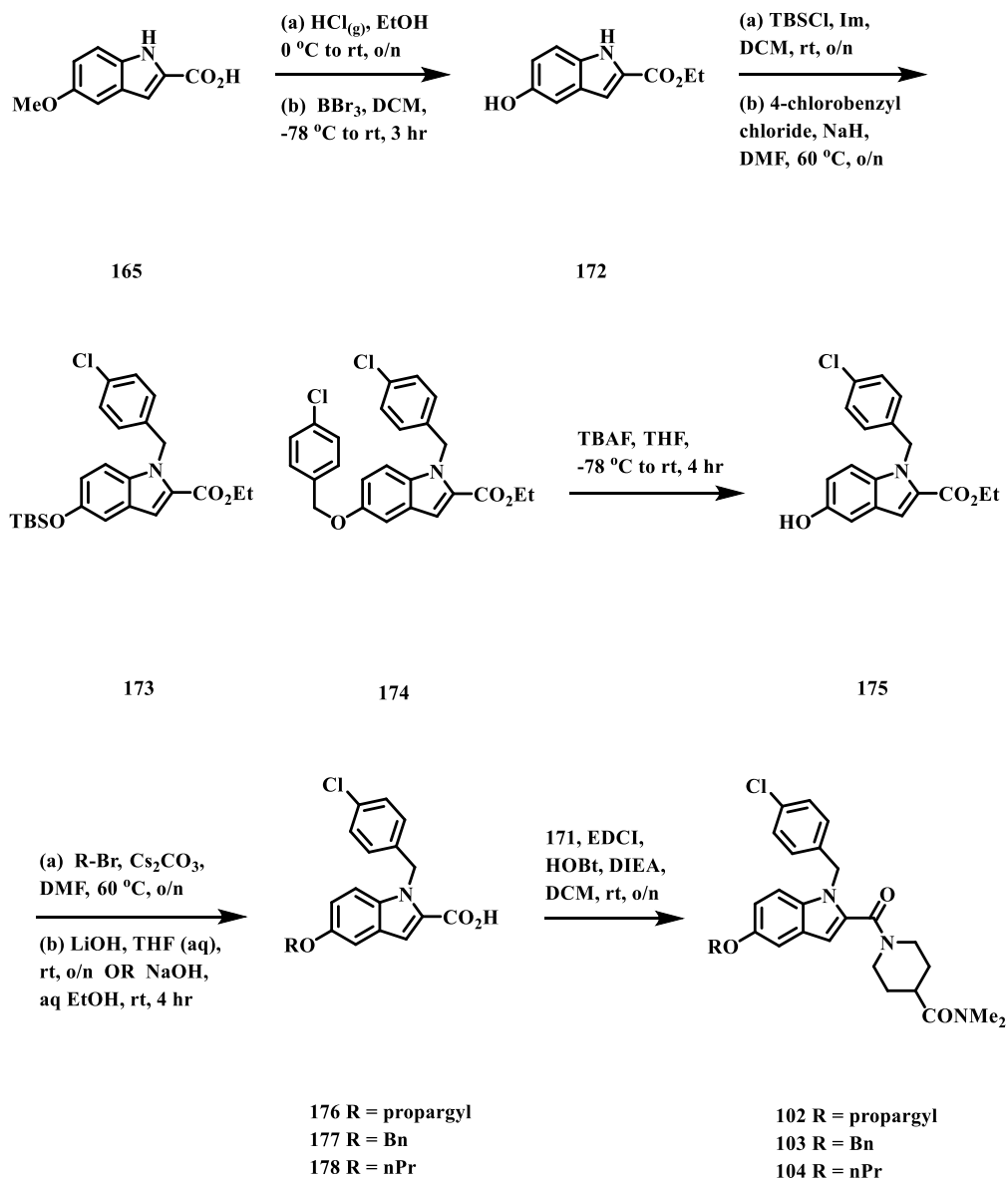


Scheme 4: Initial 5-hydroxy indole analogs



Scheme 5: Synthesis of synthon **167**

Inhibitor **105** was then protected using tert-butyldiphenylsilyl chloride to generate compound **180**. The TBDPS ether was used instead of the TBS ether in an attempt to minimize the bisalkylation found with the TBS ether by slowing chloride-induced desilylation (Scheme 7). Gratifyingly, alkylation using 4-chlorobenzyl iodide in the presence of a cesium carbonate resulted in intermediate **181**. Only trace amounts of the bisalkylated product were seen following the transition to the TBDPS ether. Removal of the silyl protecting group was ultimately accomplished using tetrabutylammonium fluoride to generate **101**.

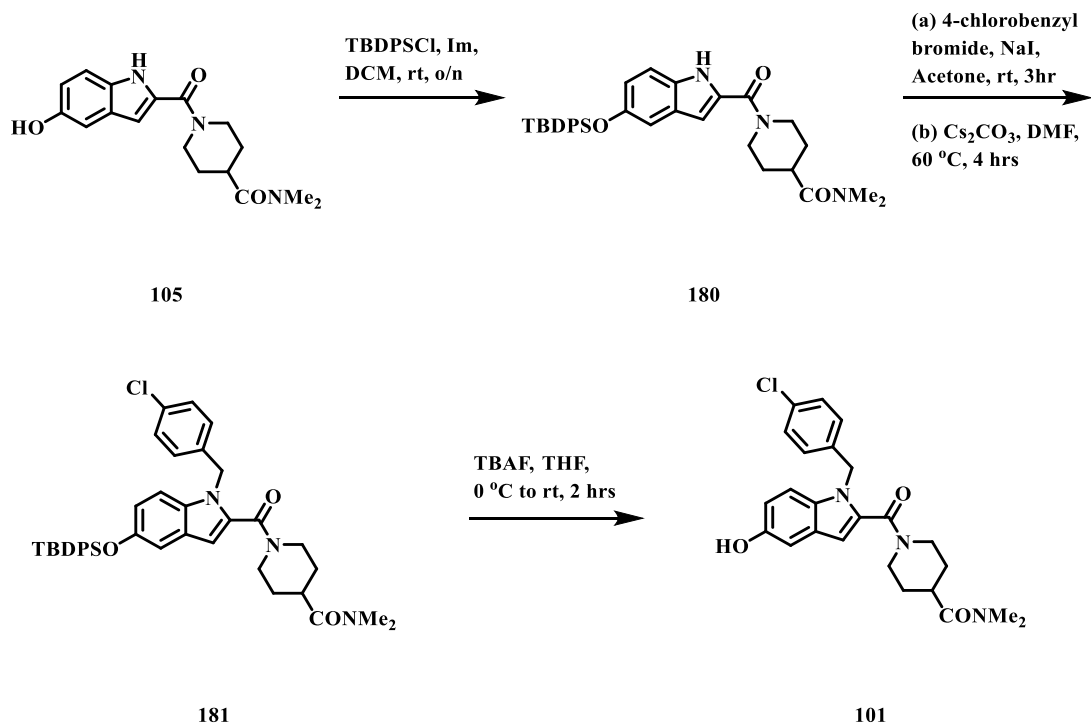


Scheme 6: Synthesis of inhibitors **102**, **103**, and **104**

We elected to explore the 5-hydroxy indole SAR with the dimethyl carboxamide in order to minimize molecular weight. This replacement was considered a valid substitution because the original indole lead (**10**) and the dimethyl carboxamide (**20**) shown in Table 2 were equipotent compounds. Larger lipophilic substituents on the 5-OH group (**103** and **104**) resulted in similar potencies as **20**. On the contrary, smaller

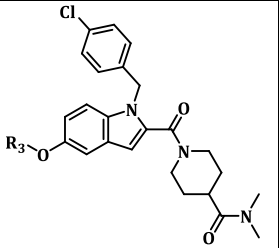
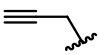
substitutions (**100-102**) resulted in a decrease or complete loss of potency. The contrasting activities between the sizes of the lipophilic groups may simply be due to an increase in cellular permeability. When comparing inhibitors **101** and **105**, the complete loss in potency in **105** indicated substitution at the N1-indole position is required for activity.

Another hypothesis is that **20** has a different binding mode compared to **10**. When considering a possible change in binding mode, it is possible that the larger, hydrophobic substituents found in **103**, **104**, and **20** are now interacting with the hydrophobic binding site that was previously occupied by the benzyl carboxamide functionality in **10**. The smaller, lipophilic substitutions such as the methyl (**100**) and the propargyl group (**102**) are not sufficient to make proper contact with the target resulting in the loss of potency.



Scheme 7: Synthesis of compound **101**

Table 4: 5-hydroxy indole SAR

	CCG Number	R ₃	IC ₅₀ (μM) ^a	CC ₅₀ (μM) ^b
100	211759	Me	> 50	> 50
101	222701	H	23.2 ± 8.0	>100
102	212058		> 50	> 50
103	212151	Bn	8.1 ± 2.0	50.7
104	212138	Pr	7.3 ± 4.7	15.1
105^c	212051	H	> 50	> 50

^aInhibition of luciferase expression in WEEV replicon assay. Ribavirin as positive control has an IC₅₀ in the assay of 16 μM. Values are mean of at least n=3 independent experiments ± SE. ^bCell viability determined by inhibition of mitochondrial reduction of MTT. Values are mean of at least n=3 independent experiments. ^cunalkylated N1-indole position. Data provided by Dr. David Miller and Craig Dobry

Conclusions

Early SAR development demonstrated that derivatization of the carboxamide position in **10** modulates antiviral activity while the N1-indole and 5-hydroxy indole positions did not provide significant change in potency compared to **10**. Also, we discovered two enantiomeric compounds (**11** and **12**) with widely differing activity, indicating that our target of interest may have a chiral character, and evidence of a hydrogen bonding motif (**22**) in its binding site. Furthermore, we have demonstrated that we are able to elicit *in vivo* activity against NSV through improvements in potency and

metabolic stability. A key factor in improving metabolic stability was the transition from the thienopyrrole template to bioisosteric indole.

CHAPTER III. SECOND GENERATION INDOLE-2-CARBOXAMIDE ANALOGS

Rationale

The SAR defined in Chapter II indicated that substituents on the terminal carboxamide position are able to modulate activity. Both hydrophobic and hydrophilic modifications were effective to various degrees. Of most significance was the increase in activity observed with a 4-pyridylmethyl carboxamide (**22**, $IC_{50} = 6.8 \mu\text{M}$) versus benzyl amide inhibitor **10** ($IC_{50} = 15 \mu\text{M}$), a modification that would be expected to *decrease* cell permeability and non-specific protein binding. This result strongly suggested that a potential hydrogen bonding interaction between the target and ligand is available to increase potency further. The following SAR focused on modulating the hydrogen bonding capability of the pyridylmethyl carboxamide.

SAR development

Inhibitors based on **22** were synthesized according to Scheme 2. These analogs were made to probe hydrophilic interactions. As illustrated by Table 5, substituents with increased basicity such as **35** and **38**, significantly decreased potency compared to inhibitor **22**. However, a non-basic, saturated heterocycle such as a morpholine (**39**) resulted in an inhibitor with similar potency as the original lead indole **10**. Increasing the hydrogen bonding capability and altering ring size with an imidazole and a pyrazole (**33**

and **34**) resulted in a drastic loss of activity, although the increase in TPSA with these two analogs (TPSA_{33, 34} = 68.25 vs. TPSA₂₂ = 65.01) could have impeded cell permeability.¹⁰⁷ Similarly, inhibitors capable of making multiple hydrogen bonds (**36** and **37**) were inactive. The position of the pyridine nitrogen also has an effect on potency. Transitioning from the *para*-position (**22**) to the *meta*- position (**30**), in relation to the carboxamide, generated a less active inhibitor. This loss in potency may be due to the incorrect directionality of the hydrogen bonding pair resulting in a weaker interaction between the target and inhibitor.¹⁰⁸ Addition of a methylene resulted in our first submicromolar inhibitor (**50**) which has a 40-fold increase in potency compared to the indole lead **10**.

Chirality

Considering the target's enantiospecificity and the previous success in increasing potency by adding chirality in both the thienopyrrole and indole series (Figure 6), it was hypothesized that adding chirality to 4-pyridyl carboxamide would increase potency. The racemic α -methyl-4-pyridylmethyl amide (**32**) was more active than inhibitor **22**. Based on previous SAR, it was hypothesized that only the *R*-isomer (**31**) would show activity. In fact the *R*-isomer (**31**) was more active than the racemic α -methyl-pyridylmethyl amide (**22**) and the racemic α -methyl-4-pyridylmethyl amide (**32**), consistent with our previous SAR and indicative of retention of the overall binding mode.

Antiviral activity

Due to the increased potency of **32** and **31**, the antiviral activity of these two compounds was examined. A related alphavirus, Fort Morgan virus (FMV) was used

because similar to NSV, FMV requires a lower biosafety level for safe handling compared to WEEV. Antiviral activity was measured at 25 μ M of inhibitor in human BE(2)-C neuronal cell line. Figure 11 illustrates the significant decrease in viral titer compared to the standard ribavirin and previous lead **12**. Even though the enantiopure analog, **31**, showed an improvement in potency compared to the racemate (**32**) in the replicon assay, it had a higher viral titer than **32** in an FMV infection study. Compounds **32** and **31** increased cellular viability compared to ribavirin and **12**. Racemate **32** reduced viral titer and significantly increased cellular viability in WEEV infection.

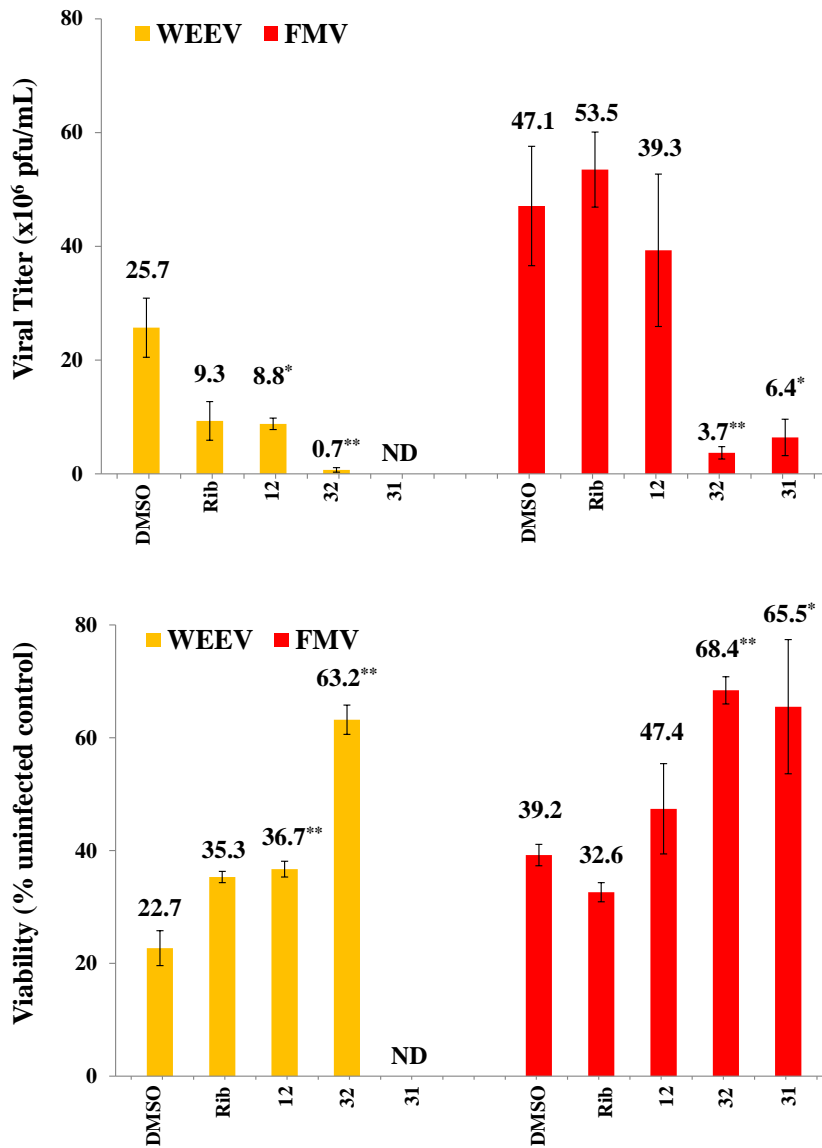
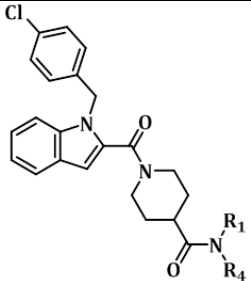
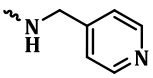
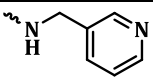
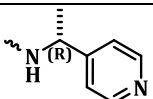
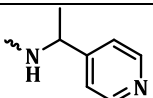
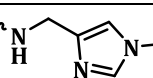
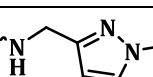
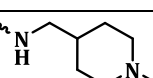
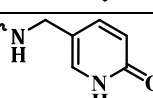
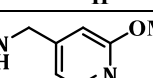
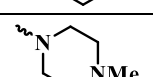
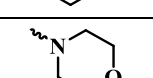
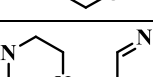
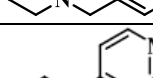


Figure 11: Viral Titer and Viability results for 32 and 31

Human BE(2)-C neuronal cells were infected with WEEV or FMV and incubated with inhibitors at 25 μ M. Cell viability and viral titers were measured 24 h post infection via MTT and plaque assays. Ribavirin(Rib) as positive control; DMSO negative. ND = not determined. $P < 0.05^*$ or 0.005^{**}
Graph courtesy of Dr. David Miller

Table 5: CCG 203929 (22) analogs

	CCG Number	NR ₁ R ₄	IC ₅₀ (μM) ^a	CC ₅₀ (μM) ^b
22	203929		6.8 ± 1.7	>100
30	205422		14.4 ± 0.4	>100
31	212090		0.6 ± .3	92.3
32	206329		2.4 ± 0.8	90.1
33	205455		>50	>50
34	205454		76.9 ± 30.8	>100
35	205429		>50	>50
36^δ	211760		>100	>100
37	208787		>50	>50
38	204023		31.4 ± 16.7	75.6
39	204024		12.8 ± 4.6	>100
40	205430		13.1 ± 2.0	63.3
50	205432		0.5 ± 0.2	49.9

^aInhibition of luciferase expression in WEEV replicon assay. Ribavirin as positive control has an IC₅₀ in the assay of 16 μM. Values are mean of at least n=3 independent experiments ± SE. ^bCell viability determined by inhibition of mitochondrial reduction of MTT. Values are mean of at least n=3 independent experiments.

Physicochemical properties

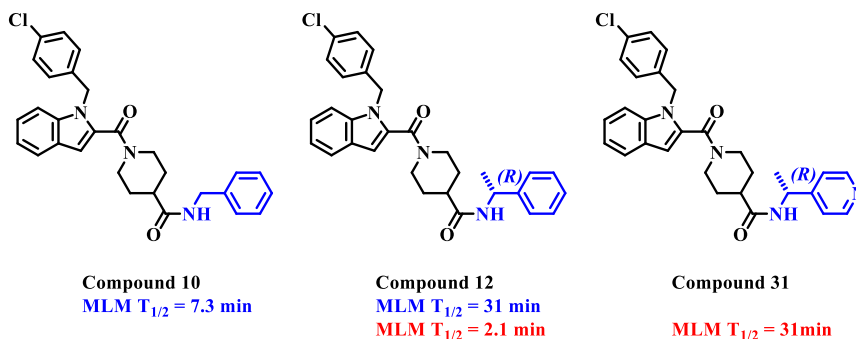


Figure 12: Select metabolic stability

^aHalf-life in mouse liver microsome incubations. ^bBlue and red indicates two different batches of MLM used to determine half-lives. Values are mean of ≥ 2 independent incubations. Performed by Scott J. Barraza

As previously discussed, addition of the α -methyl substitution in **12** increased metabolic stability compared to lead inhibitor **10**. Figure 12 shows the metabolic stability of select compounds. The figure above shows two half-lives for compound **12**. This is due to the two different batches of mouse liver microsomes used. The two experiments are differentiated by the colors. Transitioning to the α -methyl pyridyl carboxamide, the metabolic stability significantly increased compared to the corresponding α -methyl benzyl analog **12**. The increased metabolic stability may be due to the lowered lipophilicity. The metabolic stability of the 4-pyridylmethyl carboxamide (**22**) was not measured because of the increased metabolic stability in **12** induced by the presence of an α -methyl group, we assumed the pyridyl analog lacking the α -methyl would be less stable. This experiment emphasized the importance of having a known control when performing a metabolic stability experiment due to the potential for differences in activity between batches of microsomes.

Figure 10 (page 27) showed that the presence of 4-pyridylmethyl caboxamide substituents (**22**, **31**, and **32**) did not significantly change the passive permeability of the inhibitors. However, these series of compounds had an increased Pgp recognition. A third generation of carboxamide inhibitors based on **50** was subsequently pursued because of the dramatic 40-fold increase in potency compared to original indole lead **10**.

Conclusions

This chapter further explored the interaction between the terminal carboxamide of our inhibitors and the hydrogen bonding motif hypothesized to be present in the binding site of our molecular target. These modifications identified two compounds that have nanomolar activity (**31** and **50**) in the replicon assay, improved *in vitro* antiviral activity compared to indole lead **12**, and significantly improved metabolic stability in MLM.

CHAPTER IV. THIRD GENERATION INDOLE-2-CARBOXAMIDE ANALOGS

Rationale

Because of the significant increase in potency, a series of analogs were generated based on compound 4-pyridylethyl amide **50**. Similar to the strategy employed to derivatives based on **22**, the analogs explored both hydrophobic and hydrophilic modifications. In addition, they examined alternative hydrogen bonding motifs to explore the hypothesis that main chain amides of the molecular target were being engaged.

SAR development

These third generation indole analogs were synthesized according to Scheme 2. Similar to the trend seen in the 4-pyridylmethyl carboxamide series (Table 5) the progressive movement of the pyridine nitrogen from *para*-position to the *ortho*-position (**50**, **53**, and **57**) resulted in a decrease in potency from 0.5 μM to 22.4 μM (Table 6). This result indicated that the pyridine nitrogen must be in the *para*-position in order to make an ideal interaction with the target. The distance between the carboxamide and the pyridine motif was also examined. The 4-pyridylpropyl carboxamide (**63**) analog was less active than **50**. Taken together with the previously observed activity of the shorter

single methylene analog **22**, this indicates that the optimum distance between the 4-pyridine and amide functionalities is two methylenes.

Additions of lipophilic motifs such as aliphatic groups or halogens can aid in increasing cellular permeability which results in an increase in intracellular concentration of inhibitors. Lipophilic inhibitors (**52**, **56**, **58**, **59**, and **62**) showed lower activity than **50**. These compounds suggest that even though the target is capable of making hydrophobic interactions, the protein of interest has a hydrophilic binding site that prefers to make hydrogen bonds with motifs such as the pyridine in **50**.

Conformationally restricting potential inhibitors can lead to increases in potency, mitigate metabolic instability, and alter Pgp recognition. Restricting rotation about the ethylene linker of **50** was initially done by the sequential addition of methyl groups. N-methylation of **50** resulted in analog **51**; however, this analog resulted in a slight decrease in potency. This may be due to the different rotomers that **51** has and only one rotomer is in the right conformation to achieve the requisite hydrogen bond for increased potency. Monomethylation at the β -methylene of the 4-pyridylethyl carboxamide (**54**) resulted in a compound of similar potency to **50**. This result suggests that **50** and **54** are able to achieve similar spatial conformation that allows them to bind to the target in a similar fashion. However, greater conformational restriction by adding the gemdimethyl (**55**) restricts the molecule in a less than ideal three-dimensional shape limiting its capabilities to hydrogen bond to the target. One can imagine that covalently restricting the movement of the ethylene linker with the dihydrofuran ring (**64**) may result in a decrease in potency; however, this analog had better potency than its gemdimethyl (**55**) counterpart. This recovery in potency may be attributed to a better conformation than **55**

or the presence of the oxygen in **64**. This oxygen may be participating in the same hydrogen bonding system that the pyridine nitrogen is involved in; however, it is not of the appropriate distance, orientation or strength of hydrogen bond resulting in a lower potency than **50**.

Hydrogen bonding substitutions

Hydrogen bonds, which can influence interactions between drugs and their targets are integral interactions in drug discovery.¹⁰⁹ They can have significant impact on potency, selectivity, permeability and solubility.¹¹⁰ The relative strengths of these bonds are not only determined by the type of functionality, but also their shape and their local environment. For example, lactams are better hydrogen bond acceptors than acyclic amides. Also, electron donating or withdrawing functionalities affect the hydrogen bonding acceptor capabilities of aromatic systems.¹¹⁰ In addition, local environments influence the strength and significance of a hydrogen bond in a protein-drug interaction. Hydrogen bond networks can provide significant stability to an interaction.^{110, 111} Of particular interest, heteroaromatic rings are key components of most drugs.^{112, 113} They aid in determining molecular shape and recognition by proteins.^{112, 114} Aromatic heterocycles participates in hydrophobic, polar, hydrogen bonding, cation- π , amide- π , halogen- π , and π -stacking interactions.¹¹⁵⁻¹²⁰

Based on the key increase in potency observed with our lead inhibitor **50** upon introduction of the 4-pyridyl group, Dr. Paul Kirchoff performed a substructure search of the PDB for compounds that contained a pyridine in their bound ligands. The database search primarily identified ATP competitive kinase inhibitors that interacted with the

protein backbone amides instead of the side chains. Therefore, we hypothesized that our pyridyl amide might be interacting with main chain amides. To test this hypothesis, we prepared analogs incorporating hydrogen bonding groups known to interact strongly with the hinge region of kinases.

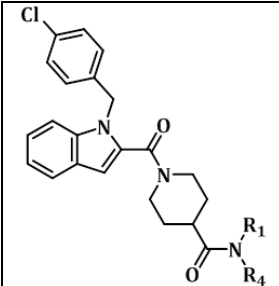
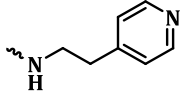
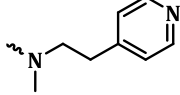
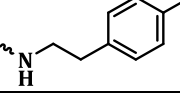
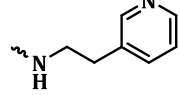
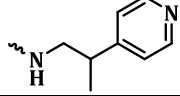
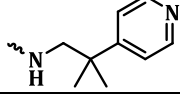
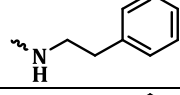
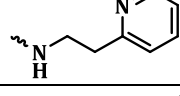
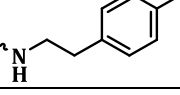
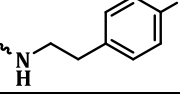
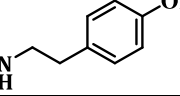
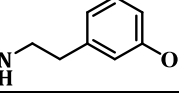
Hydrogen bonding substitution SAR development

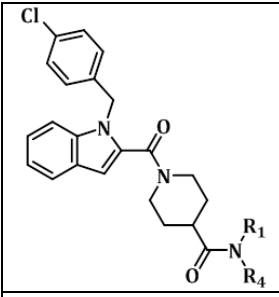
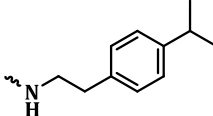
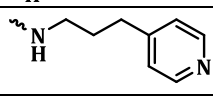
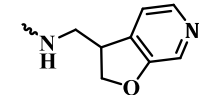
These derivatives explored other hydrogen bonding motifs as a possible replacement for the pyridine found in **50**. Bicyclic compounds **70** and **75** are regioisomeric indazoles and capable of making both π - π and hydrogen bond interactions with the target. Even though these two compounds lost significant potency compared to **50**, they do highlight that structural changes not only affect potency but also cytotoxicity. The 4-indazolyl carboxamide (**70**) was significantly more cytotoxic than the 5-indazolyl (**75**). Also, the 1-methylpyrazolyl carboxamide (**76**) is significantly more cytotoxic than its unmethylated counterpart (**78**). Interestingly, tryptamine carboxamide (**74**) and 7-azatryptamine carboxamide (**71**) showed that the two hydrogen bonding motifs in **71** results in a more potent inhibitor than **74**, which is what would have been predicted for an interaction with main chain amides. The most active analog from this group was the simple N-unsubstituted pyrazole **78**. Increasing the distance between the amide and pyrazole motif did not improve potency (**73** v. **78**).

3,4-dichlorophenethyl carboxamide (**72**) has the potential to establish an interaction referred to as halogen bonding.^{117, 121, 122} This interaction is seen to increase efficacy, potency, and selectivity in inhibitors for kinases such as CDK9.^{121, 123-125} C-X bonds where X is a halogen are capable of making interactions with electrophiles,

nucleophiles, and other halogens.¹²⁶ Halogens, excluding fluorine, have an uneven distribution of electrons where a slight positive charge is found opposite of the C-X bond. This is called the σ -hole.^{109, 122} Similar to kinases where the carbonyl backbone acts as the primary hydrogen bond acceptor for the ATP site binding inhibitors, the carbonyl also functions as the primary halogen bond acceptor.¹²² Unfortunately, the 3,4-dichlorophenylethyl amide (**72**) was not significantly more active than the simple phenethylamide (**56**, Table 6), suggesting that no productive halogen bonding with an amide backbone was realized.

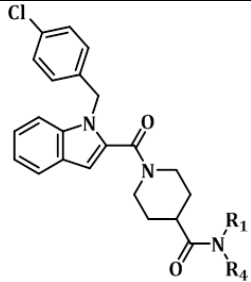
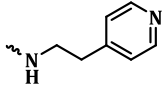
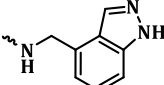
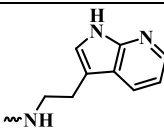
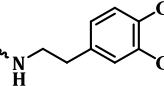
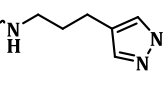
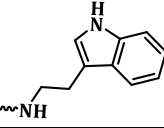
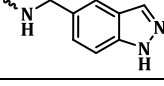
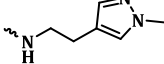
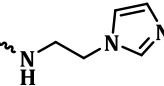
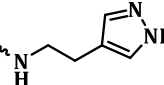
Table 6: Inhibitor 50 derivatives

	CCG Number	NR ₁ R ₄	IC ₅₀ (μM) ^a	CC ₅₀ (μM) ^b
50	205432		0.5 ± 0.2	49.9
51	211761		1.6 ± 0.8	47.9
52	102518		5.5 ± 2.2	75.2
53	205433		5.3 ± 1.1	39.4
54	206580		1.7 ± 1.2	98.2
55	209022		19.3 ± 21.0	43.6
56	206397		15.2 ± 9.3	62.2
57	205456		22.4 ± 10.0	86.2
58	206400		8.1 ± 1.1	40.4
59	206396		21.4 ± 18.8	18.6
60	206398		15.5 ± 14.6	11.3
61	206395		11.1 ± 3.8	>100

	CCG Number	NR ₁ R ₄	IC ₅₀ (μM) ^a	CC ₅₀ (μM) ^b
62	206461		10.8 ± 3.3	27.2
63	208788		31.9 ± 37.9	71.5
64	206581		3.6 ± 1.7	75.8

^aInhibition of luciferase expression in WEEV replicon assay. Ribavirin as positive control has an IC₅₀ in the assay of 16 μM. Values are mean of at least n=3 independent experiments ± SE. ^bCell viability determined by inhibition of mitochondrial reduction of MTT. Values are mean of at least n=3 independent experiments. Provided by Dr. David Miller and Craig Dobry

Table 7: CCG 205432 hydrogen bonding exploration

	CCG Number	NR ₁ R ₄	IC ₅₀ (μM) ^a	CC ₅₀ (μM) ^b
50	205432		0.5 ± 0.2	49.9
70	215061		14.0 ± 0.9	47.3
71	222940		3.40 ± 0.3	88.9
72	222720		11.0	>100
73	222760		1.34 ± 0.8	45.5
74	222900		13.4 ± 0.9	98.0
75	215060		12.5 ± 2.6	>100
76	215080		2.33 ± 0.3	10.0
77	206582		4.9 ± 2.6	99.6
78	215153		1.0 ± .1	56.0

^aInhibition of luciferase expression in WEEV replicon assay. Ribavirin as positive control has an IC₅₀ in the assay of 16 μM. Values are mean of at least n=3 independent experiments ± SE. ^bCell viability determined by inhibition of mitochondrial reduction of MTT. Values are mean of at least n=3 independent experiments. Provided by Dr. David Miller and Craig Dobry

Physicochemical Properties

Metabolic stability was performed in a similar fashion as described in Chapter I. Studies indicated that **50** and **77** had longer half-lives than the first generation indole inhibitor **12** (MLM $T_{1/2}$ = 2.1 min), but were both less stable than **31** (Figure 13). This decrease in half life might be due to the reintroduction of an unsubstituted methylene group. This site was shown (**10** v **12**, Chapter III) to be metabolically labile and addition of a methyl group decreased its susceptibility to metabolism. Also, it is possible that having two methylenes allowed better binding of the pyridine in the CYP450 binding site, making it more prone to oxidation.

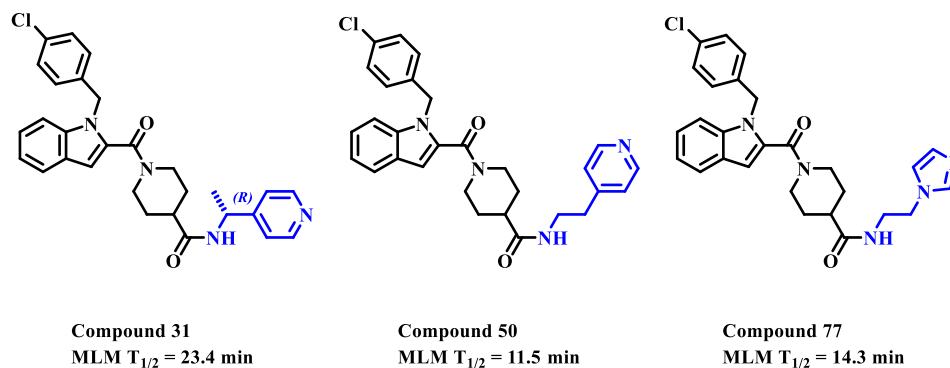


Figure 13: Select metabolic stability
Half-life in mouse liver microsome incubations. Values are mean of ≥ 2 independent incubations.
Performed by Scott J. Barraza

Pgp recognition and passive permeability were measured for select compounds. As shown by Figure 14, the N-methylated analog of **50** (**51**) led to increased recognition by Pgp. However, unlike **51**, methylation at the β -carbon (**54**) slightly decreased Pgp recognition relative to **50**. This result emphasizes that Pgp recognition is not only affected by changes in functional groups, but also molecular shape. Regioisomers (**50**, **53**, **57**) had similar Pgp recognition. Extending the distance between the carboxamide

and pyridine (**63**) and conformationally restricting the ethylene linker (**64**) increased Pgp recognition compared to **50**. The more basic imidazoleethyl carboxamide (**77**) decreased Pgp recognition in comparison to **50**. In addition, its increased polarity resulted in a log reduction in passive permeability (Figure 14).

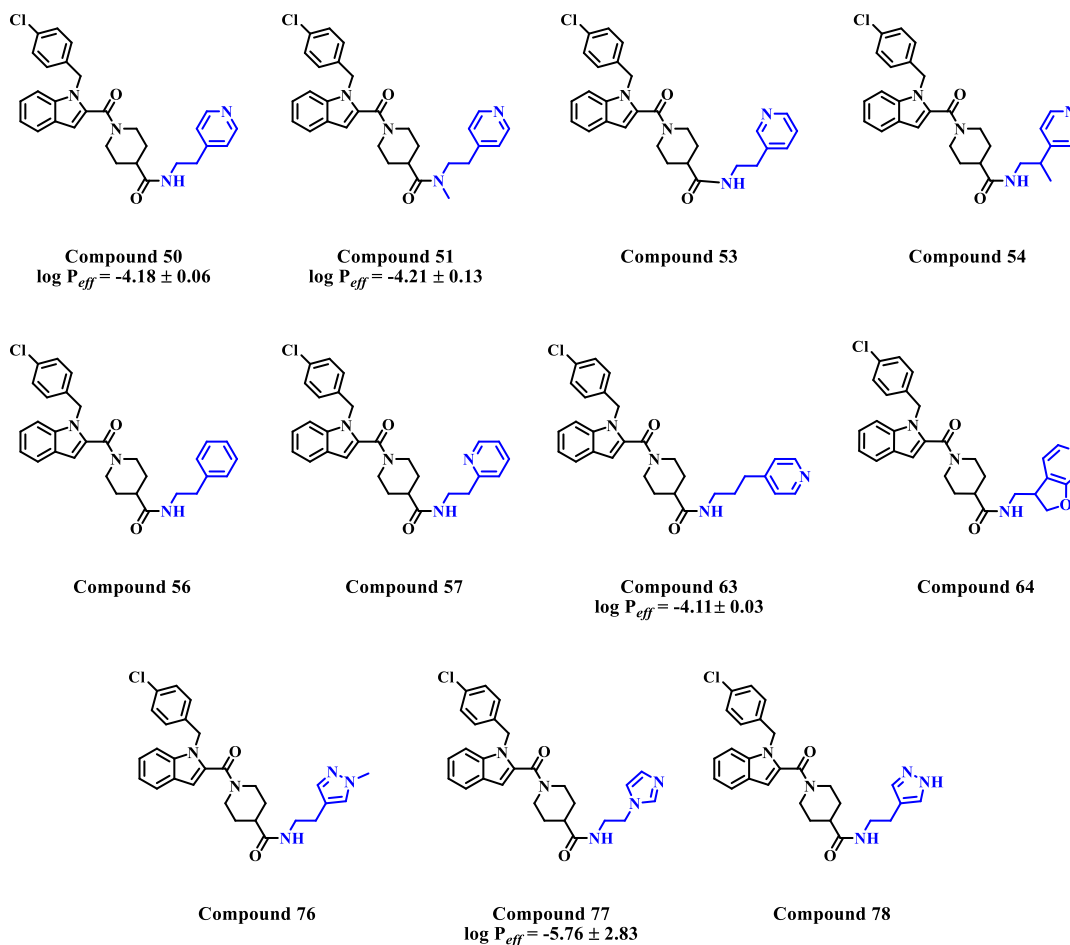
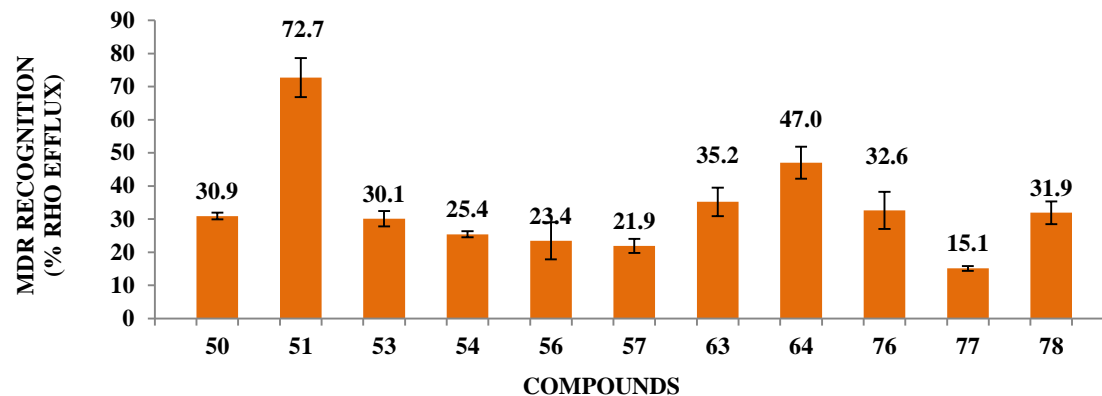


Figure 14: Pgp recognition and passive permeability for pyridylethyl carboxamide analogs Rhodamine 123 (Rho 123) uptake was measured in MDR1-MDCKII cells utilizing Glomax Multi Detection System (Promega). ‘MDR1 recognition’ was assessed by measuring uptake in the presence of MDR inhibitor, tariquidar (5 μ M), and either 30 μ M of anti-viral or vehicle, and calculating: % Rho 123_{eff} = $(C_{av} - C_{veh}) * 100 / (C_{tar} - C_{veh})$, where C_{av} = concentration of Rho 123 in the presence of anti-viral, C_{veh} = concentration in the presence of vehicle, C_{tar} = concentration of Rho 123 in the presence of tariquidar. In the presence of tariquidar, Rho 123 uptake was $1123 \pm 54\%$ of vehicle controls (n=44). MDR recognition provided by Dr. Richard Keep and Jianming Xiang

In vitro antiviral and viability studies

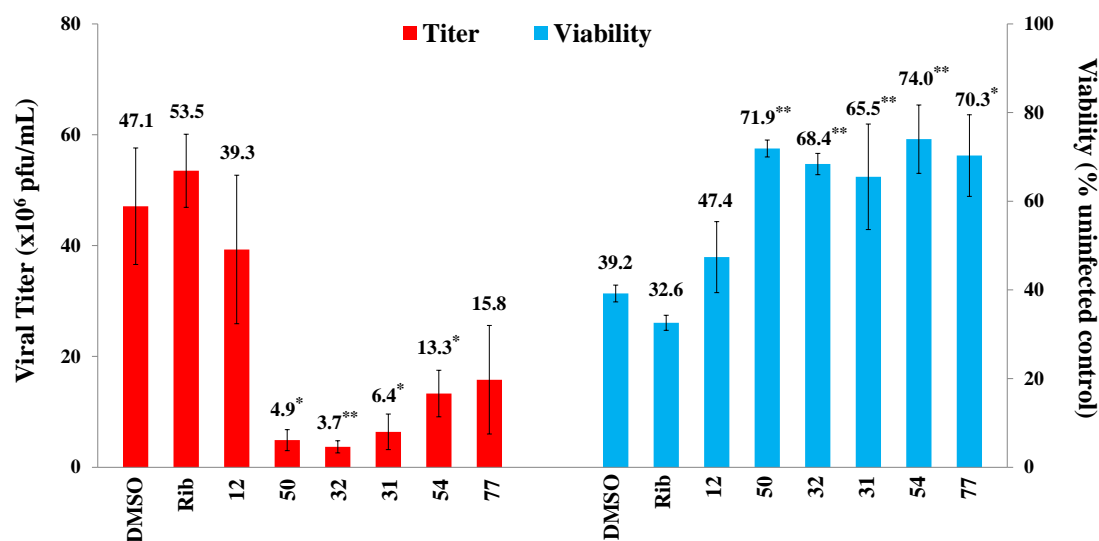


Figure 15: FMV antiviral viral results for compound **50** analogs

Human BE(2)-C neuronal cells were infected with FMV and incubated with inhibitors at 25 μ M. Cell viability and viral titers were measured 24 h post infection via MTT and plaque assays. Ribavirin(Rib) as positive control; DMSO negative. $P < 0.05^*$ or 0.005^{**} Data courtesy of Dr. David Miller and Craig Dobry

Similar to the previous studies, antiviral and viability studies were done at 25 μ M inhibitor concentration in neuronal cells infected with FMV. Figure 15 showed all the compounds were capable of reducing viral titer and increasing cellular viability compared to Ribavirin and **12**. Inhibitor **50** was efficacious in reducing viral titer to similar levels as **32** and **31**. The less potent β -monomethylated analog **54** did not reduce viral titer compared to **50**. However, both significantly increased viability to the same level compared to Ribavirin and **12**. These antiviral activities showed progress towards better antiviral and increased cellular viability.

***In vivo* WEEV infection study**

Due to its increase in metabolic stability and 40-fold increase in potency, **50** was taken into a WEEV infection mice study. Female C57BL/6 mice 5-6 weeks of age were infected with a highly virulent strain of WEEV, Cba-87. Mice were infected subcutaneously with 10^3 pfu of WEEV. Treatment was administered via intraperitoneal injection at 30 mg/kg, twice daily starting the day of infection until day 7. The mice were monitored until day 14, at which time they were euthanized. Disease severity was scored according to the same scale described in Chapter II. Figure 16 showed **50** decreased disease severity (clinical score) and increased survival compared to DMSO treated mice.¹²⁷

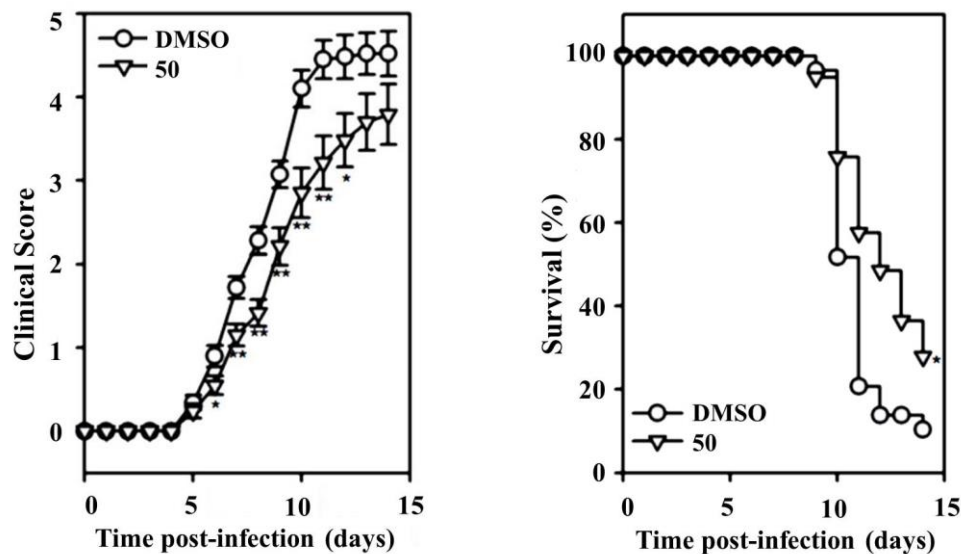


Figure 16: *In vivo* WEEV infection treatment with compound **50**. Mice were infected with 10^3 pfu/mL of WEEV and treated with **50** using 30 mg/kg/dose or vehicle. Animals were treated via IP injection every 12 hours beginning 12 hours after virus challenge. Composite of four independent experiments, where n=4-10 mice per group per experiment. (A) Disease severity (B) Survival Graph courtesy of Dr. David Irani, Dr. David Miller, and Penelope Blakely. Figure adapted from Ref. 125

Conclusions

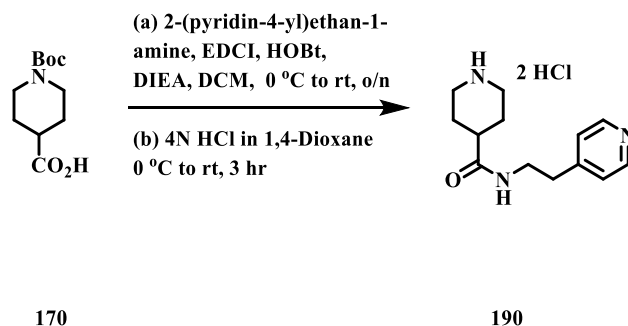
This chapter explored in detail SAR at the terminal amide, reinforcing that the 4-pyridylethyl amide (**50**) was an optimal amide substitution pattern, leading to a nanomolar activity in the replicon assay, improved metabolic stability, and *in vivo* activity against WEEV. In addition, modifications at the amide were able to modulate physicochemical properties identifying compounds with lower Pgp recognition and further increased metabolic stability.

CHAPTER V. INDOLE SUBSTITUTION

Rationale

The carboxamide position had been extensively probed, leading to the discovery of optimal inhibitor **50**. This compound is 40-fold more potent than the original indole lead (**10**). In our early SAR studies, both the N1-indole and 5-hydroxy indole substitutions did not improve potency compared to **10**, resulting in a majority of subsequent SAR being optimized for the 4-chlorobenzyl and 5-H indole scaffold. It was on this scaffold that the 4-pyridylethyl carboxamide was found necessary to give the best potency. We thus elected to revisit the role of the indole and its impact on activity, cytotoxicity and physicochemical properties in the presence of the optimal 4-pyridylethyl carboxamide. Many of these analogs were also designed to further improve metabolic stability.

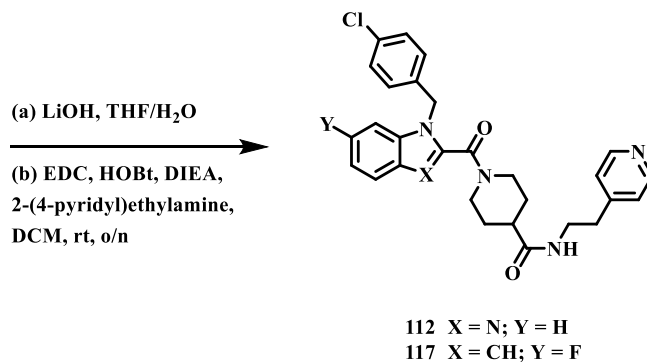
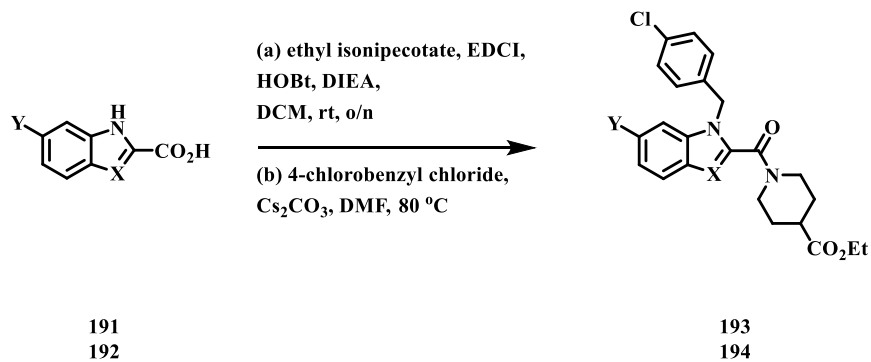
Synthesis



Scheme 8: Synthesis of synthon **190**

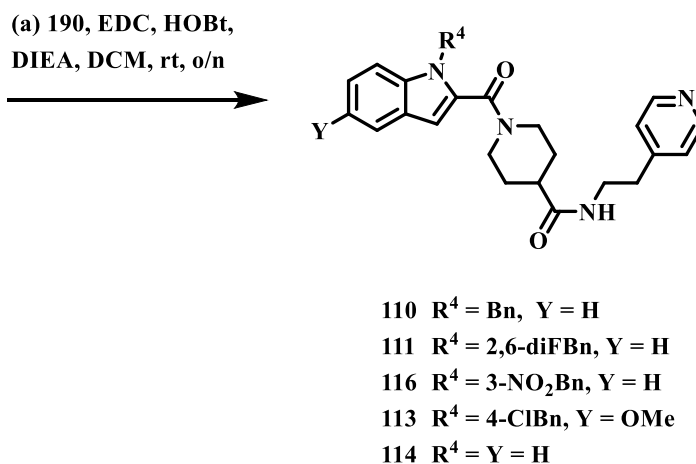
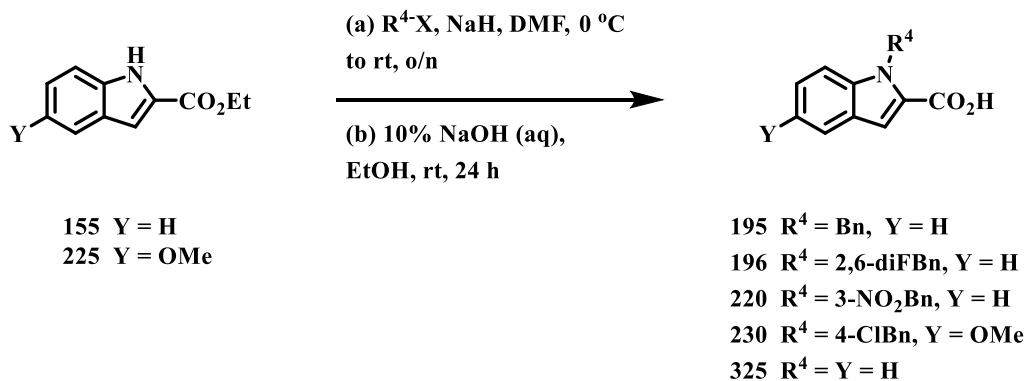
To streamline analog synthesis, the complete piperidine amide portion of **50** was first prepared. Previously synthesized intermediate **170** was coupled with 2-(pyridine-4-yl)ethan-1-amine. Subsequent exposure to hydrochloric acid resulted in synthon **190** (Scheme 8).

6-fluoro-1*H*-indole-2-carboxylic acid and 1*H*-benzo[*d*]imidazole-2-carboxylic acid were coupled to ethyl isonipicotate and the resulting ester was alkylated with 4-chlorobenzyl chloride to generate intermediate **193** and **194**. Saponification in the presence of lithium hydroxide followed by a second peptide coupling with 2-(pyridine-4-yl)ethan-1-amine gave inhibitors **112** and **117** (Scheme 9).



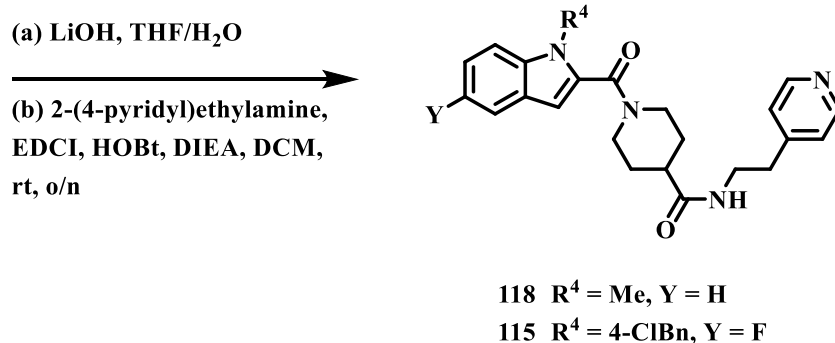
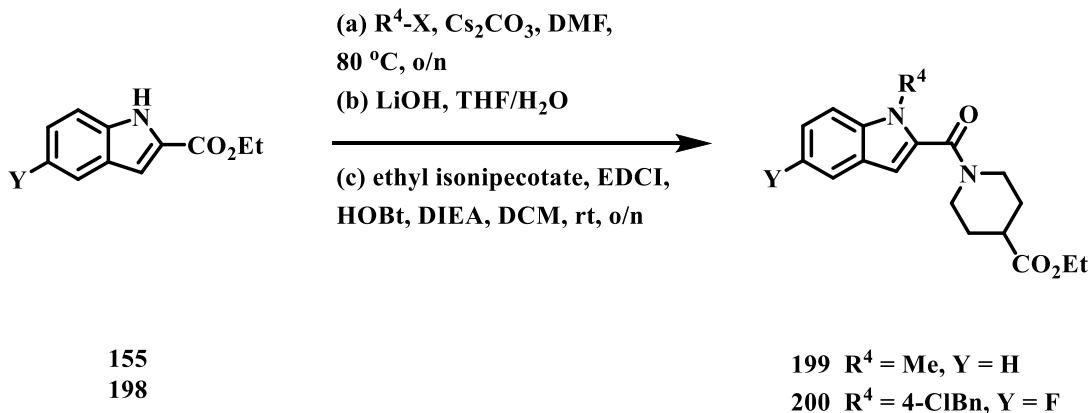
Scheme 9: Synthesis of analogs **112** and **117**

The synthesis of compounds **110**, **111**, and **116** began with the alkylation of ethyl indole-2-carboxylate with the requisite benzyl halides. Subsequent hydrolysis resulted in carboxylic acids **195**, **196**, and **220**. Coupling with synthon **190** resulted in inhibitors **110**, **111**, and **116**. Ester **225** was alkylated with 4-chlorobenzyl chloride then hydrolyzed to give acid **230**. Coupling with **190** gave compound **113**. To generate inhibitor **114**, ester **155** was hydrolyzed to give **235**. Coupling with synthon **190** gave the desired inhibitor (Scheme 10).



Scheme 10: Synthesis of analog **110**, **111**, **113**, **114**, **116**

Indole **155** was methylated in the presence of methyl iodide to generate ethyl 1-methyl-1*H*-indole-2-carboxylate (Scheme 11). Alkylation of ethyl 5-fluoro-1*H*-indole-2-carboxylate (**198**) with 4-chlorobenzyl chloride generated ethyl 1-(4-chlorobenzyl)-5-fluoro-1*H*-indole-2-carboxylate (**200**). Both esters were hydrolyzed and the resulting carboxylic acids were coupled with ethyl isonipicotate using EDCI and HOBt to give **199** and **200**. Esters **199** and **200** were hydrolyzed followed by a coupling with 2-(4-pyridyl)ethylamine to give inhibitors **118** and **115**.



Scheme 11: Synthesis of analog **115** and **118**

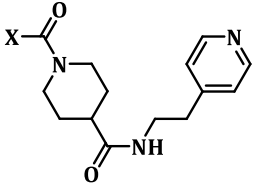
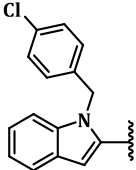
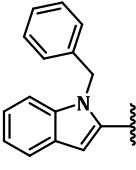
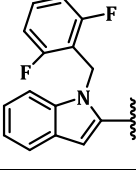
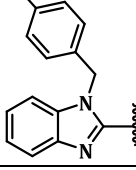
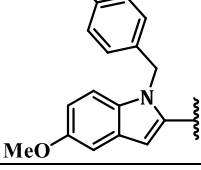
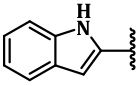
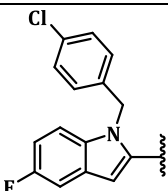
SAR development

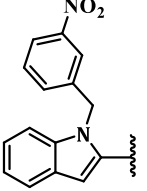
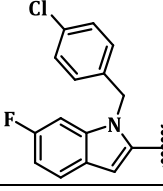
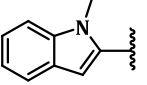
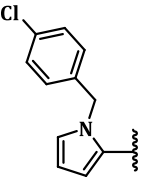
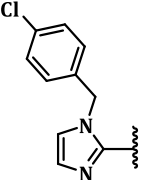
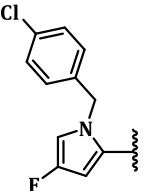
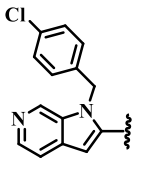
Table 8 lists the various indole modification analogs synthesized. The 4-chlorobenzyl was replaced with a methyl and a hydrogen (**118** and **114**, respectively). These two analogs were completely inactive indicating a benzylic type motif is necessary for activity at the N1-indole position. The 5-methoxy indole substitution (**113**) did not affect potency; however, it increased cytotoxicity. Replacement of the indole with an electron deficient benzimidazole (**112**) or 6-azaindole (**143**) resulted in about a 10-fold

loss of potency. Both were intended to mitigate oxidative metabolism of the indole ring. The N1-benzyl substitution (**110**) showed slightly reduced potency to **50**, indicating that the chlorine was contributing to potency, perhaps just through better cell permeability. Monocyclic analogs (**140** and **141**) were synthesized by Scott J. Barraza. These compounds were intended to decrease the molecular weight in order to better coincide with the properties of marketed CNS drugs listed on page 15. Compound **140** exhibited similar potency and better cytotoxicity than **50**; however, in a preliminary *in vivo* study it caused severe neurotoxicity exhibited by seizures. Imidazole analog (**141**) resulted in a total loss of potency.

Several fluorine-containing inhibitors have been synthesized (**111**, **115**, **117**, and **142**). Fluorine is a substituent in medicinal chemistry that is capable of modulating activity, cytotoxicity, physicochemical and pharmacokinetic properties.¹²⁸⁻¹³⁰ In addition, it adds lipophilicity to the compound and yet it is capable of generating hydrogen bonding interactions.¹³¹ For CNS drugs, it is capable of increasing BBB permeability due to its impact on lipophilicity.¹³⁰ It is able to mitigate CYP450 metabolism. Our fluorinated analogs were intended to improve metabolic stability. Unfortunately, they did not improve potency. However, the 4-fluoropyrrole inhibitor (**142**) resulted in a significant increase in toxicity.

Table 8: Indole Substitution

	CCG Number	X	IC ₅₀ (μM) ^a	CC ₅₀ (μM) ^b
50	205432		0.5 ± 0.2	49.9
110	209023		1.6 ± 0.5	45.6
111	209024		1.3 ± 0.8	34.5
112	206565		4.1 ± 1.0	74.6
113	209025		0.47 ± 0.2	21.0
114	212059		>50	>50
115	208919		0.9 ± 0.8	52.5

116	212150		1.7 ± 0.2	53.3
117	208918		0.6 ± 0.7	43.1
118	206484		>50	>50
140*	206381		0.7 ± 0.1	>100
141*	208916		>50	>50
142*	209021		0.9 ± 0.3	8.0
143*	211751		4.4 ± 0.8	77.1

^aInhibition of luciferase expression in WEEV replicon assay. Ribavirin as positive control has an IC₅₀ in the assay of 16 μM. Values are mean of at least n=3 independent experiments ± SE. ^bCell viability determined by inhibition of mitochondrial reduction of MTT. Values are mean of at least n=3 independent experiments. Data provided by Dr. David Miller and Craig Dobry. *Synthesized by Scott J. Barraza

Antiviral activity

Figure 17 shows the FMV antiviral results for selected indole modified analogs. These experiments used similar conditions as the previous antiviral experiments. As shown, inhibitor **50** significantly decreased viral titer compared to its pyrrole analog inhibitor **140**. 6-fluoroindole **117** reduced viral titer better than **50** but had similar effects on cellular viability. Surprisingly, the less replicon-active benzimidazole analog (**112**) showed a reduction in viral titer and an improvement in viability better than **140**. N-benzyl indole **110** was slightly less potent than inhibitor **50**; however, it reduced viral titer to similar levels as **50** and increased cellular viability better than **50** and ribavirin. Unexpectedly, 6-azaindole **143** did not reduce viral titer even though it was equipotent to benzimidazole **112**. Compound **112** sufficiently decreased viral titer compared to Ribavirin.

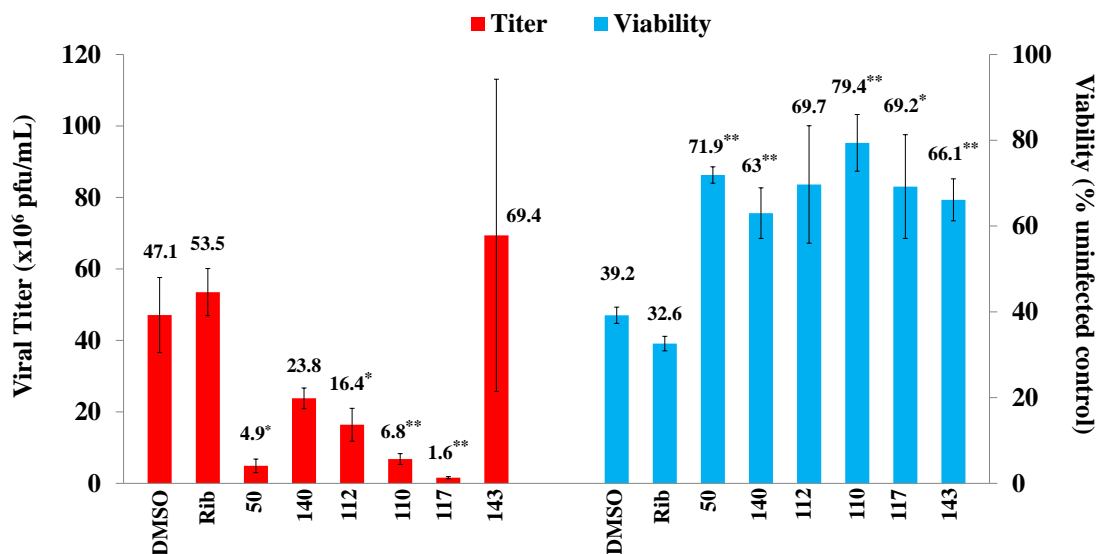


Figure 17: Indole replacement antiviral results

Human BE(2)-C neuronal cells were infected with FMV and incubated with inhibitors at 25 μ M. Cell viability and viral titers were measured 24 h post infection via MTT and plaque assays. Ribavirin(Rib) as positive control; DMSO negative. $P < 0.05^*$ or 0.005^{**} Data courtesy of Dr. David Miller and Craig Dobry

Physicochemical Properties

Select compounds were subjected to metabolic stability in mouse liver microsomes. These experiments were performed in a similar manner as those described in Chapter I. Figure 18 showed that pyrrole **140** was very unstable to CYP450. This indicated that the pyrrole is likely a major site of metabolism. Generating electron deficient scaffolds, such as the benzoimidazole (**112**) and 6-azaindole (**143**), restored some metabolic stability, but surprisingly these were not much different than indole **50**. The N1-benzyl derivative, **110**, on the other hand showed a dramatic increase in stability. This result indicates that the N-benzylic substituent is not likely to be a metabolically labile group, and that the improvement in metabolic stability is rather due to an overall reduction in lipophilicity.

These indole substitution analogs were unable to improve passive permeability compared to **50**. The fluorinated analogs (**111**, **115** and **117**) were intended to reduce metabolic liabilities at the indole and benzyl positions; however, these inhibitors were unable to produce inhibitors with increased activities compared to **50** (Table 8). Similarly, they were also unable to improve Pgp recognition compared to **50** (Figure 19). The difference in Pgp recognition between **115** and **117**, differing only in the position of a fluorine atom, demonstrates that small changes can have a large impact on Pgp recognition levels. Electron deficient bicyclic inhibitors (**112** and **143**) markedly reduced recognition relative to indole **50**. Monocyclic inhibitors **140** and **141** eliminated Pgp recognition. Reducing lipophilicity by removing the chlorine (**110**) reduced Pgp recognition (Figure 19). Overall, these results indicate that Pgp recognition of this series of inhibitors can be attenuated by reducing lipophilicity, either by removal of halogens,

replacement of aromatic CH with N, or replacement of the bicyclic indole with monocyclic heteroaromatics.

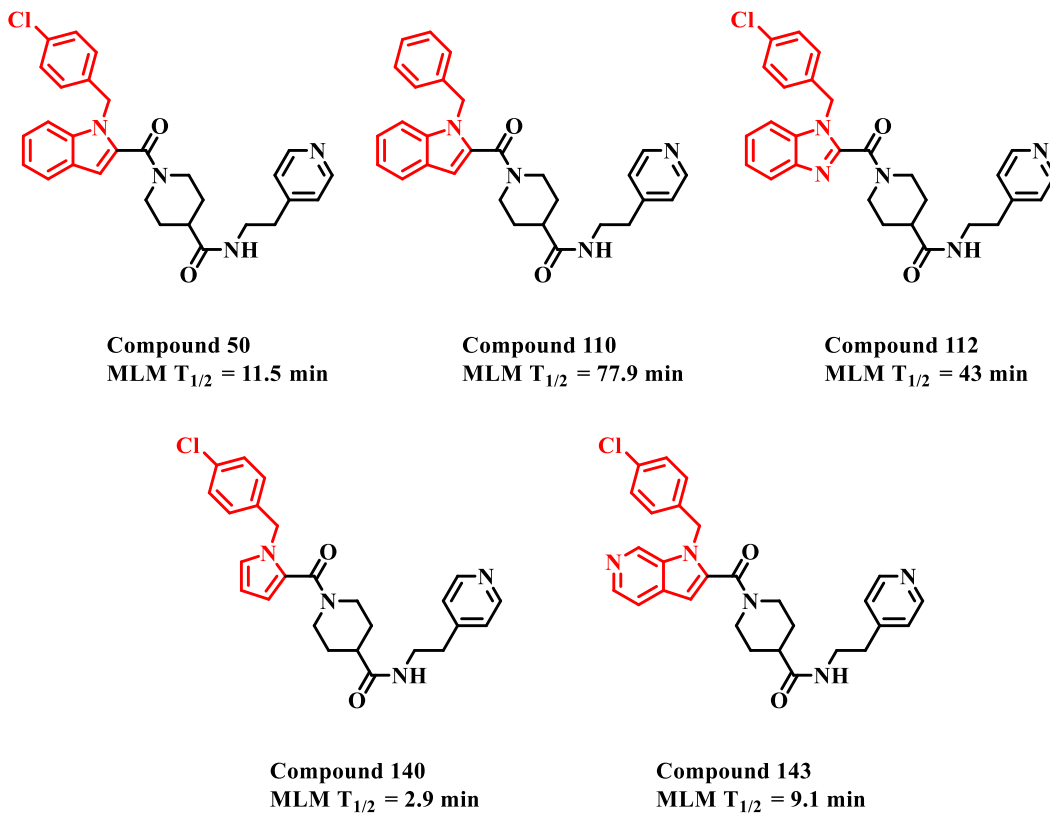


Figure 18: Metabolic stability of indole substituents
Half-life in mouse liver microsomal incubations. Values are mean of ≥ 2 independent incubations.
Performed by Scott J. Barraza

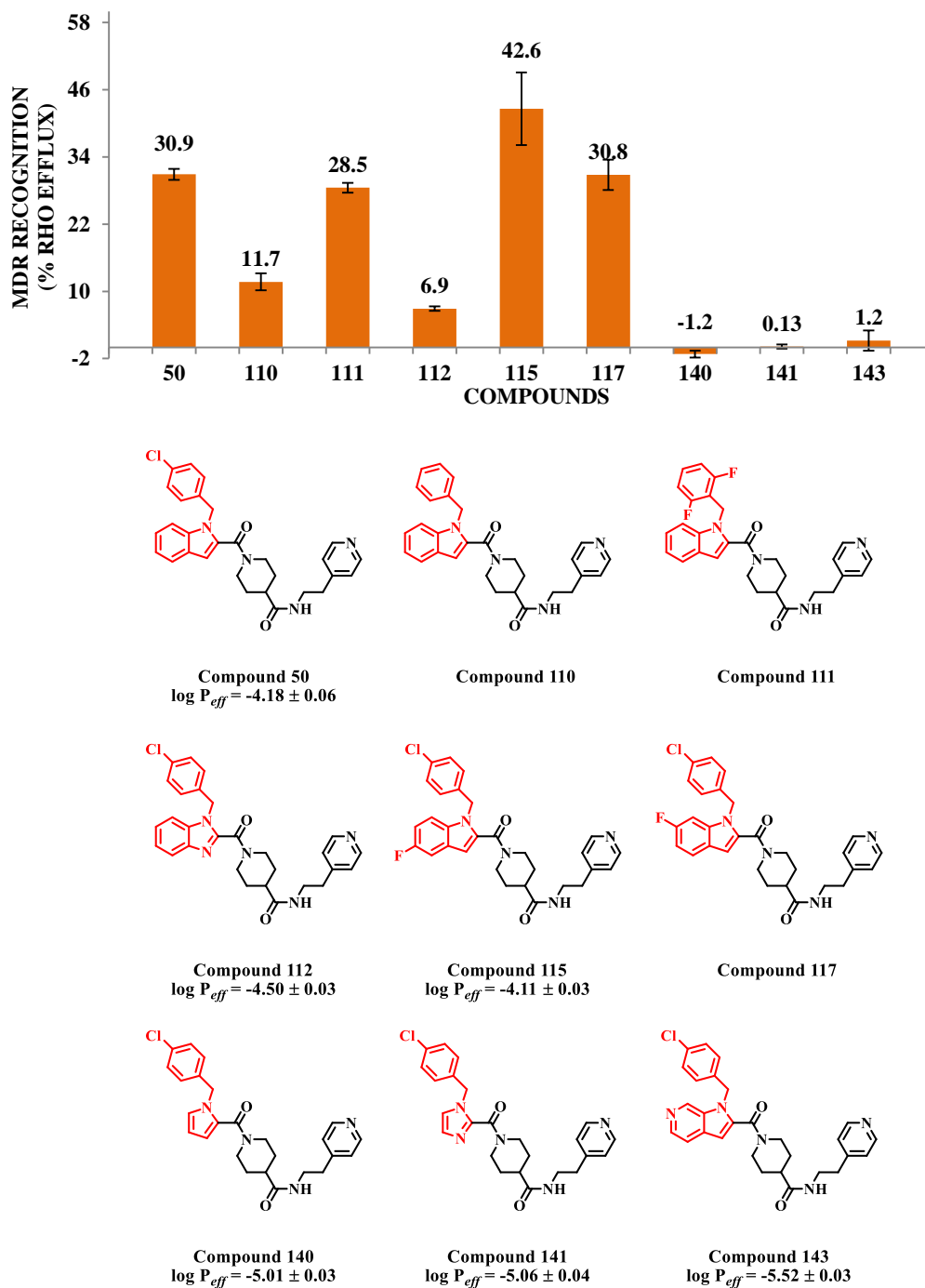


Figure 19: MDR recognition and PAMPA-BBB measurements

Rhodamine 123 (Rho 123) uptake was measured in MDR1-MDCKII cells utilizing Glomax Multi Detection System (Promega). ‘MDR1 recognition’ was assessed by measuring uptake in the presence of MDR1 inhibitor, tariquidar (5 μ M), and either 30 μ M of anti-viral or vehicle, and calculating: % Rho 123_{eff} = $(C_{av} - C_{veh}) * 100 / (C_{tar} - C_{veh})$, where C_{av} = concentration of Rho 123 in the presence of anti-viral, C_{veh} = concentration in the presence of vehicle, C_{tar} = concentration of Rho 123 in the presence of tariquidar. In the presence of tariquidar, Rho 123 uptake was $1123 \pm 54\%$ of vehicle controls (n=44). MDR recognition provided by Dr. Richard Keep and Jianming Xiang

WEEV *in vivo* infection study

Even though inhibitor **110** resulted in a slight decrease in potency compared to **50**, it had a significant increase in metabolic stability and lower Pgp recognition. Because of these two factors, inhibitor **110** was taken into a preliminary *in vivo* study. The study was performed similarly to the *in vivo* experiment for **50** (Chapter IV). Figure 20 showed that inhibitor **110** was capable of decreasing disease severity and increasing survival. Compared to **50** (page 58), **110** had survival rate of approximately 15% whereas **50** increased survival to approximately 25% compared to DMSO at day 14. In addition, at the end of the 14 days, the overall disease severity is lower when mice were treated with **110**.

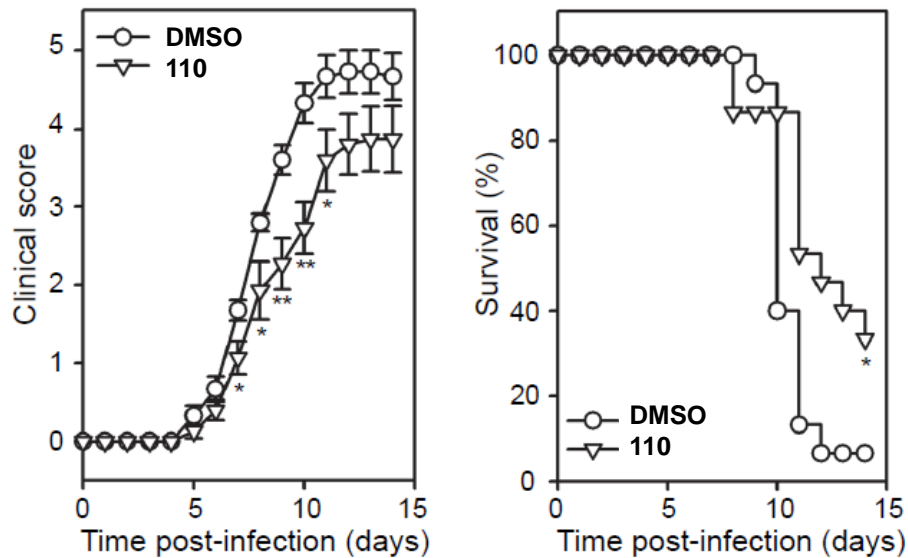
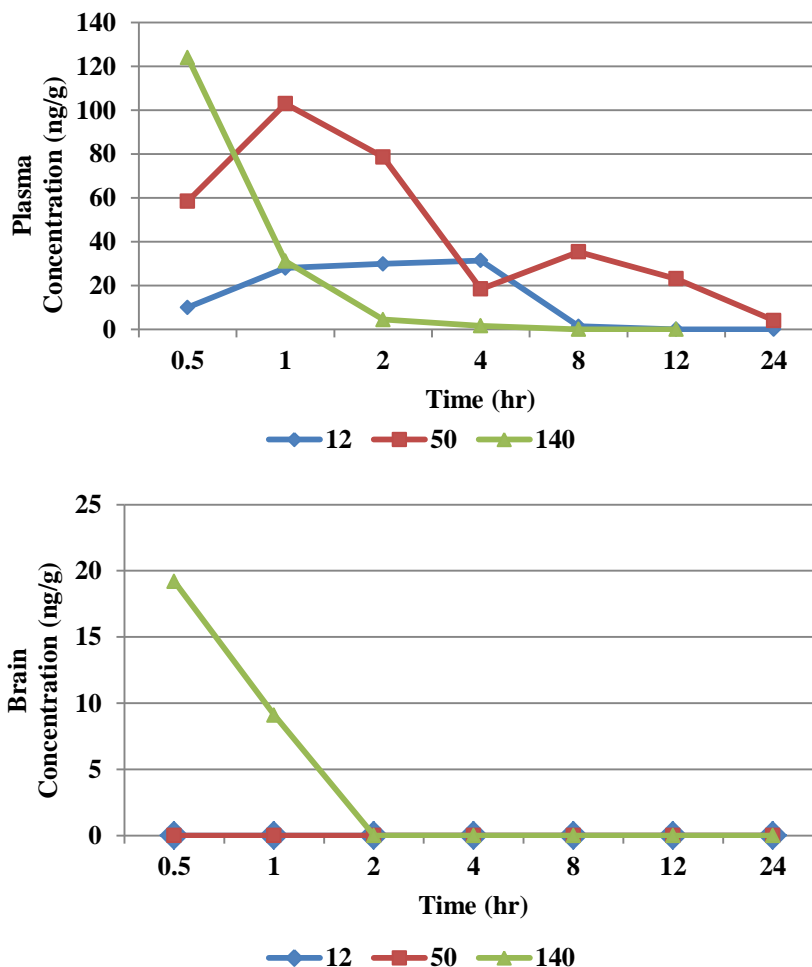


Figure 20: *In vivo* WEEV infection treatment with compound **110**

Mice were infected with 10^3 pfu/mL of WEEV and treated with **110** using 30 mg/kg/dose or vehicle. Animals were treated via IP injection every 12 hours beginning 12 hours after virus challenge. Composite of two independent experiments, where $n=5-10$ mice per group per experiment (A) Disease severity (B) Survival Graph courtesy of Dr. David Irani, Dr. David Miller, and Penelope Blakely. $P < 0.05^*$ and 0.005^{**} . Figure adapted from Ref. 125

Pharmacokinetic experiments



Compound	MLM $T_{1/2}$ (min)	%Rho efflux
12	2.1	24.4
50	11.5	30.9
140	2.9	-1.2

Figure 21: Plasma and brain concentration for **12**, **50**, and **140**

Six-week old C57BL/6 mice were injected via IP with a single dose of 30mg/kg of 12 and 50 and 10 mg/kg. Blood samples were taken at 7-intervals (30 min, 1h, 2h, 3h, 4h, 8h, 12 h). Brain tissues were harvested from the cerebrum. Plasma and brain levels were measured using LC/MS/MS. Each value shown is an average of two mice per dose. **In vivo* work done by Penelope Blakely; plasma and brain levels measured by Xiaoqin Li.

Compounds that were taken into *in vivo* studies (**12**, **50**, and **140**) were also evaluated in pharmacokinetic studies. Six-week old female C57BL/6 mice were injected via IP with a single dose 30 mg/kg of **12** and **50** and 20 mg/kg of **140**. Blood samples were taken at 7 time intervals and brain tissue from the cerebrum was harvested. The samples were analyzed for drug concentrations via LC/MS/MS by Xiaoqin Li. Figure 21 shows the different concentrations found in the plasma and brain tissue. As shown, only inhibitor **140** had detectable drug levels in the brain. This result validated the results of the Pgp recognition and metabolic stability experiments. The compound least recognized by Pgp (**140**) achieved measurable brain levels, while the compound with the greatest stability in mouse liver microsomes (**50**) had the highest level in the plasma. Both **140** and **50** had higher brain levels and plasma levels, respectively, than **12**.

Conclusions

In this chapter we reexamined the role of the indole in the presence of optimized 4-pyridylethyl amide. Importantly, we demonstrated a correlation between our Pgp-recognition and *in vitro* MLM experiments with pharmacokinetic properties. In addition, we were able to derive some information about metabolically labile sites in these replication inhibitors from the MLM SAR, namely that the indole ring is a likely major site of metabolism. Finally, this series of derivatives led to the identification of **110**, which has improved physicochemical properties compared to **50** and *in vivo* activity against WEEV.

CHAPTER VI. TARGET IDENTIFICATION

Rationale

Currently the target of our RNA replication inhibitors is unknown. Target identification is a very important aspect of drug discovery. The current cell-based assay used in our project is dependent on multiple variables such as cell growth, transfection of BHK cells with the WEEV genome, permeability of compounds, and other cellular interactions, including metabolism. Isolation of a target would allow the transition from a cell-based assay to a biochemical assay, which would allow a more direct SAR interpretation. It would provide an opportunity to define the binding region by structural biology. Knowing the specific protein of interest would allow the development of molecules that selectively manipulate desired biological processes.¹³² In addition, identifying other proteins that bind to the compound may aid in predicting off-targets.^{133,}

134

Biological target identification and Mode of Action

Dr. David Miller focused on elucidating the mode of action and biological targets for our indole-2-carboxamide inhibitors through various proteomics and genomic techniques. The breadth of antiviral activity of **50** and **140** against several families of viruses: *Togaviridae* (VEEV), *Bunyaviridae* (California encephalitis virus - CEV), *Picornaviridae* (EMCV), *Paramyxoviridae* (Sendai Virus - SeV) and *Flaviridae* (Dengue Virus - DENV) were examined. These experiments were performed in BE(2)-C cells

with a viral inoculation of MOI = 0.1. Viral titers for VEEV, CEV and EMCV were measured 24 hours post-infection. For DENV, RNA virus levels were measured 96 hours post infection. Both **50** and **140** were used at 25 μ M and 2.5 μ M. As shown by Figure 22, **50** and **140** were able to decrease viral titer against VEEV, CEV, EMCV and SeV. Compound **50** was able to decrease viral titer better than **140**. However, both compounds were unable to decrease RNA virus levels compared to RNA replication inhibitor, mycophenolic acid.¹²⁷ Compounds **50** and **140** were able to inhibit the replication of other RNA viruses, but not DENV. Even though both **50** and **140** were able to inhibit replication in other RNA viruses, their activity remains limited.

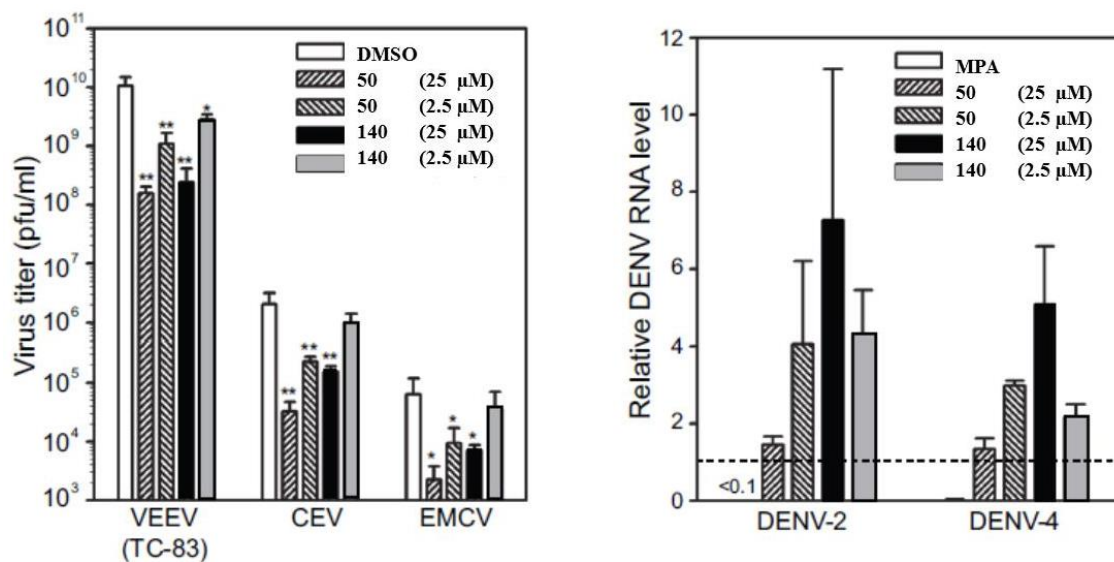


Figure 22: Broad spectrum activity against of compound **50** and **140**

^aVEEV (Venezuelan equine encephalitis virus), CEV (California encephalitis virus), EMCV (Encephalomyocarditis virus), DENV (Dengue Fever), MPA (mycophenolic acid) ^b experiments were performed in BE(2)-C cells with viral inoculation at an MOI = 0.1. Virus titer were measured 24 hours post infection. ^cDENV RNA levels were measured 96 hours post infection and compared to mycophenolic acid. ^dSeV (Sendai Virus) results not shown. $P < 0.05^*$ or $< 0.005^{**}$. Experiments performed by Dr. David Miller. Figure adapted from Ref. 127

In a time course study, BE(2)-C cells were infected with FMV at an MOI of 10. Untreated cells showed viral RNA accumulated after 6 hours post infection and a rapid increase around 10-12 hours. Cells were treated with 25 μ M of **50** 2 hours prior to FMV infection to 18 hours post infection. In the presence of **50**, viral titer increase was delayed 10-12 hours, at which point the effectiveness of **50** was diminished.

A WEEV pseudoinfectious particle (PIP), similar to those made for SINV and VEEV, was developed and it contained a fLuc gene seen in the replicon system.^{73, 127, 135} Since WEEV is naturally a recombinant virus whose glycoprotein is derived from Sindbis (SINV) virus, a well-developed antibody against SINV glycoprotein E2 can be used as a positive control for viral replication inhibition. When the PIPs were pre-incubated with the antibody before addition to HEK293 cells, it showed a suppression of fLuc expression. In contrast, **50** was unable to decrease fLuc activity when pre-incubated with PIPs before addition to cells. However, when cells were allowed to bind to PIPs before the addition of **50**, fLuc expression decreased.¹²⁷ Both the time course study and the PIPs experiment support the notion that **50** inhibits viral replication beyond viral binding and entry and its activity can be attributed to inhibition of viral RNA replication.

The use of cell-based assay allows inhibitors to target both host and viral proteins. Alphaviruses generate their replication complexes on intracellular membranes.^{7, 49, 51} The complex can be isolated through differential centrifugation.¹³⁶ Therefore, RNA replication activity of the virus can be measured in a cell free system. It was determined that **50** did not suppress RNA-dependent RNA-polymerase activity *in vitro*. The rapid rate of mutation of RdRp lends itself to the generation of drug-resistant mutants. However, compound **50** was not able to generate resistant virus, indicating that it did not

target RdRp or any viral enzymatic proteins.¹²⁷ WEEV replicons were treated in combination with **50**, **140**, MPA (purine biosynthesis inhibitor) or actimycin A (mitochondrial electron transport chain and pyrimidine biosynthesis inhibitor). Treatment with **50** and **140** showed additive effects in reducing replication; however, treatment with **50** and MPA or **50** and actimycin A did not show significant synergism. Also, addition of excess purine or pyrimidine did not rescue replicon activity. These results indicated that **50** and **140** acts on similar pathways that are not involved in purine or pyrimidine synthesis.¹²⁷

A study using Ingenuity Pathway Analysis software identified 22 pathways that may be modulated by **50** or **140**. Of those identified, the eIF2 pathway was shown to be most affected by **50** and **140**. The eIF2 pathway is involved in gene expression, translational control, cellular stress response including to viral infections.^{127, 137}

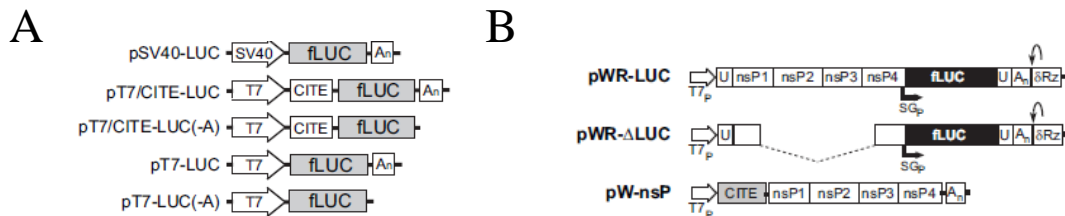


Figure 23: fLuc-encoding reporter plasmids
 (A) Plasmid description shown in left. Promoters are designated by broad arrows; CITE (cap-independent translation element); A_n (polyadenylation tail) (B) U (untranslated region), δRz (hepatitis δ virus), SG_p (subgenomic promoter), A_n (polyadenylated tail) Images adapted from Ref. 127

In order to elucidate whether **50** and **140** were able to inhibit cellular functions, the Miller lab utilized the four plasmids shown in **Figure 23A** to determine fLuc suppression. The pSV40-fLuc represents the nuclear transcription of capped and polyadenylated mRNAs and was used with a plasmid containing the pSV40 promoter.

Transcription in the cytoplasm was determined using a bacteriophage T7 RNA polymerase promoter. T7 RNA polymerase promoters express RNAs that are mainly uncapped and without a polyadenylated tail; therefore, a CITE (cap-independent translation element) sequence was included in order to improve translation turn over. Compounds **50** and **140** were able to inhibit translation using the pSV40-fLuc plasmid, but not those with T7 RNA polymerase promoter and CITE. These results indicated that **50** and **140** may be inhibiting a mechanism involving cap-dependent translation.

Expanding on the transfection study above, two plasmids were generated (**Figure 23B**). These plasmids utilized the original pWR-Luc plasmid used in the replicon system; however, one plasmid (pWR- Δ Luc) had the nonstructural proteins removed and the other (pW-nsP) only contained the nonstructural proteins in the presence of T7 promoter and CITE sequence. It was shown that if cells were transfected with either pWR- Δ Luc or pW-nsP they showed minimal fLuc expression; however, transfection with both plasmids increased fLuc expression. In the presence of **50** and **140**, fLuc expression was not significantly suppressed indicating that these inhibitors do not target a viral protein; instead, they affect host machinery.

The results of the various biological experiments highlight various aspects of the mode of action and target of these indole-2-carboxamide inhibitors. First, they are able to inhibit replication of various, but not all, RNA viruses. Second, they affect replication after viral entry into the host cell. Finally, they do not target viral enzymatic activity; instead they modulate a cap-dependent host factor in order to elicit antiviral activity.

Tag-free photoaffinity probes

One method to explore target identification is the use of photoaffinity probes. In contrast to traditional biotinylated probes or affinity matrices, tag-free photoaffinity probes allow the testing of potential probes for similar activity in the same cell-based assay as the parent compound, identification of targets low in quantity and/or affinity, and purification of the protein and ligand complex after cell lysis.¹³⁸ A photoprobe for our project needs to be used in a live cell assay, and the compound must interact with the target in a similar fashion as the parent compound. As the SAR becomes more defined, the proper location for the photolabile group can be identified where it does not compromise biological activity. The probes first bind their target, and subsequent UV irradiation generates a new covalent bond between the probe and the target. The cells are lysed and the complex may then be tagged with biotin using click chemistry and purified without dissociation using a streptavidin column. The process we proposed to use for target identification using tag-free photoprobes is shown in Figure 24 using the synthesized photoprobe **126**.

Photoprobes utilize reactive functional groups such as azides, diazirines, and benzophenones.¹³² Each of the functionalities has its own favorable characteristics as a probe. Phenyl azides have been used the most in photoaffinity labeling. Its popularity is mainly from its small size and ease of introduction.^{133, 139} Its reactivity is dependent on the amino acid reacting with the azide. Cysteine reacts the fastest while glycine is unreactive.¹⁴⁰ However, azides do not give stoichiometric labeling.¹⁴¹ The low photolabeling yields may be caused by several factors. First, the singlet nitrene intermediate upon irradiation interconverts to ketenimine azepine. However, this

intermediate has high stability and is not ideal for rapid protein capturing (Figure 25).¹⁴² Second, photoproducts may be unstable to degradation techniques. Third, the wavelength necessary to excite azides (254 nm) may damage biological systems.¹³⁹ Finally, the azide functionality itself may be unstable, especially to light.^{143, 144}

Mechanistically, unsubstituted, benzyl azides covalently bind to proteins in two ways: the ketenimine azepine intermediate is nucleophilically attacked by amino and hydroxyl functionalities in proteins and a triplet nitrene reacts with •NH-, •O-, and •C- of proteins. Both singlet and triplet nitrene intermediates of 4- tetrafluorophenyl azides may insert into CH, NH₂, and OH bonds of proteins (Figure 25A).^{139, 145, 146}

Upon excitement with ~350 nm wavelength, benzophenones generate a triplet diradical species.¹⁴⁷ The stable radical intermediate abstracts α -hydrogens from amino acids (Figure 25C).¹⁴⁷ Benzophenones abstract α -hydrogens at different rates: α to nitrogen > α to sulfur > allylic > methylene > methyl. The lack of an abstractable proton results in the regeneration of the photoprobe.^{132, 139, 148} This reversible photoactivation allows for higher yielding and more specific labeling.

Diazirines are small, non-bulky functionalities. It has been shown that the position of the diazirine functionality in alkyl chains can have great effects on its photoreactivity.¹⁴⁹ Diazirines have been shown to provide the NH-, CH, OH inserted products (Figure 25B).¹³⁹

An azide or acetylene group can be used as a clickable linker between the photoprobe and the biotin or fluorophore tag. We chose to use a terminal acetylene group due to its higher lipophilicity relative to an azide group, allowing it to better penetrate the cellular membrane. The terminal acetylene provides a synthetic handle for the Click

chemistry to occur in order to tag the target compound with biotin *after* photocrosslinking and cell lysis.¹³⁸ Varying the position of the acetylene and the photolizable group will maximize the chances of successfully labeling and isolating/visualizing the target.¹⁵⁰

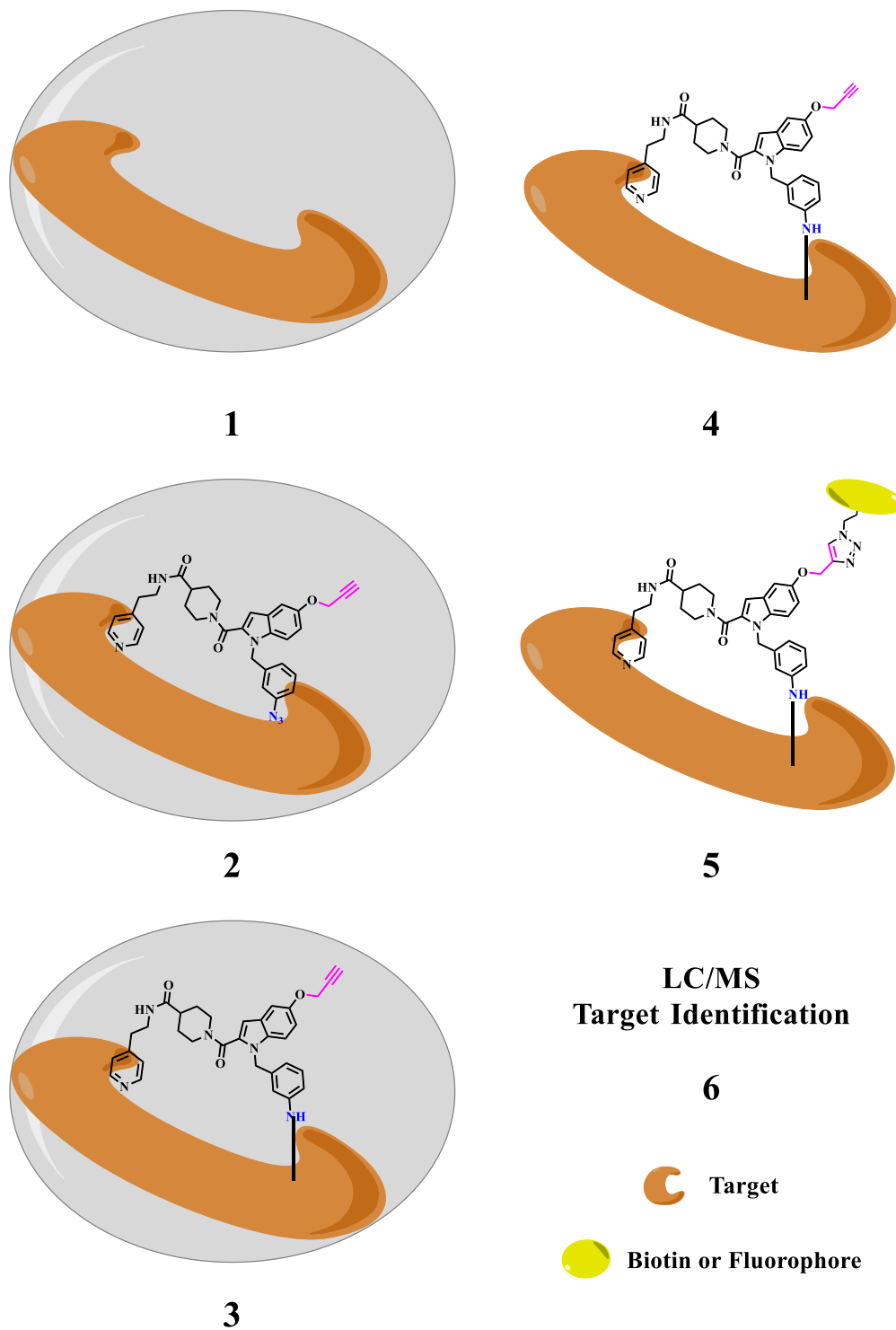


Figure 24: Representative tag free photoaffinity probe sequence with 126
 (1) Live cell (2) photoprobe incubated with cell (3) Covalent bonding due to UV irradiation (4) Lyse cell (5) Click chemistry to tag compound with biotin or fluorophore (6) Purification and identification of target through LC/MS

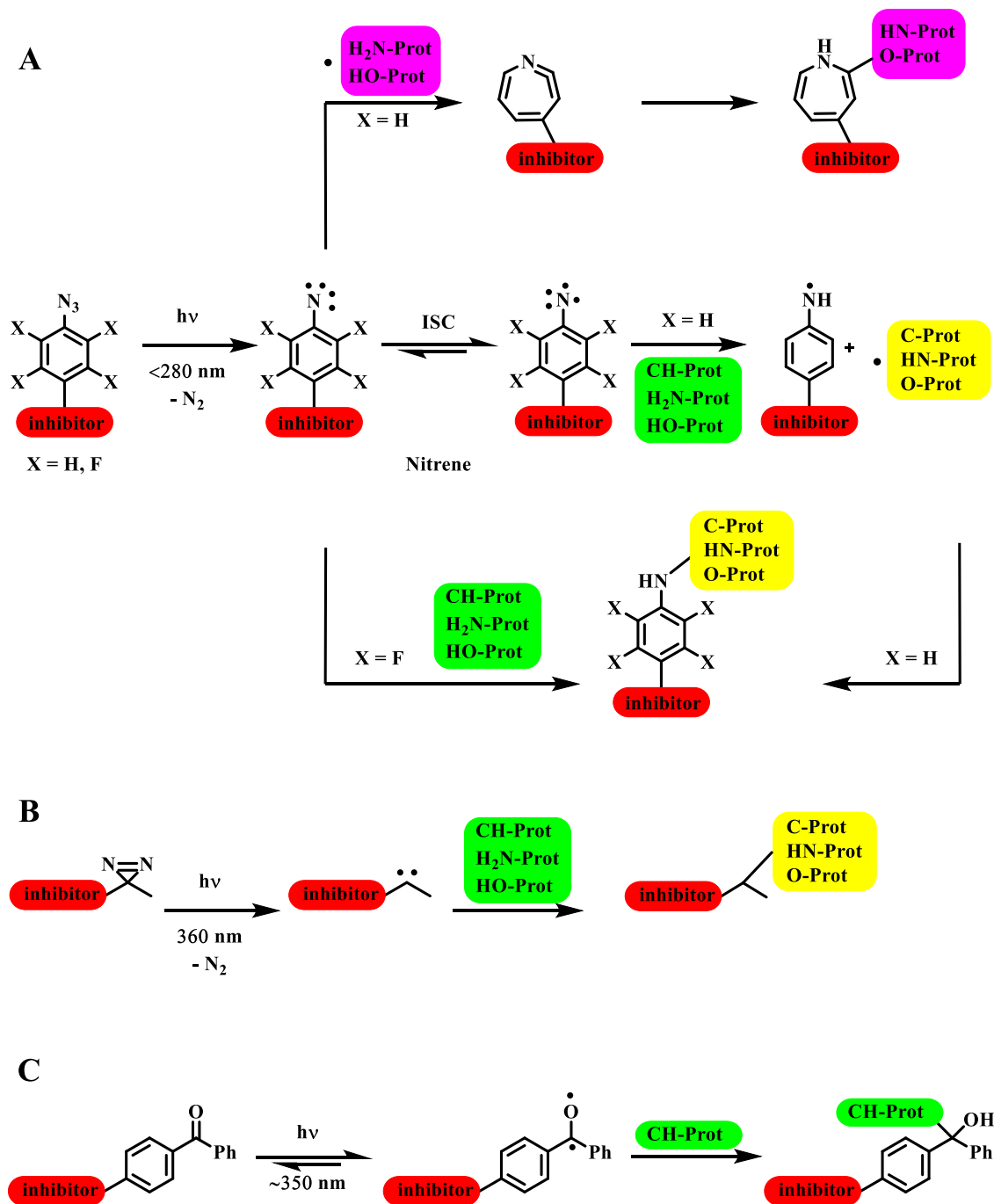
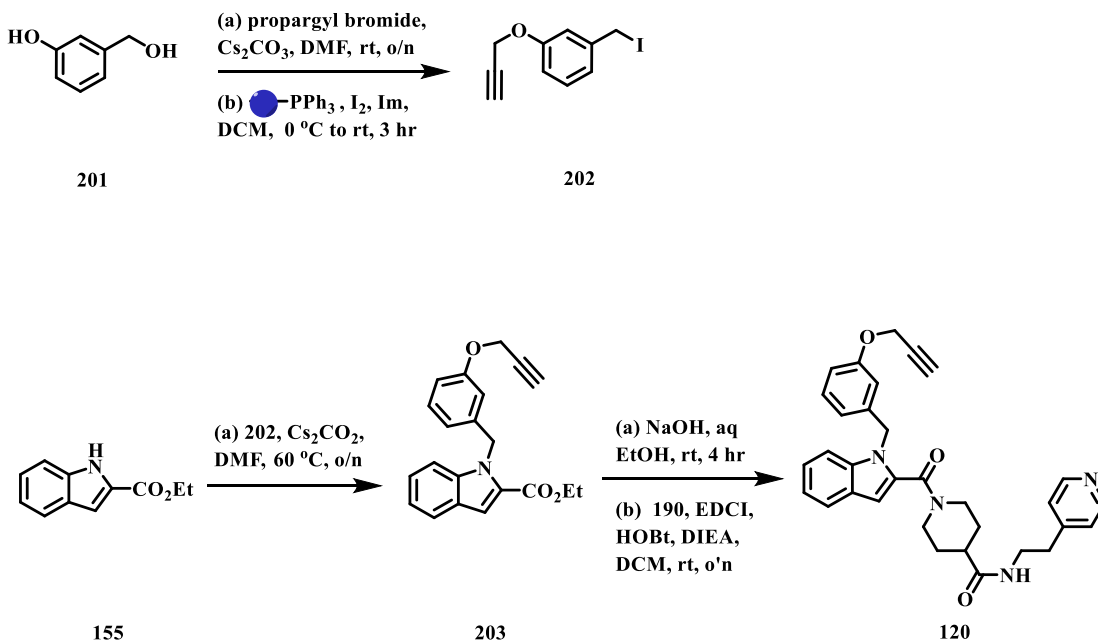


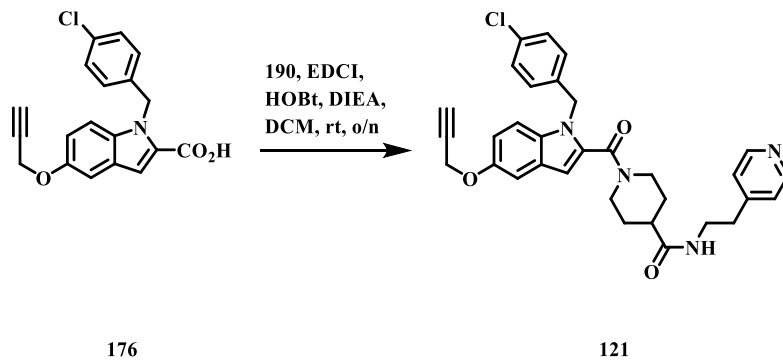
Figure 25: (A) azide (B) diazirine (C) benzophenone photoprobes protein labeling mechanism. Figure adapted from Ref.

Synthesis

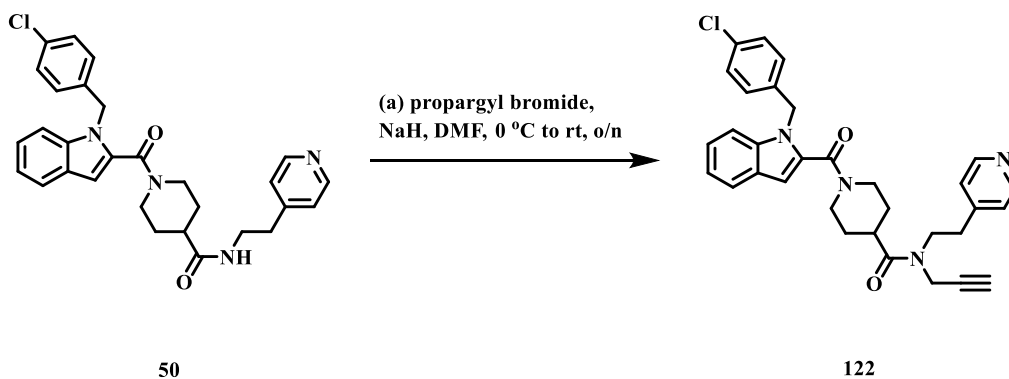


Scheme 12: Synthesis of analog **120**

Several analogs exploring the optimum position of the propargyl group were synthesized. Scheme 12 shows the synthesis of analog **120**. 3-hydroxybenzyl alcohol (**201**) was selectively alkylated using propargyl bromide and cesium carbonate. Iodination in the presence of solid supported triphenylphosphine and iodine resulted in **202**.¹⁵¹ Solid supported triphenylphosphine was used for ease of purification. Ethyl-2-indole carboxylate was alkylated with **202** to generate **203**. Subsequent saponification with sodium hydroxide and amide coupling with **190** resulted in analog **120**. Another analog **121** was synthesized through a peptide coupling using **176** and **190** (Scheme 13). Finally, alkylation of **50** with propargyl bromide generated analog **122** (Scheme 14).



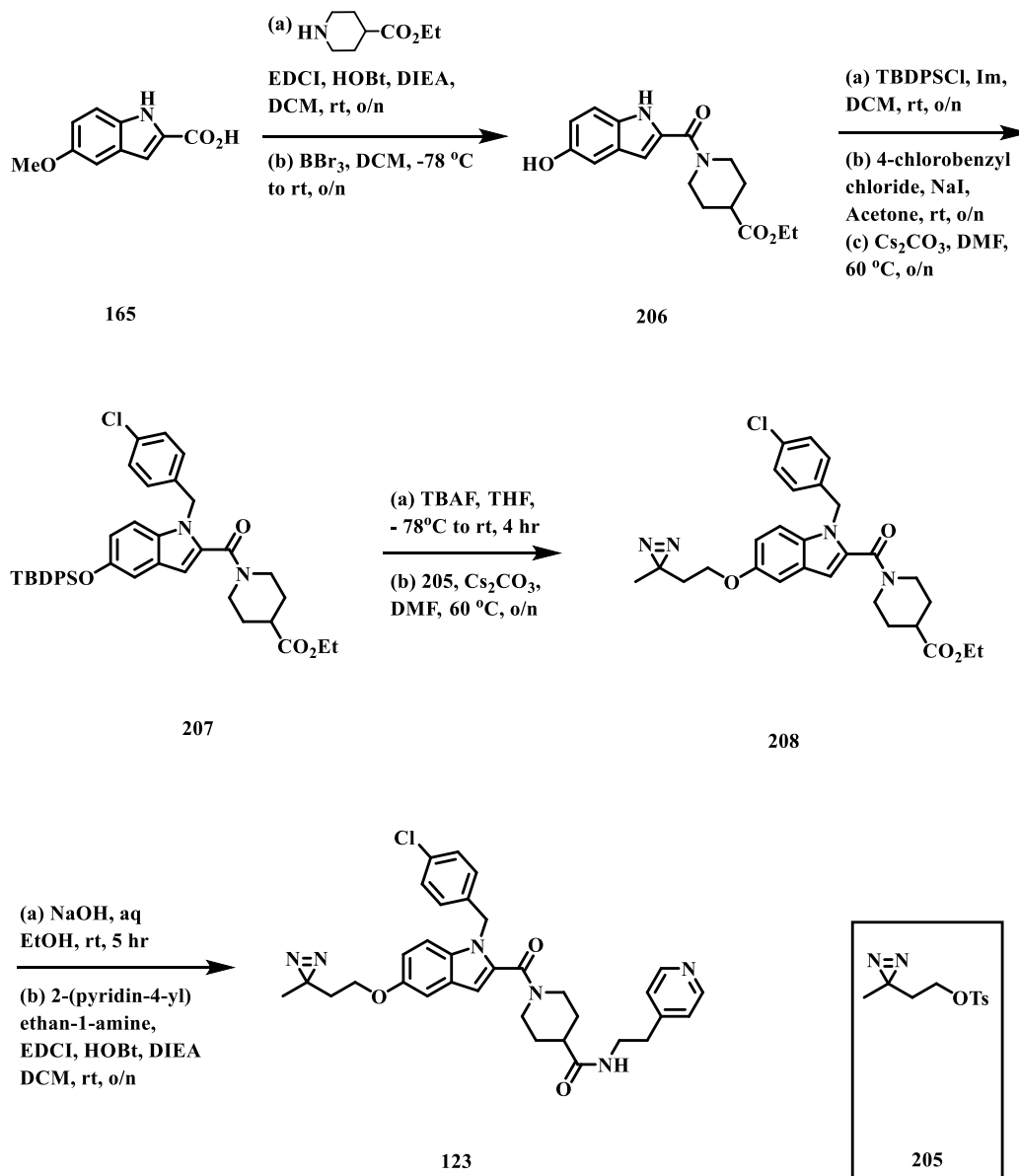
Scheme 13: Synthesis of analog **121**



Scheme 14: Synthesis of analog **122**

Two analogs were synthesized in order to examine the proper position of the photolabile group. The photolabile functionalities chosen were diazirine and azide. Scheme 15 describes the synthesis of analog **123**. Indole **165** was coupled to ethyl isonipicote. The resulting ester was demethylated using boron tribromide to generate **206**. Intermediate **206** was TBDPS-protected. Alkylation then proceeded in two steps. A Finkelstein reaction between 4-chlorobenzyl chloride and sodium iodide resulted in 4-chlorobenzyl iodide. The resulting alkyl iodide was used to alkylate the TBDPS protected **206**. This sequence of reactions resulted in intermediate **207**. Deprotection using TBAF and subsequent alkylation with diazirine **205**, synthesized as described by

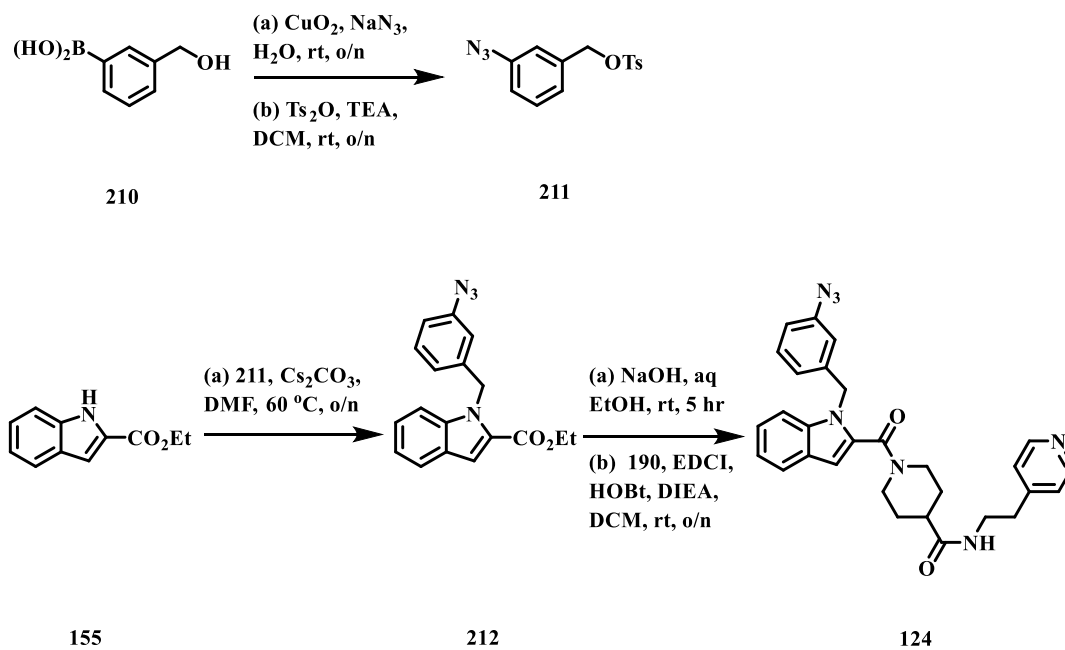
Dr. Bryan Yestrepky, resulted in **208**.¹⁵² Ester hydrolysis followed by amide coupling with 2-(pyridine-4-yl)ethan-1-amine resulted in analog **123**.



Scheme 15: Synthesis of analog **123**

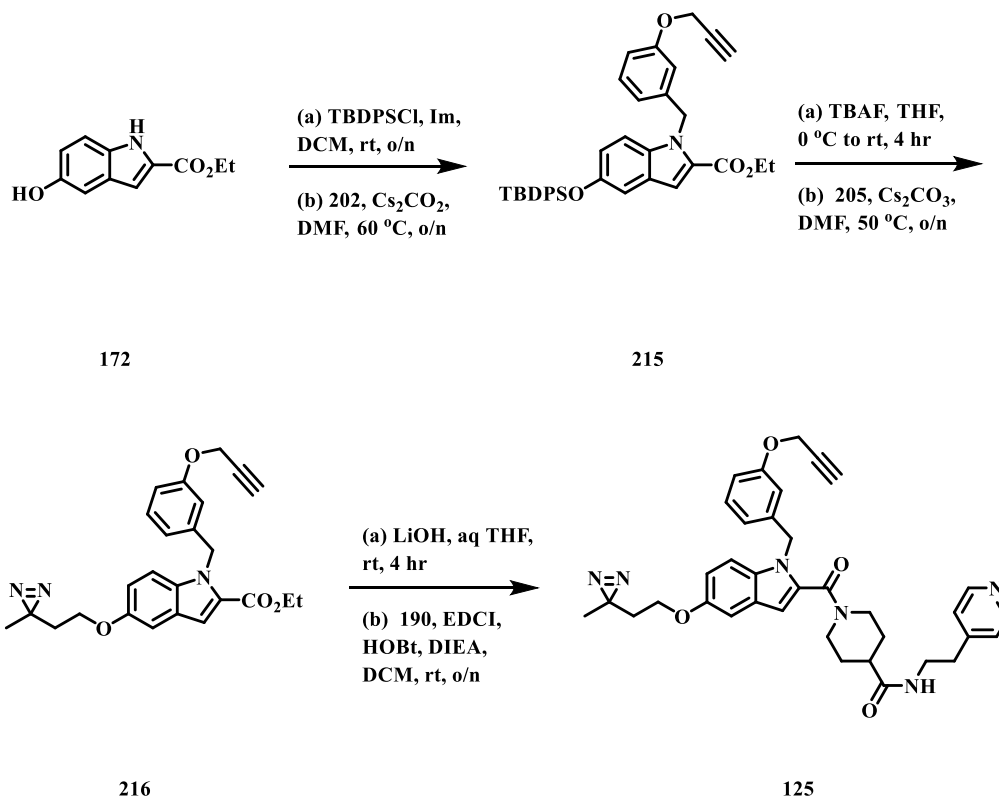
Analog **124** synthesis began with the transformation of the boronic acid **210** to aryl azide **211** through a copper mediated azidation.¹⁵³ Indole **155** was alkylated with

aryl azide **211** to give ester **212**. Hydrolysis of **212** followed by peptide coupling with synthon **190** resulted in **124** (Scheme 16).



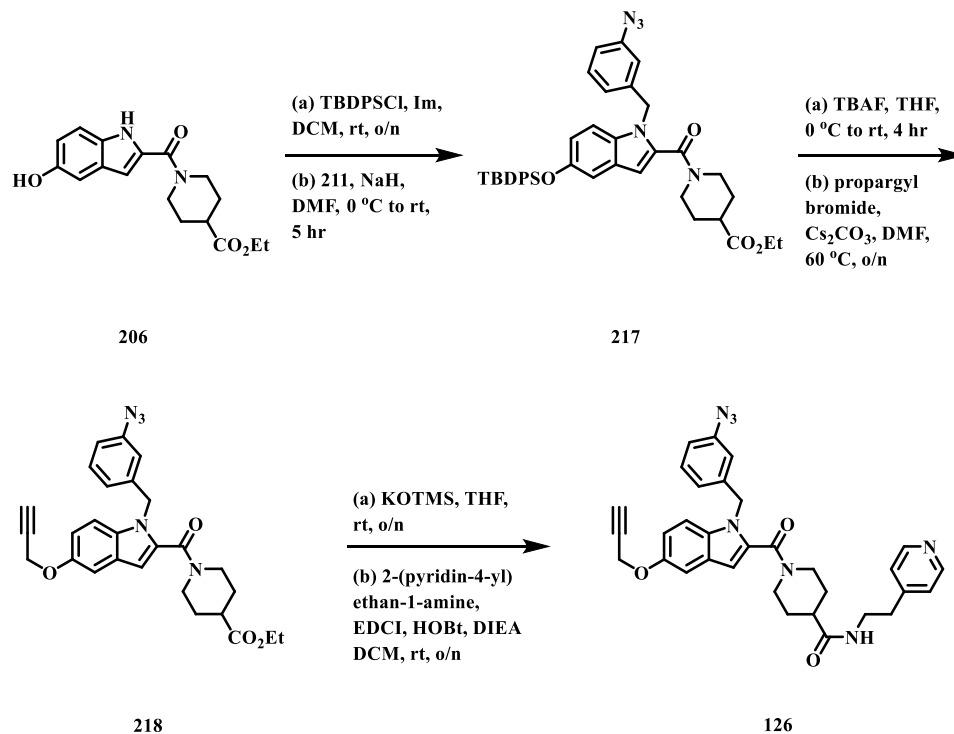
Scheme 16: Synthesis of analog **124**

Indole **172** was silyl protected using tert-butyldiphenylsilyl chloride. The resulting protected indole was alkylated with **202** in the presence of cesium carbonate. TBAF deprotection and alkylation with diazirine **205** resulted in **216**. Hydrolysis followed by coupling with **190** resulted in photoprobe **125** (Scheme 17).



Scheme 17: Synthesis of photoprobe 125

Compound **206** was silyl protected using TBDPSCl. The silyl protected **206** was alkylated with **211**. TBAF deprotection followed by alkylation using propargyl bromide resulted in intermediate **218**. Hydrolysis followed by coupling with 2-(pyridine-4-yl)ethan-1-amine resulted in photoprobe **126** (Scheme 18).



Scheme 18: Synthesis of photoprobe **126**

SAR development

Early in the SAR development, two benzophenone derivatives (**127** and **128**) were synthesized (Table 9). Both of these compounds were inactive indicating that benzophenones in the carboxamide position were not well tolerated. However, further SAR development led to compound **50**. It demonstrated that the presence of a 4-pyridylethyl carboxamide motif was necessary for high potency. Therefore, further photoprobe development contained such a motif.

First, it was necessary to explore both the position of the photolabile and the acetylene functionality. Analogs **120-122** demonstrated that placement of the propargyl group on the N1-indole or 5-hydroxy indole position was tolerated by the target;

however, N-propargylation of the carboxamide position was detrimental to activity. These results indicated that the propargyl group could be placed in the final photoprobes either on the N-benzyl group or the 5-hydroxy group with expectation that activity would be retained. Considering the lack of information regarding the binding site of the target, it is possible that these inhibitors are binding in different modes. Compound **121** (Table 9) may be interacting through the 4-pyridylethyl amide in a hydrogen bonding network while the inactive dimethyl amide **102** ($IC_{50} > 50 \mu M$,

Table 4) binds the target through the 5-hydroxy indole position and the propargyl group is not sufficient in making optimal contacts with the target.

Secondly, the proper placement of the photolabile group is necessary for photolabeling success. In the indole substitution SAR studies (Table 8), it was discovered that compound **113** ($IC_{50} = .47 \mu\text{M}$) and **116** ($IC_{50} = 1.7 \mu\text{M}$) maintained activity compared to **50** ($IC_{50} = 0.5 \mu\text{M}$). Compound **113** suggested that a small aliphatic substitution in the 5-hydroxy indole position is tolerated. The presence of a highly polar nitro group on the N1-benzyl group suggested a small, polar substitution such as an azide might be tolerated.

Direct comparisons of **50** containing photolabile groups at different positions (**123** and **124**) were synthesized. Both compounds maintained potency compared to **50**; however, **123** gained substantial toxicity. Regardless of the cytotoxicity, the azide and the diazirine at the N1-indole and 5-hydroxy indole positions, respectively, maintained activity. Based on the preliminary SAR, the two photoprobes we elected to synthesize were **125** and **126**. Of these two, **126** was equipotent to **50** while **125** was about 10-fold less potent. Compound **126** was therefore selected for initial target identification studies.

Current status of target identification

This pilot experiment was performed by Dr. David Miller. The experiment used BHK cells with or without replicon. Probe **126** was examined at 2.5 μM and 25 μM . The initial experiment was performed with compound **50** at 25 μM as the competitor. A larger excess of **50** is needed to effectively compete with the photoprobes to differentiate specific from non-specific labeling. As the probes bind to various proteins and are

irradiated, they will bind to many different protein targets. However, the large excess of **50** will identify specific binding by competing off the probe; therefore, when irradiated, bands that are specifically labeled should decrease in intensity.

An azide-biotin hapten was used for labeling. An experimental difficulty that arose from using biotin as a tagging mechanism is that biotinylated cellular proteins are also going to be detected. Figure 26 shows bands labeled with probe **126** at 25 μM in cells with or without replicon. Possible targets are indicated with question marks. The bands that are visible in the absence of probe identify cellular biotinylated compounds. In this preliminary experiment, it is clear that there was a very low overall level of labeling, suggesting that the conditions for photolabeling need to be carefully optimized in the future (e.g. irradiation time, wavelength, concentration of competitor, concentration of inhibitor, etc.). Furthermore, the issue of biotinylated protein labeling could be avoided by using a fluorophore to simply visualize the labeled proteins or by using a streptavidin pull-down experiment before attaching the azide-biotin hapten label. Once we have successfully visualized bands that are decreased in intensity in the presence of competitor, we will repeat the experiment with Click biotinylation and protein isolation on a streptavidin column. After bands are isolated, the target will be characterized by proteomics.

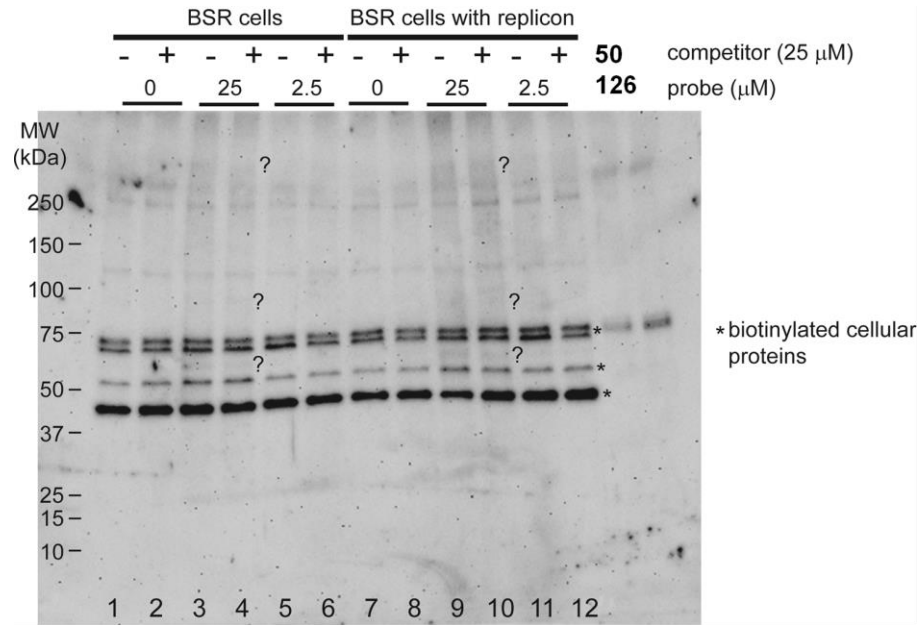
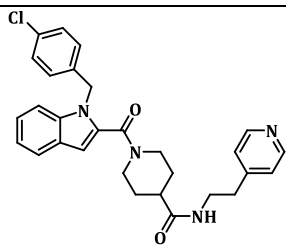
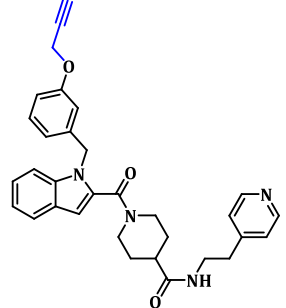
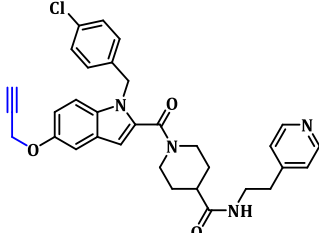
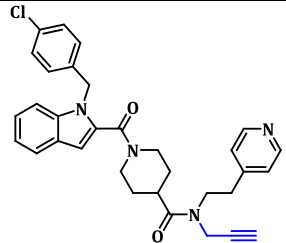
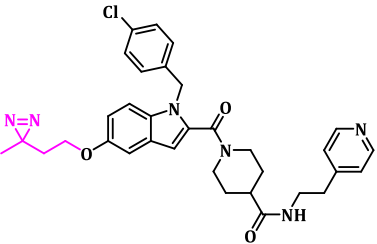


Figure 26: Pilot target identification experiment with photoprobe **126**
 *Figure provided by Dr. David Miller.

Conclusions

Dr. David Miller and his laboratory have determined that **50** and **140** inhibits virus replication by inhibiting a cap-dependent process targeting a host factor instead of a viral enzymatic protein. These inhibitors are active against other RNA viruses, but not all. Finally, preliminary target identification using tag-free photoaffinity probes have shown possible targets for **50** and related inhibitors.

Table 9: Photoaffinity probes

		Structure	IC₅₀ (μM)^a	CC₅₀ (μM)^b
50	205432		0.5 ± 0.2	49.9
120	212370		1.9 ± 0.5	45.5
121	212057		3.1 ± 5.6	6.4
122	212050		10.9 N=2	59.4
123	222802		0.55 ± 0.2	29.0

		Structure	IC ₅₀ (μM) ^a	CC ₅₀ (μM) ^b
124	222881		0.43 ± 0.1	45.1
125	222700		5.20 ± .69	89.9
126	223882		0.52 ± 0.12	>100
127	208785		>50	>50
128*	208920		57.0	>50

^aInhibition of luciferase expression in WEEV replicon assay. Ribavirin as positive control has an IC₅₀ in the assay of 16 μM. Values are mean of at least n=3 independent experiments ± SE. ^bCell viability determined by inhibition of mitochondrial reduction of MTT. Values are mean of at least 3 independent experiments. Data provided by Dr. David Miller and Craig Dobry. *n=2

CHAPTER VII. FUTURE DIRECTION

Photoprobes

Presently, the molecular target of our compounds remains unknown. Even though two photoprobes have been synthesized that have similar potencies as the lead inhibitor **50**, preliminary results indicate low labeling efficiency. Additional photolabile groups are available that may lead to more efficient target capture. We would propose to prepare the two photoprobes in Figure 27. The trifluoroethyldiazirinephenyl group has been shown to give higher yields for labeling proteins than its aliphatic ethyl diazirine counterpart.¹⁵⁴ It efficiently inserts into both C-H and O-H bonds.¹⁵⁵ This functionality is also stable in the presence of both mild acidic and basic environments.¹⁵⁶ Tetrafluorophenylazide photoprobes also show greater yields of labeling than simple benzyl azide analogs.^{139, 157} Both of these inhibitors generate intermediates that have greater lifetimes; therefore, increasing their chances in capturing proteins.

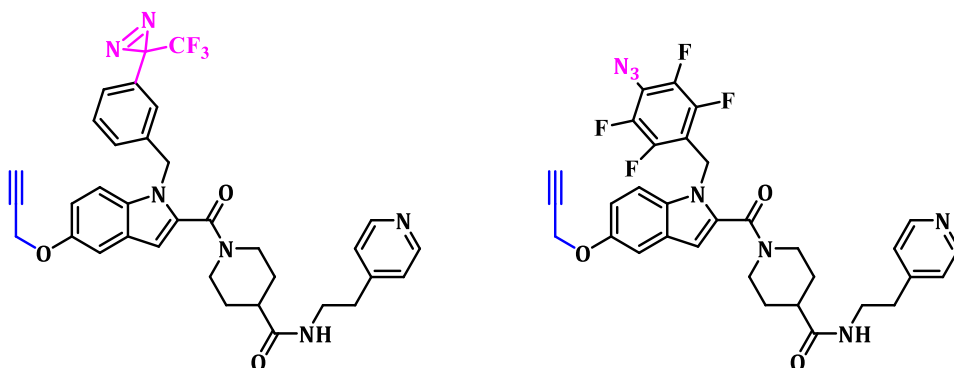


Figure 27: Fluorinated photoprobes

***In vivo* Survival Studies with Neuroprotective Agents.**

Presently, Dr. David Irani and Penelope Blakely are examining the effects on survival and disease severity when mice are treated with compound **110** in combination with telmisartan, a neuroprotective agent. Telmisartan is an antagonist of the renin-angiotensin pathway, leading to angiotensin II inhibition. Even though the angiotensin II dysregulation has been attributed to hypertension, it has also been shown to contribute to cerebrovascular inflammation through oxidative stress.¹⁵⁸ This results in the decrease of the BBB integrity and increasing xenobiotic permeability into the CNS. Angiotensin II is upregulated in neurons during viral infections. It has been previously shown that angiotensin II blockade results in faster recovery from the West Nile Virus (WNV).¹⁵⁹ Therefore, regulating the angiotensin II expression in neurons is essential in developing neuroprotective agents.

Chikungunya Virus

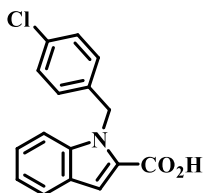
The Chikungunya Virus (CHIKV) is an alphavirus related to WEEV. The virus is endemic in India, Southeast Asia, and most sub-Saharan Africa.⁷ However, the virus has emerged in the Caribbean and the United States. Several factors may have contributed to the spread of the disease: urbanization, minimal mosquito control, and changing global demographics.¹⁶⁰ CHIKV causes severe arthritis and maculopapular rash. Joint pains may last for several months after the original infection.⁷ Since compound **50** and **140** have been shown to inhibit replication in other RNA viruses, it is possible that these inhibitors may also be active against CHIKV.

CHAPTER VIII. EXPERIMENTALS

All reagents were used as received from commercial sources unless otherwise noted. ^1H and ^{13}C spectra were obtained in $\text{DMSO-}d_6$ or CDCl_3 at room temperature, unless otherwise noted, on a Varian Inova 400 MHz, Varian Inova 500 MHz or Bruker Avance DRX 500 instruments. Chemical shifts for the ^1H NMR and ^{13}C NMR spectra were recorded in parts per million (ppm) on the δ scale from an internal standard of residual tetramethylsilane (0 ppm). Rotomers are described as a ratio of rotomer A and B if possible. Otherwise, NMR peaks are described as multiplets. Mass spectroscopy data were obtained on a Waters Corporation LCT. HPLC retention times were recorded in minutes (min) using an Agilent 1100 Series with an Agilent Zorbax Eclipse Plus – C18 column with the gradient 10% ACN/water (1 min), 10-90% ACN/water (6 min), 90% ACN/water (2 min), and 90-10% ACN/water (2 min) (Gradient A). Solvent abbreviations used: MeOH (methanol), DCM (dichloromethane), EtOAc (ethyl acetate), Hex (hexanes), DMSO (dimethylsulfoxide), DMF (dimethylformamide), H_2O (water), THF (tetrahydrofuran), ACN (acetonitrile). Reagent abbreviations used: HOBt (1-hydroxy-1,2,3-benzotriazole), EDCI (N-(3-dimethylaminopropyl)-N'-ethylcarbodiimide hydrochloride), DIEA (diisopropylethylamine), PPh_3 (triphenylphosphine), MgSO_4 (magnesium sulfate), Na_2SO_4 (sodium sulfate), NaHCO_3 (sodium bicarbonate), Na_2CO_3 (sodium carbonate), NH_4Cl (ammonium chloride), K_2HCO_3 (potassium bicarbonate), K_2CO_3 (potassium carbonate), KOH (potassium hydroxide), HCl (hydrogen chloride).

Assay abbreviations: LUC(luciferase), MTT ((3-(4,5-Dimethylthiazol-2-yl)-2,5-diphenyltetrazolium bromide).

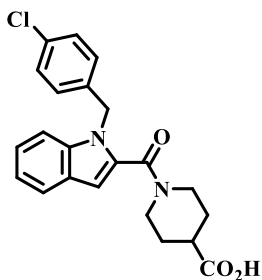
Carboxamide Derivatives



1-(4-Chlorobenzyl)-1H-indole-2-carboxylic acid (156): Ethyl 1-(4-chlorobenzyl)-1H-indole-2-carboxylate: Ethyl 1H-indole-2-carboxylate **155** (1.50 g, 7.93 mmol) and potassium carbonate (1.42 g, 10.3 mmol) were dissolved in 10 mL of DMF. A 5.0 mL DMF solution of 1-chloro-4-(chloromethyl)benzene (1.66 g, 10.3 mmol) was added. The reaction was placed under nitrogen and heated at 60 °C for 24 hours. The reaction was cooled to room temperature and diluted with water (50 mL) and extracted with ethyl acetate (80 mL). The organic layers were combined, washed with saturated sodium chloride solution (100 mL x 3), dried over magnesium sulfate, and concentrated in vacuo to afford a tan solid. Trituration with methanol afforded product as a white solid (1.8 g, 72%). TLC R_f (50% EA/Hex): 0.5. ¹H NMR (400 MHz, DMSO-*d*₆) δ = 7.74 (d, *J* = 8.0 Hz, 1H), 7.59 (d, *J* = 8.5 Hz, 1H), 7.41-7.30 (m, 4H), 7.16 (t, *J* = 7.5 Hz, 1H), 7.04 (d, *J* = 8.3 Hz, 2H), 5.85 (s, 2H), 4.29 (q, *J* = 7.1 Hz, 2H), 1.29 (t, *J* = 7.1 Hz, 3H). TOF ES+ MS: 314.0 (M+H), 336.0 (M+Na). HPLC (gradient A): ret. time = 7.88 min; purity = >95%.

Ethyl 1-(4-chlorobenzyl)-1H-indole-2-carboxylate and lithium hydroxide (1.53 g, 63.9 mmol) were dissolved in 10 mL of THF and 20 mL of water. The reaction was

heated at 60 °C overnight. The reaction was cooled and diluted with water and washed with diethyl ether. The aqueous solution was acidified using 2N HCl acid to pH 2. The resulting suspension was extracted with ethyl acetate. The organic layer was dried over magnesium sulfate, filtered, and concentrated in vacuo to obtain pure product as a white solid (1.47 g, 81%). TLC R_f (50% EA.Hex): 0.2. ¹H NMR (400 MHz, DMSO-*d*₆) δ = 13.02 (s, 1H), 7.72 (d, *J* = 8.0 Hz, 1H), 7.54 (d, *J* = 8.5 Hz, 1H), 7.37-7.26 (m, 4H), 7.14 (t, *J* = 7.5 Hz, 1H), 7.05 (d, *J* = 5.6 Hz, 2H), 5.87 (s, 2H). TOF ES+ MS: 286.0 (M+H). HPLC (gradient A): ret. time = 7.88 min; purity = >95%.



1-(1-(4-Chlorobenzyl)-1*H*-indole-2-carbonyl)piperidine-4-carboxylic acid (157):

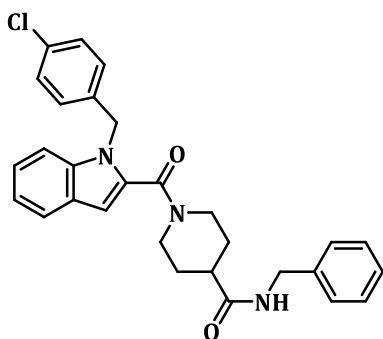
Ethyl 1-(1-(4-chlorobenzyl)-1*H*-indole-2-carbonyl)piperidine-4-carboxylate: Compound 156 (1.00 g, 3.50 mmol), EDCI (1.34 g, 6.99 mmol), and 1-hydroxybenzotriazole (0.946 g, 7.00 mmol) were added to an oven dried RBF. The solids were dissolved in 4.0 mL of DCM and allowed to stir at room temperature for 15 minutes. Ethyl piperidine-4-carboxylate (1.08 ml, 7.01 mmol) and DIEA (1.22 ml, 7.00 mmol) were added sequentially. The reaction was allowed to stir overnight at room temperature. The reaction was diluted with water and ethyl acetate. The layers were separated. The ethyl acetate layer was washed with saturated sodium chloride. The organic layer was dried over magnesium sulfate, filtered through a silica gel plug, and concentrated to obtain an oily product. The crude material was triturated in ethyl acetate to obtain white solid as

the product. (1.29 g, 87%) TLC R_f (60% EA/Hex): 0.5. ¹H NMR (400 MHz, DMSO-*d*₆) δ 7.63-7.55 (m, 2H), 7.33-7.28 (m, 2H), 7.22 (t, *J* = 7.1 Hz, 1H), 7.12-7.02 (m, 3H), 6.72 (s, 1H), 5.49 (s, 2H), 4.25 (s, 1H), 4.06 (q, *J* = 7.1, 4.2 Hz, 2H), 3.88 (s, 2H), 2.60-2.52 (m, 1H), 1.75 (s, 2H), 1.44-1.01 (m, 6H). TOF ES+ MS: 286.0 (M+H). HPLC (gradient A): ret. time = 7.88 min; purity = >95%.

Ethyl 1-(1-(4-chlorobenzyl)-1*H*-indole-2-carbonyl)piperidine-4-carboxylate (4.2 g, 9.8 mmol) and lithium hydroxide hydrate (4.1 g, 98 mmol) were dissolved in 10 mL of THF and 40 mL of water. The reaction was allowed to stir overnight. The reaction was diluted with water and diethyl ether. The aqueous layer was washed with another aliquot of diethyl ether before it was acidified with 2N HCl to pH ~ 2. The aqueous layer solution was washed with ethyl acetate (3 x 200 mL). The ethyl acetate layers were combined and washed with saturated aqueous solution of sodium chloride, dried over magnesium sulfate, filtered and concentrated *in vacuo* to obtain the product as a white solid. (3.33 g, 86%) TLC R_f (60% EA/Hex): 0.25. ¹H NMR (400 MHz, DMSO-*d*₆) δ 12.30 (s, 1H), 7.66 (d, *J* = 7.9 Hz, 1H), 7.59 (d, *J* = 8.4 Hz, 1H), 7.35 (d, *J* = 8.4 Hz, 2H), 7.25 (t, *J* = 11.4, 3.9 Hz, 1H), 7.16-7.09 (m, 3H), 6.75 (s, 1H), 5.52 (s, 2H), 4.29 (s, 1H), 4.04 (s, 1H), 3.06 (s, 2H), 2.52-2.47 (m, 1H), 1.80 (s, 2H), 1.22 (s, 2H). TOF ES+ MS: (M+H). HPLC (gradient A): ret. time = 6.98 min; purity = >95%.

Representative Procedure for Carboxamide Analogs (Method A):

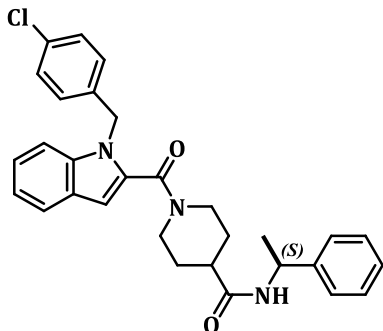
1-(1-(4-Chlorobenzyl)-1*H*-indole-2-carbonyl)piperidine-4-carboxylic acid 157 (1.0 eq), EDCI (2.0 eq), and 1-hydroxybenzotriazole (2.0 eq) were dissolved in DCM (3.0 mL) and allowed to stir at room temperature for 15 minutes. DIEA (2.0 eq) and desired amine (2.0 eq) were added. The reaction was allowed to stir at room temperature overnight. The reaction was diluted with water and ethyl acetate. The organic layer was washed with water, saturated sodium bicarbonate, 1N HCl, and saturated sodium chloride. The organic layer was dried over magnesium sulfate, filtered, and concentrated *in vacuo*. The crude material was recrystallized in diethyl ether/ethyl acetate to afford desired product.



***N*-benzyl-1-(1-(4-chlorobenzyl)-1*H*-indole-2-carbonyl)piperidine-4-carboxamide**

(CCG 102516, 10): Prepared by Method A using benzylamine. TLC R_f (70% EA/Hex):

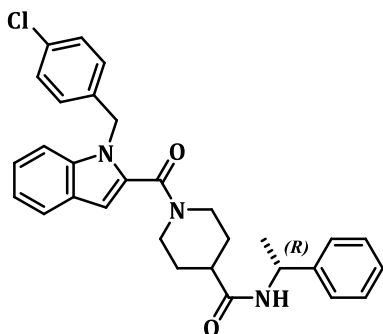
0.2. ^1H NMR (400 MHz, $\text{DMSO-}d_6$) δ 8.35 (t, $J = 5.9$ Hz, 1H), 7.63 (d, $J = 7.9$ Hz, 1H), 7.55 (d, $J = 8.3$ Hz, 1H), 7.38-7.29 (m, 4H), 7.27-7.29 (m, 4H), 7.27-7.18 (m, 4H), 7.14-7.08 (m, 3H), 6.74 (s, 1H), 5.50 (s, 2H), 4.43 (bs, 1H), 4.28 (d, $J = 5.9$ Hz, 2H), 4.04 (bs, 1H), 2.95 (bs, 2H), 2.48-2.42 (m, 2H), 1.74 (bs, 2H), 1.47 (bs, 2H). ^{13}C NMR (500 MHz, $\text{DMSO-}d_6$) 173.4, 161.8, 139.5, 137.1, 136.7, 131.7, 126.1, 123.0, 121.3, 120.1, 110.6, 103.30. TOF ES+ MS: 486.1 (M+H), 508.0 (M+Na). HPLC (gradient A): ret. time = 7.73 min; purity = >95%



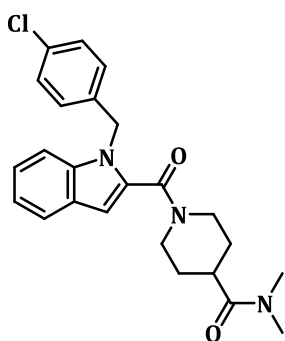
(S)-1-(1-(4-chlorobenzyl)-1H-indole-2-carbonyl)-N-(1-phenylethyl)piperidine-4-

carboxamide (CCG 203927, 11): Prepared by Method A using (S)-1-phenylethylamine.

White solid (32.9 mg, 26%). TLC R_f (70% EA/Hex): 0.2. ^1H NMR (400 MHz, DMSO- d_6) δ 8.25 (d, $J = 8.0$ Hz, 1H), 7.62 (d, $J = 7.9$ Hz, 1H), 7.53 (d, $J = 8.4$ Hz, 1H), 7.35-7.25 (m, 5H), 7.21 (t, $J = 7.3$ Hz, 2H), 7.09 (d, $J = 7.7$ Hz, 3H), 6.72 (s, 1H), 5.48 (s, 2H), 4.97-4.82 (m, 1H), 4.42 (bs, 1H), 4.03 (bs, 1H), 2.89 (bs, 2H), 2.46-2.39 (m, 1H), 1.68 (bs, 2H), 1.52-1.26 (m, 5H). ^{13}C NMR (400 MHz, DMSO- d_6) 172.6, 161.8, 144.8, 137.1, 136.7, 131.8, 131.7, 128.7, 128.3, 128.1, 126.4, 126.1, 125.7, 123.0, 121.3, 120.1, 110.6, 103.3, 47.4, 46.1, 41.4, 22.4. TOF ES+ MS: 500.0 (M+H), 522.1 (M+Na). HPLC (gradient A): ret. time = 7.88 min; purity = >95%. [CHN] C = 71.8%, H = 6.07%, N = 8.37%. Theoretical [CHN]: C = 72.06%, 6.05%, 8.4%

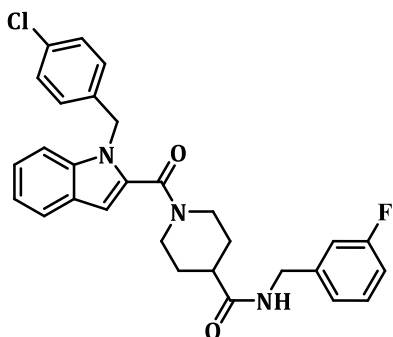


(R)-1-(1-(4-chlorobenzyl)-1H-indole-2-carbonyl)-N-(1-phenylethyl)piperidine-4-carboxamide (CCG 203926, 12): Prepared by Method A using (R)-1-phenylethylamine. White solid (282 mg, 45%). TLC R_f (70% EA/Hex): 0.2. ^1H NMR (400 MHz, DMSO- d_6) δ 8.25 (d, $J = 8.1$ Hz, 1H), 7.62 (d, $J = 7.9$ Hz, 1H), 7.53 (d, $J = 8.3$ Hz, 1H), 7.36-7.26 (m, 6H), 7.21 (t, $J = 7.4$ Hz, 2H), 7.10 (d, $J = 8.2$ Hz, 3H), 6.72 (s, 1H), 5.48 (s, 2H), 4.90 (p, $J = 7.1$ Hz, 1H), 4.41 (bs, 1H), 4.03 (bs, 1H), 2.89 (bs, 2H), 2.47-2.38 (m, 1H), 1.69 (bs, 2H), 1.52-1.25 (m, 5H). ^{13}C NMR (400 MHz, DMSO- d_6) 172.6, 161.8, 144.7, 137.1, 136.7, 131.8, 131.7, 128.7, 128.3, 128.1, 126.4, 126.1, 125.7, 123.0, 121.3, 120.1, 110.6, 103.3, 47.4, 46.1, 41.4, 22.4. TOF ES+ MS: 500 (M+H), 522.1 (M+Na). HPLC (gradient A): ret. time = 7.87 min; purity = >95% [CHN] C = 71.93%, H = 6.06%, N = 8.39%. Theoretical [CHN]: C = 72.06%, 6.05%, 8.4%.



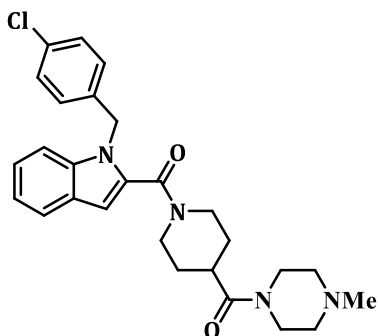
1-(1-(4-chlorobenzyl)-1H-indole-2-carbonyl)-N,N-dimethylpiperidine-4-carboxamide (CCG 204022, 13). Prepared by Method A using dimethylamine. Purified

by flash chromatography with a gradient of 100% DCM to 5% 7M ammonia in methanol diluted with 95% DCM. The product was obtained as a white solid. Yield: 68%. ^1H NMR (400 MHz, $\text{DMSO-}d_6$) δ 7.63 (d, $J = 7.8$ Hz, 1H), 7.54 (d, $J = 8.4$ Hz, 1H), 7.38 – 7.27 (m, 2H), 7.26 – 7.17 (m, 1H), 7.13 – 7.08 (m, 3H), 6.73 (s, 1H), 5.50 (s, 2H), 4.44 (bs, 1H), 3.99 (bs, 1H), 3.19 – 2.84 (m, 6H), 2.81 (s, 3H), 1.62 (bs, 2H), 1.36 (bs, 2H). TOF ES+ MS: 424.0 (M+H). HPLC ret. time = 7.09 min; purity > 95%.

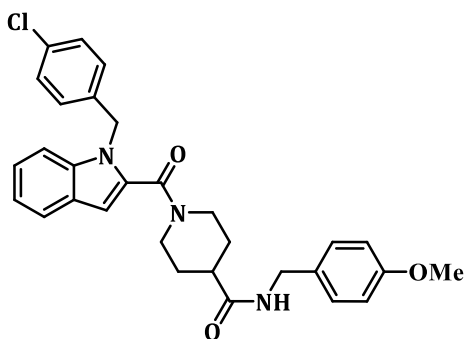


1-(1-(4-chlorobenzyl)-1H-indole-2-carbonyl)-N-(3-fluorobenzyl)piperidine-4-carboxamide (CCG 206399, 14) Prepared by Method A using (3-fluorophenyl)

methanamine. ^1H NMR (500 MHz, $\text{DMSO-}d_6$) δ 8.40 (t, $J = 6.0$ Hz, 1H), 7.58 (dd, $J = 41.7, 8.1$ Hz, 2H), 7.40 – 7.29 (m, 3H), 7.24 – 7.18 (m, 1H), 7.14 – 7.00 (m, 6H), 6.73 (s, 1H), 5.49 (s, 2H), 4.59 – 4.21 (m, 3H), 4.00 (bs, 1H), 3.16 – 2.69 (m, 2H), 2.45 (tt, $J = 11.4, 3.7$ Hz, 1H), 1.90 – 1.26 (m, 4H). TOF ES+ MS: 504.9 (M+H). HPLC (gradient A): ret. time = 7.80 min; purity > 95%

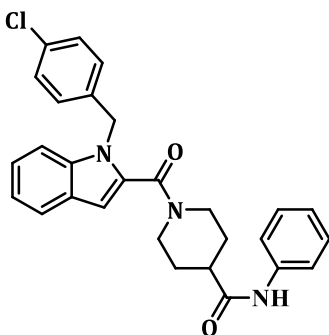


(1-(4-chlorobenzyl)-1*H*-indol-2-yl)(4-(4-methylpiperazine-1-carbonyl)piperidin-1-yl)methanone (CCG 204023, 15). Prepared by Method A using 4-methylpiperazine. The crude material was purified by medium pressure chromatography using 100% DCM to 5% 7M ammonia in MeOH/95% DCM. The product was obtained as a white solid. Yield: 57%. ¹H NMR (400 MHz, DMSO-*d*₆) δ 7.62 (d, *J* = 7.9 Hz, 1H), 7.54 (d, *J* = 8.7 Hz, 1H), 7.37 – 7.29 (m, 2H), 7.26 – 7.17 (m, 1H), 7.14 – 7.05 (m, 3H), 6.73 (s, 1H), 5.49 (s, 2H), 4.52 – 3.90 (m, 2H), 3.57 – 3.39 (m, 4H), 3.19 – 2.78 (m, 3H), 2.39 – 2.11 (m, 7H), 1.77 – 1.20 (m, 4H). TOF ES+ MS: 479.1 (M+H). HPLC ret. time = 5.37 min; purity = 92%.



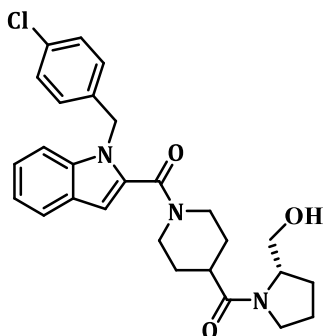
1-(1-(4-chlorobenzyl)-1*H*-indole-2-carbonyl)-*N*-(4-methoxybenzyl)piperidine-4-carboxamide (CCG 204025, 16): Prepared by Method A using 4-methoxybenzylamine. Trituration in methanol afforded 16 as white solid (104 mg, 80%). TLC R_f (70% EA/Hex): 0.2. ¹H NMR (400 MHz, DMSO-*d*₆) δ 8.25 (t, *J* = 5.8 Hz, 1H), 7.57 (dd, *J* =

34.9, 8.1 Hz, 2H), 7.33 (d, $J = 8.4$ Hz, 2H), 7.20 (t, $J = 7.7$ Hz, 1H), 7.11 (m, 4H), 6.86 (d, $J = 8.6$ Hz, 2H), 6.72 (s, 1H), 5.48 (s, 2H), 4.43 (s, 1H), 4.18 (d, $J = 5.8$ Hz, 2H), 4.01 (s, 1H), 3.71 (s, 3H), 2.93 (s, 2H), 2.41 (d, $J = 11.7$ Hz, 1H), 1.70 (s, 2H), 1.42 (s, 2H). TOF ES+ MS: 516.1 (M+H), 538.1 (M+Na). HPLC (gradient A): ret. time = 8.27 min; purity = 91%.

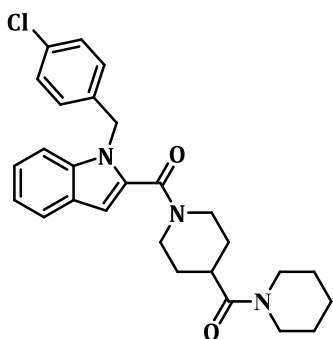


1-(1-(4-chlorobenzyl)-1H-indole-2-carbonyl)-N-phenylpiperidine-4-carboxamide

(CCG 206334, 17): Prepared by Method A using aniline. Compound 17 was obtained as a white solid (77 mg, 65%). TLC R_f (70% EA/Hex): 0.2. ^1H NMR (400 MHz, DMSO- d_6) δ 9.89 (s, 1H), 7.66-7.52 (m, 4H), 7.37-7.18 (m, 5H), 7.13-7.07 (m, 3H), 7.02 (t, $J = 7.4$ Hz, 1H), 6.75 (s, 1H), 5.51 (s, 2H), 4.45 (bs, 1H), 4.03 (bs, 1H), 2.95 (bs, 2H), 2.64-2.55 (m, 1H), 1.79 (bs, 2H), 1.47 (bs, 2H). TOF ES+ MS: 472.1 (M+H), 494.1 (M+Na). HPLC (gradient A): ret. time = 8.01 min; purity = >95%.

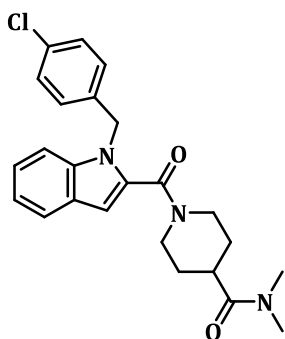


(S)-1-(4-chlorobenzyl)-1H-indol-2-yl(4-(2-(hydroxymethyl)pyrrolidine-1-carbonyl)piperidin-1-yl)methanone (CCG 204021, 18). Prepared by Method A using *L*-prolinol. The crude material was purified using flash chromatography with a gradient of 100% DCM to 5% 7M ammonia in methanol diluted with 95% DCM. The product was obtained as a white solid. Yield: 98%. $^1\text{H NMR}$ (400 MHz, $\text{DMSO-}d_6$) δ 7.62 (d, $J = 8.1$ Hz, 1H), 7.58 – 7.50 (m, 1H), 7.39 – 7.30 (m, 2H), 7.26 – 7.17 (m, 1H), 7.17 – 7.05 (m, 3H), 6.73 (s, 1H), 5.50 (s, 2H), 4.60 – 3.87 (m, 3H), 3.53 – 3.43 (m, 2H), 3.29 – 3.16 (m, 1H), 3.14 – 2.77 (m, 2H), 2.72 – 2.64 (m, 1H), 1.98 – 1.19 (m, 8H). TOF ES+ MS: 480.1 (M+H). HPLC ret. time = 6.82 min; purity = 94%.



1-(4-chlorobenzyl)-1H-indol-2-yl(4-(piperidine-1-carbonyl)piperidin-1-yl)methanone (CCG 203928, 19): Prepared by Method A using piperidine. Flash chromatography with 0-5% methanolic ammonia: DCM afforded 19 as a white solid (48 mg, 41%). TLC R_f (0-5% methanolic ammonia: DCM): 0.2. $^1\text{H NMR}$ (400 MHz,

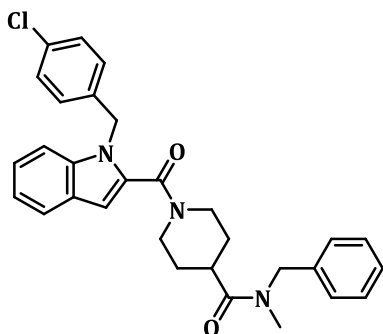
DMSO- d_6) δ 7.62 (d, $J = 7.8$ Hz, 1H), 7.54 (d, $J = 8.3$ Hz, 1H), 7.33 (d, $J = 8.5$ Hz, 2H), 7.21 (t, $J = 11.8, 4.6$ Hz, 1H), 7.13-7.07 (m, 3H), 6.73 (s, 1H), 5.49 (s, 2H), 4.44 (bs, 1H), 4.02 (bs, 1H), 3.43 (s, 4H), 3.20-3.83 (m, 3H), 1.79-1.20 (m, 10H). TOF ES+ MS: 464.1 (M+H), 486.1 (M+Na). HPLC (gradient A): ret. time = 7.95 min; purity = >95%.



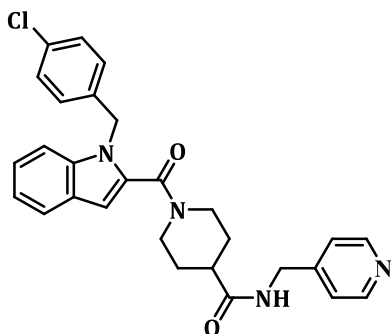
1-(1-(4-chlorobenzyl)-1H-indole-2-carbonyl)-N,N-dimethylpiperidine-4-

carboxamide (CCG 204022, 20). Prepared by Method A using dimethylamine as

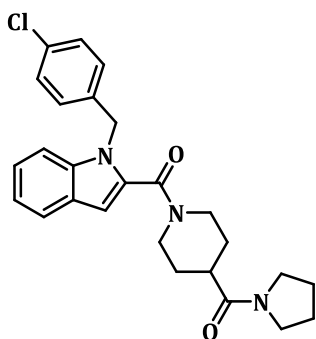
described for 20. Purified by flash chromatography with a gradient of 100% DCM to 5% 7M ammonia in methanol diluted with 95% DCM. The product was obtained as a white solid. Yield: 68%. ^1H NMR (400 MHz, DMSO- d_6) δ 7.63 (d, $J = 7.8$ Hz, 1H), 7.54 (d, $J = 8.4$ Hz, 1H), 7.38 – 7.27 (m, 2H), 7.26 – 7.17 (m, 1H), 7.13 – 7.08 (m, 3H), 6.73 (s, 1H), 5.50 (s, 2H), 4.44 (bs, 1H), 3.99 (bs, 1H), 3.19 – 2.84 (m, 6H), 2.81 (s, 3H), 1.62 (bs, 2H), 1.36 (bs, 2H). TOF ES+ MS: 424.0 (M+H). HPLC ret. time = 7.09 min; purity > 95%.



***N*-benzyl-1-(1-(4-chlorobenzyl)-1*H*-indole-2-carbonyl)-*N*-methylpiperidine-4-carboxamide (CCG 203930, 21)** Compound **157** (150 mg, 0.378 mmol), HOBt (102 mg, 0.756 mmol), and EDCI (145 mg, 0.756 mmol) were dissolved in 1.5 mL of DCM. The reaction was allowed to stir for ten minutes before *N*-methyl-1-phenylmethanamine (45.8 mg, 0.378 mmol) and DIEA (0.132 ml, 0.756 mmol) were added. The reaction was stirred for two days before it was diluted with water and ethyl acetate. The layers were separated and the organic layer was washed with the following saturated aqueous solutions: citric acid, sodium bicarbonate, and sodium chloride. The organic layer was dried over magnesium sulfate, filtered and concentrated. The crude mixture was purified using 50% Ethyl Acetate/Hexanes. The product was obtained as a white solid. Yield: 64 mg (34%). ¹H NMR (400 MHz, DMSO- *d*₆) 1.5:1 mixture of rotamers δ 7.67 – 7.59 (m, 1H), 7.58 – 7.50 (m, 1H), 7.41 – 7.17 (m, 8H), 7.14 – 7.07 (m, 3H), 6.75 (rotamer A, s), 6.71 (rotamer B, s, 1H), 5.53 – 5.47 (m, 2H), 4.65 (rotamer A, s, 1H), 4.53 – 4.33 (m, 2H), 4.01 (bs, 1H), 3.20 – 2.89 (m, 5H), 2.78 (rotamer B, s, 1H), 1.52 (bm, 4H). TOF ES+ MS: 500 (M+H). HPLC ret. time = 8.23 min; purity = 94%

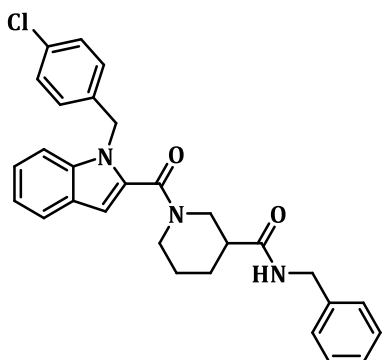


1-(1-(4-chlorobenzyl)-1*H*-indole-2-carbonyl)-*N*-(pyridin-4-ylmethyl)piperidine-4-carboxamide (CCG 203929, 22): Prepared by Method A using 4-aminomethyl pyridine to afford 22 as a white solid (61 mg, 50%). TLC R_f (100% EA): 0.1. ^1H NMR (400 MHz, DMSO- d_6) δ 8.68-8.59 (m, 4H), 7.63 (d, $J = 7.8$ Hz, 1H), 7.54 (d, $J = 8.4$ Hz, 1H), 7.49 (d, $J = 5.9$ Hz, 4H), 7.36-7.30 (m, 3H), 7.22 (t, $J = 7.6$ Hz, 1H), 7.14-7.07 (m, 2H), 6.74 (s, 1H), 5.49 (s, 2H), 4.56-4.14 (m, 4H), 2.97 (bs, 2H), 1.76 (bs, 2H), 1.43 (bs, 2H). TOF ES+ MS: 487.1 (M+H). HPLC (gradient A): ret. time = 8.00 min; purity = >95%.



(1-(4-chlorobenzyl)-1*H*-indol-2-yl)(4-(pyrrolidine-1-carbonyl)piperidin-1-yl)methanone (CCG 102514, 23): Prepared by Method A using pyrrolidine. Purified by flash chromatography with a gradient of 100% DCM to 5% 7M ammonia in methanol diluted with 95% DCM. The product was obtained as a white solid. Yield: 73%. ^1H NMR (400 MHz, DMSO- d_6) δ 7.63 (d, $J = 7.8$ Hz, 1H), 7.54 (d, $J = 8.1$ Hz, 1H), 7.38 – 7.30

(m, 2H), 7.26 – 7.17 (m, 1H), 7.16 – 7.05 (m, 3H), 6.73 (s, 1H), 5.50 (s, 2H), 4.63 – 3.86 (m, 2H), 3.47 (t, $J = 6.7$ Hz, 2H), 3.27 (t, $J = 6.9$ Hz, 2H), 3.13 – 2.80 (m, 2H), 2.77 – 2.64 (m, 1H), 1.87 (p, $J = 6.7$ Hz, 2H), 1.81 – 1.27 (m, 6H). TOF ES+ MS: 450.0 (M+H). HPLC ret. time = 7.35 min; purity > 95%.



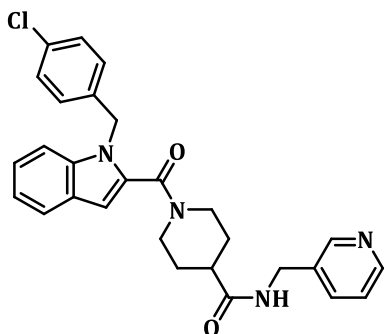
***N*-benzyl-1-(1-(4-chlorobenzyl)-1*H*-indole-2-carbonyl)piperidine-3-carboxamide**

(CCG 205483, 24): Compound **156** (100 mg, 0.319 mmol), EDC (134 mg, 0.699 mmol) and 1-hydroxybenzotriazole (95.0 mg, 0.703 mmol) were dissolved in DCM (Volume: 3.0 ml). The reaction was allowed to stir for 10 minutes before the addition of DIEA (0.122 ml, 0.700 mmol) and ethyl piperidine-3-carboxylate (0.109 ml, 0.707 mmol). The reaction was allowed to stir overnight at room temperature. The reaction was diluted with water and ethyl acetate. The organic phase was washed with water, 1N HCl, saturated sodium bicarbonate, and saturated sodium chloride. The organic layer was dried over magnesium sulfate, filtered, and concentrated in vacuo. The crude material was purified using Biotage SP1 system with 0-45% ethyl acetate/hexanes to afford ethyl 1-(1-(4-chlorobenzyl)-1*H*-indole-2-carbonyl)piperidine-3-carboxylate as white solid. (100 mg, 67%) TLC R_f (60% EA/Hex): 0.5. ^1H NMR (400 MHz, DMSO- d_6). δ 7.63 (d, $J = 7.9$ Hz, 1H), 7.55 (d, $J = 8.3$ Hz, 1H), 7.33 (d, $J = 8.4$ Hz, 2H), 7.22 (t, $J = 7.3$ Hz, 1H), 7.16-7.06 (m, 3H), 6.73 (s, 1H), 5.46 (s, 2H), 4.47 – 3.63 (m, 5H), 3.29-2.70 (m, 2H), 1.94-

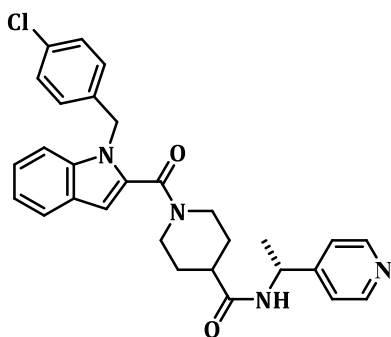
1.03 (m, 4H). TOF ES+ MS: 425.1(M+H), 447.1 (M+Na). HPLC (gradient A): ret. time = 8.36 min; purity = >95%.

Ethyl 1-(1-(4-chlorobenzyl)-1*H*-indole-2-carbonyl)piperidine-3-carboxylate (100 mg, 0.235 mmol) and solid lithium hydroxide (99 mg, 2.4 mmol) were dissolved in 1.5 mL of THF and 3.0 mL of water. The reaction was allowed to stir overnight. After 24 hours at room temperature, the reaction was diluted with water and extracted twice with diethyl ether. The aqueous layer was acidified with 2N HCl aqueous solution to pH 2 and extracted with three times with ethyl acetate. The organic layers were combined and washed with saturated sodium chloride solution, dried over magnesium sulfate, filtered and concentrated in vacuo to obtain a white solid. The crude material was taken directly to the next step without further purification. (50 mg, 53%) TLC R_f (60% EA/Hex): 0.2. ¹H NMR (400 MHz, DMSO-*d*₆) δ 12.26 (s, 1H), 7.63 (d, *J* = 7.9 Hz, 1H), 7.54 (d, *J* = 8.4 Hz, 1H), 7.33 (d, *J* = 8.4 Hz, 2H), 7.22 (t, *J* = 7.6 Hz, 1H), 7.16-7.04 (m, 3H) 6.73 (s, 1H), 5.46 (s, 2H), 4.21 (s, 1H), 3.94 (s, 1H), 3.02 (s, 2H), 1.99 (s, 1H), 1.96-1.52 (m, 2H), 1.40-0.97 (m, 2H). TOF E+ MS: 397.1 (M+H), 419.1 (M+Na). HPLC (gradient A): ret. time = 6.98 min; purity = >95%

CCG 205483 (24) was prepared by Method A using 1-(1-(4-chlorobenzyl)-1*H*-indole-2-carbonyl)piperidine-3-carboxylic acid and benzylamine. Flash chromatography with 0-5% methanolic ammonia: DCM afforded 24 as a white solid (38 mg, 62%). TLC R_f (70% EA/Hex): 0.2. ¹H NMR (400 MHz, DMSO-*d*₆) δ 8.44 (s, 1H), 7.60 (d, *J* = 7.9 Hz, 1H), 7.49 (s, 1H), 7.36-7.03 (m, 12H), 6.72 (s, 1H), 5.46 (s, 2H), 4.58-3.74 (m, 4H), 2.93 (bs, 2H), 2.30 (s, 1H), 1.93-1.48 (m, 3H). TOF ES+ MS: 486.1 (M+H), 508.1 (M+Na). HPLC (gradient A): ret. time = 7.99 min; purity = >95%.

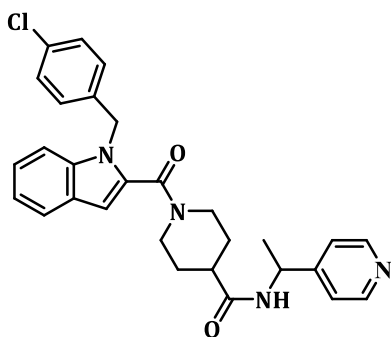


1-(1-(4-chlorobenzyl)-1*H*-indole-2-carbonyl)-*N*-(pyridin-3-ylmethyl)piperidine-4-carboxamide (CCG 205422, 30): Prepared by Method A using 3-aminomethyl pyridine to afford 30 as a white solid (315 mg, 70%). TLC R_f (100% EA): 0.1. ^1H NMR (400 MHz, DMSO- d_6) δ ppm 8.43 - 8.49 (m, 2 H), 8.39 (t, $J=5.8$ Hz, 1 H), 7.68 (d, $J=7.8$ Hz, 1 H), 7.59 (d, $J=7.8$ Hz, 1 H), 7.51 (d, $J=8.4$ Hz, 1 H), 7.39 (dd, $J=7.5, 5.0$ Hz, 1 H), 7.33 - 7.26 (m, 2 H), 7.18 (t, $J=7.6$ Hz, 1 H), 7.04 - 7.11 (m, 3 H), 6.70 (s, 1 H), 5.46 (s, 2 H), 3.84 - 4.59 (m, 4 H), 2.92 (br. s., 2 H), 2.42 (tt, $J=11.2, 3.9$ Hz, 1 H), 1.27 - 1.82 (m, 4 H) TOF ES+ MS: 487.1 (M+H). HPLC (gradient A): ret. time = 5.62 min; purity = >95%.

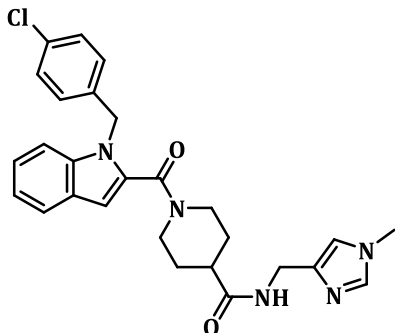


(*R*)-1-(1-(4-chlorobenzyl)-1*H*-indole-2-carbonyl)-*N*-(1-(pyridin-4-yl)ethyl)piperidine-4-carboxamide (CCG 212090, 31): Prepared by Method A using (*R*)-1-(pyridin-4-yl)ethanamine. The crude solid was recrystallized using diethyl ether/ethyl acetate. The product was obtained as a white solid after filtration. Yield: 55%. ^1H NMR (500 MHz, DMSO- d_6) δ 8.51 - 8.46 (m, 2H), 8.37 (d, $J = 7.7$ Hz, 1H), 7.62 (d, $J = 7.9$ Hz, 1H), 7.54

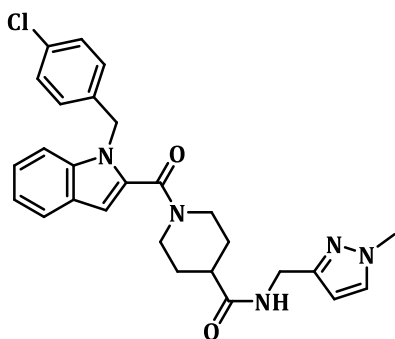
(d, $J = 8.3$ Hz, 1H), 7.36 – 7.25 (m, 4H), 7.25 – 7.18 (m, 1H), 7.13 – 7.06 (m, 3H), 6.73 (s, 1H), 5.48 (s, 2H), 4.88 (p, $J = 7.2$ Hz, 1H), 4.44 (bs, 1H), 4.02 (bs, 1H), 3.13 – 2.70 (m, 2H), 2.50 – 2.44 (m, 1H), 1.85 – 1.30 (m, 7H). TOF ES+ MS: 501.2 (M+H). HPLC ret. time = 5.62 min; purity >95% .



1-(1-(4-chlorobenzyl)-1H-indole-2-carbonyl)-N-(1-(pyridin-4-yl)ethyl)piperidine-4-carboxamide (CCG 206329, 32): Prepared by Method A using 1-(pyridin-4-yl)ethanamine . Crude material was triturated with ether and ethyl acetate and filtered to obtain 27a as a white solid. Yield: 37.9 mg, 30% ^1H NMR (400 MHz, DMSO- d_6) δ 8.52 – 8.45 (m, 2H), 8.35 (d, $J = 7.7$ Hz, 1H), 7.62 (d, $J = 7.8$ Hz, 1H), 7.53 (d, $J = 8.8$ Hz, 1H), 7.37 – 7.17 (m, 5H), 7.14 – 7.05 (m, 3H), 6.72 (s, 1H), 5.48 (s, 2H), 4.87 (p, $J = 7.1$ Hz, 1H), 4.03 (m, 2H), 2.95 (bs, 2H), 2.49 – 2.42 (m, 1H), 1.79 – 1.28 (m, 7H). TOF ES+ MS: 501.2 (M+H). HPLC ret. time = 5.73 min; purity >95% .

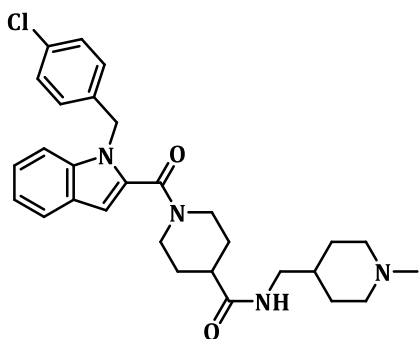


1-(1-(4-chlorobenzyl)-1H-indole-2-carbonyl)-N-((1-methyl-1H-imidazol-4-yl)methyl)piperidine-4-carboxamide (CCG 205455, 33). Prepared by Method A using (1-methyl-1H-imidazol-4-yl)methanamine. The crude material was triturated with ether and ethyl acetate and filtered to obtain white solid as a product. Yield: 23%. ^1H NMR (400 MHz, DMSO- d_6) δ 8.07 (t, $J = 5.5$ Hz, 1H), 7.62 (d, $J = 7.9$ Hz, 1H), 7.53 (d, $J = 8.3$ Hz, 1H), 7.46 (s, 1H), 7.38 – 7.30 (m, 2H), 7.26 – 7.16 (m, 1H), 7.15 – 7.05 (m, 3H), 6.87 (s, 1H), 6.73 (s, 1H), 5.49 (s, 2H), 4.49 – 3.92 (m, 4H), 3.32 (s, 3H), 2.90 (bs, 2H), 2.48 – 2.36 (m, 1H), 1.78 – 1.33 (m, 4H). TOF ES+ MS: 490.1 (M+H). HPLC ret. time = 5.48 min; purity > 95%.

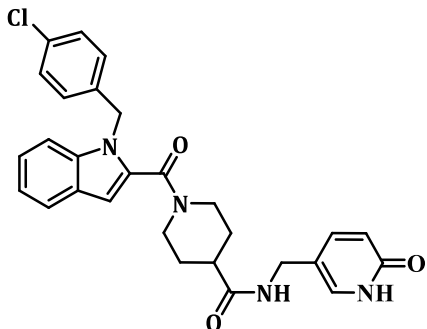


1-(1-(4-chlorobenzyl)-1H-indole-2-carbonyl)-N-((1-methyl-1H-pyrazol-3-yl)methyl)piperidine-4-carboxamide (CCG 205454, 34). Prepared by Method A using (1-methyl-1H-pyrazol-3-yl)methanamine. The crude product was triturated with ethyl acetate to obtain white solid as the product. Yield: 18%. ^1H NMR (400 MHz, DMSO-

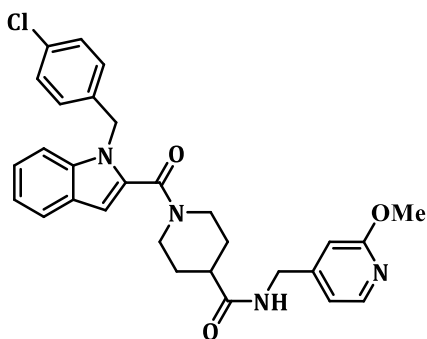
d_6) δ 8.17 (t, $J = 5.7$ Hz, 1H), 7.66 – 7.50 (m, 3H), 7.38 – 7.29 (m, 2H), 7.25 – 7.16 (m, 1H), 7.15 – 7.05 (m, 3H), 6.72 (s, 1H), 6.04 (d, $J = 2.2$ Hz, 1H), 5.49 (s, 2H), 4.17 (m, 4H), 3.76 (s, 3H), 2.92 (bs, 2H), 2.47 – 2.37 (m, 1H), 1.81 – 1.23 (m, 4H). TOF ES+ MS: 490.1 (M+H). HPLC ret. time = 6.62 min; purity = 94% .



1-(1-(4-chlorobenzyl)-1H-indole-2-carbonyl)-N-((1-methylpiperidin-4-yl)methyl)piperidine-4-carboxamide (CCG 205429, 35). Prepared by Method A using (1-methylpiperidin-4-yl)methanamine. The crude product was triturated with diethyl ether/ethyl acetate to afford the product as a white solid. Yield: 65%. ^1H NMR (400 MHz, DMSO- d_6) δ 7.79 (t, $J = 5.8$ Hz, 1H), 7.62 (d, $J = 7.9$ Hz, 1H), 7.54 (d, $J = 8.0$ Hz, 1H), 7.38 – 7.29 (m, 2H), 7.26 – 7.17 (m, 1H), 7.15 – 7.05 (m, 3H), 6.72 (s, 1H), 5.49 (s, 2H), 4.61 – 3.82 (m, 2H), 2.99 – 2.73 (m, 4H), 2.44 – 2.30 (m, 1H), 2.19 (s, 3H), 1.96 – 1.05 (m, 13H). TOF ES+ MS: 507.1 (M+H). HPLC ret. time = 5.41 min; purity > 95% .

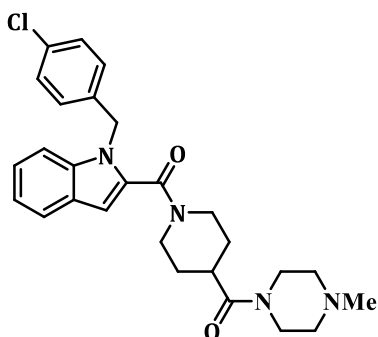


1-(1-(4-chlorobenzyl)-1H-indole-2-carbonyl)-N-((6-oxo-1,2,3,6-tetrahydropyridin-3-yl)methyl)piperidine-4-carboxamide (CCG 211760, 36). Prepared by Method A using 5-(aminomethyl)pyridin-2(1H)-one. Yield: 33 mg, 26 %. ^1H NMR (500 MHz, $\text{DMSO-}d_6$) δ 11.42 (br. s., 1 H), 8.18 (t, $J=5.5$ Hz, 1 H), 7.58 (dd, $J=33.0, 7.8$ Hz, 2 H), 7.27 - 7.37 (m, 3 H), 7.16 - 7.25 (m, 2 H), 7.04 - 7.14 (m, 3 H), 6.72 (s, 1 H), 6.30 (d, $J=9.5$ Hz, 1 H), 5.49 (br. s., 2 H), 4.44 (br. s., 1 H), 3.78 - 4.17 (m, 3 H), 2.70 - 3.10 (m, 2 H), 2.39 (tt, $J=11.3, 3.6$ Hz, 1 H), 1.18 - 1.86 (m, 4 H). TOF ES+ MS: 503.2 (M+H); 525.2 (M+Na). HPLC (gradient A): ret. time = 6.00 min; purity > 95 %



1-(1-(4-chlorobenzyl)-1H-indole-2-carbonyl)-N-((2-methoxypyridin-4-yl)methyl)piperidine-4-carboxamide (CCG 208787, 37) Prepared by Method A using (2-methoxypyridin-4-yl)methanamine. Yield: 60 mg, 41 %. ^1H NMR (400 MHz, $\text{DMSO-}d_6$) δ 8.41 (t, $J=6.2$ Hz, 1 H), 8.07 (d, $J=5.1$ Hz, 1 H), 7.59 (dd, $J=26.0, 7.6$ Hz, 2 H), 7.29 - 7.37 (m, 2 H), 7.18 - 7.26 (m, 1 H), 7.06 - 7.14 (m, 3 H), 6.83 (d, $J=5.3$ Hz, 1

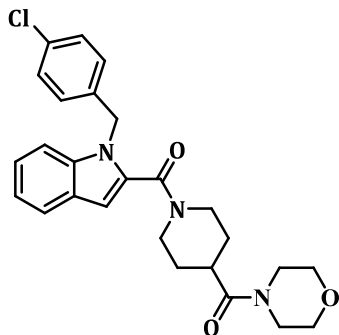
H), 6.74 (s, 1 H), 6.61 (s, 1 H), 5.49 (s, 2 H), 4.44 (br. s, 1 H), 4.24 (d, $J=6.1$ Hz, 2 H), 4.07 (br. s., 1 H), 3.82 (s, 3 H), 2.91 (br. s., 2 H), 2.46 (tt, $J=9.8, 3.9$ Hz, 1 H), 1.27 - 1.89 (m, 4 H). TOF ES+ MS: 516.9 (M+H), 538.9 (M+Na). HPLC (gradient A): ret. time = 6.62 min; purity = 94 %



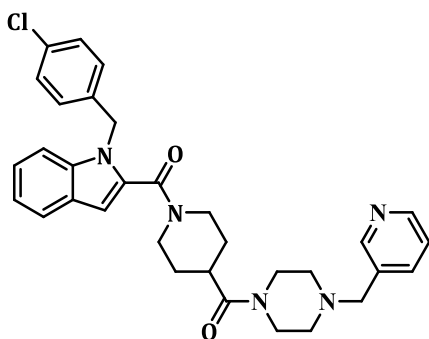
(1-(4-chlorobenzyl)-1H-indol-2-yl)(4-(4-methylpiperazine-1-carbonyl)piperidin-1-yl)methanone (CCG 204023, 38). Prepared by Method A using 4-methylpiperazine.

The crude material was purified by medium pressure chromatography using 100% DCM to 5% 7M ammonia in MeOH/95% DCM. The product was obtained as a white solid.

Yield: 57%. ^1H NMR (400 MHz, DMSO- d_6) δ 7.62 (d, $J = 7.9$ Hz, 1H), 7.54 (d, $J = 8.7$ Hz, 1H), 7.37 – 7.29 (m, 2H), 7.26 – 7.17 (m, 1H), 7.14 – 7.05 (m, 3H), 6.73 (s, 1H), 5.49 (s, 2H), 4.52 – 3.90 (m, 2H), 3.57 – 3.39 (m, 4H), 3.19 – 2.78 (m, 3H), 2.39 – 2.11 (m, 7H), 1.77 – 1.20 (m, 4H). TOF ES+ MS: 479.1 (M+H). HPLC ret. time = 5.37 min; purity = 92%.

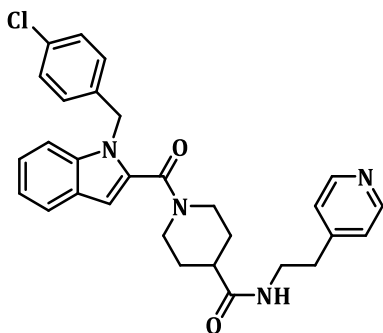


(1-(4-chlorobenzyl)-1H-indol-2-yl)(4-(morpholine-4-carbonyl)piperidin-1-yl)methanone (CCG 204024, 39). Prepared by Method A using morpholine. Purified by flash chromatography with a gradient of 100% DCM to 5% 7M ammonia in methanol diluted with 95% DCM. The product was obtained as a white solid. Yield: 73%. ¹H NMR (400 MHz, DMSO-*d*₆) δ 7.63 (d, *J* = 7.8 Hz, 1H), 7.54 (d, *J* = 8.4 Hz, 1H), 7.37 – 7.29 (m, 2H), 7.26 – 7.17 (m, 1H), 7.14 – 7.05 (m, 3H), 6.73 (s, 1H), 5.49 (s, 2H), 4.43 (bs, 1H), 4.01 (bs, 1H), 3.58 – 3.38 (m, 8H), 3.11 – 2.85 (m, 3H), 1.77 – 1.20 (m, 4H). TOF ES+ MS: 466.1 (M+H). HPLC ret. time = 7.00 min; purity > 95%.

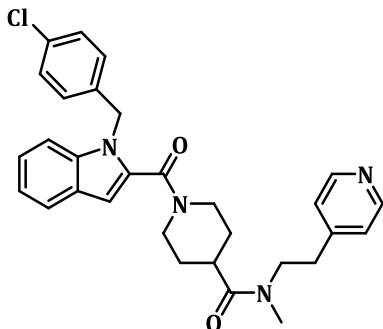


1-(1-(4-chlorobenzyl)-1H-indole-2-carbonyl)-N-((4-(pyridin-3-ylmethyl)piperazin-1-yl)methyl)piperidine-4-carboxamide (CCG 205430, 40) Prepared by Method A using 1-(pyridin-3-ylmethyl)piperazine. Yield: 105 mg, 75% ¹H NMR (400 MHz, DMSO-*d*₆) δ 8.47 (d, *J*=1.8 Hz, 1 H), 8.45 (dd, *J*=4.9, 1.8 Hz, 1 H), 7.68 (dt, *J*=7.5, 1.9 Hz, 1 H), 7.47

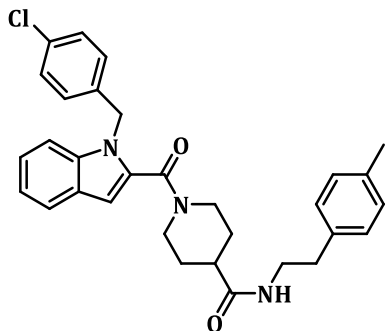
- 7.62 (m, 2 H), 7.27 - 7.36 (m, 3 H), 7.14 - 7.22 (m, 1 H), 7.03 - 7.11 (m, 3 H), 6.70 (s, 1 H), 5.46 (s, 2 H), 4.36 (br. s., 1 H), 4.00 (br. s., 1 H), 3.38 - 3.56 (m, 6 H), 2.75 - 3.12 (m, 3 H), 2.21 - 2.40 (m, 5 H), 1.22 - 1.76 (m, 4 H). TOF ES+ MS: 556.1 (M+H). HPLC (gradient A): ret. time = 5.73 min.; purity > 95%



1-(1-(4-chlorobenzyl)-1H-indole-2-carbonyl)-N-(2-(pyridin-4-yl)ethyl)piperidine-4-carboxamide (CCG 205432, 50). Prepared by Method A using 2-(pyridin-4-yl)ethanamine. The crude material was triturated with ethyl acetate to afford the product as a white solid. Yield: 328 mg, 80%. ¹H NMR (500 MHz, DMSO-*d*₆) δ 8.48 – 8.42 (m, 2H), 7.89 (t, *J* = 5.5 Hz, 1H), 7.63 (d, *J* = 7.8 Hz, 1H), 7.54 (d, *J* = 8.5 Hz, 1H), 7.37 – 7.30 (m, 2H), 7.25 – 7.18 (m, 3H), 7.13 – 7.07 (m, 3H), 6.71 (s, 1H), 5.48 (s, 2H), 4.53 – 3.82 (m, 2H), 3.32 – 3.29 (m, 2H), 3.08-2.67 (m, 4H), 2.36 – 2.27 (m, 1H), 1.75 – 1.18 (m, 4H). ¹³C NMR (500 MHz, DMSO-*d*₆) 226.99, 183.03, 173.53, 161.90, 149.39, 148.39, 137.21, 136.81, 131.91, 131.80, 128.80, 128.49, 126.16, 124.27, 123.15, 121.41, 120.27, 110.67, 103.40, 46.13, 41.42, 38.79, 34.20, 14.12, 14.09 [CHN] C = 69.28%, H = 5.88%, N = 11.23%. Theoretical [CHN]: C = 69.52%, H = 5.83%, N = 11.18% TOF ES+ MS: 501.0 (M+H). HPLC ret. time = 5.50 min; purity >95%.

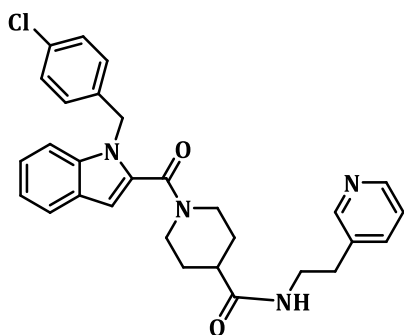


1-(1-(4-chlorobenzyl)-1H-indole-2-carbonyl)-N-methyl-N-(2-(pyridin-4-yl)ethyl)piperidine-4-carboxamide (CCG 211761, 51). Prepared by Method A using N-methyl-2-(pyridin-4-yl)ethanamine. The resulting crude material was purified using SP1 Biotage chromatography with a 25 g silica cartridge and a gradient of 20% ethyl acetate/hexanes to 100% ethyl acetate. The product was obtained as a white solid. Yield: 32%. ¹H NMR (400 MHz, DMSO- *d*₆) 1.3:1 mixture of rotamers δ 8.49 – 8.45 (m, 2H), 7.64 – 7.61 (m, 1H), 7.54 (t, J = 10Hz, 1H), 7.35 – 7.30 (m, 3H), 7.24-7.19 (m, 2H), 7.12 – 7.08 (m, 3H), 6.72 (rotamer A, s), 6.70 (rotamer B, s, 1H), 4.50 – 4.75 (m, 2H), 4.41 (bs, 1H), 3.97 (bs, 1H), 3.63 (t, J = 6.8 Hz, 1H), 3.53 (t, J = 7.3 Hz, 1H), 3.09 - 2.69 (m, 8H), 2.84- 2.50 (m, 1H), 1.17 – 1.10 (m, 4H). TOF ES+ MS: 515.3 (M+H). HPLC ret. time = 5.84 min; purity > 95%.



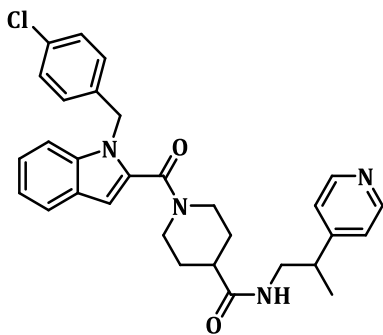
1-(1-(4-chlorobenzyl)-1H-indole-2-carbonyl)-N-(4-methylphenethyl)piperidine-4-carboxamide (CCG 102518, 52): Prepared by Method A using 4-methyl

phenethylamine. Flash chromatography with 0-5% methanolic ammonia: DCM afforded 52 as a white solid (24 mg, 19%). TLC R_f (0-5% methanolic ammonia: DCM): 0.25. ^1H NMR (400 MHz, DMSO- d_6). δ 7.86 (t, $J = 5.5$ Hz, 1H), 7.64 (d, $J = 8.0$ Hz, 1H), 7.56 (d, $J = 8.3$ Hz, 1H), 7.35 (d, $J = 8.4$ Hz, 2H), 7.23 (t, $J = 7.6$ Hz, 1H), 7.14-7.03 (m, 7H), 6.73 (s, 1H), 5.50 (s, 2H), 4.40 (bs, 1H), 3.91 (bs, 1H), 3.24 (q, $J = 12.0, 6.3$ Hz, 2H), 2.90 (bs, 2H), 2.66 (t, $J = 7.3$ Hz, 2H), 2.40-2.30 (m, 1H), 2.27 (s, 3H), 1.65 (bs, 2H), 1.36 (bs, 2H). TOF ES+ MS: 514.1 (M+H), 536.1 (M+Na). HPLC (gradient A): ret. time = 8.15 min; purity = >95%.

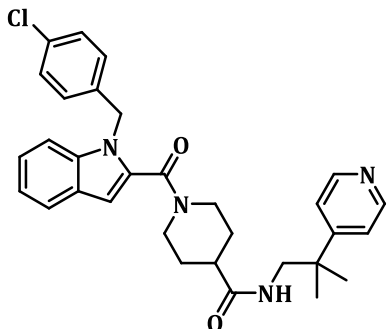


1-(1-(4-chlorobenzyl)-1H-indole-2-carbonyl)-N-(2-(pyridin-3-yl)ethyl)piperidine-4-carboxamide (CCG 205433, 53). Prepared by Method A using 2-(pyridin-3-

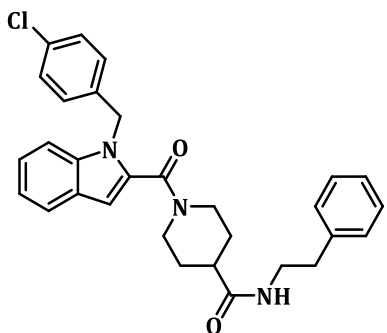
yl)ethanamine-HCl. The reaction was diluted with water and ethyl acetate. The organic layer was washed with saturated sodium bicarbonate, 10% aqueous citric acid solution, followed by saturated sodium chloride solution. The organic layer was dried over magnesium sulfate, filtered and concentrated. The resulting solid was triturated with ethyl acetate to obtain the product as a white solid. Yield: 20%. ^1H NMR (400 MHz, DMSO- d_6) δ 8.44 – 8.37 (m, 2H), 7.88 (t, J = 5.7 Hz, 1H), 7.66 – 7.50 (m, 3H), 7.38 – 7.26 (m, 3H), 7.26 – 7.17 (m, 1H), 7.14 – 7.06 (m, 3H), 6.71 (s, 1H), 5.48 (s, 2H), 4.63 – 3.80 (m, 2H), 3.34 – 3.25 (m, 2H), 2.89 (bs, 2H), 2.73 (t, J = 7.0 Hz, 2H), 2.38 – 2.27 (m, 1H), 1.74 – 1.21 (m, 4H). TOF ES+ MS: 501.0 (M+H), 523.1 (M+Na). HPLC ret. time = 5.46 min; purity >95%.



1-(1-(4-chlorobenzyl)-1H-indole-2-carbonyl)-N-(2-(pyridin-4-yl)propyl)piperidine-4-carboxamide (CCG 206580, 54). Prepared by Method A using 2-(pyridin-4-yl)propan-1-amine. The crude material was triturated in ethyl acetate to obtain product. Yield: 40%. ^1H NMR (500 MHz, CDCl_3) δ 8.58 – 8.52 (m, 2H), 7.68 – 7.61 (m, 1H), 7.37 – 7.31 (m, 1H), 7.31 – 7.10 (m, 5H), 7.06 – 6.99 (m, 2H), 6.62 (s, 1H), 5.46 (s, 2H), 5.31 (t, J = 5.1 Hz, 1H), 4.68 – 3.98 (m, 3H), 3.64 – 3.54 (m, 1H), 3.37 – 3.26 (m, 1H), 3.04 – 2.96 (m, 1H), 2.88 – 2.81 (m, 1H), 2.22 – 2.13 (m, 1H), 1.85 – 1.20 (m, 6H). TOF ES+ MS: 515.1 (M+H). HPLC ret. time = 5.80 min; purity = 85% .

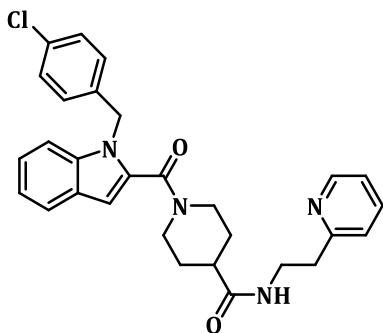


1-(1-(4-chlorobenzyl)-1*H*-indole-2-carbonyl)-*N*-(2-methyl-2-(pyridin-4-yl)propyl)piperidine-4-carboxamide (CCG 209022, 55). Prepared by Method A using 2-methyl-2-(pyridin-4-yl)propan-1-amine. The crude material was triturated in ethyl acetate. The white solid was filtered to obtain product. Yield: 23%. ¹H NMR (500 MHz, DMSO- *d*₆) δ 8.49 – 8.45 (m, 2H), 7.69 – 7.59 (m, 2H), 7.53 (d, *J* = 8.5 Hz, 1H), 7.36 – 7.31 (m, 4H), 7.25 – 7.17 (m, 1H), 7.14 – 7.06 (m, 3H), 6.71 (s, 1H), 5.48 (s, 2H), 4.55 – 3.79 (m, 2H), 3.28 (d, *J* = 6.2 Hz, 2H), 2.88 (bs, 2H), 2.42 – 2.34 (m, 1H), 1.67 – 1.19 (m, 10H). TOF ES+ MS: 529.3 (M+H). HPLC ret. time = 6.01 min; purity > 95%.

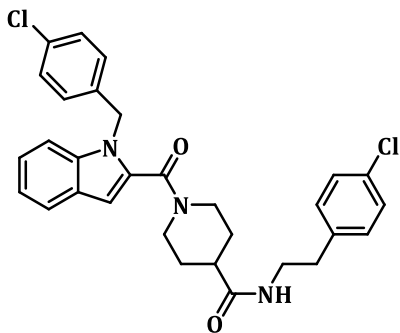


1-(1-(4-chlorobenzyl)-1*H*-indole-2-carbonyl)-*N*-phenethylpiperidine-4-carboxamide (CCG 206397, 56): Prepared by Method A using 2-phenethylamine. White solid (76 mg, 60%). TLC R_f (70% EA/Hex): 0.2. ¹H NMR (400 MHz, DMSO-*d*₆) δ 7.85 (t, *J* = 5.4 Hz, 1H), 7.62 (d, *J* = 7.8 Hz, 1H), 7.53 (d, *J* = 8.4 Hz, 1H), 7.36-7.05 (m, 10H), 6.71 (s, 1H), 5.48 (s, 2H), 4.38 (bs, 1H), 4.01 (bs, 1H), 3.26 (q, *J* = 13.6, 6.7 Hz, 2H), 2.90 (bs, 2H),

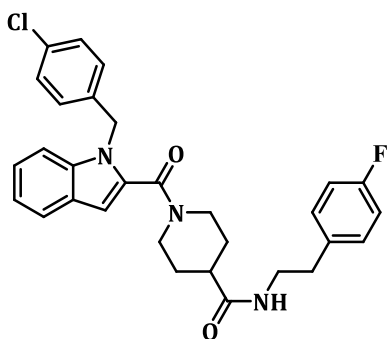
2.69 (t, $J = 13.6, 6.5$ Hz, 2H), 2.39-2.28 (m, 2H), 1.61 (bs, 2H), 1.36 (bs, 2H). TOF ES+ MS: 500.2 (M+H), 522.1 (M+Na). HPLC (gradient A): ret. time = 7.90 min; purity = >95%.



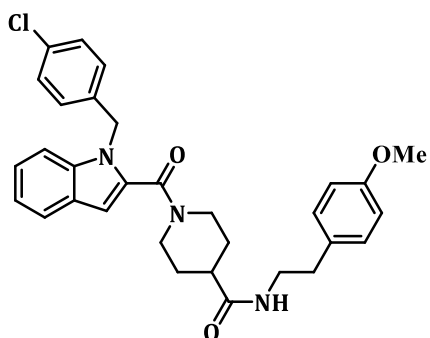
1-(1-(4-chlorobenzyl)-1H-indole-2-carbonyl)-N-(2-(pyridin-2-yl)ethyl)piperidine-4-carboxamide (CCG 205456, 57). Prepared by Method A using 2-(pyridin-2-yl)ethanamine. The crude material was triturated with ether and ethyl acetate and filtered to obtain the product as a white solid. Yield: 10%. ^1H NMR (400 MHz, DMSO- d_6) δ 8.52 – 8.45 (m, 1H), 7.87 (t, $J = 5.6$ Hz, 1H), 7.72 – 7.66 (m, 1H), 7.63 (d, $J = 7.9$ Hz, 1H), 7.54 (d, $J = 8.3$ Hz, 1H), 7.38 – 7.30 (m, 2H), 7.25 – 7.17 (m, 3H), 7.14 – 7.05 (m, 3H), 6.72 (s, 1H), 5.49 (s, 2H), 4.52 – 3.78 (m, 2H), 3.40 (q, $J = 6.9$ Hz, 2H), 3.08 – 2.76 (m, 4H), 2.38 – 2.29 (m, 1H), 1.74 – 1.23 (m, 4H). TOF ES+ MS: 501.1 (M+H), 523.1 (M+Na). HPLC ret. time = 5.51 min; purity >95%



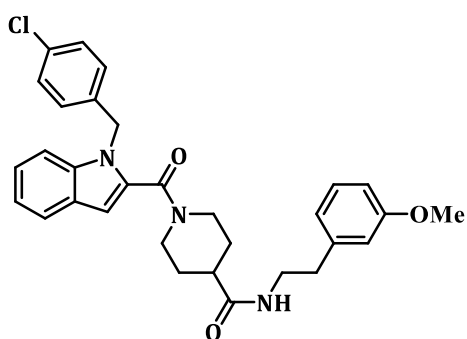
1-(1-(4-chlorobenzyl)-1*H*-indole-2-carbonyl)-*N*-(4-chlorophenethyl)piperidine-4-carboxamide (CCG 206400, 58). Prepared by Method A using 2-(4-chlorophenyl)ethanamine. The crude material was triturated in ethyl acetate to give the product as a white solid. Yield: 45%. ¹H NMR (400 MHz, DMSO- *d*₆) δ 7.85 (t, *J* = 5.7 Hz, 1H), 7.63 (d, *J* = 7.8 Hz, 1H), 7.54 (d, *J* = 8.4 Hz, 1H), 7.37 – 7.30 (m, 4H), 7.26 – 7.17 (m, 3H), 7.14 – 7.06 (m, 3H), 6.71 (s, 1H), 5.49 (s, 2H), 4.54 – 3.86 (m, 2H), 3.26 (q, *J* = 6.7 Hz, 2H), 2.90 (bs, 2H), 2.69 (t, *J* = 7.1 Hz, 2H), 2.36 – 2.30 (m, 1H), 1.76 – 1.22 (m, 4H). TOF ES+ MS: 534.1 (M+H), 556.1 (M+Na). HPLC ret. time = 8.25 min; purity > 95%.



1-(1-(4-chlorobenzyl)-1*H*-indole-2-carbonyl)-*N*-(4-fluorophenethyl)piperidine-4-carboxamide (CCG 206396, 59) Prepared by Method A using 2-(4-fluorophenyl)ethanamine. The crude material was triturated with ethyl acetate to obtain product as a white solid. Yield: 85%. ¹H NMR (400 MHz, DMSO- *d*₆) δ 7.84 (t, *J* = 5.7 Hz, 1H), 7.62 (d, *J* = 7.9 Hz, 1H), 7.54 (d, *J* = 8.4 Hz, 1H), 7.37 – 7.30 (m, 2H), 7.26 – 7.17 (m, 3H), 7.14 – 7.05 (m, 5H), 6.71 (s, 1H), 5.49 (s, 2H), 4.52 – 3.78 (m, 2H), 3.25 (q, *J* = 6.9 Hz, 2H), 2.91 (bs, 2H), 2.69 (t, *J* = 7.2 Hz, 2H), 2.38 – 2.28 (m, 1H), 1.62 (bs, 2H), 1.36 (bs, 2H). TOF ES+ MS: 518.1 (M+H), 540.1 (M+Na). HPLC ret. time = 7.91 min; purity > 95%.

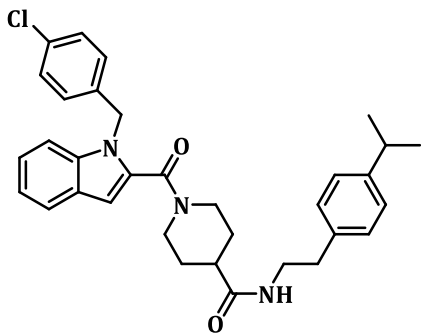


1-(1-(4-chlorobenzyl)-1H-indole-2-carbonyl)-N-(4-methoxyphenethyl)piperidine-4-carboxamide (CCG 206398, 60). Prepared by Method A using 2-(4-methoxyphenyl)ethanamine. The crude material was triturated with ethyl acetate to obtain product as a white solid. Yield: 63%. $^1\text{H NMR}$ (400 MHz, $\text{DMSO-}d_6$) δ 7.83 (t, $J = 5.6$ Hz, 1H), 7.63 (d, $J = 7.8$ Hz, 1H), 7.54 (d, $J = 8.4$ Hz, 1H), 7.37 – 7.30 (m, 2H), 7.26 – 7.17 (m, 1H), 7.14 – 7.05 (m, 6H), 6.88 – 6.81 (m, 2H), 6.71 (s, 1H), 5.49 (s, 2H), 4.49 – 3.84 (m, 2H), 3.71 (s, 3H), 3.22 (q, $J = 6.8$ Hz, 2H), 2.91 (bs, 2H), 2.63 (t, $J = 7.3$ Hz, 2H), 2.39 – 2.28 (m, 1H), 1.62 (bs, 2H), 1.37 (bs, 2H). TOF ES+ MS: 530.1 (M+H), 552.1 (M+Na). HPLC ret. time = 7.81 min; purity > 95%.

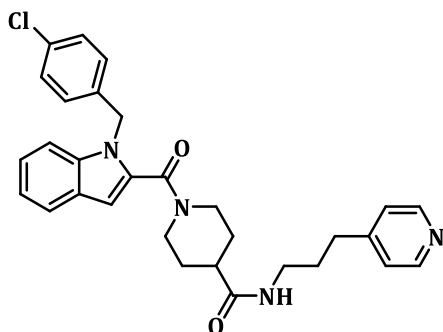


1-(1-(4-chlorobenzyl)-1H-indole-2-carbonyl)-N-(3-methoxyphenethyl)piperidine-4-carboxamide (CCG 206395, 61). Prepared by Method A using 2-(3-methoxyphenyl)ethanamine. The crude material was triturated with ethyl acetate to obtain product as a white solid. Yield: 67%. $^1\text{H NMR}$ (400 MHz, $\text{DMSO-}d_6$) δ 7.85 (t, J

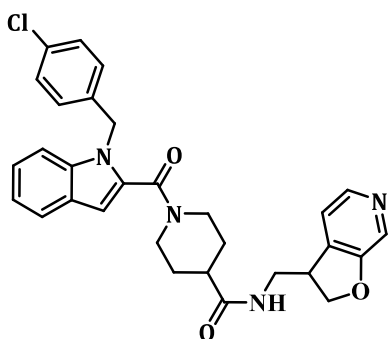
= 5.6 Hz, 1H), 7.63 (d, $J = 7.8$ Hz, 1H), 7.54 (d, $J = 8.4$ Hz, 1H), 7.37 – 7.30 (m, 2H), 7.26 – 7.14 (m, 2H), 7.14 – 7.06 (m, 3H), 6.78 – 6.73 (m, 3H), 6.71 (s, 1H), 5.49 (s, 2H), 4.51 – 3.86 (m, 2H), 3.72 (s, 3H), 3.26 (q, $J = 6.7$ Hz, 2H), 2.94 (s, 2H), 2.67 (t, $J = 7.2$ Hz, 2H), 2.37 – 2.30 (m, 1H), 1.62 (s, 2H), 1.37 (s, 2H). TOF ES+ MS: 530.1 (M+H), 552.1 (M+Na). HPLC ret. time = 7.86 min; purity > 95%.



1-(1-(4-chlorobenzyl)-1H-indole-2-carbonyl)-N-(4-isopropylphenethyl)piperidine-4-carboxamide (CCG 206461, 62). Prepared by Method A using 2-(4-isopropylphenyl)ethanamine. The crude material purified using medium pressure silica gel chromatography with a gradient of 0-60% ethyl acetate/hexanes to obtain product as a white solid. Yield: 37%. ^1H NMR (500 MHz, DMSO- d_6) δ 7.89 (t, $J = 5.7$ Hz, 1H), 7.62 (d, $J = 7.9$ Hz, 1H), 7.55 (d, $J = 8.3$ Hz, 1H), 7.37 – 7.31 (m, 2H), 7.26 – 7.18 (m, 1H), 7.17 – 7.07 (m, 7H), 6.71 (s, 1H), 5.49 (s, 2H), 4.52 – 3.83 (m, 2H), 3.24 (q, $J = 6.9$ Hz, 2H), 3.10 – 2.75 (m, 3H), 2.66 (t, $J = 7.4$ Hz, 2H), 2.39 – 2.31 (m, 1H), 1.85 – 1.10 (m, 10H). TOF ES+ MS: 542.2 (M+H), 564.1 (M+Na). HPLC ret. time = 8.71 min; purity > 95%.

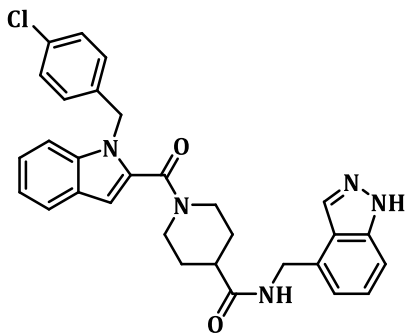


1-(1-(4-chlorobenzyl)-1H-indole-2-carbonyl)-N-(3-(pyridin-4-yl)propyl)piperidine-4-carboxamide (CCG 208788, 63). Prepared by Method A using 3-(pyridin-4-yl)propan-1-amine. The crude solid was triturated with ethyl acetate, giving a white solid. Yield: 40 mg, 31%. $^1\text{H NMR}$ (400 MHz, DMSO- d_6) δ 8.48 – 8.41 (m, 2H), 7.85 (t, $J = 5.6$ Hz, 1H), 7.62 (d, $J = 7.9$ Hz, 1H), 7.54 (d, $J = 8.4$ Hz, 1H), 7.37 – 7.30 (m, 2H), 7.26 – 7.17 (m, 3H), 7.14 – 7.05 (m, 3H), 6.72 (s, 1H), 5.49 (s, 2H), 4.41 (bs, 2H), 4.14 – 3.99 (m, 4H), 3.10 – 2.75 (m, 4H), 2.62 – 2.50 (m, 2H), 2.38 – 2.30 (m, 1H), 1.77 – 1.64 (m, 4H), 1.49 – 1.25 (m, 2H). TOF ES+ MS: 514.9 (M+H). HPLC ret. time = 5.58 min; purity > 95%

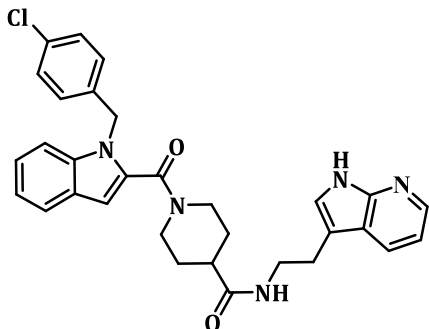


1-(1-(4-chlorobenzyl)-1H-indole-2-carbonyl)-N-((2,3-dihydrofuro[2,3-c]pyridin-3-yl)methyl)piperidine-4-carboxamide (CCG 206581, 64). Prepared by Method A using (2,3-dihydrofuro[2,3-c]pyridin-3-yl)methanamine. The crude material was triturated in ethyl acetate, filtered and concentrated to obtain a white solid. Yield: 50%. $^1\text{H NMR}$ (500

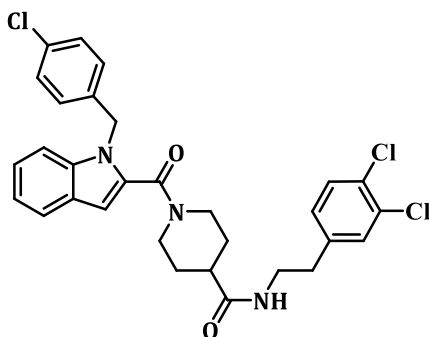
MHz, DMSO- d_6) δ 8.14 – 8.06 (m, 3H), 7.63 (d, $J = 7.9$ Hz, 1H), 7.55 (d, $J = 8.3$ Hz, 1H), 7.37 – 7.28 (m, 4H), 7.25 – 7.18 (m, 1H), 7.14 – 7.06 (m, 2H), 6.72 (s, 1H), 5.49 (s, 2H), 4.63 – 4.55 (m, 1H), 4.39 – 4.32 (m, 2H), 4.14 – 3.87 (m, 2H), 3.73 – 3.63 (m, 1H), 3.17 (d, $J = 5.3$ Hz, 1H), 2.86 – 2.82 (m, 2H), 2.40 – 2.34 (m, 1H), 1.76 – 1.15 (m, 4H). TOF ES+ MS: 529.1 (M+H). HPLC ret. time = 5.78 min; purity > 95%.



N-((1H-indazol-4-yl)methyl)-1-(1-(4-chlorobenzyl)-1H-indole-2-carbonyl)piperidine-4-carboxamide (CCG 215061, 70) Prepared by Method A using (1H-indazol-4-yl)methanamine. Product isolated as white solid. Yield: 32 %. ^1H NMR (500 MHz, DMSO- d_6) δ ppm 13.09 (s, 1 H), 8.43 (t, $J=6.1$ Hz, 1 H), 8.00 - 8.20 (m, 1 H), 7.63 (d, $J=8.1$ Hz, 1 H), 7.54 (d, $J=8.3$ Hz, 1 H), 7.42 (d, $J=8.3$ Hz, 1 H), 7.32 - 7.37 (m, 2 H), 7.25 - 7.30 (m, 1 H), 7.19 - 7.24 (m, 1 H), 7.08 - 7.14 (m, 3 H), 6.95 (d, $J=6.8$ Hz, 1 H), 6.73 (s, 1 H), 5.49 (d, $J=0.5$ Hz, 2 H), 3.89 - 4.65 (m, 4 H), 2.68 - 3.12 (m, 2 H), 2.46 (tt, $J=11.2, 3.9$ Hz, 1 H), 1.30 - 1.90 (m, 4 H). TOF ES+ MS: 526.2 (M+H), 548.1 (M+Na). HPLC (gradient A): ret. time = 6.85 min; purity > 95 %

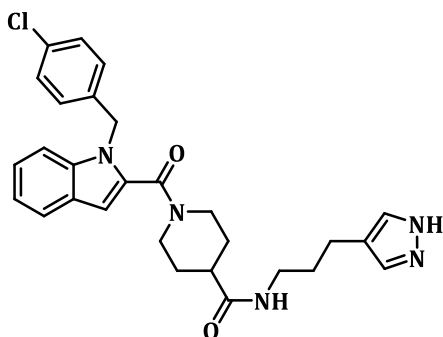


N-(2-(1H-pyrrolo[2,3-b]pyridin-3-yl)ethyl)-1-(1-(4-chlorobenzyl)-1H-indole-2-carbonyl)piperidine-4-carboxamide (CCG 222940, 71) Prepared by Method A using 2-(1H-pyrrolo[2,3-b]pyridin-3-yl)ethan-1-amine. Product isolated as white solid. Yield: 20 %. $^1\text{H NMR}$ (500 MHz, $\text{DMSO-}d_6$) δ ppm 11.34 (s, 1 H), 8.18 (dd, $J=4.6, 1.7$ Hz, 1 H), 7.84 - 8.01 (m, 2 H), 7.63 (d, $J=7.8$ Hz, 1 H), 7.54 (d, $J=8.5$ Hz, 1 H), 7.29 - 7.40 (m, 2 H), 7.15 - 7.29 (m, 2 H), 7.06 - 7.15 (m, 3 H), 7.03 (dd, $J=7.8, 4.6$ Hz, 1 H), 6.72 (s, 1 H), 5.49 (s, 2 H), 4.40 (br. s., 1 H), 3.96 (br. s., 1 H), 3.31 (q, $J=7.1$ Hz, 1 H), 2.73 - 3.09 (m, 4 H), 2.34 (tt, $J=11.1, 3.5$ Hz, 1 H), 1.24 - 1.81 (m, 4 H). TOF ES+ MS: 540.1 (M+H). HPLC (gradient A): ret. time = 5.84 min; purity > 95 %



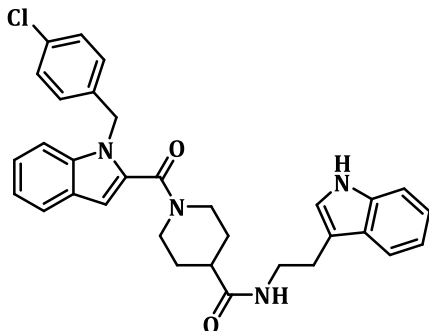
1-(1-(4-chlorobenzyl)-1H-indole-2-carbonyl)-N-(3,4-dichlorophenethyl)piperidine-4-carboxamide (CCG 222720, 72) Prepared by Method A using 2-(3,4-dichlorophenyl)ethan-1-amine. Isolated product as white solid. Yield: 37% $^1\text{H NMR}$

(500 MHz, DMSO- d_6) δ ppm 7.85 (t, $J=5.5$ Hz, 1 H), 7.63 (d, $J=8.1$ Hz, 1 H), 7.54 (dd, $J=8.3, 3.2$ Hz, 2 H), 7.44 - 7.48 (m, 1 H), 7.34 (d, $J=8.3$ Hz, 2 H), 7.16 - 7.25 (m, 2 H), 7.07 - 7.13 (m, 3 H), 6.71 (s, 1 H), 5.49 (br. s., 2 H), 4.40 (br. s., 1 H), 3.95 (br. s., 1 H), 3.28 (q, $J=6.8$ Hz, 2 H), 2.99 (br. s., 1 H), 2.84 (br. s., 1 H), 2.71 (t, $J=6.8$ Hz, 2 H), 2.32 (tt, $J=11.2, 3.9$ Hz, 1 H), 1.17 - 1.77 (m, 4 H). TOF ES+ MS: 568.0 (M+H), 590.0 (M+Na). HPLC (gradient A): ret. time = 8.41 min; purity > 95%

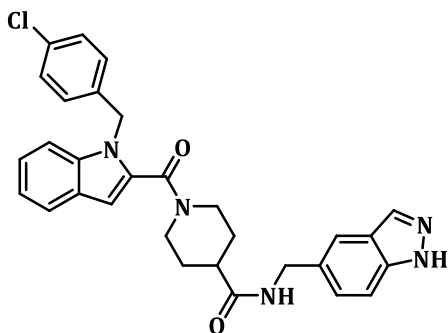


N-(3-(1H-pyrazol-4-yl)propyl)-1-(1-(4-chlorobenzyl)-1H-indole-2-

carbonyl)piperidine-4-carboxamide (CCG 222760, 73) Prepared by Method A using 3-(1H-pyrazol-4-yl)propan-1-amine. Product isolated as white solid. Yield: 35 %. ^1H NMR (500 MHz, DMSO- d_6) δ ppm 12.51 (brs, 1 H), 7.81 (t, $J=5.5$ Hz, 1 H), 7.52 - 7.64 (m, 2 H), 7.49 (brs, 1 H), 7.28 - 7.36 (m, 3 H), 7.19 - 7.24 (m, 1 H), 7.07 - 7.13 (m, 3 H), 6.72 (s, 1 H), 5.49 (brs, 2 H), 4.41 (brs, 1 H), 4.02 (brs, 1 H), 2.76 - 3.10 (m, 4 H), 2.31 - 2.44 (m, 3 H), 1.32 - 1.83 (m, 7 H). TOF ES+ MS: 504.3 (M+H). HPLC (gradient A): ret. time = 6.02 min; purity > 95 %.

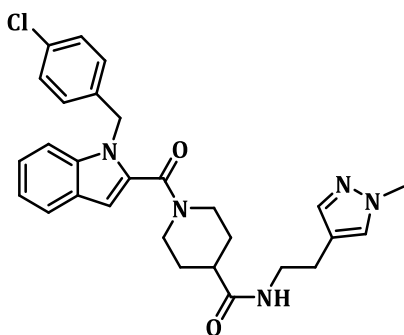


N-(2-(1H-indol-3-yl)ethyl)-1-(1-(4-chlorobenzyl)-1H-indole-2-carbonyl)piperidine-4-carboxamide (CCG222900, 74) Prepared by Method A using 2-(1H-indol-3-yl)ethan-1-amine. Product isolated as white solid. Yield: 30 %. ^1H NMR (500 MHz, DMSO- d_6) δ 10.80 (s, 1H), 7.91 (t, $J = 5.6$ Hz, 1H), 7.63 (d, $J = 7.9$ Hz, 1H), 7.54 (t, $J = 7.2$ Hz, 2H), 7.37 – 7.30 (m, 3H), 7.22 (t, $J = 7.4$ Hz, 1H), 7.15 – 7.08 (m, 4H), 7.06 (t, $J = 7.2$ Hz, 1H), 6.97 (t, $J = 7.3$ Hz, 1H), 6.72 (s, 1H), 5.49 (s, 2H), 4.54 – 3.81 (m, 2H), 3.32 (q, $J = 7.0, 6.4$ Hz, 2H), 3.07 – 2.76 (m, 4H), 2.36 (tt, $J = 11.2, 3.5$ Hz, 1H), 1.74 – 1.26 (m, 4H). TOF ES+ MS: 539.1 (M+H). HPLC (gradient A): ret. time = 7.69 min; purity > 95 %

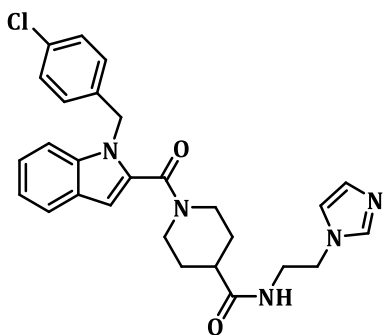


N-((1H-indazol-5-yl)methyl)-1-(1-(4-chlorobenzyl)-1H-indole-2-carbonyl)piperidine-4-carboxamide (CCG 215060, 75) Prepared by Method A using (1H-indazol-5-yl)methanamine. Isolated product as white solid. Yield: 53%. ^1H NMR (500 MHz, DMSO- d_6) δ ppm 13.00 (s, 1 H), 8.35 (t, $J=6.0$ Hz, 1 H), 8.02 (t, $J=1.3$ Hz, 1 H), 7.63 (d, $J=7.8$ Hz, 1 H), 7.58 (s, 1 H), 7.54 (d, $J=8.3$ Hz, 1 H), 7.48 (d, $J=8.8$ Hz, 1 H), 7.32 - 7.37

(m, 2 H), 7.19 - 7.26 (m, 2 H), 7.07 - 7.14 (m, 3 H), 6.73 (s, 1 H), 5.49 (s, 2 H), 4.26 - 4.58 (m, 3 H), 4.00 (br. s., 1 H), 2.73 - 3.10 (m, 2 H), 2.45 (tt, $J=11.2, 3.7$ Hz, 1 H), 1.30 - 1.89 (m, 4 H). TOF ES+ MS: 526.2 (M+H), 548.1 (M+Na). HPLC (gradient A): ret. time = 6.74 min; purity > 95%

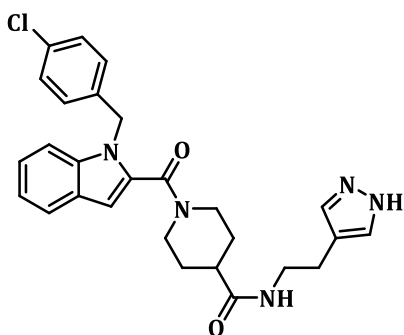


1-(1-(4-chlorobenzyl)-1H-indole-2-carbonyl)-N-(2-(1-methyl-1H-pyrazol-4-yl)ethyl)piperidine-4-carboxamide (CCG 215080, 76) Prepared by Method A using 2-(1-methyl-1H-pyrazol-4-yl)ethan-1-amine. Isolated product as white solid. Yield: 45 %. ^1H NMR (500 MHz, DMSO- d_6) δ ppm 7.86 (t, $J=5.7$ Hz, 1 H), 7.63 (dt, $J=8.1, 1.0$ Hz, 1 H), 7.54 (dd, $J=8.3, 0.7$ Hz, 1 H), 7.46 (s, 1 H), 7.32 - 7.36 (m, 2 H), 7.20 - 7.24 (m, 2 H), 7.09 - 7.13 (m, 3 H), 6.72 (d, $J=0.7$ Hz, 1 H), 5.49 (s, 2 H), 4.41 (br. s., 1 H), 3.97 (br. s., 1 H), 3.76 (s, 3 H), 3.12 - 3.21 (m, 2 H), 2.75 - 3.09 (m, 2 H), 2.50 (m, 2H), 2.35 (tt, $J=11.3, 3.7$ Hz, 1 H), 1.22 - 1.82 (m, 4 H). TOF ES+ MS: 504.1 (M+H), 526.1 (M+Na). HPLC (gradient A): ret. time = 6.45 min; purity > 95 %



***N*-(2-(1*H*-imidazol-1-yl)ethyl)-1-(1-(4-chlorobenzyl)-1*H*-indole-2-**

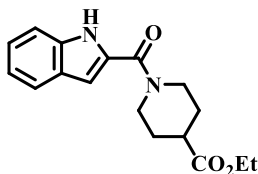
carbonyl)piperidine-4-carboxamide (CCG 206582, 77). Prepared by Method A using 2-(1*H*-imidazol-1-yl)ethanamine-HCl. The resulting crude solid was triturated with ethyl acetate to give a white solid. Yield: 18%. ¹H NMR (500 MHz, DMSO- *d*₆) δ 7.94 (t, *J* = 5.6 Hz, 1H), 7.63 (d, *J* = 7.9 Hz, 1H), 7.57 – 7.51 (m, 2H), 7.37 – 7.31 (m, 2H), 7.25 – 7.18 (m, 1H), 7.13 – 7.06 (m, 4H), 6.87 (s, 1H), 6.71 (s, 1H), 5.49 (s, 2H), 4.39 (s, 1H), 4.07 – 3.99 (m, 3H), 3.39 – 3.31 (m, 2H), 2.93 (bs, 2H), 2.39 – 2.29 (m, 1H), 1.79 – 1.20 (m, 4H). TOF ES+ MS: 490.1 (M+H). HPLC ret. time = 5.69 min; purity = 90%.



***N*-(2-(1*H*-pyrazol-4-yl)ethyl)-1-(1-(4-chlorobenzyl)-1*H*-indole-2-carbonyl)piperidine-**

4-carboxamide (CCG 215153, 78) Prepared by Method A using 2-(1*H*-pyrazol-4-yl)ethan-1-amine. Product obtained as white solid. Yield: 43 %. ¹H NMR (500 MHz, DMSO-*d*₆) δ ppm 12.53 (br. s., 1 H), 7.87 (t, *J*=5.5 Hz, 1 H), 7.63 (d, *J*=7.8 Hz, 1 H), 7.54 (d, *J*=8.3 Hz, 1 H), 7.42 (br. s., 1 H), 7.32 - 7.36 (m, 2 H), 7.18 - 7.25 (m, 1 H), 7.07 - 7.14 (m, 3 H), 6.72 (s, 1 H), 5.49 (s, 2 H), 4.42 (br. s., 1 H), 3.98 (br. s., 1 H), 3.19 (q, *J*=7.0 Hz, 2 H), 2.71 - 3.09 (m, 2 H), 2.55 (t, *J*=7.3 Hz, 2 H), 2.36 (tt, *J*=11.4, 3.8 Hz, 1 H), 1.25 - 1.84 (m, 4 H). TOF ES+ MS: 489.9 (M+H), 511.9 (M+Na). HPLC (gradient A): ret. time = 5.90 min; purity > 95%

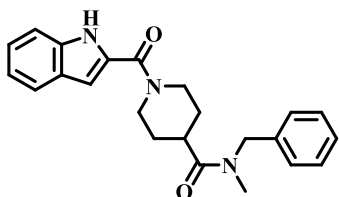
N1-indole derivatives



Ethyl 1-(1*H*-indole-2-carbonyl)piperidine-4-carboxylate (160). Ethyl 1*H*-indole-2-carboxylate (155, 3.0 g, 16 mmol) and lithium hydroxide, H₂O (3.3 g, 79 mmol) were dissolved in 2/1 water/THF (30 mL). The reaction was stirred overnight. The reaction was diluted with water and diethyl ether. The water layer was washed with diethyl ether twice. The aqueous layer was acidified to pH 2 using 2N HCl. The suspension was extracted using ethyl acetate. The organic layer was washed with saturated sodium chloride solution, dried over magnesium sulfate, filtered and concentrated to obtain 1*H*-Indole-2-carboxylic acid as a white solid. Yield: 2.39 g, 94%. ¹H NMR (400 MHz, DMSO- *d*₆) δ 12.95 (s, 1H), 11.74 (s, 1H), 7.67 – 7.60 (m, 1H), 7.47 – 7.39 (m, 1H), 7.28 – 7.19 (m, 1H), 7.11 – 7.01 (m, 2H).

1*H*-indole-2-carboxylic acid (2.49 g, 15.45 mmol), EDCI (4.44 g, 23.18 mmol), and HOBT (3.55 g, 23.18 mmol) were dissolved in THF (30 mL). The reaction was allowed to stir for 15 minutes before DIEA (4.05 ml, 23.18 mmol) and ethyl piperidine-4-carboxylate (3.57 mL, 23.18 mmol) were added to the reaction. The reaction was diluted with water and ethyl acetate. The organic layer was washed with saturated sodium bicarbonate, 1M HCl, and saturated sodium chloride. The organic layer was then dried over magnesium sulfate, filtered and concentrated. The resulting solid was triturated with ethyl acetate to obtain the product as a white solid. Yield: 3.27 g, 71%. ¹H NMR (400 MHz, DMSO- *d*₆) δ 11.55 (s, 1H), 7.60 (d, *J* = 8.1 Hz, 1H), 7.41 (d, *J* = 8.2 Hz, 1H), 7.22

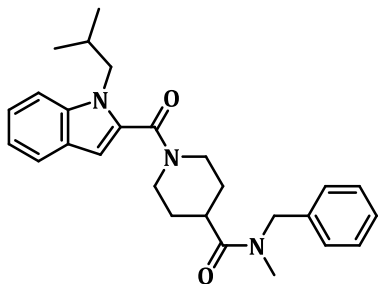
– 7.13 (m, 1H), 7.08 – 7.00 (m, 1H), 6.80 – 6.74 (m, 1H), 4.34 (dt, $J = 13.4, 3.9$ Hz, 2H), 4.09 (q, $J = 7.1$ Hz, 2H), 3.18 (bs, 2H), 2.76 – 2.64 (m, 1H), 1.99 – 1.88 (m, 2H), 1.65 – 1.50 (m, 2H), 1.20 (t, $J = 7.1$ Hz, 3H).



***N*-benzyl-1-(1*H*-indole-2-carbonyl)-*N*-methylpiperidine-4-carboxamide (90)** Ester **160** (3.0 g, 10 mmol) and lithium hydroxide, H₂O (4.19 g, 100 mmol) were dissolved in THF (Ratio: 1, Volume: 20 ml) and Water (Ratio: 2, Volume: 40.0 ml) and allowed to stir overnight at room temperature. The reaction was diluted with water, and extracted with diethyl ether. The aqueous layer was acidified using 2N HCl to pH ~2. A fine, white suspension resulted. The aqueous layer was extracted with ethyl acetate twice. The combined ethyl acetate layers were dried over magnesium sulfate, filtered and concentrated to afford the 1-(1*H*-indole-2-carbonyl)piperidine-4-carboxylic acid as a white solid. Yield: 678 mg, 25%. ¹H NMR (400 MHz, DMSO- *d*₆) δ 12.33 (s, 1H), 11.54 (s, 1H), 7.60 (d, $J = 8.0$ Hz, 1H), 7.41 (d, $J = 7.5$ Hz, 1H), 7.22 – 7.13 (m, 1H), 7.08 – 6.99 (m, 1H), 6.79 – 6.74 (m, 1H), 4.32 (d, $J = 13.3$ Hz, 2H), 3.17 (bs, 1H), 2.65 – 2.54 (m, 1H), 1.96 – 1.87 (m, 2H), 1.63 – 1.49 (m, 2H). HPLC ret. time = 5.31 min; purity > 95%.

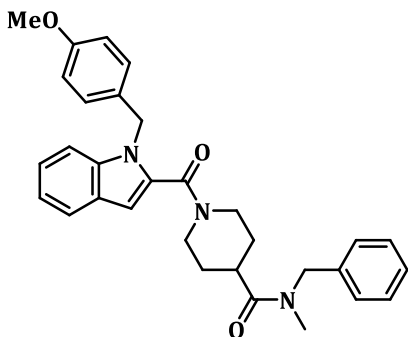
1-(1*H*-indole-2-carbonyl)piperidine-4-carboxylic acid (1.00g, 3.67 mmol), EDCI (1.408 g, 7.34 mmol), and HOBt hydrate (1.125 g, 7.34 mmol) were dissolved in DCM (10 ml). The reaction was allowed to stir for 10 minutes before adding DIEA (1.283 ml, 7.34 mmol) and *N*-methyl-1-phenylmethanamine (0.836 ml, 7.34 mmol). The reaction

was allowed to stir overnight at room temperature. The reaction was diluted with water and ethyl acetate. The organic phase was washed with saturated sodium bicarbonate, 1N HCl, and saturated sodium chloride solution. The organic layer was dried over magnesium sulfate, filtered and concentrated. The crude material was purified by silica gel chromatography using 30% to 60% ethyl acetate: hexanes to obtain product as a white solid. Yield: 1.03 g, 75% ¹H NMR (400 MHz, DMSO- *d*₆) 1.7:1 mixture of rotamers δ 11.59 – 11.53 (m, 1H), 7.64 – 7.56 (m, 1H), 7.45 – 7.13 (m, 7H), 7.09 – 6.99 (m, 1H), 6.78 (rotamer A, s), 6.75 (rotamer B, s, 1H), 4.69 (rotamer A, s, 1H), 4.54 – 4.37 (m, 3H), 3.28 – 2.92 (m, 5H), 2.79 (rotamer B, s, 1H), 1.86 – 1.77 (m, 1H), 1.75 – 1.55 (m, 3H). TOF ES+ MS: 376.2 (M+H), 398.1 (M+Na). HPLC ret. time = 6.10 min; purity = 93%.



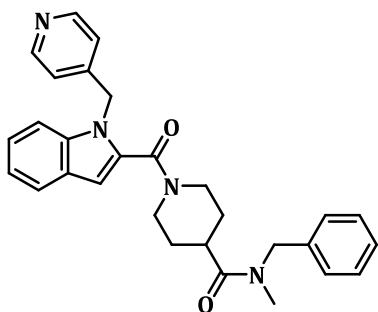
***N*-benzyl-1-(1-isobutyl-1*H*-indole-2-carbonyl)-*N*-methylpiperidine-4-carboxamide (CCG 206332, 80).** Compound **90** (100 mg, 0.27 mmol) was dissolved in 1.0 mL of DMF and added to a suspension of sodium hydride (12.8 mg, 0.32 mmol) in 2.0 mL of DMF. The reaction was stirred at 80 °C for 10 minutes before adding 1-iodo-2-methylpropane (0.061 mL, 0.53 mmol). The reaction was allowed to stir overnight. After 18 hours, the reaction was cooled to room temperature before diluting with water and ethyl acetate. The organic phase was washed with water followed by saturated sodium chloride, dried over magnesium sulfate, filtered and concentrated. The crude material was purified via column chromatography using 50% ethyl acetate/hexanes to 100% ethyl

acetate. The purification provided the product as a white solid. Yield: 28 mg (25%). ^1H NMR (400 MHz, $\text{DMSO-}d_6$) δ 7.64 – 7.50 (m, 2H), 7.42 – 7.15 (m, 6H), 7.12 – 7.03 (m, 1H), 6.67 (rotamer A, s), 6.64 (rotamer B, s, 1H), 4.67 (rotamer A, s, 1H), 4.60-4.26 (s, 3H), 4.24-3.98 (m, 2H), 3.00 (s, 5H), 2.79 (s, 1H), 2.06 – 1.92 (m, 1H), 1.78 (bs, 1H), 1.72 – 1.49 (m, 3H), 0.84 – 0.71 (m, 6H). TOF ES+ MS: 432.2 (M+H), 454.2 (M+Na). HPLC ret. time = 7.80 min; purity = 94%.



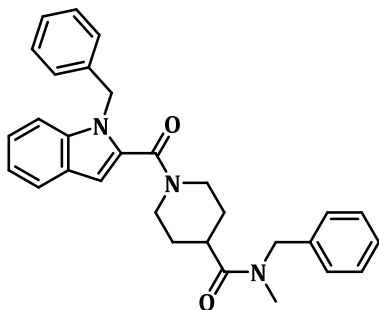
***N*-benzyl-1-(1-(4-methoxybenzyl)-1*H*-indole-2-carbonyl)-*N*-methylpiperidine-4-carboxamide (CCG 205477, 81)** Compound **90** (100 mg, 0.266 mmol) was added to a suspension of sodium hydride (12.8 mg, 0.32 mmol) in THF (1.5 mL). The reaction was stirred for 10 minutes before 1-(bromomethyl)-4-methoxybenzene (0.039 mL, 0.27 mmol) was added. The reaction was allowed to stir at room temperature overnight. The reaction was diluted with water and extracted with ethyl acetate. The organic layer was washed with water and saturated sodium chloride solution. It was dried over magnesium sulfate, filtered and concentrated. The crude material was purified by flash chromatography using a gradient of 50% - 100% ethyl acetate in hexanes to obtain the product as a white solid. Yield: 42 mg (32%). ^1H NMR (400 MHz, $\text{DMSO-}d_6$) 1.7:1 mixture of rotamers δ 7.66 – 7.57 (m, 2H), 7.40 – 7.04 (m, 8H), 6.85-6.81(m, 3H), 6.69 (rotamer A, s), 6.65 (rotamer B, s, 1H), 5.46 – 5.39 (m, 2H), 4.64 (rotamer A, s, 1H),

4.53-4.20 (m, 2H), 3.97 (bs, 1H), 3.69-3.66(m, 3H), 3.19 – 2.83 (m, 5H), 2.78 (rotamer B, s, 1H), 1.82 – 1.24 (m, 4H). TOF ES+ MS: 496.1 (M+H), 518.1 (M+Na). HPLC ret. time = 7.83 min; purity = 92%.

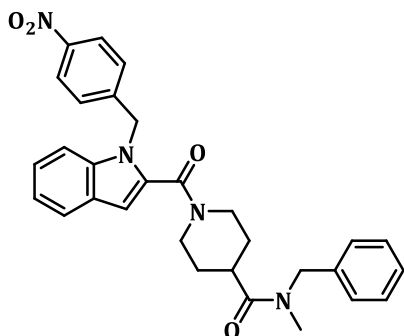


***N*-benzyl-*N*-methyl-1-(1-(pyridin-4-ylmethyl)-1*H*-indole-2-carbonyl)piperidine-4-carboxamide (CCG 208789, 82)** Pyridin-4-ylmethanol (180 mg, 1.65 mmol) and TEA (0.22 mL, 1.6 mmol) were dissolved in THF (7 mL) and cooled to 0 °C. Methanesulfonyl chloride (0.125 mL, 1.6 mmol) was added dropwise and the reaction was allowed to warm to room temperature and stirred overnight. To a suspension of 60 wt% sodium hydride (21.5 mg, 0.538 mmol) in 3.5 mL of DMF, compound 90 (200 mg, 0.533 mmol) was added as a 1.0 mL DMF solution. The reaction was allowed to stir for 10 minutes before a 0.5 mL DMF solution of mesylated alcohol was added. The reaction was stirred at room temperature overnight. After 15 hours, the reaction was diluted with water and ethyl acetate. The aqueous phase was washed with another aliquot of ethyl acetate. The combined organic phases were washed with saturated sodium chloride, dried over magnesium sulfate, filtered and concentrated. The crude black oil was purified via SP1 Biotage using a gradient of 100% ethyl acetate to 10% methanol: ethyl acetate. The product isolated as a white solid. Yield: 25 mg (10%). ¹H NMR (500 MHz, DMSO- *d*₆) 1.8:1 mixture of rotamers δ 8.48 – 8.42 (m, 2H), 7.69 – 7.62 (m, 1H), 7.51 – 7.45 (m, 1H), 7.41 – 7.08 (m, 7H), 7.02 – 6.96 (m, 2H), 6.80 (rotamer A, s), 6.77 (rotamer B, s,

1H), 5.59 – 5.53 (m, 2H), 4.65 (rotamer A, s, 1H), 4.52 – 4.48 (m, 2H), 4.11 (bs, 1H), 3.17 (d, $J = 5.3$ Hz, 2H), 3.10-2.87 (m, H), 2.77 (rotamer B, s, 1H), 1.86-1.33 (bm, 4H). TOF ES+ MS: 467.0(M+H). HPLC ret. time = 5.52 min; purity > 95%.



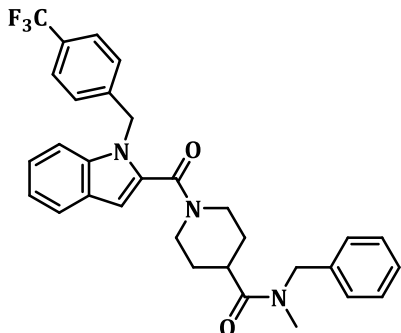
***N*-benzyl-1-(1-benzyl-1*H*-indole-2-carbonyl)-*N*-methylpiperidine-4-carboxamide (CCG 205404, 83)** Compound **90** (50 mg, 0.133 mmol) was dissolved in 0.5 mL of DMF and cooled to 0 °C. Lithium bis(trimethylsilyl)amide (0.146 ml, 0.146 mmol) was added dropwise and the reaction was allowed to stir for 10 minutes. Benzyl bromide (0.024 ml, 0.20 mmol) was added to the reaction, and it was allowed to stir overnight at room temperature. The reaction was quenched with water. It was then extracted with ethyl acetate. The organic extracts were washed with saturated sodium chloride solution three times and dried over magnesium sulfate, filtered and concentrated. The crude material was purified through flash silica gel chromatography using 25% EtOAc:DCM to give the product as a white solid. Yield: 41 mg (66%). ¹H NMR (400 MHz, DMSO- *d*₆) 1.6:1 mixture of rotamers δ 7.68 – 7.52 (m, 2H), 7.45 – 6.98 (m, 12H), 6.72 (rotamer A, s), 6.69 (rotamer B, s, 1H), 5.54-5.41 (m, 2H), 4.64 (s, 1H), 4.52 – 4.23 (m, 2H), 4.01 (bs, 1H), 3.18 – 2.85 (m, 5H), 2.78 (rotamer B, s, 1H), 1.73 – 1.23 (m, 4H). TOF ES+ MS: 466.2 (M+H), 488.2 (M+Na). HPLC ret. time = 7.86 min; purity > 95%.



***N*-benzyl-*N*-methyl-1-(1-(4-nitrobenzyl)-1*H*-indole-2-carbonyl)piperidine-4-**

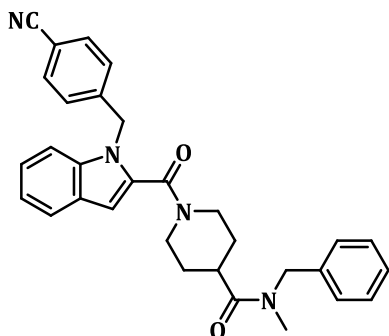
carboxamide (CCG 205484, 84) Compound **90** (50 mg, 0.133 mmol) was added to a suspension of sodium hydride (60 wt% in oil, 8.0 mg, 0.20 mmol) in DMF (2 ml). The reaction was allowed to stir for 10 minutes at 60 °C. 1-(chloromethyl)-4-nitrobenzene (45.7 mg, 0.266 mmol) and potassium iodide (44.2 mg, 0.266 mmol) were added and the reaction was stirred overnight at 60 °C. The reaction was diluted with water and ethyl acetate. The organic layer was washed with water and saturated sodium chloride solution. It was dried over magnesium sulfate, filtered and concentrated. The crude material was purified using 40-100% ethyl acetate: hexanes to afford the product as a white solid.

Yield: 11 mg, 16%. ¹H NMR (400 MHz, DMSO- *d*₆) 1.7:1 mixture of rotamers δ 8.20 – 8.11 (m, 2H), 7.70 – 7.62 (m, 1H), 7.55 (d, *J* = 8.4 Hz, 1H), 7.40 – 7.10 (m, 9H), 6.80 (rotamer A, s), 6.77 (rotamer B, s, 1H), 5.70 – 5.63 (m, 2H), 4.62 (rotamer A, s, 1H), 4.49 – 4.25 (m, 2H), 4.08 (bs, 1H), 3.18 – 2.87 (m, 5H), 2.74 (rotamer B, s, 1H), 1.39 (bm, 4H). TOF ES+ MS: 511.1 (M+H). HPLC ret. time = 7.56 min; purity > 95%.



***N*-benzyl-*N*-methyl-1-(1-(4-(trifluoromethyl)benzyl)-1*H*-indole-2-**

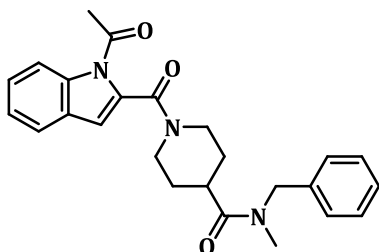
carbonyl)piperidine-4-carboxamide (CCG 208917, 85) Compound 90 (200 mg, 0.533 mmol), Cs₂CO₃ (347 mg, 1.065 mmol), and 1-(bromomethyl)-4-(trifluoromethyl)benzene (0.124 mL, 0.799 mmol) were dissolved in DMF (5.0 mL) and heated to 70 °C overnight. The reaction was diluted with water and ethyl acetate and ether (1:1). The aqueous layer was back extracted with ethyl acetate. The organic phase was washed with saturated sodium chloride (3x), dried over sodium sulfate, filtered and concentrated. The resulting crude material was purified via SP1 Biotage with a gradient of 30% ethyl acetate/hexanes to 100% ethyl acetate. The product was isolated as a white solid. Yield: 90 mg (32%). ¹H NMR (500 MHz, DMSO- *d*₆) 2:1 mixture of rotamers δ 7.68 – 7.61 (m, 3H), 7.55 – 7.49 (m, 1H), 7.41 – 7.07 (m, 9H), 6.79 (rotamer A, s), 6.75 (rotamer B, s, 1H), 5.64 – 5.59 (m, 2H), 4.64 (s, 1H), 4.51 – 4.25 (m, 1H), 4.09 (bs, 1H), 2.96 (s, 5H), 2.77 (s, 1H), 1.86 – 1.22 (m, 4H). TOF ES+ MS: 534.0 (M+H), 556.0 (M+Na). HPLC ret. time = 8.25 min; purity = 92%.



***N*-benzyl-1-(1-(4-cyanobenzyl)-1*H*-indole-2-carbonyl)-*N*-methylpiperidine-4-**

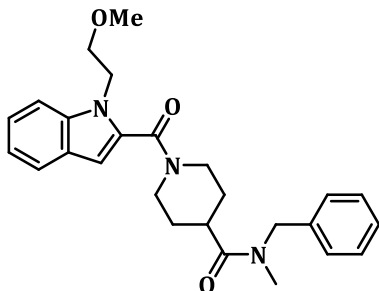
carboxamide (CCG 206330, 86) Sodium iodide (99 mg, 0.660 mmol) and 4-(chloromethyl)benzonitrile (100 mg, 0.660 mmol) were dissolved in acetone (2.2 mL) and allowed to stir at room temperature for 4 hours. The resulting solid was filtered and the filtrate concentrated to obtain crude 4-(iodomethyl)benzonitrile (130 mg, 0.535 mmol, 81% yield) as an orange oil. It was taken directly to the next step without characterization and purification. Compound **90** (100 mg, 0.266 mmol) was dissolved in 1.0 mL of DMF and added to a suspension of sodium hydride (12.78 mg, 0.320 mmol) in 2.0 of DMF. The reaction was stirred at 80 °C for 10 minutes before adding 4-(iodomethyl)benzonitrile (129 mg, 0.533 mmol) dissolved in 2.0 mL of DMF. The reaction was allowed to stir overnight. After 18 hours, the reaction was cooled to room temperature before diluting with water and ethyl acetate. The organic phase was washed with water followed by saturated sodium chloride, dried over magnesium sulfate, filtered and concentrated. The crude material was purified via flash column chromatography using a gradient of 50% ethyl acetate/hexanes to 100% ethyl acetate. The purification provided product as a white solid. Yield: 50 mg, 38%. ¹H NMR (400 MHz, DMSO-*d*₆) 1.7:1 mixture of rotamers δ 7.78 – 7.70 (m, 2H), 7.69 – 7.61 (m, 1H), 7.52 (d, *J* = 8.4 Hz, 1H), 7.43 – 7.07 (m, 9H), 6.78 (rotamer A, s), 6.75 (rotamer B, s, 1H), 5.64 – 5.57 (m,

2H), 4.64 (rotamer A, s, 1H), 4.52 – 4.25 (m, 2H), 4.04 (bs, 1H), 3.18 - 2.84 (m, 5H), 2.78 (rotamer B, s, 1H), 1.78 – 1.17 (m, 4H). TOF ES+ MS: 491.1 (M+H). HPLC ret. time = 7.54 min; purity = 94%.



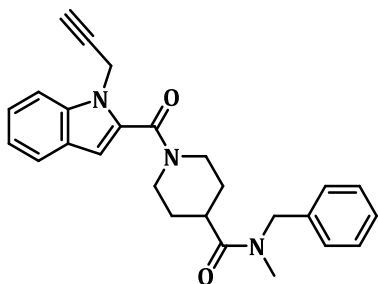
1-(1-acetyl-1H-indole-2-carbonyl)-N-benzyl-N-methylpiperidine-4-carboxamide

(CCG 206333, **87**) A solution of compound **90** (100 mg, 0.27 mmol) in 1 mL of DMF was added to a suspension of sodium hydride (11.7 mg, 0.29 mmol) in 2.0 mL DMF. The reaction was stirred at 80 °C for 10 minutes before adding acetic anhydride (0.050 mL, 0.53 mmol). The reaction was allowed to stir for 5 hours before it was cooled to room temperature and diluted with ammonium chloride and ethyl acetate. The organic phase was washed with saturated ammonium chloride twice, followed by saturated sodium chloride, dried over magnesium sulfate, filtered and concentrated. The crude material was purified via flash chromatography using a gradient of 50% ethyl acetate/hexanes to 100% ethyl acetate. Purification afforded the product as a white. Yield: 13 mg (12%). ¹H NMR (400 MHz, DMSO-*d*₆) 1.6:1 mixture of rotamers δ 8.15 – 8.07 (m, 1H), 7.69 – 7.61 (m, 1H), 7.44 – 7.15 (m, 6H), 6.91 (rotamer A, s), 6.88 (rotamer B, s, 1H), 4.67 (rotamer A, s, 1H), 4.56 – 4.33 (m, 2H), 4.00 – 3.84 (m, 1H), 3.21 – 2.85 (m, 5H), 2.79 (s, 1H), 2.61 (rotamer A, s, 2H), 2.59 (rotamer B, s, 1H), 1.91 – 1.48 (m, 4H). TOF ES+ MS: 418.1 (M+H), 440.1 (M+Na). HPLC ret. time = 6.52 min; purity > 95%.



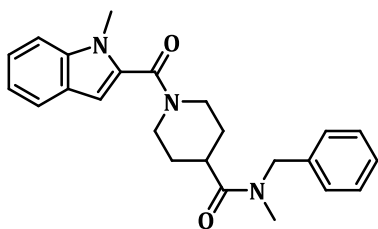
***N*-benzyl-1-(1-(2-methoxyethyl)-1*H*-indole-2-carbonyl)-*N*-methylpiperidine-4-**

carboxamide (CCG 206331, 88) Compound **90** (50 mg, 0.13 mmol) dissolved in 0.5 mL of DMF was added to a suspension of sodium hydride (7.99 mg, 0.200 mmol) in 1.0 mL of DMF. The reaction was heated at 70 °C for ten minutes before adding 2-methoxyethyl 4-methylbenzenesulfonate (0.144 mL, 0.266 mmol). The reaction was allowed to stir overnight. After 18 hours, the reaction was cooled to room temperature before diluting with water and ethyl acetate. The organic phase was washed with water followed by saturated sodium chloride, dried over magnesium sulfate, filtered and concentrated. The crude material was purified via flash column chromatography using a gradient of 50-80% ethyl acetate/hexanes. The purification provided the product as a white solid. Yield: 20 mg (35%). ¹H NMR (400 MHz, DMSO-*d*₆) 1.7:1 mixture of rotamers δ 7.63 – 7.50 (m, 2H), 7.42 – 7.15 (m, 6H), 7.13 – 7.03 (m, 1H), 6.64 (rotamer A, s), 6.60 (rotamer B, s, 1H), 4.68 (s, 1H), 4.61 – 4.37 (m, 4H), 4.18 (bs, 1H), 3.62 – 3.44 (m, 2H), 3.19 – 3.14 (m, 3H), 3.11 – 2.92 (m, 5H), 2.79 (s, 1H), 1.89 – 1.48 (m, 4H). TOF ES+ MS: 434.2 (M+H), 456.1 (M+Na). HPLC ret. time = 7.03 min; purity > 95%.



N-benzyl-N-methyl-1-(1-(prop-2-yn-1-yl)-1H-indole-2-carbonyl)piperidine-4-

carboxamide (CCG 206401, 89) sodium hydride (12.78 mg, 0.320 mmol) was added to an oven dried flask and placed under nitrogen. It was then suspended in 1.0 mL of DMF. The suspension was placed in a 70 °C oil bath before adding N-benzyl-1-(1H-indole-2-carbonyl)-N-methylpiperidine-4-carboxamide **90** (100 mg, 0.266 mmol) as a 0.5 mL DMF solution. The reaction was allowed to stir for 20 minutes before the addition of 3-bromoprop-1-yne (0.047 ml, 0.533 mmol) dropwise. The reaction was allowed to stir overnight. The reaction was cooled and diluted with saturated ammonium chloride and ethyl acetate. The organic layer was washed with saturated ammonium chloride followed by saturated sodium chloride. The organic layer was dried over magnesium sulfate, filtered, and concentrated. The yellow crude material was purified via Biotage column 30-70% ethyl acetate:hexanes 4 gram silicycle column to obtain white solid. Yield: 50 mg, 46% ¹H NMR (500 MHz, DMSO-*d*₆) □ ppm 7.55 - 7.69 (m, 2 H), 7.08 - 7.43 (m, 7 H), 6.75 (rotomer A, s, 0.6 H), 6.71 (rotomer B, s, 0.3 H), 5.09 - 5.17 (m, 2 H), 3.87 - 4.71 (m, 4 H), 3.23 - 3.29 (m, 1 H), 2.89 - 3.13 (m, 5 H), 2.79 (s, 1 H), 1.51 - 2.00 (m, 4 H). ES+ MS: 414.1 (M+H), 436.1 (M+Na). HPLC (gradient A): ret. time = 7.10 min; purity = 93 %



N-benzyl-N-methyl-1-(1-methyl-1H-indole-2-carbonyl)piperidine-4-carboxamide

(CCG 205428, 91) N-benzyl-1-(1H-indole-2-carbonyl)-N-methylpiperidine-4-

carboxamide (100 mg, 0.266 mmol) was added to a suspension of sodium hydride (12.78

mg, 0.320 mmol) in THF (Volume: 1.5 mL) at 0 °C. The reaction was stirred for 10

minutes before iodomethane (0.200 mL, 3.20 mmol) was added. The reaction was

allowed to stir at room temperature overnight. The reaction was diluted with water and

extracted with ethyl acetate. The organic layer was washed with water and saturated

sodium chloride solution. It was dried over magnesium sulfate, filtered and concentrated.

The crude material was purified using 50% - 100% ethyl acetate in hexanes. To obtain

product as white solid. Yield: 42 mg, 40 %. ¹H NMR (400 MHz, DMSO-*d*₆) δ ppm

7.54 - 7.60 (m, 1 H), 7.45 - 7.50 (m, 1 H), 7.13 - 7.39 (m, 6 H), 7.03 - 7.09 (m, 1 H), 6.57

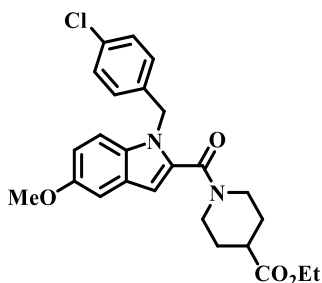
- 6.63 (m, 1 H), 4.65 (s, 1 H), 3.95 - 4.55 (m, 2 H), 3.67 - 3.77 (m, 3 H), 2.82 - 3.18 (m, 4

H), 2.76 (s, 1 H), 1.48 - 1.86 (m, 4 H). ES+ MS: 390.1 (M+H), 412.1 (M+Na). HPLC

(gradient A): ret. time = 6.92 min; purity > 95 %

HPLC (gradient A): ret. time = 4.32 min; purity > 95 %

5-hydroxy indole derivatives



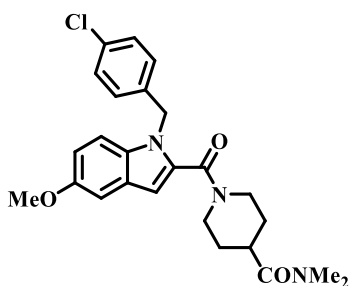
ethyl 1-(1-(4-chlorobenzyl)-5-methoxy-1H-indole-2-carbonyl)piperidine-4-

carboxylate (166)

ethyl 1-(5-methoxy-1H-indole-2-carbonyl)piperidine-4-carboxylate was prepared by Method A using 5-methoxy-1H-indole-2-carboxylic acid (3.0 g, 15.7 mmol) and ethyl piperidine-4-carboxylate (4.8 mL, 31.4 mmol). Product obtained as a peach solid. Yield: 3.2 g, 62.1 %. $^1\text{H NMR}$ (500 MHz, $\text{DMSO-}d_6$) δ ppm 11.40 (s, 1 H), 7.30 (d, $J=8.8$ Hz, 1 H), 7.06 (d, $J=2.4$ Hz, 1 H), 6.83 (dd, $J=8.9, 2.6$ Hz, 1 H), 6.68 (d, $J=1.5$ Hz, 1 H), 4.33 (dt, $J=13.5, 4.1$ Hz, 2 H), 4.09 (q, $J=7.1$ Hz, 2 H), 3.75 (s, 3 H), 3.17 (br. s., 2 H), 2.69 (tt, $J=11.0, 4.0$ Hz, 1 H), 1.88 - 1.97 (m, 2 H), 1.48 - 1.64 (m, 2 H), 1.20 (t, $J=7.1$ Hz, 3 H)

1-chloro-4-(chloromethyl)benzene (366 mg, 2.270 mmol) and sodium iodide (340 mg, 2.270 mmol) were dissolved in Acetone (Ratio: 1.000, Volume: 5.00 mL) and stirred overnight. The resulting precipitate was filtered and the filtrate was concentrated to obtain 4-chlorobenzyl iodide. Ethyl 1-(5-methoxy-1H-indole-2-carbonyl)piperidine-4-carboxylate (500 mg, 1.513 mmol), cesium carbonate (986 mg, 3.03 mmol), and 4-chlorobenzyl iodide were dissolved in DMF (Ratio: 1.000, Volume: 5 mL) and heated to 60 °C overnight. The reaction was diluted with water and ethyl acetate. The aqueous layer was washed with another portion of ethyl acetate. The organic phases were

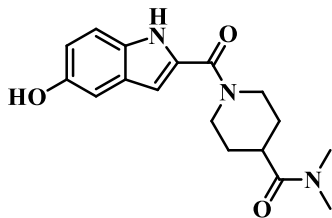
combined, washed with saturated sodium chloride, dried over sodium sulfate, filtered and concentrated. The crude material was purified using flash chromatography with 10-70% ethyl acetate/hexanes to obtain product as a white solid. Yield: 606 mg, 88 %. ^1H NMR (500 MHz, $\text{DMSO-}d_6$) δ ppm 7.48 (d, $J=9.0$ Hz, 1 H), 7.27 - 7.35 (m, 2 H), 7.11 (d, $J=2.4$ Hz, 1 H), 7.01 - 7.08 (m, 2 H), 6.87 (dd, $J=8.9, 2.6$ Hz, 1 H), 6.63 (s, 1 H), 5.45 (s, 2 H), 3.81 - 4.42 (m, 2 H), 3.76 (s, 3 H), 2.68 - 3.25 (m, 1 H), 2.57 (tt, $J=11.0, 3.9$ Hz, 1 H), 0.97 - 1.95 (m, 5 H).



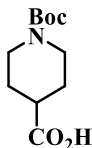
1-(1-(4-chlorobenzyl)-5-methoxy-1H-indole-2-carbonyl)-N,N-dimethylpiperidine-4-carboxamide (CCG 211759, 100) 166 (1.2 g, 2.64 mmol) was dissolved in Ethanol (Volume: 30 ml). Aqueous lithium hydroxide (26.4 ml, 26.4 mmol). The reaction was stirred overnight at room temperature. It was concentrated under vacuum to remove the ethanol. The resulting crude material was diluted with diethyl ether/ethyl acetate solution and water. The aqueous phase was acidified using 2N HCl to pH 2. The resulting suspension was washed with ethyl acetate. The organic phase was washed with saturated sodium chloride, dried over sodium sulfate, filtered and concentrated to obtain 1-(1-(4-chlorobenzyl)-5-methoxy-1H-indole-2-carbonyl)piperidine-4-carboxylic acid. Yield: 915 mg, 81 %. ^1H NMR (500 MHz, $\text{DMSO-}d_6$) δ ppm 12.27 (br. s., 1 H), 7.45 (d, $J=9.0$ Hz, 1 H), 7.23 - 7.38 (m, 2 H), 7.10 (d, $J=2.4$ Hz, 1 H), 7.01 - 7.09 (m, 2 H), 6.86 (dd, $J=8.8,$

2.4 Hz, 1 H), 6.63 (s, 1 H), 5.45 (s, 2 H), 3.80 - 4.49 (m, 1 H), 3.76 (s, 3 H), 3.03 (br. s., 1 H), 2.47 (tt, $J=11.0, 3.9$ Hz, 1 H), 1.12 - 1.88 (m, 2 H)

A large pressure vessel was purged with nitrogen. 1-(1-(4-chlorobenzyl)-5-methoxy-1H-indole-2-carbonyl)piperidine-4-carboxylic acid (907 mg, 2.125 mmol), 1-Hydroxybenzotriazole (574 mg, 4.25 mmol), EDCI (815 mg, 4.25 mmol) were dissolved in DCM (Volume: 20 ml). The reaction was cooled using an ice bath stirred for 15 minutes before Hunig's Base (0.742 ml, 4.25 mmol) and Dimethylamine in THF (2.125 ml, 4.25 mmol) were added. The pressure vessel was tightly sealed and the reaction was allowed to warm to room temperature overnight. The reaction was diluted with water and ethyl acetate. The organic phase was washed with 1N HCl, saturated sodium chloride, dried over sodium sulfate, filtered and concentrated. The crude material was purified using 10-80% ethyl acetate/hexanes to obtain product. Yield: 743 mg, 77 %. ^1H NMR (500 MHz, $\text{DMSO-}d_6$) δ ppm 7.43 (d, $J=8.8$ Hz, 1 H), 7.28 - 7.38 (m, 2 H), 7.04 - 7.14 (m, 3 H), 6.85 (dd, $J=9.0, 2.4$ Hz, 1 H), 6.63 (s, 1 H), 5.45 (br. s., 2 H), 4.41 (br. s, 1 H), 4.03 (br. s, 1 H), 3.70 - 3.80 (m, 3 H), 2.83 - 3.24 (m, 6 H), 2.76 - 2.83 (m, 3 H), 1.20 - 1.87 (m, 4 H). TOF ES+ MS: 476.2 (M+Na). HPLC (gradient A): ret. time = 6.92 min; purity = 90 %

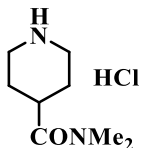


1-(5-hydroxy-1H-indole-2-carbonyl)-N,N-dimethylpiperidine-4-carboxamide (CCG 212051, 105) 100 (100 mg, 0.220 mmol) was dissolved in anhydrous DCM (Volume: 3 mL) and cooled to -78°C . BBr_3 (0.661 mL, 0.661 mmol) was added dropwise. The reaction was allowed to warm to room temperature and stirred until the TLC showed complete consumption of starting material. The reaction was cooled with an ice bath before slowly adding saturated sodium bicarbonate. The reaction was diluted with ethyl acetate. The organic phase was washed with saturated sodium bicarbonate until the aqueous layer from the separatory funnel is basic. It was washed with saturated sodium chloride and dried over sodium sulfate, filtered and concentrated. The crude material was purified using 10-80% ethyl acetate/hexanes to obtain product as a white solid. Yield: 24 mg, 34 %. $^1\text{H NMR}$ (500 MHz, $\text{DMSO}-d_6$) δ ppm 11.25 (s, 1 H), 8.79 (s, 1 H), 7.20 (d, $J=8.8$ Hz, 1 H), 6.83 - 6.93 (m, 1 H), 6.65 - 6.78 (m, 1 H), 6.51 - 6.61 (m, 1 H), 4.34 - 4.50 (m, 2 H), 3.02 - 3.21 (m, 4 H), 2.98 (tt, $J=11.1, 3.6$ Hz, 1 H), 2.82 (s, 3 H), 1.67 - 1.78 (m, 2 H), 1.45 - 1.59 (m, 2 H). TOF ES+ MS: 316.1 (M+H), 338.1 (M+Na).



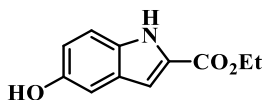
1-(tert-Butoxycarbonyl)piperidine-4-carboxylic acid (170). ethyl piperidine-4-carboxylate (0.490 mL, 3.18 mmol) and Hunig'sBase (0.833 mL, 4.77 mmol) were added to 6.0 mL of THF. Di-tert-butyl dicarbonate (1041 mg, 4.77 mmol) was added as a 3.0 mL solution of THF. The reaction was stirred overnight. The reaction was diluted with water and ethyl acetate. The organic layer was washed with saturated, aqueous solution of sodium chloride, dried over magnesium sulfate, filtered and concentrated. The TLC of the reaction mixture showed conversion of starting material to product. 1-tert-butyl 4-ethyl piperidine-1,4-dicarboxylate was taken directly to the next step.

1-tert-butyl 4-ethyl piperidine-1,4-dicarboxylate (10 g, 38.9 mmol) was placed in Ethanol (Ratio: 1.000, Volume: 100 ml) and 2N NaOH (Ratio: 1.000, Volume: 100 ml). The reaction was stirred for 2 days. It was concentrated to half volume. The resulting suspension was diluted with minimal water to allow free movement of a stir bar. The suspension was cooled by an ice bath and acidified using 2N HCl to pH 2. The suspension was extracted using ethyl acetate. The aqueous phase was washed with another aliquot of ethyl acetate. The combined organic phases were washed with saturated sodium chloride, filtered and concentrated to obtain product as a white solid. Yield: 8.1 g, 91 %. $^1\text{H NMR}$ (400 MHz, DMSO- d_6) δ 12.25 (s, 1H), 3.81 (d, $J = 13.3$ Hz, 2H), 2.78 (s, 2H), 2.38 (tt, $J = 11.1, 3.9$ Hz, 1H), 1.76 (dd, $J = 13.3, 3.1$ Hz, 2H), 1.47 – 1.24 (m, 10H).



N,N-dimethylpiperidine-4-carboxamide hydrochloride (171): A large pressure vessel was purged with nitrogen. **170** (1.5 g, 6.54 mmol), DMAP (0.799 g, 6.54 mmol), EDCI (2.508 g, 13.08 mmol) were dissolved in DCM (Volume: 25 ml). The reaction was cooled using an ice bath stirred for 15 minutes before Hunig'sBase (2.285 ml, 13.08 mmol) and dimethylamine in THF (6.54 ml, 13.08 mmol) were added. The pressure vessel was tightly sealed and the reaction was allowed to warm to room temperature overnight. The reaction was diluted with water and ethyl acetate. The organic phase was washed with 1N HCl, saturated sodium chloride, dried over sodium sulfate, filtered and concentrated. Product was taken directly to the next step. TOF ES+ MS: 279.2 (M+Na).

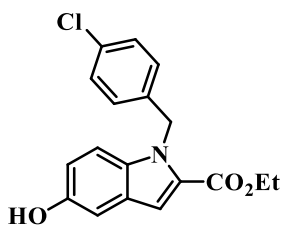
Tert-butyl 4-(dimethylcarbamoyl)piperidine-1-carboxylate (700 mg, 2.73 mmol) was dissolved in 1,4 Dioxane (Volume: 2.0 ml). HCl in 1,4 dioxane (6.83 ml, 27.3 mmol) was added and after 10 minutes, a peach solid formed. the reaction was stirred for an additional 30 minutes before it was concentrated under vacuum. It was placed under high vacuum to isolate **171** as sticky peach solid. TOF ES+ MS: 193.2 (M+H).



Ethyl 5-hydroxy-1H-indole-2-carboxylate (172) 5-methoxy-1H-indole-2-carboxylic acid (6.0 g, 31.4 mmol) was dissolved in EtOH (Volume: 150 mL) and cooled by an ice bath. HCl (g) (0.954 mL, 31.4 mmol) was bubbled to saturation. The reaction was stirred overnight. Nitrogen gas was bubbled into the reaction for 30 minutes. After which point, the reaction was concentrated under vacuum. The crude slurry was dissolved with ethyl

acetate. The organic phase was cooled by an ice bath before saturated sodium carbonate was added slowly. The layers were separated using a separatory funnel. The organic phase was washed with saturated sodium carbonate (2x) then saturated sodium chloride. The organic phase was dried over sodium sulfate. Filtered and concentrated to obtain ethyl 5-methoxy-1H-indole-2-carboxylate. Yield: 5.86 g, 85 %. ^1H NMR (500 MHz, $\text{DMSO-}d_6$) δ ppm 11.75 (br. s., 1 H), 7.35 (d, $J=9.0$ Hz, 1 H), 7.10 (d, $J=2.4$ Hz, 1 H), 7.05 (dd, $J=2.4, 0.7$ Hz, 1 H), 6.92 (dd, $J=8.8, 2.4$ Hz, 1 H), 4.33 (q, $J=7.1$ Hz, 2 H), 3.76 (s, 3 H), 1.34 (t, $J=7.2$ Hz, 3 H).

Using an oven dried flask charged with argon, ethyl 5-methoxy-1H-indole-2-carboxylate (3.0 g, 13.68 mmol) was dissolved in DCM (Volume: 150 ml). It was cooled to -78 °C before adding BBr_3 in DCM (27.4 ml, 27.4 mmol) via addition funnel. The reaction was allowed to warm slowly to room temperature. After 3 hours, the reaction was cooled to 0 °C and slowly diluted with water. The resulting suspension was transferred to a separatory funnel and further diluted with water and ethyl acetate. The organic phase was washed with saturated sodium bicarbonate until the aqueous layer showed to be basic by pH paper. The organic phase was washed with saturated sodium chloride, dried over sodium sulfate, filtered, and concentrated to obtain pure product. ^1H NMR (500 MHz, $\text{DMSO-}d_6$) δ ppm 11.58 (s, 1 H), 8.92 (br. s., 1 H), 7.26 (d, $J=8.8$ Hz, 1 H), 6.89 - 6.97 (m, 2 H), 6.81 (dd, $J=8.8, 2.4$ Hz, 1 H), 4.31 (q, $J=7.2$ Hz, 2 H), 1.32 (t, $J=7.1$ Hz, 3 H)

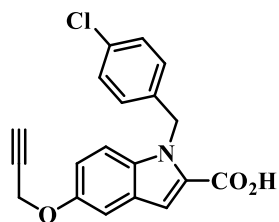


Ethyl 1-(4-chlorobenzyl)-5-hydroxy-1H-indole-2-carboxylate (175): 172 (780 mg, 3.80 mmol) and imidazole (776 mg, 11.40 mmol) were dissolved in DCM (35.0 mL) and stirred at room temperature for 30 minutes. TBS-Cl (1146 mg, 7.60 mmol) was dissolved in DCM (10.0 mL) and stirred at room temperature overnight. The reaction was diluted with ethyl acetate and water. The organic phase was washed with 1N HCl and saturated sodium chloride. The organic phase was dried over sodium sulfate, filtered and concentrated. The crude material was purified via flash chromatography 0 - 40% ethyl acetate/hexanes to obtain ethyl 5-((tert-butyldimethylsilyl)oxy)-1H-indole-2-carboxylate. Yield: 1.2 g, 99%. $^1\text{H NMR}$ (500 MHz, $\text{DMSO-}d_6$) δ ppm 11.74 (s, 1 H), 7.33 (d, $J=9.0$ Hz, 1 H), 7.05 – 7.02 (m, 2 H), 6.83 (dd, $J=6.5, 2.5$ Hz, 1 H), 4.33 (q, $J=7.0$ Hz, 2 H), 1.33 (t, $J=7.0$ Hz, 3 H), 0.97 (s, 9H), .17 (s, 6H).

In a dried flask, purged with argon, sodium hydride (28.2 mg, 0.704 mmol) was added and suspended in DMF (1.0 mL) and cooled using an ice bath. Ethyl 5-((tert-butyldimethylsilyl)oxy)-1H-indole-2-carboxylate (150 mg, 0.470 mmol) was dissolved in DMF (1.0 mL) and added dropwise to the flask. The reaction was stirred for 10 minutes before a 1-chloro-4-(chloromethyl)benzene (0.066 mL, 0.516 mmol) dissolved in DMF (0.5 mL) was added. The reaction was allowed to warm to room temperature and stirred for an additional 30 minutes before it was diluted with saturated sodium chloride and ethyl acetate. The aqueous phase was washed with another aliquot with ethyl acetate. The organic phases were combined and washed with saturated sodium chloride. It was

dried over sodium sulfate, filtered and concentrated. Ethyl 5-((tert-butyl dimethylsilyl)oxy)-1-(4-chlorobenzyl)-1H-indole-2-carboxylate and ethyl 1-(4-chlorobenzyl)-5-((4-chlorobenzyl)oxy)-1H-indole-2-carboxylate was isolated in a 3:1 ratio. The mixture was taken directly to the next step.

Ethyl 5-((tert-butyl dimethylsilyl)oxy)-1-(4-chlorobenzyl)-1H-indole-2-carboxylate and ethyl 1-(4-chlorobenzyl)-5-((4-chlorobenzyl)oxy)-1H-indole-2-carboxylate (473 mg, 1.065 mmol) was dissolved in THF (Volume: 6 mL) and cooled to 0 °C. TBAF in THF (1.598 mL, 1.598 mmol) was added dropwise and then warmed to room temperature. The reaction was stirred overnight. Then it was diluted with ethyl acetate and water. The organic phase was washed with saturated sodium chloride, filtered and concentrated. The crude material was purified using 0-20% ethyl acetate: hexanes biotage 4 g column. To obtain **175** as a white solid. Yield: 226 mg, 64 %. ¹H NMR (500 MHz, DMSO-*d*₆) δ ppm 9.08 (s, 1 H) 7.38 (d, *J*=9.03 Hz, 1 H) 7.31 - 7.35 (m, 2 H) 7.19 (d, *J*=0.73 Hz, 1 H) 6.99 - 7.04 (m, 2 H) 6.98 (d, *J*=2.20 Hz, 1 H) 6.85 (dd, *J*=9.03, 2.44 Hz, 1 H) 5.76 (s, 2 H) 4.25 (q, *J*=7.08 Hz, 2 H) 1.27 (t, *J*=7.08 Hz, 3 H)

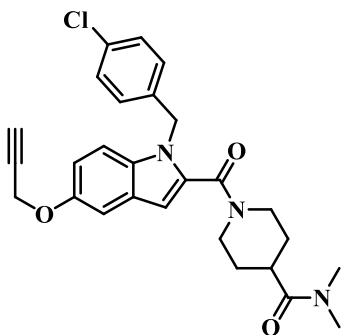


1-(4-chlorobenzyl)-5-(prop-2-yn-1-yloxy)-1H-indole-2-carboxylic acid (176)

Compound **175** (200mg, 0.606 mmol) and cesium carbonate (296 mg, 0.910 mmol) were dissolved in DMF (Volume: 5 mL). 3-bromoprop-1-yne (0.092 mL, 1.213 mmol) was added. The reaction was allowed to stir at room temperature overnight before it was diluted with saturated sodium chloride and ethyl acetate. The aqueous phase was washed

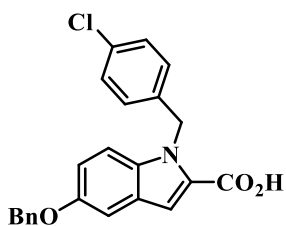
with ethyl acetate. The organic phases were combined and washed with saturated sodium chloride. It was dried over sodium sulfate, filtered and concentrated. The crude material was purified using 0-60% ethyl acetate/hexanes to obtain ethyl 1-(4-chlorobenzyl)-5-(prop-2-yn-1-yloxy)-1H-indole-2-carboxylate as a white solid. Yield: 160 mg, 72 %. ¹H NMR (500 MHz, DMSO-*d*₆) δ ppm 7.52 (d, *J*=9.0 Hz, 1 H), 7.33 (d, *J*=8.5 Hz, 2 H), 7.29 (s, 1H), 7.26 (d, *J*=2 Hz, 1H), 7.01 - 7.03 (m, 3 H), 5.81 (s, 2H), 4.79 (d, *J*=2.0 Hz, 2 H), 4.27 (q, *J*=7.0 Hz, 2 H), 3.56 (t, *J*=2.0 Hz, 1 H), 1.28 (t, *J*=7.0 Hz, 3H).

Ethyl 1-(4-chlorobenzyl)-5-(prop-2-yn-1-yloxy)-1H-indole-2-carboxylate (160 mg, 0.435 mmol) was dissolved in Ethanol (Ratio: 1.000, Volume: 6.00 ml) and aq. NaOH (Ratio: 1.000, Volume: 6 ml) and allowed to stir overnight. The reaction was concentrated by half of the volume, cooled to 0 °C, acidified with 2M HCl. The resulting suspension filtered under vacuum. The solid was dried under vacuum to obtain **176** as a white solid. Yield: 83 mg, 57 %. ¹H NMR (500 MHz, DMSO-*d*₆) δ ppm 12.98 (s, 1 H), 7.47 (d, *J*=9.0 Hz, 1 H), 7.31 - 7.36 (m, 2 H), 7.23 - 7.26 (m, 2 H), 7.00 - 7.04 (m, 2 H), 6.98 (dd, *J*=9.0, 2.4 Hz, 1 H), 5.83 (s, 2 H), 4.79 (d, *J*=2.4 Hz, 2 H), 3.56 (t, *J*=2.4 Hz, 1 H). HPLC (gradient A): ret. time = 7.37 min; purity > 95 %.



1-(1-(4-chlorobenzyl)-5-(prop-2-yn-1-yloxy)-1H-indole-2-carbonyl)-N,N-dimethylpiperidine-4-carboxamide (CCG 212058, 102) 176 (36 mg, 0.106 mmol),

EDCI (40.6 mg, 0.212 mmol) and 1-Hydroxybenzotriazole (28.6 mg, 0.212 mmol) were dissolved in DCM (Ratio: 3.00, Volume: 3 ml) and stirred for 30 minutes at room temperature. **171** (57.3 mg, 0.212 mmol) was added as a DCM (Ratio: 1.000, Volume: 1 ml) solution, followed by Hunig'sBase (0.043 ml, 0.247 mmol). The reaction was further stirred at room temperature overnight at room temperature. The reaction was diluted with water and ethyl acetate. The organic phase was washed with saturated sodium carbonate, 1N HCl, and brine. The organic phase was dried over sodium sulfate, filtered and concentrated. The crude material was purified via Biotage SP1 with 30% to 60% ethyl acetate/hexanes. The product was a white solid. Yield: 24 mg, 48%. ¹H NMR (500 MHz, DMSO-*d*₆) δ ppm 7.46 (d, *J*=9.0 Hz, 1 H), 7.31 - 7.36 (m, 2 H), 7.19 (d, *J*=2.7 Hz, 1 H), 7.07 - 7.12 (m, 2 H), 6.90 (dd, *J*=8.9, 2.6 Hz, 1 H), 6.65 (s, 1 H), 5.46 (s, 2 H), 4.77 (d, *J*=2.2 Hz, 2 H), 4.44 (br. s., 1 H), 4.03 (br. s., 1 H), 3.54 (t, *J*=2.3 Hz, 1 H), 2.85 - 3.21 (m, 6 H), 2.81 (s, 3 H), 1.21 - 1.83 (m, 4 H). TOF ES+ MS: 478.3 (M+H), 500.3 (M+Na). HPLC (gradient A): ret. time = 6.93 min; purity > 95 %

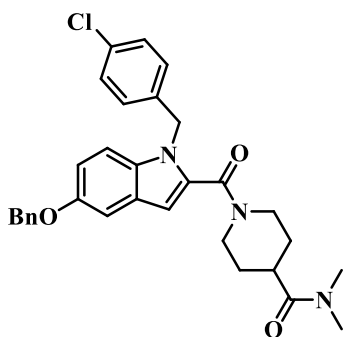


5-(benzyloxy)-1-(4-chlorobenzyl)-1H-indole-2-carboxylic acid (177) Cesium

carbonate (222 mg, 0.682 mmol) and ethyl 1-(4-chlorobenzyl)-5-hydroxy-1H-indole-2-carboxylate (150 mg, 0.455 mmol) were dissolved in DMF (Volume: 4.0 ml). It was stirred for 20 minutes before benzyl bromide (0.081 ml, 0.682 mmol) was added. The reaction was stirred overnight. The reaction was diluted by water and ethyl acetate/diethyl ether. The water phase was washed again with ethyl acetate/diethyl ether.

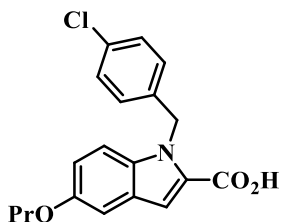
The combined organic phases were washed with saturated sodium carbonate followed by saturated sodium chloride. It was dried over saturated sodium sulfate, filtered, and concentrated. The crude material was purified via sp1 biotage using 0-45% ethyl acetate-hexanes gradient. The product was obtained as a white solid. TOF ES+ MS: 420.0 (M+H), 442.2 (M+Na). HPLC (gradient A): ret. Time = 9.88 min; purity > 95%

Ethyl 5-(benzyloxy)-1-(4-chlorobenzyl)-1H-indole-2-carboxylate (150 mg, 0.357 mmol) was dissolved in Ethanol (Ratio: 1.000, Volume: 2 ml), 2N NaOH (Ratio: 1.000, Volume: 2.000 ml). It was stirred overnight. The reaction was concentrated to half volume and diluted with water to allow free movement of a stir bar. It was cooled by an ice bath and acidified using 2N HCl to pH 2. The resulting suspension was extracted with ethyl acetate (2X). The organic phases were combined and washed with saturated sodium chloride, dried over sodium sulfate, filtered and concentrated. The product was isolated as a white solid. Yield: 106 mg, 76 %. ¹H NMR (500 MHz, DMSO-*d*₆) δ ppm 12.96 (br. s., 1 H), 7.45 - 7.49 (m, 3 H), 7.37 - 7.42 (m, 2 H), 7.31 - 7.35 (m, 3 H), 7.27 (d, *J*=2.4 Hz, 1 H), 7.22 (s, 1 H), 6.99 - 7.05 (m, 3 H), 5.83 (s, 2 H), 5.10 (s, 2 H). HPLC (gradient A): ret. Time = 8.29 min; purity > 95%



1-(5-(benzyloxy)-1-(4-chlorobenzyl)-1H-indole-2-carbonyl)-N,N-dimethylpiperidine-4-carboxamide (CCG 212151, 103) Compound **177** (87 mg, 0.222 mmol), EDCI (85

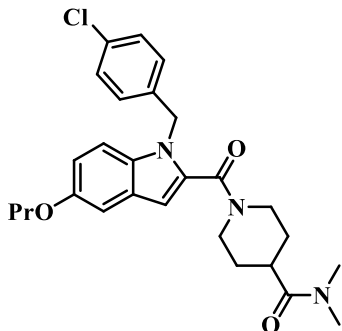
mg, 0.444 mmol) and 1-Hydroxybenzotriazole (60.0 mg, 0.444 mmol) were dissolved in DCM (Ratio: 3.00, Volume: 3 ml) and stirred for 30 minutes at room temperature. **171** (120 mg, 0.444 mmol) was added as a DCM (Ratio: 1.000, Volume: 1 ml) solution, followed by Hunig'sBase (0.043 ml, 0.247 mmol). The reaction was further stirred at room temperature overnight at room temperature. The reaction was diluted with water and ethyl acetate. The organic phase was washed with saturated sodium carbonate, 1N HCl, and brine. The organic phase was dried over sodium sulfate. The drying agent was used filtered and crude material concentrated. The crude material was purified via Biotage SP1 with 50% ethyl acetate/hexanes to 100% ethyl acetate. The product was a white solid. Yield: 40 mg, 34%. ¹H NMR (500 MHz, DMSO-*d*₆) δ ppm 7.42 - 7.49 (m, 3 H), 7.37 - 7.42 (m, 2 H), 7.30 - 7.35 (m, 3 H), 7.19 (d, *J*=2.4 Hz, 1 H), 7.07 - 7.11 (m, 2 H), 6.94 (dd, *J*=9.0, 2.4 Hz, 1 H), 6.62 (s, 1 H), 5.45 (br. s., 2 H), 5.10 (s, 2 H), 4.44 (br. s., 1 H), 4.04 (br. s., 1 H), 2.85 - 3.21 (m, 6 H), 2.81 (s, 3 H), 1.23 - 1.82 (m, 4 H). ES+ MS: 552.0 (M+Na). HPLC (gradient A): ret. time = 7.96 min; purity > 95 %



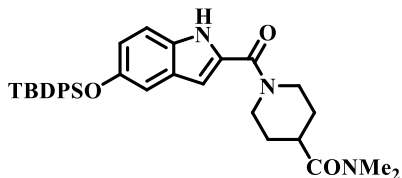
1-(4-chlorobenzyl)-5-propoxy-1H-indole-2-carboxylic acid (178) Cesium carbonate (222 mg, 0.682 mmol) and ethyl 1-(4-chlorobenzyl)-5-hydroxy-1H-indole-2-carboxylate (150 mg, 0.455 mmol) were dissolved in DMF (Volume: 4.0 ml). It was stirred for 20 minutes before 1-bromopropane (0.042 ml, 0.455 mmol) was added. The reaction was stirred at room temperature overnight. The reaction was diluted by water and ethyl

acetate/diethyl ether. The water phase was washed again with ethyl acetate/diethyl ether. The combined organic phases were washed with saturated sodium carbonate followed by saturated sodium chloride. It was dried over saturated sodium sulfate, filtered, and concentrated. The crude material was purified via spl biotage using 0-45% ethyl acetate-hexanes gradient. ethyl 1-(4-chlorobenzyl)-5-propoxy-1H-indole-2-carboxylate was obtained as a white solid. Yield: 155 mg, 92 %. ¹H NMR (500 MHz, DMSO-*d*₆) δ ppm 7.47 (d, *J*=9.0 Hz, 1 H), 7.31 - 7.35 (m, 2 H), 7.26 (s, 1 H), 7.17 (d, *J*=2.2 Hz, 1 H), 6.99 - 7.02 (m, 2 H), 6.97 (dd, *J*=9.0, 2.4 Hz, 1 H), 5.80 (s, 2 H), 4.27 (q, *J*=7.1 Hz, 2 H), 3.92 (t, *J*=6.6 Hz, 2 H), 1.74 (sxt, *J*=7.1 Hz, 2 H), 1.28 (t, *J*=7.1 Hz, 3 H), 0.99 (t, *J*=7.3 Hz, 3 H)

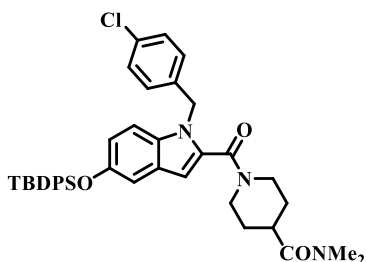
Ethyl 1-(4-chlorobenzyl)-5-propoxy-1H-indole-2-carboxylate (150 mg, 0.403 mmol) was dissolved in Ethanol (Ratio: 1.000, Volume: 2 ml) and 2N NaOH (Ratio: 1.000, Volume: 2.000 ml). It was stirred overnight. The reaction was concentrated to half volume and diluted with water to allow free movement of a stir bar. It was cooled by an ice bath and acidified using 2N HCl to pH 2. The resulting suspension was extracted with ethyl acetate (2X). The organic phases were combined and washed with saturated sodium chloride, dried over sodium sulfate, filtered and concentrated. The product was isolated as a white solid. Yield: 56 mg, 40 %. ¹H NMR (500 MHz, DMSO-*d*₆) δ ppm 12.93 (br. s., 1 H), 7.43 (d, *J*=9.3 Hz, 1 H), 7.31 - 7.35 (m, 2 H), 7.22 (s, 1 H), 7.15 (d, *J*=2.4 Hz, 1 H), 7.01 (m, *J*=8.3 Hz, 2 H), 6.94 (dd, *J*=9.0, 2.4 Hz, 1 H), 5.82 (s, 2 H), 3.92 (t, *J*=6.6 Hz, 2 H), 1.74 (sxt, *J*=7.1 Hz, 2 H), 0.99 (t, *J*=7.4 Hz, 3 H).



1-(1-(4-chlorobenzyl)-5-propoxy-1H-indole-2-carbonyl)-N,N-dimethylpiperidine-4-carboxamide (CCG 212138, 104) 178 (50 mg, 0.145 mmol), EDCI (55.8 mg, 0.291 mmol) and 1-Hydroxybenzotriazole (39.3 mg, 0.291 mmol) were dissolved in DCM (Ratio: 3.00, Volume: 3 ml) and stirred for 30 minutes at room temperature. **171** (79 mg, 0.291 mmol) was added as a DCM (Ratio: 1.000, Volume: 1 ml) solution, followed by Hunig's Base (0.043 ml, 0.247 mmol). The reaction was further stirred at room temperature overnight at room temperature. The reaction was diluted with water and ethyl acetate. The organic phase was washed with saturated sodium carbonate, 1N HCl, and brine. The organic phase was dried over sodium sulfate. The drying agent was used filtered and crude material concentrated. The crude material was purified via Biotage SP1 with 50% ethyl acetate/hexanes to 100% ethyl acetate. The product was a white solid. Yield: 22 mg, 32%. ¹H NMR (500 MHz, Chloroform-*d*) δ ppm 7.19 - 7.23 (m, 2 H), 7.17 (d, $J=9.0$ Hz, 1 H), 7.06 (d, $J=2.4$ Hz, 1 H), 7.00 - 7.04 (m, 2 H), 6.91 (dd, $J=8.8, 2.4$ Hz, 1 H), 6.57 (s, 1 H), 5.42 (s, 2 H), 4.11 - 4.84 (m, 2 H), 3.94 (t, $J=6.6$ Hz, 2 H), 3.05 (s, 3 H), 2.87 - 3.00 (m, 5 H), 2.75 (quin, $J=7.3$ Hz, 1 H), 1.58 - 1.87 (m, 6 H), 1.05 (t, $J=7.4$ Hz, 3 H). TOF ES+ MS: 482.4 (M+H), 504.4 (M+Na). HPLC (gradient A): ret. time = 7.83 min; purity > 95 %

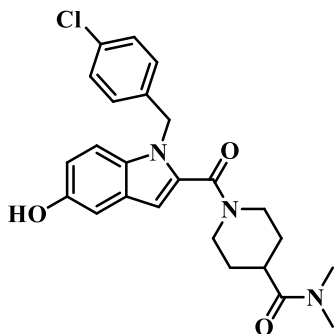


1-(5-((tert-butyldiphenylsilyl)oxy)-1H-indole-2-carbonyl)-N,N-dimethylpiperidine-4-carboxamide (180) Imidazole (23.31 mg, 0.342 mmol) and **105** (72 mg, 0.228 mmol) were dissolved in DCM (Volume: 5 ml) and stirred at room temperature for 10 minutes. TBDPS-Cl (0.088 ml, 0.342 mmol) was added. The reaction was stirred for another 2 hours before it was diluted with ethyl acetate and water. The organic phase was washed with 1N HCl, saturated sodium carbonate, then saturated sodium chloride. It was then dried over sodium sulfate, filtered and concentrated. The crude material was purified using 0-60% ethyl acetate/hexanes to obtain product as an off white solid. Yield: 124 mg, 98%. TOF ES+ MS: 554.1 (M+H) , 576.1 (M+Na).



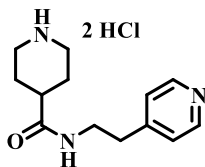
1-(5-((tert-butyldiphenylsilyl)oxy)-1-(4-chlorobenzyl)-1H-indole-2-carbonyl)-N,N-dimethylpiperidine-4-carboxamide (181) 1-(bromomethyl)-4-chlorobenzene (21.71 mg, 0.106 mmol) and sodium iodide (10.56 mg, 0.070 mmol) were dissolved in Acetone (Ratio: 1.000, Volume: 5.00 ml) and stirred for 3 hours. The resulting suspension was filtered and the filtrate was concentrated to obtain 4-chlorobenzyl iodide. **180** (39 mg, 0.070 mmol), cesium carbonate (34.4 mg, 0.106 mmol) and 4-chlorobenzyl iodide were

dissolved in DMF and stirred at 60 °C for 4 hours. The reaction was diluted with water and ethyl acetate. The aqueous phase was washed with ethyl acetate (2X). The organic phases were combined and washed with saturated sodium chloride (2X). It was dried over sodium sulfate, filtered and concentrated. The resulting crude material was purified using 0-60% ethyl acetate/hexanes to obtain product. Yield: 40 mg, 84 %. TOF ES+ MS: 678.1 (M+H)



1-(1-(4-chlorobenzyl)-5-hydroxy-1H-indole-2-carbonyl)-N,N-dimethylpiperidine-4-carboxamide (CCG 222701, 101) 181 (34 mg, 0.050 mmol) was dissolved in THF (Volume: 5002 μ l) and cooled to -78 °C. TBAF (55.1 μ l, 0.055 mmol) was added dropwise and the reaction was stirred for 2 hours before it was diluted with water and ethyl acetate. The organic phase was washed with saturated sodium chloride, dried over sodium sulfate, filtered and concentrated. The crude material was purified using 0-80% ethyl acetate/hexanes to obtain white solid as a product. Yield: 17 mg, 78% ^1H NMR (500 MHz, DMSO- d_6) δ ppm 8.91 (s, 1 H), 7.28 - 7.36 (m, 3 H), 7.09 (d, $J=8.5$ Hz, 2 H), 6.90 (d, $J=2.2$ Hz, 1 H), 6.72 (dd, $J=8.8, 2.4$ Hz, 1 H), 6.54 (s, 1 H), 5.41 (s, 2 H), 3.92 - 4.61 (m, 2 H), 2.77 - 3.20 (m, 9 H), 1.23 - 1.79 (m, 4 H). TOF ES+ MS: 440.1 (M+H), 462.1 (M+Na). HPLC (gradient A): ret. time = 5.70 min; purity > 95 %

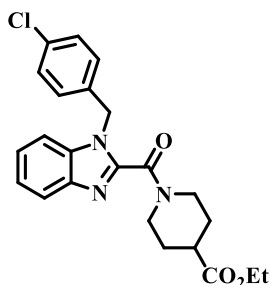
Indole replacement derivatives



N-(2-(pyridin-4-yl)ethyl)piperidine-4-carboxamide dihydrochloride (190). The following was added to DCM: **170** (600 mg, 2.62 mmol), DIEA (1.37 mL, 7.85 mmol), EDCI (552 mg, 2.88 mL), HOBt (441 mg, 2.88 mmol), and 2-(4-pyridylethyl)amine (0.34 mL, 2.88 mL). The solution was stirred at rt for 17 h, at which time the DCM was stripped off and 10% aq. sodium carbonate was added. Material was extracted out with EtOAc (3X). The organic extractions were pooled, dried over magnesium sulfate, and concentrated *in vacuo*. The residue was taken up in a small amount of EtOAc and diethyl ether was added. The precipitate was collected over a filter and washed with diethyl ether to give tert-butyl 4-((2-(pyridin-4-yl)ethyl)carbamoyl)piperidine-1-carboxylate as an off-white solid. Yield: 634 mg (73%). ¹H NMR (400 MHz, CDCl₃) δ 8.49 (d, *J* = 5.9 Hz, 2H), 7.09 (d, *J* = 5.9 Hz, 2H), 5.59 (t, *J* = 5.3 Hz, 1H), 4.22 – 3.95 (m, 2H), 3.52 (q, *J* = 6.8 Hz, 2H), 2.81 (t, *J* = 6.9 Hz, 2H), 2.68 (t, *J* = 12.5 Hz, 2H), 2.14 (tt, *J* = 11.6, 3.8 Hz, 1H), 1.77 – 1.65 (m, 2H), 1.56 (qd, *J* = 12.1, 4.3 Hz, 2H), 1.43 (s, 9H).

Tert-Butyl 4-((2-(pyridin-4-yl)ethyl)carbamoyl)piperidine-1-carboxylate (575 mg, 1.72 mmol) was suspended in diethyl ether at room temperature, and 4M HCl in dioxane (6 mL, 24 mmol) was added. The mixture was stirred at room temperature for 30 min, at which time the organic solution was decanted off and the solid material collected and dried *in vacuo*. The title compound was thus obtained as a tan powder. Yield: 448 mg (97%). ¹H NMR (400 MHz, DMSO-d₆) δ 9.22 (bs, 1H), 8.91 (bs, 1H), 8.79 (d, *J* = 6.4

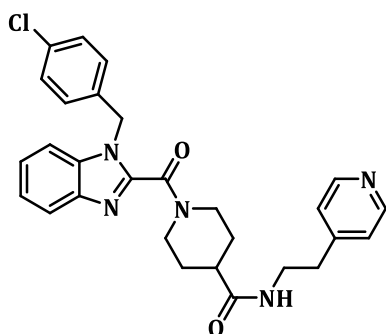
Hz, 2H), 8.18 (t, $J = 5.6$ Hz, 1H), 7.89 (d, $J = 6.3$ Hz, 2H), 3.40 (q, $J = 6.2$ Hz, 2H), 3.15 (d, $J = 12.6$ Hz, 2H), 3.00 (t, $J = 6.4$ Hz, 2H), 2.83 – 2.69 (m, 2H), 2.39 – 2.26 (m, 1H), 1.80 – 1.59 (m, 4H). TOF ES+ MS: (M+H) 234.2, (M+Na) 256.1.



Ethyl 1-(1-(4-chlorobenzyl)-1H-benzo[d]imidazole-2-carbonyl)piperidine-4-

carboxylate (193). 1H-benzo[d]imidazole-2-carboxylic acid hydrate **191** (500 mg, 2.78 mmol), EDCI (1170 mg, 6.11 mmol), and HOBt (825 mg, 6.11 mmol) were dissolved in DCM. The reaction was allowed to stir for 10 minutes before DIEA (1.066 mL, 6.11 mmol) and ethyl piperidine-4-carboxylate (0.941 mL, 6.11 mmol) were added. The reaction was allowed to stir overnight at room temperature. The reaction was diluted with water and ethyl acetate. The organic phase was washed with 1N HCl, saturated sodium bicarbonate, and saturated sodium chloride solution. The ethyl acetate layer was dried over magnesium sulfate, filtered and concentrated. The resulting crude material was triturated with ethyl acetate to obtain ethyl 1-(1H-benzo[d]imidazole-2-carbonyl)piperidine-4-carboxylate as a white solid. Yield: 113 mg (14%). ¹H NMR (400 MHz, DMSO- *d*₆) δ 13.09 (s, 1H), 7.63 (dd, $J = 84.6, 8.0$ Hz, 2H), 7.28 (dt, 2H), 5.30 (d, $J = 13.5$ Hz, 1H), 4.42 (d, $J = 13.0$ Hz, 1H), 4.09 (q, $J = 14.2, 7.0$ Hz, 2H), 3.48 (t, $J = 11.7$ Hz, 1H), 3.05 (t, $J = 11.3$ Hz, 1H), 2.77 – 2.65 (m, 1H), 1.97 (d, $J = 13.7$ Hz, 2H), 1.69 – 1.52 (m, 2H), 1.19 (t, $J = 7.1$ Hz, 3H). TOF ES+ MS: 302.1 (M+H), 324.1 (M+Na). HPLC ret. time = 5.44 min; purity > 95%.

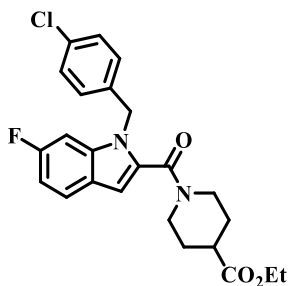
Ethyl 1-(1*H*-benzo[*d*]imidazole-2-carbonyl)piperidine-4-carboxylate (80 mg, 0.265 mmol) and cesium carbonate (130 mg, 0.398 mmol) were dissolved in DMF (Volume: 2.0 ml). 1-Chloro-4-(chloromethyl)benzene (0.051 ml, 0.40 mmol) was added and the reaction was heated at 80 °C overnight. After 18 hours, the reaction was cooled to room temperature and diluted with water and ethyl acetate. The organic phase was washed with saturated sodium chloride four times before it was dried over magnesium sulfate, filtered and concentrated. The isolated beige solid was taken directly to the next step without purification. Yield: 85 mg (75%). ¹H NMR (400 MHz, DMSO- *d*₆) δ 7.74 (d, *J* = 7.7 Hz, 1H), 7.66 (d, *J* = 7.7 Hz, 1H), 7.49 – 7.27 (m, 6H), 5.63 – 5.48 (m, 1H), 5.15 (s, 1H), 4.42 – 4.32 (m, 1H), 4.08 (q, *J* = 8 Hz, 8Hz, 2H), 3.97 – 3.86 (m, 1H), 3.22 – 3.10 (m, 1H), 3.05 – 2.93 (m, 1H), 2.70 – 2.55 (m, 1H), 1.97 – 1.88 (m, 1H), 1.76 – 1.67 (m, 1H), 1.53 – 1.38 (m, 1H), 1.21 (t, *J* = 8 Hz, 3H). TOF ES+ MS: 426.0 (M+H), 448.0 (M+Na).



1-(1-(4-chlorobenzyl)-1*H*-benzo[*d*]imidazole-2-carbonyl)-*N*-(2-(pyridin-4-yl)ethyl)piperidine-4-carboxamide (CCG 206565, 112). 193 (60 mg, 0.141 mmol) and lithium hydroxide, H₂O (23.6 mg, 0.564 mmol) were dissolved in 2/1 water/THF (0.75 ml). The reaction was stirred for two hours before it was diluted with water and diethyl ether. The aqueous phase was washed with diethyl ether twice. It was then acidified to

pH ~ 2 and extracted with ethyl acetate. The organic phase was washed with saturated sodium chloride, dried over magnesium sulfate, filtered and concentrated to obtain crude acid as a white solid. No further purification was performed. Yield: 54 mg, 96%. ^1H NMR (400 MHz, DMSO- d_6) δ 12.31 (s, 1H), 7.74 (d, $J = 7.8$ Hz, 1H), 7.63 (d, $J = 7.7$ Hz, 2H), 7.41 – 7.20 (m, 6H), 5.55 (s, 2H), 4.39 – 4.30 (m, 1H), 3.95 – 3.86 (m, 1H), 3.21 – 3.09 (m, 1H), 3.06 – 2.95 (m, 1H), 1.98 – 1.85 (m, 1H), 1.76 – 1.68 (m, 1H), 1.50 – 1.42 (m, 1H), 1.30 – 1.22 (m, 1H). TOF ES+ MS: 398.1 (M+H), 420.1 (M+Na). HPLC ret. time = 6.01 min; purity > 95%.

The crude acid from above (50 mg, 0.13 mmol), EDCI (48.2 mg, 0.251 mmol), and HOBt (34.0 mg, 0.251 mmol) were dissolved in DCM (2.0 mL). The reaction was allowed to stir for 10 minutes before the addition of DIEA (0.044 mL, 0.251 mmol) and 2-(pyridin-4-yl)ethanamine (0.030 mL, 0.251 mmol). The reaction was allowed to stir overnight. The reaction was diluted with water and ethyl acetate. The organic layer was washed with saturated sodium bicarbonate and saturated sodium chloride. The ethyl acetate layer was dried over magnesium sulfate, filtered and concentrated. The crude material was triturated in diethyl ether/ethyl acetate to obtain **112** white solid. Yield: 19 mg (30%). ^1H NMR (500 MHz, DMSO- d_6) δ 8.48 – 8.43 (m, 2H), 7.92 (t, $J = 5.7$ Hz, 1H), 7.74 (d, $J = 8.8$ Hz, 1H), 7.61 (d, $J = 8.1$ Hz, 1H), 7.42 – 7.19 (m, 8H), 5.61 – 5.49 (m, 2H), 4.45 (d, $J = 13.3$ Hz, 1H), 3.98 (d, $J = 13.6$ Hz, 1H), 3.35 – 3.28 (m, 2H), 3.10 – 3.00 (m, 1H), 2.92 – 2.83 (m, 1H), 2.73 (t, $J = 7.0$ Hz, 2H), 2.41 – 2.31 (m, 1H), 1.79 – 1.31 (m, 4H). TOF ES+ MS: 502.1 (M+H), 524.1 (M+Na). HPLC ret. time = 5.20 min; purity > 95%.

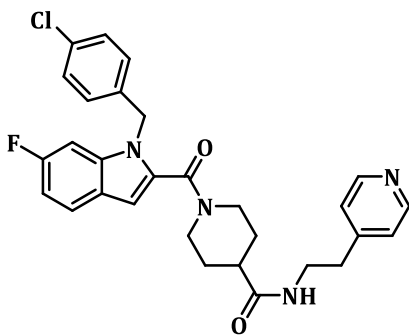


Ethyl 1-(1-(4-chlorobenzyl)-6-fluoro-1H-indole-2-carbonyl)piperidine-4-carboxylate

(194). 6-fluoro-1H-indole-2-carboxylic acid 192 (500 mg, 2.79 mmol), EDCI (1070 mg, 5.58 mmol), and HOBt (754 mg, 5.58 mmol) were dissolved in DCM (14 mL). The reaction was allowed to stir for 20 minutes before adding ethyl piperidine-4-carboxylate (0.860 mL, 5.58 mmol) and DIEA (0.975 mL, 5.58 mmol). The reaction was stirred at room temperature overnight. After 18 hours, it was diluted with water and ethyl acetate. The organic phase was washed with 1N HCl, saturated sodium carbonate, and saturated sodium chloride. It was dried over sodium sulfate, filtered and concentrated. No further purification was done on the material. Yield: 140 mg (16%). ¹H NMR (500 MHz, DMSO- *d*₆) δ 11.64 (s, 1H), 7.62 (dd, *J* = 8.7, 5.5 Hz, 1H), 7.13 (dd, *J* = 10.0, 2.5 Hz, 1H), 6.96 – 6.88 (m, 1H), 6.81 (dd, *J* = 2.3, 0.9 Hz, 1H), 4.33 (dt, *J* = 13.3, 3.2 Hz, 2H), 4.09 (q, *J* = 7.1 Hz, 2H), 3.19 – 3.08 (m, 2H), 2.75 – 2.65 (m, 1H), 1.97 – 1.89 (m, 2H), 1.57 (q, *J* = 11.1 Hz, 2H), 1.20 (t, *J* = 7.1 Hz, 3H). TOF ES+ MS: 319.0 (M+H), 341.0 (M+Na). HPLC ret. time = 6.76 min; purity > 95%

Ethyl 1-(6-fluoro-1H-indole-2-carbonyl)piperidine-4-carboxylate (140 mg, 0.440 mmol) and Cs₂CO₃ (287 mg, 0.880 mmol) were dissolved in DMF (5.0 mL). 1-chloro-4-(chloromethyl)benzene (0.617 ml, 4.83 mmol) was added as a liquid. The reaction was heated at 60 °C overnight. The reaction was cooled and diluted with water and ethyl acetate. The aqueous layer was washed with another aliquot of ethyl acetate. The

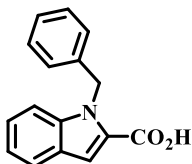
combined organic phases were washed with saturated sodium chloride solution four times. It was dried over sodium sulfate, filtered and concentrated. The crude oil was purified using flash chromatography (0-10% ethyl acetate/hexanes). The product was isolated as a white solid. Yield: 170 mg (87%). $^1\text{H NMR}$ (500 MHz, $\text{DMSO-}d_6$) δ 7.64 (dd, $J = 8.7, 5.5$ Hz, 1H), 7.54 (dd, $J = 10.5, 2.3$ Hz, 1H), 7.36 – 7.29 (m, 2H), 7.10 – 7.04 (m, 2H), 7.02 – 6.94 (m, 1H), 6.75 (d, $J = 0.8$ Hz, 1H), 5.50 – 5.46 (m, 2H), 4.30 (bs, 1H), 4.07 (q, $J = 7.1$ Hz, 2H), 3.88 (bs, 1H), 2.99 (m, 2H), 2.62 – 2.52 (m, 2H), 2.01 – 1.54 (m, 4H), 1.18 (t, $J = 7.1$ Hz, 3H). TOF ES+ MS: 443.1 (M+H), 465.0 (M+Na). HPLC ret. time = 8.39 min; purity >95%.



1-(1-(4-chlorobenzyl)-6-fluoro-1H-indole-2-carbonyl)-N-(2-(pyridin-4-yl)ethyl)piperidine-4-carboxamide (CCG 208918, 117). 194 (140 mg, 0.316 mmol) and lithium hydroxide, H_2O (133 mg, 3.16 mmol) were dissolved in 1/1 THF/water (4 ml). The reaction was stirred overnight at room temperature. After 16 hours, the reaction was concentrated until a suspension formed. It was cooled by an ice bath and diluted with minimal amount of water to allow a stir bar to move freely. 2N HCl was added dropwise until pH 2 was reached. The resulting suspension was diluted with ethyl acetate. The aqueous phase was washed with another aliquot of ethyl acetate. The organic phases were combined and washed with saturated sodium chloride, filtered, and concentrated. No

further purification was performed. The product was isolated as a white solid. Yield: 106 mg, 81% ^1H NMR (400 MHz, $\text{DMSO-}d_6$) δ 12.28 (s, 1H), 7.64 (dd, $J = 8.8, 5.5$ Hz, 1H), 7.51 (dd, $J = 10.5, 2.3$ Hz, 1H), 7.37 – 7.29 (m, 2H), 7.12 – 7.05 (m, 2H), 7.03 – 6.93 (m, 1H), 6.75 (s, 1H), 5.47 (s, 2H), 4.26 (s, 1H), 3.87 (s, 1H), 3.00 (bs, 2H), 2.48 – 2.43 (m, 1H), 1.95 – 1.21 (m, 4H). TOF ES+ MS: 415.0 (M+H), 437.0 (M+Na). HPLC ret. time = 7.02 min; purity > 95%.

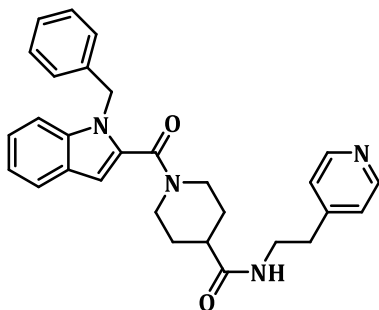
The crude acid from above (106 mg, 0.256 mmol), EDCI (98 mg, 0.511 mmol), and DMAP (62.4 mg, 0.511 mmol) were suspended in DCM (Volume: 5.0 mL). The reaction was stirred for 10 minutes before 2-(pyridin-4-yl)ethanamine (0.061 mL, 0.511 mmol) and DIEA (0.089 mL, 0.511 mmol) were added. The reaction was stirred overnight. The reaction was diluted with water and ethyl acetate. The organic phase was washed with water, saturated sodium carbonate, and saturated sodium chloride. It was dried over sodium sulfate, filtered and concentrated. The crude material was triturated using ethyl acetate. The white solid was filtered to obtain the desired product 117. Yield: 90 mg (68%). ^1H NMR (500 MHz, $\text{DMSO-}d_6$) δ 8.48 – 8.43 (m, 2H), 7.89 (t, $J = 5.7$ Hz, 1H), 7.64 (dd, $J = 8.7, 5.5$ Hz, 1H), 7.49 (dd, $J = 10.4, 2.3$ Hz, 1H), 7.38 – 7.32 (m, 2H), 7.24 – 7.18 (m, 2H), 7.13 – 7.08 (m, 2H), 7.01 – 6.93 (m, 1H), 6.74 (s, 1H), 5.47 (s, 2H), 4.37 (bs, 1H), 3.93 (bs, 1H), 3.34 – 3.28 (m, 2H), 3.04 – 2.70 (m, 4H), 2.36 – 2.26 (m, 1H), 1.71 – 1.18 (m, 4H). TOF ES+ MS: 519.0 (M+H). HPLC ret. time = 5.83 min; purity > 95%.



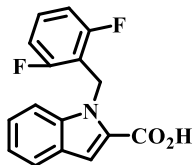
1-Benzyl-1*H*-indole-2-carboxylic acid (195). Ester **155** (1.0 g, 5.3 mmol), potassium carbonate (1.461 g, 10.57 mmol) were dissolved in DMF (15 ml) and heated to 60 °C. The reaction was stirred for 20 minutes before the addition of (bromomethyl)benzene (0.942 ml, 7.93 mmol). The reaction was stirred overnight at 60 °C. After cooling to room temperature, it was diluted with water and an ethyl acetate/diethyl ether mixture. The aqueous phase was washed with another aliquot of the same organic mixture. The organic phases were combined and washed with saturated sodium chloride (2x), dried over sodium sulfate, filtered and concentrated. The resulting crude material was purified via SP1 biotage (25 g silica cartridge) with 0-40% ethyl acetate/hexanes gradient. Ethyl 1-benzyl-1*H*-indole-2-carboxylate was obtained as an off-white solid. Yield: 396 mg, 27%. ¹H NMR (500 MHz, DMSO- *d*₆) δ 7.72 (dt, *J* = 8.0, 1.0 Hz, 1H), 7.57 (dd, *J* = 8.5, 0.9 Hz, 1H), 7.38 (d, *J* = 0.9 Hz, 1H), 7.35 – 7.11 (m, 5H), 7.05 – 6.99 (m, 2H), 5.86 (s, 2H), 4.28 (q, *J* = 7.1 Hz, 2H), 1.28 (t, *J* = 7.1 Hz, 3H). HPLC ret. time = 8.58 min; purity > 95%.

The ester from above (390 mg, 1.396 mmol) was dissolved in THF (1 ml) and 2N aqueous sodium hydroxide (3.49 ml, 6.98 mmol). The reaction was stirred for 3 hours before it was concentrated under vacuum until a white precipitate formed. The resulting suspension was cooled by an ice bath and diluted with water until a stir bar was able to stir. 2N HCl was added dropwise until pH 2 was reached. The acidic aqueous suspension was extracted with ethyl acetate. The aqueous layer was washed with another aliquot of ethyl acetate. The organic phases were combined and washed with saturated sodium chloride, filtered and concentrated. No further purification of 24f was necessary. Yield: 339 mg, 27% ¹H NMR (500 MHz, DMSO- *d*₆) δ 12.97 (s, 1H), 7.70 (dt, *J* = 8.1, 0.9 Hz,

1H), 7.54 (dd, $J = 8.5, 1.0$ Hz, 1H), 7.35 – 7.17 (m, 5H), 7.16 – 7.09 (m, 1H), 7.05 – 7.00 (m, 2H), 5.88 (s, 2H). TOF ES+ MS: 252.1(M+H), 274.1(M+Na). HPLC ret. time = 7.13 min; purity > 95%.



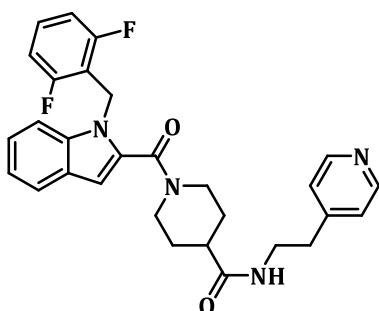
1-(1-benzyl-1H-indole-2-carbonyl)-N-(2-(pyridin-4-yl)ethyl)piperidine-4-carboxamide (CCG 209023, **110**). **195** (48.5 mg, 0.193 mmol), DMAP (23.56 mg, 0.193 mmol), and EDCI (37.0 mg, 0.193 mmol) were dissolved in THF (3.0 ml). The reaction remained a suspension after 30 minutes. Amine **190** (30 mg, 0.129 mmol) was added followed by DIEA (0.034 ml, 0.193 mmol). The reaction was stirred overnight at room temperature. The reaction was diluted with water and ethyl acetate. The organic phase was washed with water and saturated sodium chloride, then it was dried over sodium sulfate. The resulting crude material was purified using SP1 Biotage using a gradient of 30% ethyl acetate: hexanes to 100% ethyl acetate. The product was isolated as a white solid. Yield: 20 mg (33%). ^1H NMR (500 MHz, DMSO- d_6) δ 8.48 – 8.43 (m, 2H), 7.88 (t, $J = 5.6$ Hz, 1H), 7.62 (dt, $J = 7.8$ Hz, 1H), 7.58 (dd, $J = 8.4, 0.9$ Hz, 1H), 7.29 – 7.17 (m, 7H), 7.13 – 7.05 (m, 4H), 6.69 (s, 1H), 5.49 (s, 2H), 4.40 (bs, 1H), 3.92 (bs, 1H), 3.30 (m, 2H), 2.89 (bs, 2H), 2.73 (t, $J = 6.9$ Hz, 2H), 2.35 – 2.25 (m, 1H), 1.74 – 1.21 (m, 4H). TOF ES+ MS: 467.2 (M+H), 489.2 (M+Na). HPLC ret. time = 5.30 min; purity >95%.



1-(2,6-Difluorobenzyl)-1H-indole-2-carboxylic acid (196). 60 wt% sodium hydride (127 mg, 3.17 mmol) was suspended in DMF (8 ml) and cooled with an ice bath. The reaction was stirred at for twenty minutes before a DMF (2 ml) solution of 8 (500 mg, 2.64 mmol) was added dropwise. The reaction was allowed to stir for 20 minutes before 2-(bromomethyl)-1,3-difluorobenzene (821 mg, 3.96 mmol) was added dropwise as a solution in DMF (3 ml). It was allowed to stir at room temperature overnight. The reaction was diluted with saturated ammonium chloride and a mixture of ethyl acetate/diethyl ether. The aqueous phase was washed with another aliquot of ethyl acetate/diethyl ether. The organic phases were combined and washed with saturated sodium chloride, dried over sodium sulfate, filtered and concentrated. The resulting crude material was purified via SP1 Biotage (25 g silica gel column) using a gradient of 100% hexanes to 30% ethyl acetate/hexanes. The product ethyl 1-(2,6-difluorobenzyl)-1H-indole-2-carboxylate was isolated as a white solid. Yield: 586 mg (70%). ¹H NMR (500 MHz, DMSO- *d*₆) δ 7.68 (dt, *J* = 8.0, 1.0 Hz, 1H), 7.50 (dd, *J* = 8.4, 1.0 Hz, 1H), 7.39 – 7.27 (m, 3H), 7.16 – 7.09 (m, 1H), 7.08 – 7.01 (m, 2H), 5.99 (s, 2H), 4.32 (q, *J* = 7.1 Hz, 2H), 1.31 (t, *J* = 7.1 Hz, 3H). TOF ES+ MS: 316.1(M+H), 338.0 (M+Na). HPLC ret. time = 8.53 min; purity >95%.

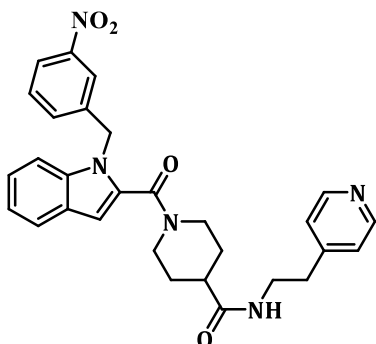
The ester from above (500 mg, 1.59 mmol) was dissolved in ethanol (3 ml) and aqueous sodium hydroxide (3.96 ml, 7.93 mmol). The reaction was stirred for 3 hours before it was concentrated under vacuum until white precipitate formed. The resulting suspension was cooled using an ice bath and diluted with water until a stir bar was

spinning freely. 2N HCl was added dropwise until the aqueous solution reached pH 2. It was diluted with ethyl acetate (2x). The organic phases were combined and washed with saturated sodium chloride, dried over sodium sulfate, filtered and concentrated. The resulting solid **196** was taken to the next step without purification. Yield: 396 mg, 87% ^1H NMR (500 MHz, DMSO- d_6) δ 12.99 (s, 1H), 7.67 (d, $J = 7.9$ Hz, 1H), 7.46 (d, $J = 8.4$ Hz, 1H), 7.40 – 7.23 (m, 3H), 7.14 – 6.99 (m, 3H), 6.02 (s, 2H). TOF ES+ MS: 288.1 (M+H), 310.1 (M+Na). HPLC ret. time = 7.10 min; purity > 95%.



1-(1-(2,6-difluorobenzyl)-1H-indole-2-carbonyl)-N-(2-(pyridin-4-yl)ethyl)piperidine-4-carboxamide (CCG 209024, 111). 196 (104 mg, 0.361 mmol), HOBt (56.3 mg, 0.417 mmol), and EDCI (80 mg, 0.417 mmol) were dissolved in THF (Volume: 3.0 ml). The reaction was stirred for 30 minutes. Solid 16 (30 mg, 0.13 mmol) was added followed by DIEA (0.073 ml, 0.417 mmol). The reaction was stirred overnight at room temperature. The reaction was diluted with water and ethyl acetate. The organic phase was washed with water and saturated sodium chloride; it was dried over sodium sulfate. The resulting crude material was purified using SP1 Biotage using a gradient of 30% ethyl acetate: hexanes to 100% ethyl acetate. The product was isolated as a white solid. Yield: 68 mg (49%). ^1H NMR (500 MHz, DMSO- d_6) δ 8.49 – 8.44 (m, 2H), 7.91 (t, $J = 5.6$ Hz, 1H), 7.61 – 7.55 (m, 2H), 7.41 – 7.31 (m, 1H), 7.28 – 7.20 (m, 3H), 7.12 – 7.01 (m, 3H), 6.67 (s, 1H), 5.63 (s, 4H), 4.42 (bs, 1H), 3.97 (bs, 1H), 3.37 – 3.29 (m, 3H), 3.03 – 2.69 (m,

4H), 2.37 – 2.27 (m, 1H), 1.73 – 1.31 (m, 4H). TOF ES+ MS: 503.2 (M+H) HPLC ret. time = 5.37 min; purity = 92%.



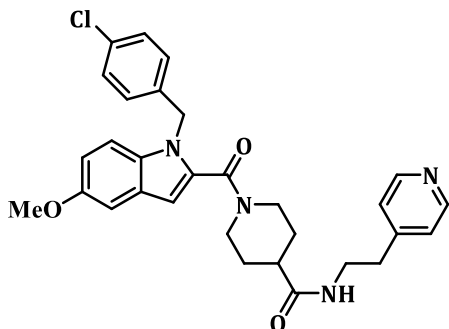
1-(1-(3-nitrobenzyl)-1H-indole-2-carbonyl)-N-(2-(pyridin-4-yl)ethyl)piperidine-4-carboxamide (212150, 116)

Cesium carbonate (2.58 g, 7.93 mmol) and **155** (1.0 g, 5.29 mmol) was dissolved in 10 mL of DMF. It was stirred at room temperature for 30 minutes before an 8 mL DMF solution of 1-(bromomethyl)-3-nitrobenzene (1.713 g, 7.93 mmol). The reaction was allowed to stir overnight. It was diluted with saturated ammonium chloride and ethyl acetate/THF. The aqueous phase was washed with the same organic phase combination. The combined organic phases were washed with saturated sodium chloride. It was dried over sodium sulfate, filtered, and concentrated. The resulting crude solid was triturated with ethyl acetate and filtered to obtain ethyl 1-(3-nitrobenzyl)-1H-indole-2-carboxylate as a white solid. Yield: 373 mg, 22 %.

Ethyl 1-(3-nitrobenzyl)-1H-indole-2-carboxylate (373 mg, 1.150 mmol) was dissolved in EtOH (Ratio: 2, Volume: 2 ml), THF (Ratio: 1.000, Volume: 1.000 ml) and 2N NaOH (Ratio: 1.000, Volume: 1.000 ml). The reaction was stirred overnight. The reaction was concentrated by half volume and diluted with water to allow free movement of a stirbar. It was cooled by and ice bath and acidified using 2N HCl. The resulting

suspension was extracted using ethyl acetate. The organic phase was washed with saturated sodium chloride, dried over sodium sulfate, filtered and concentrated. The product **220** was obtained as a white solid. The crude material was taken directly to the next step. Yield: 314 mg, 92 %

Compound **220** (160 mg, 0.539 mmol), 1-Hydroxybenzotriazole (97 mg, 0.718 mmol), and EDCI (138 mg, 0.718 mmol) were dissolved in THF (Volume: 5 ml) and stirred for 20 minutes before **190** (110 mg, 0.359 mmol) was added a solid. It was followed by the addition of Hunig'sBase (0.188 ml, 1.078 mmol). The reaction was stirred overnight. The reaction was diluted with water and ethyl acetate/THF. The organic phase was washed with sodium carbonate and saturated sodium chloride. The organic phase was dried over sodium sulfate, filtered and concentrated. The crude material was purified using sp1 biotage with gradient of 100% ethyl acetate to 10% methanol/ethyl acetate to obtain product as a white solid. $^1\text{H NMR}$ (500 MHz, DMSO- d_6) δ ppm 8.41 - 8.50 (m, 2 H), 8.10 (d, $J=8.1$ Hz, 1 H), 7.96 (s, 1 H), 7.89 (t, $J=5.6$ Hz, 1 H), 7.66 (d, $J=7.8$ Hz, 1 H), 7.55 - 7.62 (m, 2 H), 7.50 - 7.55 (m, 1 H), 7.19 - 7.27 (m, 3 H), 7.09 - 7.16 (m, 1 H), 6.77 (s, 1 H), 5.65 (s, 2 H), 4.39 (br. s., 1 H), 4.01 (br. s., 1 H), 3.30 (q, $J=6.8$ Hz, 2 H), 2.68 - 3.16 (m, 4 H), 2.31 (tt, $J=11.1, 3.6$ Hz, 1 H), 1.08 - 1.78 (m, 4 H). TOF ES+ MS: 512.1 (M+H). HPLC (gradient A): ret. time = 5.51 min; purity > 95 %



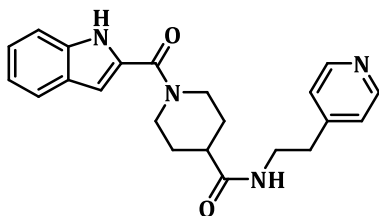
1-(1-(4-chlorobenzyl)-5-methoxy-1H-indole-2-carbonyl)-N-(2-(pyridin-4-yl)ethyl)piperidine-4-carboxamide (CCG 209025, 113) A suspension of sodium hydride (37.5 mg, 0.937 mmol) in DMF (2.0 mL) was cooled to 0 °C. A 1.0 mL DMF solution of **225** (137 mg, 0.625 mmol) was added dropwise and the reaction was stirred for 15 minutes before a 1.0 mL DMF solution of 1-chloro-4-(chloromethyl)benzene (0.120 ml, 0.937 mmol). The reaction was warmed to room temperature and stirred for 5 hours. The reaction was diluted with water and ethyl acetate. The aqueous layer was washed with another portion of ethyl acetate. The organic phases were combined and washed with saturated sodium chloride (3x), dried over sodium sulfate, filtered, and concentrated. The crude material was purified via column chromatography using 0-50% ethyl acetate/hexanes. The product was obtained as a white solid and taken directly to the next step Yield: 191 mg, 89%

Ethyl 1-(4-chlorobenzyl)-5-methoxy-1H-indole-2-carboxylate (350 mg, 1.018 mmol) was dissolved in EtOH (Volume: 2.0 ml) and 2N sodium hydroxide (5.09 ml, 10.18 mmol). The reaction was stirred for 4 hours, before it was concentrated under vacuum to remove the ethanol. The resulting thick solution was diluted with water and acidified using 2N HCl. The white suspension was sonicated for 10 minutes before the

solid was filtered to obtain **220**. The carboxylic acid was taken directly to the next step.

Yield: 260 mg, 81 %

Compound **230** (50 mg, 0.158 mmol), EDCI (45.5 mg, 0.238 mmol), DMAP (29.0 mg, 0.238 mmol) were dissolved in THF (Volume: 3.0 ml) and stirred at room temperature for 30 minutes. Compound **190** (55.5 mg, 0.206 mmol) was added as a solid. Subsequently, Hunig's Base (0.041 ml, 0.238 mmol) was added. The reaction was stirred at room temperature overnight. The reaction was diluted with water and ethyl acetate. The organic phase was washed with saturated sodium carbonate and saturated sodium chloride. It was dried over sodium sulfate, filtered and concentrated. The resulting crude material was purified via flash column chromatography using 0-70% ethyl acetate/hexanes to obtain product as a white solid. $^1\text{H NMR}$ (500 MHz, $\text{DMSO-}d_6$) δ ppm 8.43 - 8.49 (m, 2 H), 7.89 (t, $J=5.6$ Hz, 1 H), 7.43 (d, $J=9.0$ Hz, 1 H), 7.31 - 7.35 (m, 2 H), 7.19 - 7.24 (m, 2 H), 7.05 - 7.12 (m, 3 H), 6.85 (dd, $J=9.0, 2.4$ Hz, 1 H), 6.62 (s, 1 H), 5.44 (s, 2 H), 4.35 (br. s., 1 H), 3.98 (br. s., 1 H), 3.76 (s, 3 H), 3.27 - 3.32 (m, 6 H), 2.77 - 3.08 (m, 2 H), 2.73 (t, $J=7.0$ Hz, 2 H), 2.32 (tt, $J=11.1, 3.6$ Hz, 1 H), 1.21 - 1.74 (m, 4 H). TOF ES+ MS: 531.2 (M+H), 553.2 (M+Na). HPLC (gradient A): ret. time = 5.55 min; purity > 95 %



1-(1H-indole-2-carbonyl)-N-(2-(pyridin-4-yl)ethyl)piperidine-4-carboxamide (CCG

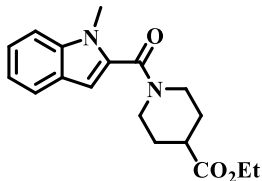
212059, 114) Ethyl 1*H*-indole-2-carboxylate (155, 3.0 g, 16 mmol) and lithium

hydroxide, H_2O (3.3 g, 79 mmol) were dissolved in 2/1 water/THF (30 mL). The reaction

was stirred overnight. The reaction was diluted with water and diethyl ether. The water layer was washed with diethyl ether twice. The aqueous layer was acidified to pH 2 using 2N HCl. The suspension was extracted using ethyl acetate. The organic layer was washed with saturated sodium chloride solution, dried over magnesium sulfate, filtered and concentrated to obtain 1*H*-Indole-2-carboxylic acid as a white solid. Yield: 2.39 g, 94%. ¹H NMR (400 MHz, DMSO-*d*₆) δ 12.95 (s, 1H), 11.74 (s, 1H), 7.67 – 7.60 (m, 1H), 7.47 – 7.39 (m, 1H), 7.28 – 7.19 (m, 1H), 7.11 – 7.01 (m, 2H).

1*H*-indole-2-carboxylic acid (100 mg, 0.621 mmol), EDCI (178 mg, 0.931 mmol), 1-Hydroxybenzotriazole (126 mg, 0.931 mmol) were dissolved in DCM (Volume: 5 ml) and stirred for 30 minutes at room temperature. N-(2-(pyridin-4-yl)ethyl)piperidine-4-carboxamide, 2HCl (285 mg, 0.931 mmol) was added as a solid, followed by Hunig'sBase (0.542 ml, 3.10 mmol). The reaction was further stirred at room temperature overnight at room temperature. The reaction was diluted with water and ethyl acetate/THF. The organic phase was washed with saturated sodium carbonate, sodium bicarbonate, and brine. The organic phase was dried over sodium sulfate. The drying agent was used filtered and crude material concentrated. The crude material was purified via Biotage SP1 with 50% ethyl acetate/hexanes to 100% ethyl acetate. The product was a white solid. Yield: 140 mg, 60 %. ¹H NMR (500 MHz, DMSO-*d*₆) δ ppm 8.43 - 8.49 (m, 2 H), 7.96 (t, *J*=5.6 Hz, 1 H), 7.60 (d, *J*=8.1 Hz, 1 H), 7.41 (d, *J*=8.1 Hz, 1 H), 7.20 - 7.25 (m, 2 H), 7.14 - 7.20 (m, 1 H), 7.01 - 7.07 (m, 1 H), 6.75 (d, *J*=1.5 Hz, 1 H), 4.42 (dt, *J*=13.4, 3.7 Hz, 2 H), 3.33 (q, *J*=6.8 Hz, 3 H), 3.05 (br. s., 2 H), 2.74 (t, *J*=7.0 Hz, 2 H), 2.41 (tt, *J*=11.3, 3.8 Hz, 1 H), 1.67 - 1.77 (m, 2 H), 1.45 - 1.60 (m, 2 H). TOF ES+ MS: 377.3 (M+H), 399.3 (M+Na). HPLC (gradient A): ret. time = 4.37 min;

purity > 95 %

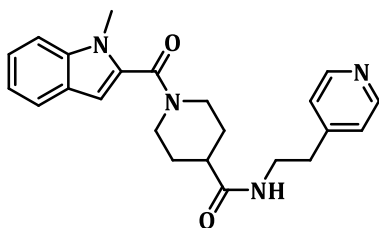


Ethyl 1-(1-methyl-1*H*-indole-2-carbonyl)piperidine-4-carboxylate (199). Ethyl 1*H*-indole-2-carboxylate **155** (1.00 g, 5.29 mmol) and K₂CO₃ (1.46 g, 10.57 mmol) were dissolved in DMF (10 ml). Iodomethane (0.99 ml, 16 mmol) was added and the reaction was stirred at 60 °C overnight. The reaction was dissolved in water and diethyl ether. The water layer was washed with diethyl ether twice. The organic layers were combined and washed with brine twice. It was then dried over magnesium sulfate, filtered, and concentrated. The crude product ethyl 1-methyl-1*H*-indole-2-carboxylate was taken directly into the next step. ¹H NMR (400 MHz, DMSO- *d*₆) δ 7.69 (d, *J* = 8.0 Hz, 1H), 7.58 (d, *J* = 8.6 Hz, 1H), 7.35 (t, *J* = 7.8 Hz, 1H), 7.27 (s, 1H), 7.14 (t, *J* = 7.5 Hz, 1H), 4.32 (q, *J* = 7.1 Hz, 2H), 4.03 (s, 3H), 1.34 (t, *J* = 7.1 Hz, 3H). TOF ES+ MS: 204.1 (M+H). HPLC ret. time = 7.85 min; purity > 95%.

Ethyl 1-methyl-1*H*-indole-2-carboxylate (1.0 g, 4.92 mmol) and lithium hydroxide (1.178 g, 49.2 mmol) were dissolved in 2/1 water/THF (6 ml). The reaction was allowed to stir overnight. The reaction was diluted with water and washed with diethyl ether. The water layer was then acidified with 1N HCl to pH 2. The resulting suspension was extracted with ethyl acetate. The organic layer was washed with saturated sodium chloride, dried over magnesium sulfate, filtered and concentrated to obtain pure 1-methyl-1*H*-indole-2-carboxylic acid as a white solid. Yield: 560 mg (65%). ¹H NMR

(400 MHz, DMSO- d_6) δ 12.91 (s, 1H), 7.67 (d, $J = 8.0$ Hz, 1H), 7.57 (d, $J = 8.5$ Hz, 1H), 7.37 – 7.29 (m, 1H), 7.22 (s, 1H), 7.16 – 7.08 (m, 1H), 4.02 (s, 3H). TOF ES+ MS: 176.1 (M+H). HPLC ret. time = 6.06 min; purity > 95%.

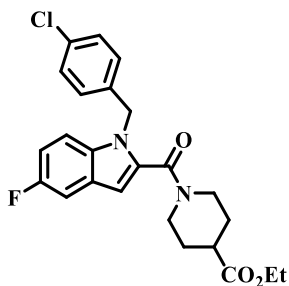
1-Methyl-1*H*-indole-2-carboxylic acid (200 mg, 1.14 mmol), HOBt (231 mg, 1.712 mmol), and EDCI (328 mg, 1.712 mmol) were dissolved in DCM (Volume: 4 ml). The reaction was allowed to stir for 10 minutes before adding DIEA (0.299 ml, 1.71 mmol) and ethyl piperidine-4-carboxylate (0.264 ml, 1.71 mmol). The reaction was stirred overnight. The reaction was diluted with water and extracted with ethyl acetate. The organic layer was washed with saturated sodium bicarbonate and 1N HCl. This was followed by a wash with saturated sodium chloride. The organic phase was dried over magnesium sulfate, filtered and concentrated to obtain 26e as a white solid. No further purification was required. Yield: 214 mg, 60%. ^1H NMR (400 MHz, DMSO- d_6) δ 7.57 (d, $J = 8.0$ Hz, 1H), 7.48 (d, $J = 9.0$ Hz, 1H), 7.21 (d, $J = 15.3$ Hz, 1H), 7.06 (t, $J = 7.5$ Hz, 1H), 6.61 (s, 1H), 4.37 – 3.83 (m, 4H), 3.71 (s, 3H), 3.10 (bs, 2H), 2.70 – 2.59 (m, 1H), 1.87 (bs, 2H), 1.61 – 1.46 (m, 2H), 1.16 (t, $J = 7.1$ Hz, 3H). TOF ES+ MS: 315.1 (M+H), 337.1 (M+Na). HPLC ret. time = 6.99 min; purity > 95%.



1-(1-methyl-1*H*-indole-2-carbonyl)-*N*-(2-(pyridin-4-yl)ethyl)piperidine-4-carboxamide (CCG 206484, 118). **199** (210 mg, 0.668 mmol) and lithium hydroxide, H₂O (280 mg, 6.68 mmol) were dissolved in 2/1 water/THF (2.3 ml). The reaction was stirred for 6 hours before it was diluted with water and diethyl ether. The aqueous layer

was acidified using 2N HCl to pH ~ 2. The suspension was extracted with ethyl acetate. The organic phase was washed with saturated sodium chloride, dried over magnesium sulfate, filtered and concentrated to obtain product as a white solid. No purification was performed on the material. The crude acid was taken directly to the next step. TOF ES+ MS: 287.1(M+H), 309.1(M+Na). HPLC ret. time = 5.60 min; purity = 94%.

1-(1-methyl-1*H*-indole-2-carbonyl)piperidine-4-carboxylic acid (100 mg, 0.349 mmol), EDCI (100 mg, 0.524 mmol), and HOBt (70.8 mg, 0.524 mmol) were dissolved in DCM (Volume: 3.0 mL). The reaction was stirred for 10 minutes before 2-(pyridin-4-yl)ethanamine (0.059 mL, 0.524 mmol) and DIEA (0.091 mL, 0.524 mmol). The reaction was stirred overnight at room temperature. The reaction was diluted with water and ethyl acetate. The organic layer was washed with saturated sodium bicarbonate solution, and finally saturated sodium chloride. the organic layer was then dried over magnesium sulfate, filtered and concentrated. The resulting solid was triturated in ethyl acetate to give 118. Yield: 50 mg (38%). ¹H NMR (400 MHz, DMSO- *d*₆) δ 8.49 – 8.42 (m, 2H), 7.94 (t, *J* = 5.6 Hz, 1H), 7.60 (d, *J* = 7.8 Hz, 1H), 7.50 (d, *J* = 8.0 Hz, 1H), 7.29 – 7.19 (m, 3H), 7.09 (t, *J* = 7.4 Hz, 1H), 6.62 (s, 1H), 4.40 (bs, 1H), 4.02 (bs, 1H), 3.74 (s, 3H), 3.32 – 3.29 (m, 2H), 3.04 (bs, 2H), 2.73 (t, *J* = 7.0 Hz, 2H), 2.41 – 2.36 (m, 1H), 1.71 – 1.66 (m, 2H), 1.57 – 1.46 (m, 2H). TOF ES+ MS: 391.1 (M+H). HPLC ret. time = 4.68 min; purity > 95%.



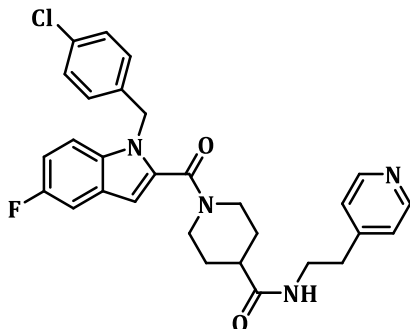
Ethyl 1-(1-(4-chlorobenzyl)-5-fluoro-1*H*-indole-2-carbonyl)piperidine-4-carboxylate

(200). Ethyl 5-fluoro-1*H*-indole-2-carboxylate **198** (0.500 g, 2.413 mmol) and Cs₂CO₃ (1.179 g, 3.62 mmol) were dissolved in DMF (15 ml). 1-chloro-4-(chloromethyl)benzene (0.617 ml, 4.83 mmol) was added as a liquid. The reaction was heated at 60 °C overnight. The reaction was cooled and diluted with water and ethyl acetate. The aqueous layer was washed with another aliquot of ethyl acetate. The combined organic phases were washed with saturated sodium chloride solution four times. It was dried over sodium sulfate, filtered and concentrated. The crude oil was purified by flash chromatography using 0-10% ethyl acetate/hexanes. The product ethyl 1-(4-chlorobenzyl)-5-fluoro-1*H*-indole-2-carboxylate was isolated as a clear oil. Yield: 600 mg (75 %). ¹H NMR (500 MHz, DMSO- *d*₆) δ 7.63 (dd, *J* = 9.0, 5.3 Hz, 1H), 7.51 (dd, *J* = 9.4, 2.4 Hz, 1H), 7.47 – 7.41 (m, 1H), 7.37 – 7.33 (m, 2H), 7.21 (td, *J* = 9.3, 2.5 Hz, 1H), 7.03 (d, *J* = 8.5 Hz, 2H), 5.85 (s, 2H), 4.28 (q, *J* = 7.1 Hz, 2H), 1.28 (t, *J* = 7.1 Hz, 3H). HPLC ret. time = 9.06 min; purity > 95%.

Ethyl 1-(4-chlorobenzyl)-5-fluoro-1*H*-indole-2-carboxylate (465 mg, 1.402 mmol) and lithium hydroxide, H₂O (588 mg, 14.0 mmol) were dissolved in 2/1 water/THF (12 ml). The reaction was allowed to stir overnight at room temperature. The reaction was diluted with water and diethyl ether. The organic phase was removed and the aqueous phase was acidified using 2N HCl to pH ~2. The resulting suspension was

extracted with ethyl acetate. The aqueous phase was washed with another aliquot of ethyl acetate. The organic phases were combined, washed with saturated sodium chloride, filtered and concentrated to obtain the product 1-(4-chlorobenzyl)-5-fluoro-1*H*-indole-2-carboxylic acid. No further purification was performed. Yield: 130 mg (31%). ¹H NMR (500 MHz, DMSO- *d*₆) δ 13.14 (s, 1H), 7.58 (dd, *J* = 9.2, 4.4 Hz, 1H), 7.49 (dd, *J* = 9.4, 2.6 Hz, 1H), 7.37 – 7.28 (m, 3H), 7.18 (td, *J* = 9.2, 2.6 Hz, 1H), 7.06 – 7.00 (m, 2H), 5.86 (s, 2H). HPLC ret. time = 7.55 min; purity > 95%.

1-(4-chlorobenzyl)-5-fluoro-1*H*-indole-2-carboxylic acid (130 mg, 0.428 mmol), EDCI (164 mg, 0.856 mmol), and DMAP (105 mg, 0.856 mmol) were dissolved in DCM (Volume: 5 ml). The reaction was allowed to stir for 20 minutes before adding ethyl piperidine-4-carboxylate (0.132 ml, 0.856 mmol) and DIEA (0.150 ml, 0.856 mmol). The reaction was stirred at room temperature overnight. After 18 hours, it was diluted with water and ethyl acetate. The organic phase was washed with 1N HCl, saturated sodium carbonate, and saturated sodium chloride. It was dried over sodium sulfate, filtered and concentrated. The crude mixture was triturated with diethyl ether and ethyl acetate. The product 26i was isolated as a pale yellow oil solid. Yield: 90 mg (100%). ¹H NMR (500 MHz, DMSO- *d*₆) δ 7.62 (dd, *J* = 9.1, 4.4 Hz, 1H), 7.40 (dd, *J* = 9.5, 2.6 Hz, 1H), 7.35 – 7.30 (m, 6H), 7.11 – 7.05 (m, 9H), 6.71 (s, 1H), 5.49 (s, 2H), 4.31 (bs, 1H), 4.07 (q, *J* = 7.1, 7.1 Hz, 2H), 3.83 (bs, 1H), 3.08 (bs, 1H), 2.92 (bs, 1H), 2.62 – 2.53 (m, 1H), 1.86 (bs, 1H), 1.66 (bs, 1H), 1.40 (bs, 1H), 1.18 (t, *J* = 7.1 Hz, 3H), 1.05 (bs, 1H). TOF ES+ MS: 443.0 (M+H), 465.0 (M+Na). HPLC ret. time = 8.28 min; purity >95%.



1-(1-(4-chlorobenzyl)-5-fluoro-1*H*-indole-2-carbonyl)-*N*-(2-(pyridin-4-

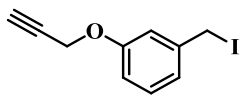
yl)ethyl)piperidine-4-carboxamide (CCG 208919, 115). 200 (190 mg, 0.429 mmol)

and lithium hydroxide, H₂O (180 mg, 4.29 mmol) were dissolved in 2/1 water/THF (4.5 ml). The reaction was stirred overnight at room temperature. After 16 hours, the reaction was concentrated until a suspension formed. It was cooled by an ice bath and diluted with minimal amount of water to allow a stir bar to move freely. 2N HCl was added dropwise until pH 2 was reached. The resulting suspension was diluted with ethyl acetate. The aqueous phase was washed with another aliquot of ethyl acetate. The organic phases were combined and washed with saturated sodium chloride, filtered, and concentrated. No further purification was performed. The product 1-(1-(4-chlorobenzyl)-5-fluoro-1*H*-indole-2-carbonyl)piperidine-4-carboxylic acid was isolated as a white solid. Yield: 129 mg, 73%. ¹H NMR (400 MHz, DMSO-*d*₆) δ 12.26 (s, 1H), 7.59 (dd, *J* = 9.0, 4.4 Hz, 1H), 7.40 (dd, *J* = 9.6, 2.6 Hz, 1H), 7.35 – 7.30 (m, 2H), 7.12 – 7.05 (m, 3H), 6.71 (s, 1H), 5.48 (s, 2H), 4.28 (bs, 1H), 3.84 (bs, 1H), 3.00 (bs, 2H), 2.48 – 2.41 (m, 1H), 1.53 (bm, 4H). HPLC ret. time = 5.51 min; purity > 95%.

1-(1-(4-chlorobenzyl)-5-fluoro-1*H*-indole-2-carbonyl)piperidine-4-carboxylic acid (106 mg, 0.256 mmol), DMAP (62.4 mg, 0.51 mmol), and EDCI (98 mg, 0.51 mmol) were dissolved in DCM (5.0 mL). The reaction was stirred for 10 minutes before

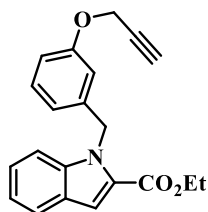
adding 2-(pyridin-4-yl)ethanamine (0.061 mL, 0.51 mmol) and DIEA (0.089 mL, 0.51 mmol). The reaction was stirred overnight at room temperature. It was diluted with water and ethyl acetate. The organic phase was washed with water, saturated sodium carbonate, and saturated sodium chloride. It was filtered and concentrated. The resulting crude material was triturated with ethyl acetate. The resulting white solid was filtered to obtain the desired product. Yield: 80 mg, 60%. $^1\text{H NMR}$ (500 MHz, $\text{DMSO-}d_6$) δ 8.48 – 8.43 (m, 2H), 7.90 (t, $J = 5.7$ Hz, 1H), 7.57 (dd, $J = 9.1, 4.4$ Hz, 1H), 7.40 (dd, $J = 9.5, 2.5$ Hz, 1H), 7.36 – 7.33 (m, 2H), 7.23 – 7.20 (m, 2H), 7.13 – 7.07 (m, 3H), 6.70 (s, 1H), 5.48 (s, 2H), 4.40 (bs, 1H), 3.90 (bs, 1H), 3.34 – 3.30 (m, 22H), 3.04 – 2.70 (m, 4H), 2.36 – 2.27 (m, 1H), 1.67 – 1.18 (m, 4H). TOF ES+ MS: 519.1 (M+H), 541.1 (M+Na). HPLC ret. time = 5.51 min; purity > 95%.

Photoaffinity probes

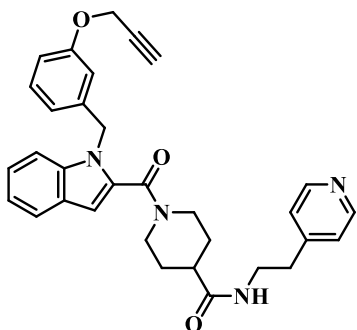


1-(iodomethyl)-3-(prop-2-yn-1-yloxy)benzene (202). To solid 3-(hydroxymethyl)phenol (5 g, 40.3 mmol) and cesium carbonate (19.7 g, 60.4 mmol) was added DMF (Volume: 134 ml). The reaction was stirred for 20 minutes at room temperature. 3-bromoprop-1-yne (3.66 ml, 48.3 mmol) was added and the reaction was stirred overnight. The reaction was diluted with water and extracted with 50:50 ethyl acetate:diethyl ether. The aqueous layer was washed again with the same organic layer mixture. The organic layers were combined and washed with saturated sodium carbonate followed by saturated sodium chloride. It was dried over sodium sulfate, filtered and concentrated. The crude material was purified via SP1 biotage, 40g silica gel column with 0-45% ethyl acetate-hexanes to obtain (3-(prop-2-yn-1-yloxy)phenyl)methanol as a slightly yellow oil. Yield: 2.6 g, 39.8%. $^1\text{H NMR}$ (500 MHz, $\text{DMSO-}d_6$) δ ppm 7.25 (t, $J=7.8$ Hz, 1 H), 6.88 - 6.97 (m, 2 H), 6.80 - 6.88 (m, 1 H), 5.20 (t, $J=5.9$ Hz, 1 H), 4.77 (d, $J=2.4$ Hz, 2 H), 4.47 (d, $J=5.9$ Hz, 2 H), 3.55 (t, $J=2.4$ Hz, 1 H). Imidazole (504 mg, 7.40 mmol), iodine (1.88 g, 7.40mmol), and polymer bound triphenylphosphine (3mmol/g loading, 1.94g, 7.40 mmol) were dissolved in DCM (20 mL) and stirred for 10 minutes at room temperature. (3-(prop-2-yn-1-yloxy)phenyl)methanol was added as a DCM (10 mL) solution. The reaction was stirred at room temperature for 3 hours at which time the reaction showed complete consumption of starting material by TLC. The reaction was filtered and polymer was washed with DCM. The resulting filtrate was washed with water followed by saturated sodium thiosulfate until organic phase was colorless. The organic phase was subsequently washed with saturated sodium chloride,

dried over sodium sulfate, filtered and concentrated to obtain 1-(iodomethyl)-3-(prop-2-yn-1-yloxy)benzene as a reddish oil. Taken directly to next step without further purification or characterization. $R_f = 0.5$ (50% EtOAc/Hex)



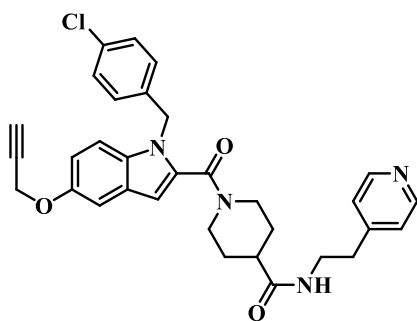
Ethyl 1-(3-(prop-2-yn-1-yloxy)benzyl)-1H-indole-2-carboxylate (203) Ethyl 1H-indole-2-carboxylate (**155**) (200 mg, 1.05 mmol) was dissolved in 3.0 mL of DMF. Cesium carbonate (448 mg, 1.37 mmol) was added to the solution. The reaction was stirred for 20 minutes before 1-(iodomethyl)-3-(prop-2-yn-1-yloxy)benzene was added as a solution in 2.0 mL of DMF. The reaction was stirred overnight at 60 °C. The reaction was diluted with water and ethyl acetate. The aqueous layer was washed with another portion of ethyl acetate. The organic layers were combined and washed with brine (3x), dried over sodium sulfate, filtered and concentrated. The resulting crude material was taken to the next step without further purification. ^1H NMR (500 MHz, DMSO- d_6) δ ppm 7.73 (d, $J=8.1$ Hz, 1 H), 7.57 (d, $J=8.3$ Hz, 1 H), 7.38 (s, 1 H), 7.29 - 7.34 (m, 1 H), 7.13 - 7.21 (m, 2 H), 6.84 (dd, $J=8.2, 2.3$ Hz, 1 H), 6.66 (s, 1 H), 6.60 (d, $J=7.8$ Hz, 1 H), 5.84 (s, 2 H), 4.71 (d, $J=2.4$ Hz, 2 H), 4.29 (q, $J=7.2$ Hz, 2 H), 3.52 (t, $J=2.3$ Hz, 1 H), 1.29 (t, $J=7.1$ Hz, 3 H). TOF ES+ MS: 334.3 (M+H), 356.2 (M+Na). HPLC (gradient A): ret. time = 8.46 min; purity 65 %.



1-(1-(3-(prop-2-yn-1-yloxy)benzyl)-1H-indole-2-carbonyl)-N-(2-(pyridin-4-yl)ethyl)piperidine-4-carboxamide (CCG 212370, 120) Compound **203** (120 mg, .360 mmol) was dissolved in ethanol (2.0 mL) and 2N NaOH (0.9 mL, 1.80 mmol). The reaction was stirred at room temperature until TLC showed consumption of starting material. The reaction was concentrated to remove ethanol. The aqueous solution was acidified to pH 2 using 2N HCl. The resulting solid was extracted using ethyl acetate (2x). The combined organic phases were washed with saturated sodium chloride, dried over magnesium sulfate, filtered and concentrated to obtain 1-(3-(prop-2-yn-1-yloxy)benzyl)-1H-indole-2-carboxylic acid. The crude material was taken directly to next step without purification. TOF ES+ MS: 306.2 (M+H), 328.2 (M+Na).

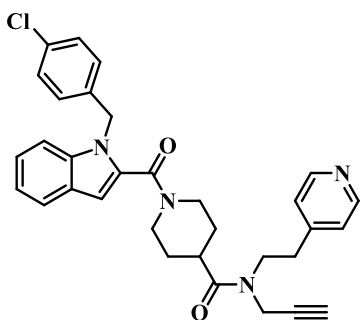
1-(3-(prop-2-yn-1-yloxy)benzyl)-1H-indole-2-carboxylic acid (90 mg, .295 mmol), EDCI (113 mg, .590 mmol), and HOBt (80 mg, .590 mmol) were suspended in 3.0 mL of DCM. The suspension was stirred for 20 minutes and turned into a homogenous solution. Solid N-(2-(pyridin-4-yl)ethyl)piperidine-4-carboxamide dihydrochloride (181 mg, .590 mmol) was added followed by DIEA (0.10 mL, 0.590). The reaction was stirred overnight at room temperature. The reaction was diluted with water and ethyl acetate:THF (10:1). The organic phase was washed with saturated sodium bicarbonate, saturated sodium carbonate, and saturated sodium chloride solutions.

It was then dried over sodium sulfate, filtered and concentrated. The crude material was purified via flash chromatography using 20% ethyl acetate-hexanes to 100% ethyl acetate. The product was obtained as a white solid. Yield: 50 mg, 33%. ¹H NMR (500 MHz, DMSO-*d*₆) δ ppm 8.44 - 8.47 (m, 2 H), 7.89 (t, *J*=5.7 Hz, 1 H), 7.59 (dd, *J*=35.2, 7.8 Hz, 2 H), 7.17 - 7.23 (m, 4 H), 7.09 (t, *J*=7.4 Hz, 1 H), 6.84 (dd, *J*=8.2, 2.3 Hz, 1 H), 6.72 (t, *J*=2.2 Hz, 1 H), 6.70 (s, 1 H), 6.64 (d, *J*=7.8 Hz, 1 H), 5.46 (s, 2 H), 4.71 (d, *J*=2.4 Hz, 2 H), 4.42 (br. s., 1 H), 3.93 (br. s., 1 H), 3.51 (t, *J*=2.3 Hz, 1 H), 3.31 (q, *J*=7.1 Hz, 2 H), 2.77 - 3.11 (m, 2 H), 2.73 (t, *J*=7.1 Hz, 2 H), 2.31 (tt, *J*=11.3, 3.9 Hz, 1 H), 1.20 - 1.76 (m, 4 H). TOF ES+ MS: 521.5 (M+H). HPLC (gradient A): ret. time = 5.17 min; purity > 95 %.



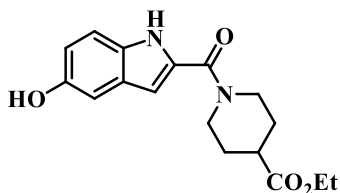
1-(1-(4-chlorobenzyl)-5-(prop-2-yn-1-yloxy)-1H-indole-2-carbonyl)-N-(2-(pyridin-4-yl)ethyl)piperidine-4-carboxamide (CCG 212057, 121) Compound **176** (42mg, 0.124 mmol), EDCI (47.4 mg, 0.247 mmol), and HOBt (33.4 mg, 0.247 mmol) were dissolved in DCM and stirred for 30 minutes at room temperature. N-(2-(pyridin-4-yl)ethyl)piperidine-4-carboxamide, 2HCl (76 mg, 0.247 mmol) was added as a solid, followed by Hunig'sBase (0.043 ml, 0.247 mmol). The reaction was further stirred at room temperature overnight at room temperature. The reaction was diluted with water and ethyl acetate/THF. The organic phase was washed with saturated sodium carbonate,

sodium bicarbonate, and brine. The organic phase was dried over sodium sulfate. The drying agent was used filtered and crude material concentrated. The crude material was purified via Biotage SP1 with 50% ethyl acetate/hexanes to 100% ethyl acetate. The product was a white solid. Yield: 40 mg, 58 % ^1H NMR (500 MHz, $\text{DMSO-}d_6$) δ ppm 8.42 - 8.49 (m, 2 H), 7.90 (t, $J=5.5$ Hz, 1 H), 7.46 (d, $J=9.0$ Hz, 1 H), 7.30 - 7.37 (m, 2 H), 7.19 (d, $J=2.4$ Hz, 1 H), 7.21 (d, $J=5.6$ Hz, 2 H), 7.06 - 7.12 (m, 2 H), 6.90 (dd, $J=8.8, 2.4$ Hz, 1 H), 6.64 (s, 1 H), 5.45 (s, 2 H), 4.77 (d, $J=2.2$ Hz, 2 H), 4.38 (br. s., 1 H), 3.96 (br. s., 1 H), 3.55 (t, $J=2.2$ Hz, 1 H), 3.31 (q, $J=5.9$ Hz, 2 H), 2.77 - 3.08 (m, 2 H), 2.73 (t, $J=7.0$ Hz, 2 H), 2.32 (tt, $J=11.2, 3.4$ Hz, 1 H), 1.20 - 1.77 (m, 4 H). TOF ES+ MS: 555.4 (M+H); 577.4 (M+Na). HPLC (gradient A): ret. time = 5.59 min; purity > 95 %



1-(1-(4-chlorobenzyl)-1H-indole-2-carbonyl)-N-(prop-2-yn-1-yl)-N-(2-(pyridin-4-yl)ethyl)piperidine-4-carboxamide (CCG 212050) Sodium hydride (9.58 mg, 0.240 mmol) was added to an oven dried flask purged with argon and suspended in 1.5 mL of DMF. The suspension was cooled to 0 °C. 1-(1-(4-chlorobenzyl)-1H-indole-2-carbonyl)-N-(2-(pyridin-4-yl)ethyl)piperidine-4-carboxamide (100 mg, 0.200 mmol) dissolved in 1.5 mL of DMF was added dropwise and stirred for 15 minutes before adding 3-bromoprop-1-yne (0.018 ml, 0.240 mmol). The reaction was allowed to warm

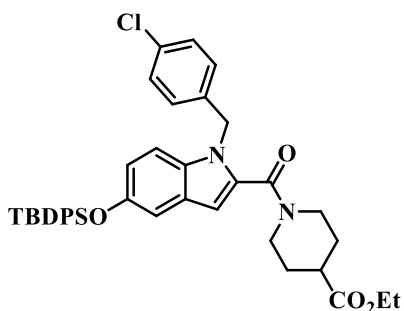
to room temperature. After 4 hours, the reaction was diluted with water and ethyl acetate. The aqueous layer was washed with another portion of ethyl acetate. The organic phases were combined, washed with saturated sodium chloride (3x), dried over sodium sulfate, filtered, and concentrated. The crude material was purified using 0-10% methanol-ethyl acetate. The product was isolated as a white solid. Yield: 36 mg, 33% Mixture of rotomers. $^1\text{H NMR}$ (500 MHz, $\text{DMSO-}d_6$) δ ppm 8.47 - 8.54 (rotomer A, m, 1 H), 8.44 - 8.47 (rotomer B, m, 1 H), 7.60 - 7.66 (m, 1 H), 7.54 (t, $J=7.7$ Hz, 1 H), 7.30 - 7.37 (m, 3 H), 7.18 - 7.27 (m, 2 H), 7.07 - 7.14 (m, 3 H), 6.74 (rotomer A, s, 0.5 H), 6.71 (rotomer B, s, 0.5 H), 5.45 - 5.53 (m, 2 H), 3.89 - 4.58 (m, 4 H), 3.72 (rotomer A, t, $J=7.0$ Hz, 1 H), 3.58 (rotomer B, t, $J=7.4$ Hz, 1 H), 3.36 (rotomer A, t, $J=2.3$ Hz, 0.5 H), 3.21 (rotomer B, t, $J=2.3$ Hz, 0.5 H), 3.08 (rotomer A, br. s., 1 H), 2.90 - 2.99 (m, 2 H), 2.83 (rotomer B, t, $J=7.6$ Hz, 1 H), 2.51 - 2.58 (m, 1 H), 1.16 - 1.71 (m, 4 H). TOF ES+ MS: 539.2 (M+H), 561.2 (M+Na). HPLC (gradient A): ret. time = 5.97min; purity 90 %



Ethyl 1-(5-hydroxy-1H-indole-2-carbonyl)piperidine-4-carboxylate (206) 165 (1.0 g, 5.23 mmol), EDCI (1.504 g, 7.85 mmol), and 1-hydroxybenzotriazole (1.060 g, 7.85 mmol) were dissolved in DCM (Volume: 25 ml). The reaction was stirred for 30 minutes. The reaction turned from a suspension to a yellow clear solution. Hunig'sBase (1.370 ml, 7.85 mmol) and ethyl piperidine-4-carboxylate (1.209 ml, 7.85 mmol) were added. The reaction was stirred at room temperature overnight. It was diluted ethyl

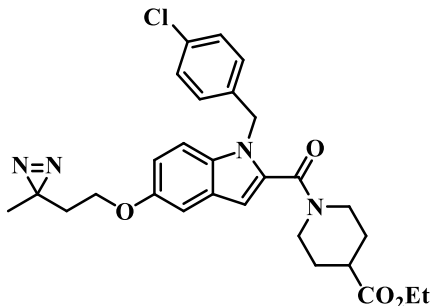
acetate and water. The phases were separated and it was sequentially washed with 1N HCl, saturated sodium carbonate, and saturated sodium chloride. It was dried over sodium sulfate, filtered and concentrated to obtain ethyl 1-(5-methoxy-1H-indole-2-carbonyl)piperidine-4-carboxylate as a white solid. The crude material did not need to be purified. Yield: 1.5 g, 85% ^1H NMR (500 MHz, $\text{DMSO-}d_6$) δ ppm 11.42 (s, 1 H), 7.30 (d, $J=8.8$ Hz, 1 H), 7.06 (d, $J=2.4$ Hz, 1 H), 6.83 (dd, $J=8.8, 2.4$ Hz, 1 H), 6.68 (d, $J=2.2$ Hz, 1 H), 4.33 (dt, $J=13.3, 3.2$ Hz, 2 H), 4.09 (q, $J=7.1$ Hz, 2 H), 3.75 (s, 3 H), 3.16 (br. s., 2 H), 2.69 (tt, $J=11.0, 3.9$ Hz, 1 H), 1.92 (dd, $J=13.3, 3.1$ Hz, 2 H), 1.50 - 1.65 (m, 2 H), 1.20 (t, $J=7.1$ Hz, 3 H)

Ethyl 1-(5-methoxy-1H-indole-2-carbonyl)piperidine-4-carboxylate (200 mg, 0.605 mmol) was dissolved in DCM (Volume: 8 ml). It was cooled to -78 $^\circ\text{C}$ and Boron tribromide in DCM (1.816 ml, 1.816 mmol) was added dropwise. The reaction was allowed to warm to room temperature. It was stirred until the reaction was complete by TLC. It was cooled to 0 $^\circ\text{C}$ and water was added slowly. The layers were separated and the organic phase was washed with saturated sodium carbonate. The organic phase was washed with saturated sodium carbonate until the water phase from the separatory funnel was basic. The ethyl acetate layer was dried over sodium sulfate, filtered, and concentrated. The crude material was purified via 0 - 70 % ethyl acetate/hexanes. The product was isolated as a white solid. Yield: 153 mg, 80 %. ^1H NMR (500 MHz, $\text{DMSO-}d_6$) δ ppm 11.25 (s, 1 H), 8.79 (s, 1 H), 7.21 (d, $J=8.8$ Hz, 1 H), 6.88 (d, $J=2.0$ Hz, 1 H), 6.71 (dd, $J=8.8, 2.2$ Hz, 1 H), 6.58 (d, $J=2.0$ Hz, 1 H), 4.33 (dt, $J=13.2, 3.4$ Hz, 2 H), 4.09 (q, $J=7.1$ Hz, 2 H), 3.15 (br. s., 2 H), 2.68 (tt, $J=11.0, 3.9$ Hz, 1 H), 1.92 (dd, $J=13.3, 3.1$ Hz, 2 H), 1.51 - 1.61 (m, 2 H), 1.19 (t, $J=7.1$ Hz, 3 H)



Ethyl 1-(5-((tert-butyl-diphenylsilyloxy)-1-(4-chlorobenzyl)-1H-indole-2-carbonyl)piperidine-4-carboxylate (207) 1-(bromomethyl)-4-chlorobenzene (0.741 g, 3.61 mmol) and sodium iodide (0.594 g, 3.97 mmol) were dissolved in Acetone (Ratio: 1.000, Volume: 20.00 ml) and stirred overnight at room temperature. The resulting suspension was filtered and the filtrate was concentrated to obtain crude 4-chlorobenzyl iodide.

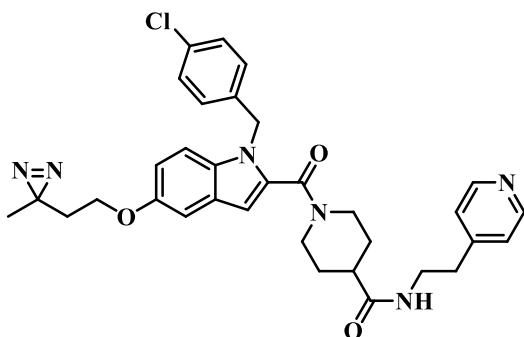
Ethyl 1-(5-((tert-butyl-diphenylsilyloxy)-1H-indole-2-carbonyl)piperidine-4-carboxylate (1.00 g, 1.803 mmol) and cesium carbonate (0.881 g, 2.70 mmol) were suspended in 15 mL of DMF. 4-chlorobenzyl iodide was dissolved in 5 mL of DMF and added to the reaction. The reaction was heated to 60 °C overnight. It was diluted with water and ethyl acetate. The aqueous layer was washed with another aliquot of ethyl acetate. The organic phases were combined and washed with saturated sodium chloride, dried over sodium sulfate, filtered and concentrated. The crude material was purified using 0-75% ethyl acetate/hexanes to obtain ethyl 1-(5-((tert-butyl-diphenylsilyloxy)-1-(4-chlorobenzyl)-1H-indole-2-carbonyl)piperidine-4-carboxylate as white solid. The resulting product was taken directly to the next step. Yield: 931 mg, 76 %.



Ethyl 1-(1-(4-chlorobenzyl)-5-(2-(3-methyl-3H-diazirin-3-yl)ethoxy)-1H-indole-2-carbonyl)piperidine-4-carboxylate (208) **207** (420 mg, 0.618 mmol) was dissolved in THF (Volume: 10 ml) and cooled with an ice bath. TBAF (0.927 ml, 0.927 mmol) was added slowly. The reaction turned from colorless to a clear yellow solution. It was stirred for an additional hour before it was diluted with water and ethyl acetate and water. The organic phase was washed with saturated sodium chloride, dried over sodium sulfate, filtered and concentrated. The crude material was purified using 0-80% ethyl acetate/hexanes to obtain product as an off white solid. Yield: 229 mg, 84%. ¹H NMR (500 MHz, DMSO-*d*₆) δ ppm 8.92 (s, 1 H), 7.36 (d, *J*=8.8 Hz, 1 H), 7.29 - 7.33 (m, 2 H), 7.05 (d, *J*=8.3 Hz, 2 H), 6.91 (d, *J*=2.2 Hz, 1 H), 6.74 (dd, *J*=8.8, 2.2 Hz, 1 H), 6.53 (s, 1 H), 5.41 (s, 2 H), 4.27 (br. s., 1 H), 3.82 - 4.11 (m, 3 H), 2.98 (br. s., 2 H), 2.57 (tt, *J*=11.0, 3.8 Hz, 1 H), 1.73 (br. s., 2 H), 1.14 - 1.51 (m, 5 H). TOF ES+ MS: 441.2 (M+H), 463.2 (M+Na). HPLC (gradient A): ret. time = 6.84 min; purity >95%

Cesium carbonate (238 mg, 0.731 mmol) and ethyl 1-(1-(4-chlorobenzyl)-5-hydroxy-1H-indole-2-carbonyl)piperidine-4-carboxylate (215 mg, 0.488 mmol) were dissolved 3.0 mL of DMF. 2-(3-methyl-3H-diazirin-3-yl)ethyl 4-methylbenzenesulfonate (186 mg, 0.731 mmol) was dissolved in 2.0 mL of DMF. The reaction was heated at 60 °C overnight. The reaction was diluted with ethyl acetate and water. The aqueous phase

was washed with another aliquot of ethyl acetate. The organic phases were combined and washed with saturated sodium chloride, filtered and concentrated. The crude material was purified via Biotage using 20-80% ethyl acetate/hexanes to obtain product as a white solid. Yield: 195 mg, 76%. ¹H NMR (500 MHz, DMSO-*d*₆) δ ppm 7.48 (d, *J*=9.0 Hz, 1 H), 7.29 - 7.34 (m, 2 H), 7.11 (d, *J*=2.4 Hz, 1 H), 7.03 - 7.07 (m, 2 H), 6.89 (dd, *J*=9.0, 2.4 Hz, 1 H), 6.62 (s, 1 H), 5.45 (s, 2 H), 4.31 (br. s., 1 H), 4.07 (q, *J*=7.1 Hz, 2 H), 3.74 - 3.97 (m, 3 H), 2.78 - 3.19 (m, 2 H), 2.57 (tt, *J*=11.0, 3.9 Hz, 1 H), 1.25 - 1.96 (m, 6 H), 1.18 (t, *J*=7.1 Hz, 3 H), 1.09 (s, 3 H). TOF ES+ MS: 523.2 (M+H), 545.2 (M+Na). HPLC (gradient A): ret. time = 8.63 min; purity = 90 %

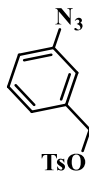


1-(1-(4-chlorobenzyl)-5-(2-(3-methyl-3H-diazirin-3-yl)ethoxy)-1H-indole-2-carbonyl)-N-(2-(pyridin-4-yl)ethyl)piperidine-4-carboxamide (CCG 222802, 123)

208 (195 mg, 0.373 mmol) was dissolved in EtOH (Ratio: 1.000, Volume: 4 ml) and 2N NaOH (Ratio: 1.000, Volume: 4.00 ml) and stirred at room temperature for 5 hours. At this point, the ethanol was removed under vacuum and the resulting solution was diluted with 4 mL of water and 4 mL of diethyl ether. The organic phase was removed, and the aqueous layer was acidified to pH 2. The resulting suspension was extracted with ethyl acetate (2x). The organic phases were combined and washed with saturated sodium chloride. It was dried over sodium sulfate, filtered and concentrated. Taken directly to

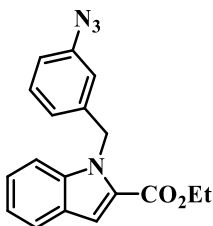
the next step. Yield: 175 mg, 95%. ^1H NMR (500 MHz, $\text{DMSO-}d_6$) δ ppm 12.30 (s, 1 H), 7.46 (d, $J=9.0$ Hz, 1 H), 7.29 - 7.35 (m, 2 H), 7.11 (d, $J=2.4$ Hz, 1 H), 7.03 - 7.09 (m, 2 H), 6.88 (dd, $J=9.0, 2.4$ Hz, 1 H), 6.62 (s, 1 H), 5.45 (s, 2 H), 4.27 (br. s., 1 H), 3.70 - 4.11 (m, 3 H), 2.85 - 3.23 (m, 2 H), 2.47 (tt, $J=10.7, 3.9$ Hz, 1 H), 1.17 - 2.00 (m, 6 H), 1.09 (s, 3 H). HPLC (gradient A): ret. time = 5.95 min; purity > 95 %

1-(1-(4-chlorobenzyl)-5-(2-(3-methyl-3H-diazirin-3-yl)ethoxy)-1H-indole-2-carbonyl)piperidine-4-carboxylic acid (175 mg, 0.354 mmol), 1-Hydroxybenzotriazole (96 mg, 0.707 mmol) and EDCI (136 mg, 0.707 mmol) were dissolved in DCM (Volume: 5 ml). It was stirred for 10 minutes before 2-(pyridin-4-yl)ethan-1-amine (0.085 ml, 0.707 mmol) and Hunig'sBase (0.124 ml, 0.707 mmol) were added. The reaction was stirred overnight at room temperature. It was diluted with water and ethyl acetate. The organic phase was washed with saturated sodium carbonate, saturated sodium chloride, dried over sodium sulfate, filtered and concentrated. The crude material was purified via Biotage using 20-80% ethyl acetate/hexanes to obtain product as an off-white solid. Yield: 40% ^1H NMR (500 MHz, $\text{DMSO-}d_6$) δ 8.49 – 8.41 (m, 2H), 7.89 (t, $J = 5.6$ Hz, 1H), 7.44 (d, $J = 9.0$ Hz, 1H), 7.37 – 7.30 (m, 2H), 7.24 – 7.18 (m, 2H), 7.13 – 7.05 (m, 3H), 6.87 (dd, $J = 9.0, 2.4$ Hz, 1H), 6.61 (s, 1H), 5.44 (s, 2H), 4.35 (bs, 1H), 4.09 – 3.74 (m, 3H), 3.30 (q, $J = 6.8$ Hz, 2H), 3.11 – 2.62 (m, 4H), 2.32 (tt, $J = 11.3, 3.8$ Hz, 1H), 1.80 (t, $J = 6.1$ Hz, 2H), 1.68 – 1.20 (m, 4H), 1.09 (s, 3H). ^{13}C NMR (126 MHz, dms) δ 173.41, 161.77, 152.92, 149.27, 148.27, 137.19, 132.13, 132.09, 131.75, 128.62, 128.34, 126.42, 124.15, 113.99, 111.44, 103.56, 102.99, 63.09, 46.13, 41.32, 38.68, 34.09, 33.39, 24.59, 19.63. TOF ES+ MS: 599.3 (M+H). HPLC (gradient A): ret. time = 6.18 min; purity > 95 %



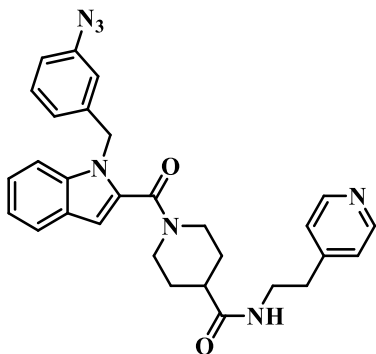
3-azidobenzyl 4-methylbenzenesulfonate (211) (3-(hydroxymethyl)phenyl)boronic acid (500 mg, 3.29 mmol) was converted to (3-azidophenyl)methanol according to literature (Ref 150). Yield: 95 mg, 19%

In a flask purged with argon, (3-azidophenyl)methanol (500 mg, 3.35 mmol) and triethylamine (1.402 ml, 10.06 mmol) were dissolved in DCM (Volume: 15 ml). Solid p-toluenesulfonic anhydride (1641 mg, 5.03 mmol) was added to the reaction. It was stirred at room temperature overnight. The reaction was diluted with water and ethyl acetate. The organic phase was washed with 1N NaOH (2x) and saturated sodium chloride. It was dried over sodium sulfate, filtered and concentrated. Yield: 661 mg, 65 % ^1H NMR (500 MHz, DMSO- d_6) δ ppm 7.77 - 7.86 (m, 2 H), 7.46 - 7.52 (m, 2 H), 7.37 - 7.43 (m, 1 H), 7.07 - 7.15 (m, 2 H), 6.97 - 7.00 (m, 1 H), 5.14 (s, 2 H), 2.43 (s, 3 H)



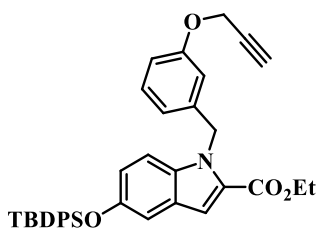
Ethyl 1-(3-azidobenzyl)-1H-indole-2-carboxylate (212) ethyl 1H-indole-2-carboxylate (234 mg, 1.236 mmol) and cesium carbonate (537 mg, 1.648 mmol) were dissolved in 10 mL of DMF. **211** (250 mg, 0.824 mmol) was added as a 5 mL DMF solution. The reaction was stirred overnight at 60 °C. It was diluted with water and ethyl acetate. The

aqueous layer was washed with another portion of ethyl acetate. The organic phases were combined and washed with 1N NaOH, saturated sodium chloride (2x), dried over sodium sulfate, filtered and concentrated. The crude material was purified using Biotage 0-50% ethyl acetate/hexanes. The product was obtained as a yellow oil. Yield: 172 mg, 65%. ¹H NMR (500 MHz, DMSO-*d*₆) δ ppm 7.73 (d, *J*=7.8 Hz, 1 H), 7.59 (dd, *J*=8.5, 0.7 Hz, 1 H), 7.39 (s, 1 H), 7.28 - 7.36 (m, 2 H), 7.13 - 7.19 (m, 1 H), 6.96 - 7.01 (m, 1 H), 6.75 - 6.80 (m, 2 H), 5.86 (s, 2 H), 4.29 (q, *J*=7.1 Hz, 2 H), 1.29 (t, *J*=7.1 Hz, 3 H)



1-(1-(3-azidobenzyl)-1H-indole-2-carbonyl)-N-(2-(pyridin-4-yl)ethyl)piperidine-4-carboxamide (CCG 222881, 124) 212 (52 mg, 0.162 mmol) was dissolved in Ethanol (Ratio: 1.000, Volume: 2 ml) and 2N NaOH (Ratio: 1.000, Volume: 2.000 ml). The reaction was stirred for 5 hours until TLC showed complete conversion. The ethanol was removed under vacuum. The resulting suspension was diluted with 1 mL of water. The aqueous phase was acidified using 2N HCl to pH ~2. The resulting solid was filtered to obtain 1-(3-azidobenzyl)-1H-indole-2-carboxylate as a peach solid. Taken directly to the next step. Yield: 50.9 mg, 95 % yield.

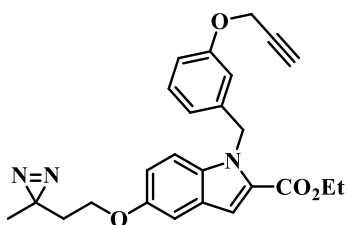
1-(3-azidobenzyl)-1H-indole-2-carboxylic acid (32 mg, 0.109 mmol), EDCI (42.0 mg, 0.219 mmol), and 1-Hydroxybenzotriazole (29.6 mg, 0.219 mmol) were dissolved in DCM (Volume: 5 ml). The reaction was stirred for 20 minutes before solid **190** (67.1 mg, 0.219 mmol) and Hunig's Base (0.038 ml, 0.219 mmol) were added. The reaction was stirred at room temperature overnight. The reaction was diluted with water and ethyl acetate. The organic phase was washed with saturated sodium bicarbonate, saturated sodium carbonate and saturated sodium chloride. It was dried over sodium sulfate, filtered and concentrated. The crude material was purified via Biotage using 10 g silica column @ 20 mL/min with 10-80% ethyl acetate/hexanes to obtain product as a glassy solid. Yield: 13 mg, 23 %. ¹H NMR (500 MHz, DMSO-*d*₆) δ ppm 8.47 - 8.56 (m, 2 H), 7.94 (t, *J*=5.9 Hz, 1 H), 7.66 (dd, *J*=24.5, 7.8 Hz, 2 H), 7.36 (t, *J*=7.8 Hz, 1 H), 7.23 - 7.31 (m, 3 H), 7.16 (t, *J*=7.6 Hz, 1 H), 7.01 - 7.07 (m, 1 H), 6.85 - 6.95 (m, 2 H), 6.77 (s, 1 H), 5.56 (s, 2 H), 4.45 (br. s., 1 H), 4.02 (br. s., 1 H), 3.36 (q, *J*=6.4 Hz, 1 H), 2.73 - 3.20 (m, 4 H), 2.37 (tt, *J*=10.0, 5.0 Hz, 1 H), 1.15 - 1.84 (m, 4 H) ¹³C NMR (126 MHz, dms) δ 173.38, 161.75, 149.27, 148.27, 140.32, 139.44, 136.78, 131.70, 130.10, 126.00, 124.15, 123.48, 123.04, 121.29, 120.16, 117.90, 117.45, 110.54, 103.31, 46.28, 41.31, 38.67, 34.10. TOF ES+ MS: 508.2 (M+H). HPLC (gradient A): ret. time = 4.73 min; purity > 95 %



Ethyl 5-((tert-butyldiphenylsilyl)oxy)-1-(3-(prop-2-yn-1-yloxy)benzyl)-1H-indole-2-carboxylate ethyl 5-((tert-butyldiphenylsilyl)oxy)-1H-indole-2-carboxylate (215)

Imidazole (1.254 g, 18.42 mmol) and ethyl 5-hydroxy-1H-indole-2-carboxylate (1.89 g, 9.21 mmol) were dissolved in DCM (Volume: 50 ml) and stirred at room temperature for 30 minutes. TBDPS-Cl (4.73 ml, 18.42 mmol) was added and the reaction and stirred overnight. The reaction was diluted with ethyl acetate and water. The layers were separated and the organic phase was washed sequentially, 1N HCl and saturated sodium chloride. It was dried over sodium sulfate filtered and concentrated. The crude material was purified via flash chromatography using 1-40% ethyl acetate/hexanes to obtain ethyl 5-((tert-butyldiphenylsilyl)oxy)-1H-indole-2-carboxylate as a clear oil that crystallized over time. Yield: 3.4 g, 82%. ¹H NMR (500 MHz, DMSO-*d*₆) δ ppm 11.71 (s, 1 H), 7.62 - 7.78 (m, 4 H), 7.34 - 7.58 (m, 6 H), 7.23 (d, *J*=8.8 Hz, 1 H), 6.87 - 6.93 (m, 2 H), 6.81 (dd, *J*=8.9, 2.3 Hz, 1 H), 4.29 (q, *J*=7.2 Hz, 2 H), 1.29 (t, *J*=7.1 Hz, 3 H), 1.05 (s, 9 H)

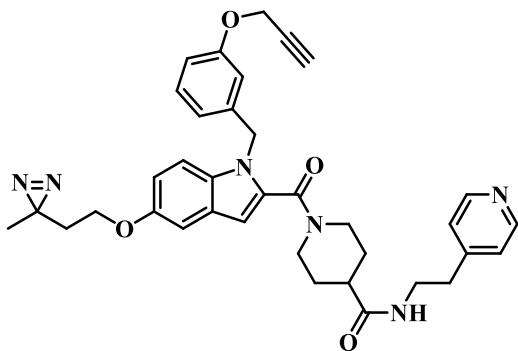
Ethyl 5-((tert-butyldiphenylsilyl)oxy)-1H-indole-2-carboxylate (215) (400 mg, 0.902 mmol) and cesium carbonate (588 mg, 1.803 mmol) were dissolved in 20 mL of DMF. 1-(iodomethyl)-3-(prop-2-yn-1-yloxy)benzene (491 mg, 1.803 mmol) was dissolved in 10 mL of DMF and added to the reaction. The reaction was stirred at 60 °C overnight. It was diluted with water and ethyl acetate. The aqueous phase was washed with ethyl acetate. The organic phases were combined and washed with saturated sodium chloride, dried over sodium sulfate, filtered and concentrated. The resulting crude material was purified using 0-40% ethyl acetate/hexanes to obtain product as a glassy solid. Yield: 318 mg, 60 mg. TOF ES+ MS: 588.0 (M+H), 610.0 (M+Na).



Ethyl 5-(2-(3-methyl-3H-diazirin-3-yl)ethoxy)-1-(3-(prop-2-yn-1-yloxy)benzyl)-1H-indole-2-carboxylate (216) 215 (81 mg, 0.138 mmol) was dissolved in THF (Volume: 3 ml) and cooled with an ice bath. TBAF (0.179 ml, 0.179 mmol) was added dropwise. The reaction turned from colorless to yellow solution. It was diluted with water and ethyl acetate. The organic phase was washed with saturated sodium chloride, dried over sodium sulfate, filtered and concentrated. The crude material was purified using 0-60% ethyl acetate/hexanes to obtain product. Yield: 46 mg, 95% ¹H NMR (500 MHz, DMSO-*d*₆) δ ppm 9.06 (s, 1 H), 7.37 (d, *J*=9.0 Hz, 1 H), 7.14 - 7.22 (m, 2 H), 6.97 (d, *J*=2.4 Hz, 1 H), 6.80 - 6.87 (m, 2 H), 6.63 (t, *J*=2.1 Hz, 1 H), 6.58 (dd, *J*=7.8, 1.0 Hz, 1 H), 5.75 (s, 2 H), 4.71 (d, *J*=2.4 Hz, 2 H), 4.27 (q, *J*=7.1 Hz, 2 H), 3.53 (t, *J*=2.4 Hz, 1 H), 1.28 (t, *J*=7.1 Hz, 3 H). HPLC (gradient A): ret. time = 7.13 min; purity > 95%

Cesium carbonate (133 mg, 0.408 mmol) and ethyl 5-hydroxy-1-(3-(prop-2-yn-1-yloxy)benzyl)-1H-indole-2-carboxylate (95 mg, 0.272 mmol) were dissolved in 2 mL of DMF and stirred at room temperature for 10 minutes before 2-(3-methyl-3H-diazirin-3-yl)ethyl 4-methylbenzenesulfonate (104 mg, 0.408 mmol) was dissolved in 2 mL of DMF before it was added to the reaction and heated to 50 °C overnight. The reaction was diluted with water and ethyl acetate. The aqueous layer was washed with ethyl acetate (2x). The organic phases were washed with saturated sodium carbonate and saturated sodium chloride, dried over sodium sulfate, filtered and concentrated. The crude product

was taken directly to next step. $^1\text{H NMR}$ (500 MHz, $\text{DMSO-}d_6$) δ ppm 7.48 (d, $J=9.3$ Hz, 1 H), 7.26 (s, 1 H), 7.16 - 7.21 (m, 2 H), 6.98 (dd, $J=9.2, 2.6$ Hz, 1 H), 6.83 (dd, $J=8.3, 2.7$ Hz, 1 H), 6.63 (t, $J=2.2$ Hz, 1 H), 6.58 (dd, $J=7.6, 0.7$ Hz, 1 H), 5.80 (s, 2 H), 4.71 (d, $J=2.2$ Hz, 2 H), 4.28 (q, $J=7.1$ Hz, 2 H), 3.88 (t, $J=6.1$ Hz, 2 H), 3.52 (t, $J=2.3$ Hz, 1 H), 1.81 (t, $J=6.1$ Hz, 2 H), 1.29 (t, $J=7.1$ Hz, 3 H), 1.09 (s, 3 H). TOF ES+ MS: 432.1 (M+H), 454.1 (M+Na). HPLC (gradient A): ret. time = 8.91 min; purity > 95 %

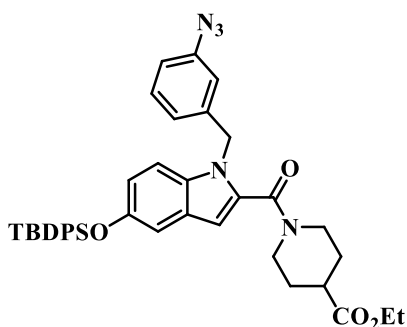


1-(5-(2-(3-methyl-3H-diazirin-3-yl)ethoxy)-1-(3-(prop-2-yn-1-yloxy)benzyl)-1H-indole-2-carbonyl)-N-(2-(pyridin-4-yl)ethyl)piperidine-4-carboxamide (222700, 125)

216 (60 mg, 0.139 mmol) was dissolved in THF (Ratio: 1.000, Volume: 1 ml) and 1 N LiOH (Ratio: 1.000, Volume: 1.000 ml). It was stirred at room temperature for 4 hours. It was diluted with water and ethyl acetate. The aqueous phase was acidified to pH ~ 2. The resulting suspension was extracted with ethyl acetate. The organic phase was washed with saturated sodium chloride, dried over sodium sulfate, filtered and concentrated. Product taken directly to the next step. Yield: 20 mg, 36%. TOF ES+ MS: 404.0 (M+H), 426.0 (M+Na).

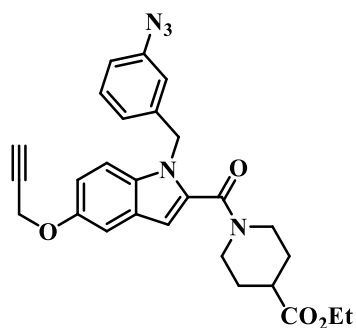
5-(2-(3-methyl-3H-diazirin-3-yl)ethoxy)-1-(3-(prop-2-yn-1-yloxy)benzyl)-1H-indole-2-carboxylic acid (34 mg, 0.084 mmol), EDCI (32.3 mg, 0.169 mmol), and 1-

hydroxybenzotriazole (22.78 mg, 0.169 mmol) were dissolved in DCM (3 ml). The reaction was stirred at room temperature for 10 minutes. Solid **190** (38.7 mg, 0.126 mmol) was added followed by Hunig'sBase (0.029 ml, 0.169 mmol). The reaction was stirred at room temperature overnight. The reaction was diluted with water and ethyl acetate. The organic phase was washed with saturated sodium carbonate and saturated sodium chloride. It was dried over sodium sulfate, filtered, and concentrated. The crude material was purified via Biotage 20-80% ethyl acetate/hexanes to obtain product as a white solid. Yield: 21 mg, 40 %. ¹H NMR (500 MHz, DMSO- *d*₆) δ ppm 8.42 - 8.49 (m, 2 H), 7.89 (t, *J*=5.9 Hz, 1 H), 7.44 (d, *J*=9.3 Hz, 1 H), 7.16 - 7.23 (m, 3 H), 7.11 (d, *J*=2.4Hz, 1 H), 6.87 (dd, *J*=8.8, 2.4 Hz, 1 H), 6.84 (dd, *J*=8.3, 2.4 Hz, 1 H), 6.70 (t, *J*=2.0 Hz, 1 H), 6.58 - 6.64 (m, 2 H), 5.41 (s, 2 H), 4.71 (d, *J*=2.4 Hz, 2 H), 4.36 (br. s., 1 H), 3.79 - 4.18 (m, 3 H), 3.51 (t, *J*=2.2 Hz, 1 H), 3.31 (q, *J*=5.9 Hz, 2 H), 2.68 - 3.11 (m, 4 H), 2.31 (tt, *J*=11.2, 3.7 Hz, 1 H), 1.80 (t, *J*=6.1 Hz, 2 H), 1.19 - 1.75 (m, 4 H), 1.09 (s, 3 H) ¹³C NMR (126 MHz, dmso) δ 173.44, 161.81, 157.15, 152.86, 149.27, 148.26, 139.77, 132.28, 132.21, 129.45, 126.37, 124.16, 119.50, 114.00, 113.89, 112.83, 111.48, 103.51, 102.80, 79.00, 78.08, 63.10, 55.22, 46.64, 41.34, 38.66, 34.11, 33.42, 24.59, 19.63. TOF ES+ MS: 619.1 (M+H). HPLC (gradient A): ret. time = 6.21 min; purity > 95 %



Ethyl 1-(1-(3-azidobenzyl)-5-((tert-butyldiphenylsilyl)oxy)-1H-indole-2-

carbonyl)piperidine-4-carboxylate (217) Sodium hydride (87 mg, 2.163 mmol) was suspended in 5 mL of DMF and cooled to 0 °C. ethyl 1-(5-((tert-butyldiphenylsilyl)oxy)-1H-indole-2-carbonyl)piperidine-4-carboxylate (800 mg, 1.442 mmol) was dissolved in 5 mL of DMF. The reaction was allowed to stir at 0 °C before a 5 mL DMF solution of **211** (656 mg, 2.163 mmol) was added. The reaction was allowed to warm to room temperature over 5 hours, before it was diluted with water and ethyl acetate. The aqueous phase was washed with ethyl acetate. The organic phases were combined and washed with saturated sodium chloride, filtered and concentrated. The crude material was purified with the biotage using 10 to 60% ethyl acetate/hexanes to obtain product. Yield: 841 mg, 85 %. TOF ES+ MS: 686.3 (M+H).

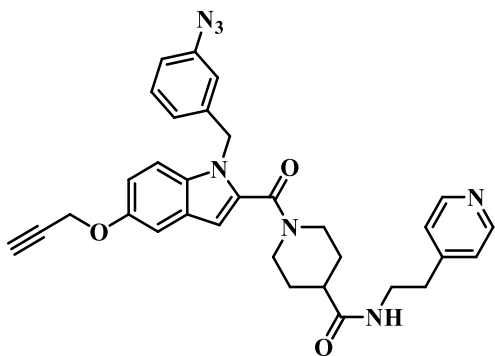


Ethyl 1-(1-(3-azidobenzyl)-5-(prop-2-yn-1-yloxy)-1H-indole-2-carbonyl)piperidine-

4-carboxylate (218) **217** (811 mg, 1.182 mmol) was dissolved in THF (Volume: 10 mL) and cooled with an ice bath. TBAF (2.365 mL, 2.365 mmol) was added dropwise. The reaction turned from colorless to yellow solution. It was diluted with water and ethyl acetate. The organic phase was washed with saturated sodium chloride, dried over sodium sulfate, filtered and concentrated. The crude material was purified with the biotage using 0-60% ethyl acetate/hexanes to obtain ethyl 1-(1-(3-azidobenzyl)-5-

hydroxy-1H-indole-2-carbonyl)piperidine-4-carboxylate. Yield: 450 mg, 85% TOF ES+ MS: 448.3 (M+H)

Cesium carbonate (889 mg, 2.73 mmol) and ethyl 1-(1-(3-azidobenzyl)-5-hydroxy-1H-indole-2-carbonyl)piperidine-4-carboxylate (814 mg, 1.819 mmol) were dissolved in DMF and stirred for 10 minutes before adding 3-bromoprop-1-yne (0.207 ml, 2.73 mmol). The reaction was heated to 60 °C overnight. The reaction was diluted with water and ethyl acetate. The organic phase was washed with saturated sodium chloride, dried over sodium sulfate, filtered and concentrated. The crude material was purified using 20-80% ethyl acetate/hexanes to obtain product. Yield: 530 mg, 60 %. ¹H NMR (500 MHz, DMSO-*d*₆) δ ppm 7.53 (d, *J*=9.0 Hz, 1 H), 7.30 (t, *J*=7.9 Hz, 1 H), 7.19 (d, *J*=2.4 Hz, 1 H), 6.96 - 7.01 (m, 1 H), 6.92 (dd, *J*=9.0, 2.7 Hz, 1 H), 6.84 (d, *J*=8.1 Hz, 1 H), 6.79 (t, *J*=2.1 Hz, 1 H), 6.66 (s, 1 H), 5.47 (br. s., 2 H), 4.78 (d, *J*=2.2 Hz, 2 H), 4.31 (br. s., 1 H), 3.79 - 4.12 (m, 3 H), 3.55 (t, *J*=2.3 Hz, 1 H), 2.79 - 3.22 (m, 2 H), 2.58 (tt, *J*=11.0, 3.9 Hz, 1 H), 1.52 - 1.97 (m, 2 H), 0.89 - 1.52 (m, 5 H)



1-(1-(3-azidobenzyl)-5-(prop-2-yn-1-yloxy)-1H-indole-2-carbonyl)-N-(2-(pyridin-4-yl)ethyl)piperidine-4-carboxamide (CCG 223882, 126) 218 (57 mg, 0.117 mmol) was dissolved in THF (Volume: 3 ml). Solid Potassium Trimethylsilanolate (16.57 mg, 0.129

mmol) was added and the reaction was stirred at room temperature overnight. The resulting suspension was concentrated and the resulting solid was acidified using 4N HCl Dioxane. The suspension was concentrated to obtain product, which was taken directly to the next step. Yield: 51 mg, 95%. TOF ES+ MS: 458.0 (M+H)

1-(1-(3-azidobenzyl)-5-(prop-2-yn-1-yloxy)-1H-indole-2-carbonyl)piperidine-4-carboxylic acid (45 mg, 0.098 mmol), EDCI (30.5 mg, 0.197 mmol) and 1-hydroxybenzotriazole (26.6 mg, 0.197 mmol) were dissolved in DCM (3 ml). The reaction was stirred at room temperature for 15 minutes before 2-(pyridin-4-yl) ethan-1-amine (0.024 ml, 0.197 mmol) and Hunig'sBase (0.034 ml, 0.197 mmol) were added. The reaction was stirred overnight at room temperature. The reaction was diluted with water and ethyl acetate. The organic phase was washed with saturated sodium bicarbonate, saturated sodium carbonate, and saturated sodium chloride. It was dried over sodium sulfate, filtered and concentrated. The crude material was purified using biotage with 25% ethyl acetate/hexanes to 100% ethyl acetate to obtain product as glassy solid. Yield: 43 mg, 75 %. ¹H NMR (500 MHz, DMSO-*d*₆) δ ppm 8.44 - 8.48 (m, 2 H), 7.88 (t, *J*=5.9 Hz, 1 H), 7.48 (d, *J*=9.3 Hz, 1 H), 7.30 (t, *J*=8.3 Hz, 1 H), 7.18 - 7.23 (m, 3 H), 6.98 (dd, *J*=7.8, 2.0 Hz, 1 H), 6.91 (dd, *J*=8.8, 2.4 Hz, 1 H), 6.79 - 6.87 (m, 2 H), 6.64 (s, 1 H), 5.46 (s, 2 H), 4.78 (d, *J*=2.4 Hz, 2 H), 4.38 (br. s., 1 H), 3.97 (br. s., 1 H), 3.54 (t, *J*=2.4 Hz, 1 H), 3.31 (q, *J*=6.8 Hz, 2 H), 2.70 - 3.14 (m, 4 H), 2.25 - 2.36 (m, 1 H), 1.13 - 1.77 (m, 4 H) ¹³C NMR (126 MHz, dmsO) δ 173.38, 170.21, 161.70, 151.91, 149.27, 148.27, 140.35, 139.42, 132.39, 132.29, 130.09, 126.22, 124.15, 123.45, 117.88, 117.43, 114.02, 111.44, 104.22, 103.01, 79.65, 77.83, 59.64, 55.82, 46.41, 41.32, 34.10, 20.65,

13.98. TOF ES+ MS: 562.0 (M+H). HPLC (gradient A): ret. time = 5.68 min; purity = 90 %

Biological experiments

Mouse Liver Microsomes (courtesy of Scott Barraza)

Experiment performed as previously described.⁸¹

Passive Permeability Experiment:

Compounds were dissolved in DMSO to generate a 10 mM compound solution. The experiment was performed using the Double-Sink protocol provided by pION, Inc. with the PAMPA Explorer® system. A cosolvent system solution was used for the experiment.

NSV, WEEV, and FMV *In Vitro* antiviral and viability experiment (Courtesy of Dr. David Miller and Craig Dobry)

Experiment performed as previously described.^{66, 81, 161}

NSV and WEEV *in vivo* experiment (Courtesy of Dr. David Irani, Dr. David Miller and Penelope Blakely)

Experiment performed as previously described.^{81, 161}

Rhodamine 123 efflux experiment (Courtesy of Dr. Richard Keep and Jianming Xiang)

Experiment performed as previously described.¹⁶¹

REFERENCES

1. Calisher, C. H., Karabatsos, N., Lazuick, J.S., Monath, T., Wolff, K., Arbovirus serogroup: definition and geographic distribution. In *The arboviruses: epidemiology and ecology*, Monath, T. P., Ed. CRC Press, Inc: Boca Raton, Fl, 1988; pp 19-57.
2. Tavakoli, N. P., Eastern and western equine encephalitis viruses. *Molecular Detection of Human Viral Pathogens* **2011**, 335.
3. Hahn, C. S.; Lustig, S.; Strauss, E. G.; Strauss, J. H., Western equine encephalitis virus is a recombinant virus. *Proceedings of the National Academy of Sciences* **1988**, 85, (16), 5997-6001.
4. Calisher, C. H.; Maness, K. S. C.; Lord, R. D.; Coleman, P. H., Identification of two South American Strains of Eastern Equine Encephalomyelitis Virus from Migrant Birds Captured on Mississippi-Delta. *Am J Epidemiol* **1971**, 94, (2), 172-&.
5. Casals, J., Antigenic Variants of Eastern Equine Encephalitis Virus. *J Exp Med* **1964**, 119, (4), 547-&.
6. Hammon, W. M.; Reeves, W. C.; Brookman, B.; Izumi, E. M., Mosquitoes and Encephalitis in the Yakima Valley, Washington: I. Arthropods Tested and Recovery of Western Equine and St. Louis Viruses From *Culex tarsalis* Coquillett. *J Infect Dis* **1942**, 70, (3), 263-266.
7. Griffin, D. E., Alphaviruses. In *Fields Virology*, Fourth ed.; D.M. Knipe, P. M. H., D.E. Griffin, R.A Lamb, M.A. Martin, B. Roizman, S.S Straus, Ed. Lippincott Williams & Wilkins: Philadelphia, 2001; pp 917-962.
8. Zacks, M. A.; Paessler, S., Encephalitic alphaviruses. *Vet Microbiol* **2010**, 140, (3-4), 281-286.
9. Griffin, D. E.; Byrnes, A. P.; Cook, S. H., Emergence and virulence of encephalitogenic arboviruses. *Arch Virol* **2004**, 21-33.
10. Nargi-Aizenman, J. L.; Havert, M. B.; Zhang, M.; Irani, D. N.; Rothstein, J. D.; Griffin, D. E., Glutamate receptor antagonists protect from virus-induced neural degeneration. *Annals of Neurology* **2004**, 55, (4), 541-549.
11. Olney, J., Brain lesions, obesity, and other disturbances in mice treated with monosodium glutamate. *Science* **1969**, 164, 719-721.
12. Choi, D.; Maulucci-Gedde, M.; Kriegstein, A., Glutamate neurotoxicity in cortical cell culture. *The Journal of Neuroscience* **1987**, 7, (2), 357-368.
13. Choi, D.; Koh, J.; Peters, S., Pharmacology of glutamate neurotoxicity in cortical cell culture: attenuation by NMDA antagonists. *The Journal of Neuroscience* **1988**, 8, (1), 185-196.
14. Gorter, J. A.; Petrozzino, J. J.; Aronica, E. M.; Rosenbaum, D. M.; Opitz, T.; Bennett, M. V. L.; Connor, J. A.; Zukin, R. S., Global Ischemia Induces Downregulation of Glur2 mRNA and Increases AMPA Receptor-Mediated Ca²⁺ Influx in Hippocampal CA1 Neurons of Gerbil. *The Journal of Neuroscience* **1997**, 17, (16), 6179-6188.

15. Rothstein, J. D.; Jin, L.; Dykes-Hoberg, M.; Kuncl, R. W., Chronic inhibition of glutamate uptake produces a model of slow neurotoxicity. *Proceedings of the National Academy of Sciences* **1993**, 90, (14), 6591-6595.
16. Nargi-Aizenman, J. L.; Griffin, D. E., Sindbis virus-induced neuronal death is both necrotic and apoptotic and is ameliorated by N-methyl-D-aspartate receptor antagonists. *J Virol* **2001**, 75, (15), 7114-7121.
17. Griffin, D. E.; Hardwick, J. M., Perspective: virus infections and the death of neurons. *Trends in Microbiology* **1999**, 7, (4), 155-160.
18. Levine, B.; Huang, Q.; Isaacs, J. T.; Reed, J. C.; Griffin, D. E.; Hardwick, J. M., Conversion of lytic to persistent alphavirus infection by the bcl-2 cellular oncogene. *Nature* **1993**, 361, (6414), 739-742.
19. Irani, D. N.; Prow, N. A., Neuroprotective interventions targeting detrimental host immune responses protect mice from fatal alphavirus encephalitis. *J Neuropathol Exp Neurol* **2007**, 66, (6), 533-44.
20. Havert, M. B.; Schofield, B.; Griffin, D. E.; Irani, D. N., Activation of Divergent Neuronal Cell Death Pathways in Different Target Cell Populations during Neuroadapted Sindbis Virus Infection of Mice. *J. Virol.* **2000**, 74, (11), 5352-5356.
21. Dropulić, B.; Masters, C. L., Entry of Neurotropic Arboviruses into the Central Nervous System: An In Vitro Study Using Mouse Brain Endothelium. *J Infect Dis* **1990**, 161, (4), 685-691.
22. Johnson, K. P. M. D.; Johnson, R. T. M. D., CALIFORNIA ENCEPHALITIS: II. STUDIES OF EXPERIMENTAL INFECTION IN THE MOUSE. *Journal of Neuropathology & Experimental Neurology* **1968**, 27, (3), 390-400.
23. Johnson, R., Virus Invasion of the Central Nervous System: A Study of Sindbis Virus Infection in the Mouse Using Fluorescent Antibody. *Am J Pathol.* **1965**, 46, (6), 929-943.
24. Earnest, M. P. M. D.; Goolishian, H. A. P. D.; Calverley, J. R. M. D.; Hayes, R. O. P. D.; Hill, H. R. M. D., Neurologic, intellectual, and psychologic sequelae following western encephalitis: A follow-up study of 35 cases. [Article].
25. Przelomski, M. M. M.; O'Rourke, E. M.; Grady, G. F. M.; Berardi, V. P.; Markley, H. G. M., Eastern equine encephalitis in Massachusetts: A report of 16 cases, 1970-1984. [Article].
26. Griffin, D. E., Arboviruses and the Central-Nervous-System. *Springer Semin Immun* **1995**, 17, (2-3), 121-132.
27. Deresiewicz, R. L.; Thaler, S. J.; Hsu, L.; Zamani, A. A., Clinical and Neuroradiographic Manifestations of Eastern Equine Encephalitis. *New England Journal of Medicine* **1997**, 336, (26), 1867-1874.
28. Nadler, J. V.; Perry, B. W.; Cotman, C. W., Intraventricular kainic acid preferentially destroys hippocampal pyramidal cells. *Nature* **1978**, 271, (5646), 676-677.
29. Olney J, F. T., de Gubareff T, Acute dendrotoxic changes in the hippocampus of kainate treated rats. *Brain Research* **1979**, 176, 91-100.
30. Darman, J.; Backovic, S.; Dike, S.; Maragakis, N. J.; Krishnan, C.; Rothstein, J. D.; Irani, D. N.; Kerr, D. A., Viral-Induced Spinal Motor Neuron Death Is Non-Cell-Autonomous and Involves Glutamate Excitotoxicity. *The Journal of Neuroscience* **2004**, 24, (34), 7566-7575.

31. Jackson, A. C., The pathogenesis of spinal cord involvement in the encephalomyelitis of mice caused by neuroadapted Sindbis virus infection. *Laboratory investigation* **1987**, 56, (4), 418-423.
32. Jackson, A. C., Basis of neurovirulence in Sindbis virus encephalomyelitis of mice. *Laboratory investigation* **1988**, 58, (5), 503-517.
33. Reeves, W. C.; Hutson, G. A.; Bellamy, R. E.; Scrivani, R. P., Chronic Latent Infections of Birds with Western Equine Encephalomyelitis Virus. *Experimental Biology and Medicine* **1958**, 97, (4), 733-736.
34. CDC Bioterrorism Agents/Diseases. <http://emergency.cdc.gov/agent/agentlist-category.asp#b>
35. NIH/NIAID Category A, B, & C Priority Pathogens. <http://www.niaid.nih.gov/topics/BiodefenseRelated/Biodefense/research/Pages/CatA.aspx>
36. Christopher, L. W.; Cieslak, L. J.; Pavlin, J. A.; Eitzen, E. M.; Jr, Biological warfare: A historical perspective. *JAMA* **1997**, 278, (5), 412-417.
37. Sidwell, R. W.; Smee, D. F., Viruses of the Bunya- and Togaviridae families: potential as bioterrorism agents and means of control. *Antivir Res* **2003**, 57, (1-2), 101-111.
38. Huxsoll, D. L., Patrick, W.C., Parrott, C.D, Veterinary services in biological disasters. *J. Am. Vet. Med. Assoc.* **1987**, 190, 714-722.
39. Bronze, M. S.; Huycke, M. M.; Machado, L. J.; Voskuhl, G. W.; Greenfield, R. A., Viral agents as biological weapons and agents of bioterrorism. *Am J Med Sci* **2002**, 323, (6), 316-25.
40. Franz, D. R.; Jahrling, P. B.; Friedlander, A. M.; et al., Clinical recognition and management of patients exposed to biological warfare agents. *JAMA* **1997**, 278, (5), 399-411.
41. Jahrling, P. B.; Navarro, E.; Scherer, W. F., Interferon induction and sensitivity as correlates to virulence of Venezuelan encephalitis viruses for hamsters. *Arch Virol* **1976**, 51, (1-2), 23-35.
42. Nagata, L. P.; Wong, J. P.; Hu, W.-g.; Wu, J. Q., Vaccines and therapeutics for the encephalitic alphaviruses. *Future Virology* 2013/07//, 2013, p 661+.
43. Griffin, D.; Levine, B.; Tyor, W.; Ubol, S.; Desprès, P., The role of antibody in recovery from alphavirus encephalitis. *Immunological Reviews* **1997**, 159, (1), 155-161.
44. Swayze, R. D.; Bhogal, H. S.; Barabé, N. D.; McLaws, L. J.; Wu, J. Q. H., Envelope protein E1 as vaccine target for western equine encephalitis virus. *Vaccine* **2011**, 29, (4), 813-820.
45. Julander, J. G.; Siddharthan, V.; Blatt, L. M.; Schafer, K.; Sidwell, R. W.; Morrey, J. D., Effect of exogenous interferon and an interferon inducer on western equine encephalitis virus disease in a hamster model. *Virology* **2007**, 360, (2), 454-460.
46. Chosewood, L. C. W., D.E. , *Biosafety in Microbiological and Biomedical Laboratories*. US Government Printing Office: Washington, 2009; p 233-267.
47. Pittman, P. R.; Makuch, R. S.; Mangiafico, J. A.; Cannon, T. L.; Gibbs, P. H.; Peters, C. J., Long-term duration of detectable neutralizing antibodies after administration of live-attenuated VEE vaccine and following booster vaccination with inactivated VEE vaccine. *Vaccine* **1996**, 14, (4), 337-343.

48. Paessler, S.; Weaver, S. C., Vaccines for Venezuelan equine encephalitis. *Vaccine* **2009**, *27*, Supplement 4, (0), D80-D85.
49. Steele, K. R., D.; Glass, P.; Hart, M.; Ludwig, G.; Pratt, W.; Parker, W.; Smith, J., Alphavirus Encephalitides. In *Medical Aspects of Biological Warfare*, Dembek, Z. F., Ed. Office of The Surgeon General Washington, DC, 2007; pp 241-270.
50. Anthony, R. P.; Brown, D. T., Protein-protein interactions in an alphavirus membrane. *J Virol* **1991**, *65*, (3), 1187-1194.
51. Strauss, J. H.; Strauss, E. G., The alphaviruses: gene expression, replication, and evolution. *Microbiological Reviews* **1994**, *58*, (3), 491-562.
52. Cross, R. K., Identification of a Unique Guanine-7-Methyltransferase in Semliki Forest Virus (Sfv) Infected Cell-Extracts. *Virology* **1983**, *130*, (2), 452-463.
53. Hardy, W. R.; Strauss, J. H., Processing the nonstructural polyproteins of sindbis virus: nonstructural proteinase is in the C-terminal half of nsP2 and functions both in cis and in trans. *J Virol* **1989**, *63*, (11), 4653-4664.
54. Barth, B. U.; Suomalainen, M.; Liljeström, P.; Garoff, H., Alphavirus assembly and entry: role of the cytoplasmic tail of the E1 spike subunit. *J Virol* **1992**, *66*, (12), 7560-7564.
55. Hoekstra, D.; Kok, J., Entry mechanisms of enveloped viruses. Implications for fusion of intracellular membranes. *Biosci Rep* **1989**, *9*, (3), 273-305.
56. Marsh, M., The entry of enveloped viruses into cells by endocytosis. (0264-6021 (Print)).
57. Wengler, G., The regulation of disassembly of alphavirus cores. *Arch Virol* **2009**, *154*, (3), 381-390.
58. Carrasco, L., The inhibition of cell functions after viral infection A proposed general mechanism. *Febs Lett* **1977**, *76*, (1), 11-15.
59. Garry, R. F.; Bishop, J. M.; Parker, S.; Westbrook, K.; Lewis, G.; Waite, M. R. F., Na⁺ and K⁺ concentrations and the regulation of protein synthesis in Sindbis virus-infected chick cells. *Virology* **1979**, *96*, (1), 108-120.
60. Sefton, B. M., Immediate glycosylation of Sindbis virus membrane proteins. *Cell* **1977**, *10*, (4), 659-668.
61. Liljeström, P.; Garoff, H., Internally located cleavable signal sequences direct the formation of Semliki Forest virus membrane proteins from a polyprotein precursor. *J Virol* **1991**, *65*, (1), 147-154.
62. de Curtis, I.; Simons, K., Dissection of Semliki Forest virus glycoprotein delivery from the trans-Golgi network to the cell surface in permeabilized BHK cells. *Proceedings of the National Academy of Sciences* **1988**, *85*, (21), 8052-8056.
63. Howard, C. R.; Simpson, D. I. H., The Biology of the Arenaviruses. *Journal of General Virology* **1980**, *51*, (1), 1-14.
64. Simons, K.; Garoff, H., The Budding Mechanisms of Enveloped Animal Viruses. *Journal of General Virology* **1980**, *50*, (1), 1-21.
65. Leung, J. Y. S., Ng, M.M.L., and Chu, J.J.H., Replication of Alphaviruses: A Review on the Entry Process of Alphaviruses into Cells. *Advances in Virology* **2011**, *2011*, 1-9.
66. Peng, W.; Peltier, D. C.; Larsen, M. J.; Kirchhoff, P. D.; Larsen, S. D.; Neubig, R. R.; Miller, D. J., Identification of thieno[3,2-b]pyrrole derivatives as novel small molecule inhibitors of neurotropic alphaviruses. *J Infect Dis* **2009**, *199*, (7), 950-7.

67. Nagai, Y.; Ito, Y.; Hamaguchi, M.; Yoshida, T.; Matsumoto, T., Relation of Interferon Production to the Limited Replication of Newcastle Disease Virus in L Cells. *Journal of General Virology* **1981**, 55, (1), 109-116.
68. Andzhaparidze, O. G.; Bogomolova, N. N.; Boriskin, Y. S.; Bektemirova, M. S.; Drynov, I. D., Comparative study of rabies virus persistence in human and hamster cell lines. *J Virol* **1981**, 37, (1), 1-6.
69. Kramer, M. J.; Dennin, R.; Kramer, C.; Jones, G.; Connell, E.; Rolon, N.; Guarin, A.; Kale, R.; Trown, P. W., Cell and Virus Sensitivity Studies with Recombinant Human Alpha Interferons. *Journal of Interferon Research* **1983**, 3, (4), 425-435.
70. Frolov, I.; Schlesinger, S., Translation of Sindbis virus mRNA: analysis of sequences downstream of the initiating AUG codon that enhance translation. *J Virol* **1996**, 70, (2), 1182-90.
71. Frolov, I.; Hoffman, T. A.; Pragai, B. M.; Dryga, S. A.; Huang, H. V.; Schlesinger, S.; Rice, C. M., Alphavirus-based expression vectors: Strategies and applications. *P Natl Acad Sci USA* **1996**, 93, (21), 11371-11377.
72. Petrakova, O.; Volkova, E.; Gorchakov, R.; Paessler, S.; Kinney, R. M.; Frolov, I., Noncytopathic replication of Venezuelan equine encephalitis virus and eastern equine encephalitis virus replicons in mammalian cells. *J Virol* **2005**, 79, (12), 7597-7608.
73. Pushko, P.; Parker, M.; Ludwig, G. V.; Davis, N. L.; Johnston, R. E.; Smith, J. F., Replicon-helper systems from attenuated venezuelan equine encephalitis virus: Expression of heterologous genes in vitro and immunization against heterologous pathogens in vivo. *Virology* **1997**, 239, (2), 389-401.
74. Kerns, E., Di, L., *Drug-like Properties: Concepts, Structure Design and Methods*. Elsevier Inc. : 2008; p 526.
75. Hollenberg, P. F.; Kent, U. M.; Bumpus, N. N., Mechanism-based inactivation of human cytochromes p450s: experimental characterization, reactive intermediates, and clinical implications. *Chem Res Toxicol* **2008**, 21, (1), 189-205.
76. Ortiz de Montellano, P. G.-L., SE., Structure of cytochrome P450: Heme-binding site and heme reactivity. *Handbook of experimental pharmacology* **1993**, 105, 169-181.
77. Guengerich, F. P., Cytochrome P450 and Chemical Toxicology. *Chemical Research in Toxicology* **2007**, 21, (1), 70-83.
78. Jones, B. C.; Middleton, D. S.; Youdim, K., 6 Cytochrome P450 Metabolism and Inhibition: Analysis for Drug Discovery. In *Progress in Medicinal Chemistry*, Lawton, G.; Witty, D. R., Eds. Elsevier: 2009; Vol. Volume 47, pp 239-263.
79. Friedman, H., *Influence of Isosteric Replacements upon Biological Activity*. The National Academies Press: 1951; Vol. 206.
80. Lemke, T. L.; Williams, D. A.; Foye, W. O., *Foye's principles of medicinal chemistry*. Lippincott Williams & Wilkins: Philadelphia, 2002; p xii, 1114 p.
81. Sindac, J. A.; Yestrepesky, B. D.; Barraza, S. J.; Bolduc, K. L.; Blakely, P. K.; Keep, R. F.; Irani, D. N.; Miller, D. J.; Larsen, S. D., Novel Inhibitors of Neurotropic Alphavirus Replication That Improve Host Survival in a Mouse Model of Acute Viral Encephalitis. *J Med Chem* **2012**, 55, (7), 3535-3545.
82. Pajouhesh, H.; Lenz, G. R., Medicinal chemical properties of successful central nervous system drugs. *NeuroRx* **2005**, 2, (4), 541-53.

83. Mahar Doan, K., Humphreys, J., Webster, L., Wring, S., Shampine, L., Serabjit-Singh, C., Adkinson, K., Polli, J., Passive Permeability and P-Glycoprotein-Mediated Efflux Differentiate Central Nervous System (CNS) and Non-CNS Marketed Drugs. *THE JOURNAL OF PHARMACOLOGY AND EXPERIMENTAL THERAPEUTICS* **2002**, 303, 1029-1037.
84. Albrecht T, F. M., Boldogh I, Rabson, A., Effects on Cells. In *Medical Microbiology*, S, B., Ed. University of Texas Medical Branch at Galveston: Galveston (TX), 1996.
85. Castorena, K. M.; Peltier, D. C.; Peng, W.; Miller, D. J., Maturation-dependent responses of human neuronal cells to western equine encephalitis virus infection and type I interferons. *Virology* **2008**, 372, (1), 208-20.
86. Lustig, S., Molecular basis of Sindbis virus neurovirulence in mice. *J Virol* **1988**, 62, (7), 2329-2336.
87. Schmued, L. C.; Albertson, C.; Slikker Jr, W., Fluoro-Jade: a novel fluorochrome for the sensitive and reliable histochemical localization of neuronal degeneration. *Brain Research* **1997**, 751, (1), 37-46.
88. Miller, D. S.; Bauer, B.; Hartz, A. M., Modulation of P-glycoprotein at the blood-brain barrier: opportunities to improve central nervous system pharmacotherapy. *Pharmacol Rev* **2008**, 60, (2), 196-209.
89. Pardridge, W. M., Blood-brain barrier delivery. *Drug Discovery Today* **2007**, 12, (1-2), 54-61.
90. Niederkorn, J. Y., See no evil, hear no evil, do no evil: the lessons of immune privilege. *Nat Immunol* **2006**, 7, (4), 354-359.
91. Abbott, N. J.; Patabendige, A. A. K.; Dolman, D. E. M.; Yusof, S. R.; Begley, D. J., Structure and function of the blood-brain barrier. *Neurobiol Dis* **2010**, 37, (1), 13-25.
92. Miller, D. S.; Bauer, B.; Hartz, A. M. S., Modulation of P-glycoprotein at the blood-brain barrier: Opportunities to improve central nervous system pharmacotherapy. *Pharmacological Reviews* **2008**, 60, (2), 196-209.
93. Schäfer, A.; Brooke, C. B.; Whitmore, A. C.; Johnston, R. E., The Role of the Blood-Brain Barrier during Venezuelan Equine Encephalitis Virus Infection. *J Virol* **2011**, 85, (20), 10682-10690.
94. Seelig, A., A general pattern for substrate recognition by P-glycoprotein. *Eur J Biochem* **1998**, 251, (1-2), 252-61.
95. Miller, D. S., Regulation of P-glycoprotein and other ABC drug transporters at the blood-brain barrier. *Trends in Pharmacological Sciences* **2010**, 31, 246-254.
96. Förster, F.; Volz, A.; Fricker, G., Compound profiling for ABCC2 (MRP2) using a fluorescent microplate assay system. *European Journal of Pharmaceutics and Biopharmaceutics* **2008**, 69, (1), 396-403.
97. Forster, S.; Thumser, A. E.; Hood, S. R.; Plant, N., Characterization of Rhodamine-123 as a Tracer Dye for Use In *In vitro* Drug Transport Assays. *PLoS ONE* **2012**, 7, (3), e33253.
98. Larsen, S. D.; Wilson, M. W.; Abe, A.; Shu, L.; George, C. H.; Kirchoff, P.; Showalter, H. D. H.; Xiang, J.; Keep, R. F.; Shayman, J. A., Property-based design of a glucosylceramide synthase inhibitor that reduces glucosylceramide in the brain. *Journal of Lipid Research* **2012**, 53, (2), 282-291.

99. Di, L.; Kerns, E. H.; Fan, K.; McConnell, O. J.; Carter, G. T., High throughput artificial membrane permeability assay for blood-brain barrier. *Eur J Med Chem* **2003**, 38, (3), 223-32.
100. Avdeef, A.; Bendels, S.; Di, L.; Faller, B.; Kansy, M.; Sugano, K.; Yamauchi, Y., PAMPA - Critical factors for better predictions of absorption. *J Pharm Sci-US* **2007**, 96, (11), 2893-2909.
101. Avdeef, A., Physicochemical profiling (solubility, permeability, and charge state). *Current Topics in Medicinal Chemistr* **2001**, 1, 277-351.
102. Ruell, J. A.; Tsinman, O.; Avdeef, A., Acid-base cosolvent method for determining aqueous permeability of amiodarone, itraconazole, tamoxifen, terfenadine and other very insoluble molecules. *Chem Pharm Bull (Tokyo)* **2004**, 52, (5), 561-5.
103. Nassar, A.-E. F.; Kamel, A. M.; Clarimont, C., Improving the decision-making process in the structural modification of drug candidates: enhancing metabolic stability. *Drug Discovery Today* **2004**, 9, (23), 1020-1028.
104. ACE and JChem acidity and basicity calculator.
<http://epoch.uky.edu/ace/public/pKa.jsp>
105. Faull, A. W.; Kettle, J. G. Preparation of indole-2-carboxylic acids as MCP-1 receptor antagonists. WO2001051466A1, 2001.
106. Anilkumar, G. N.; Bennett, F.; Chan, T.-Y.; Chen, K. X.; Sannigrahi, M.; Velazquez, F.; Venkatraman, S.; Zeng, Q.; Duca, J. S.; Lesburg, C. A.; Kozlowski, J. A.; Njoroge, F. G.; Rosenblum, S. B.; Shih, N.-Y. Preparation of substituted indole derivatives for use in treatment or prevention of hepatitis C viral infections. WO2009032124A1, 2009.
107. Gancia, E.; Montana, J. G.; Manallack, D. T., Theoretical hydrogen bonding parameters for drug design. *J Mol Graph Model* **2001**, 19, (3-4), 349-362.
108. Hao, M. H., Theoretical calculation of hydrogen-bonding strength for drug molecules. *J Chem Theory Comput* **2006**, 2, (3), 863-872.
109. Bissantz, C.; Kuhn, B.; Stahl, M., A Medicinal Chemist's Guide to Molecular Interactions. *J Med Chem* **2010**, 53, (14), 5061-5084.
110. Laurence, C.; Brameld, K. A.; Graton, J. r. m.; Le Questel, J.-Y.; Renault, E., The pKBHX Database: Toward a Better Understanding of Hydrogen-Bond Basicity for Medicinal Chemists. *J Med Chem* **2009**, 52, (14), 4073-4086.
111. Koch, O.; Bocola, M.; Klebe, G., Cooperative effects in hydrogen-bonding of protein secondary structure elements: A systematic analysis of crystal data using Seabase. *Proteins: Structure, Function, and Bioinformatics* **2005**, 61, (2), 310-317.
112. Huber, R. G.; Margreiter, M. A.; Fuchs, J. E.; von Grafenstein, S.; Tautermann, C. S.; Liedl, K. R.; Fox, T., Heteroaromatic π -Stacking Energy Landscapes. *Journal of Chemical Information and Modeling* **2014**, 54, (5), 1371-1379.
113. Feher, M.; Schmidt, J. M., Property Distributions: Differences between Drugs, Natural Products, and Molecules from Combinatorial Chemistry. *Journal of Chemical Information and Computer Sciences* **2002**, 43, (1), 218-227.
114. Meyer, E. A.; Castellano, R. K.; Diederich, F., Interactions with Aromatic Rings in Chemical and Biological Recognition. *Angewandte Chemie International Edition* **2003**, 42, (11), 1210-1250.
115. Harder, M.; Kuhn, B.; Diederich, F., Efficient Stacking on Protein Amide Fragments. *ChemMedChem* **2013**, 8, (3), 397-404.

116. Janiak, C., A critical account on π - π stacking in metal complexes with aromatic nitrogen-containing ligands. *Journal of the Chemical Society, Dalton Transactions* **2000**, (21), 3885-3896.
117. Wallnoefer, H. G.; Fox, T.; Liedl, K. R.; Tautermann, C. S., Dispersion dominated halogen-[small pi] interactions: energies and locations of minima. *Physical Chemistry Chemical Physics* **2010**, 12, (45), 14941-14949.
118. Dougherty, D. A., Cation- π Interactions in Chemistry and Biology: A New View of Benzene, Phe, Tyr, and Trp. *Science* **1996**, 271, (5246), 163-168.
119. Ma, J. C.; Dougherty, D. A., The Cation- π Interaction. *Chemical Reviews* **1997**, 97, (5), 1303-1324.
120. Gallivan, J. P.; Dougherty, D. A., Cation- π interactions in structural biology. *Proceedings of the National Academy of Sciences* **1999**, 96, (17), 9459-9464.
121. Lu, Y. X.; Shi, T.; Wang, Y.; Yang, H. Y.; Yan, X. H.; Luo, X. M.; Jiang, H. L.; Zhu, W. L., Halogen Bonding-A Novel Interaction for Rational Drug Design? *J Med Chem* **2009**, 52, (9), 2854-2862.
122. Wilcken, R.; Zimmermann, M. O.; Lange, A.; Joerger, A. C.; Boeckler, F. M., Principles and Applications of Halogen Bonding in Medicinal Chemistry and Chemical Biology. *J Med Chem* **2013**, 56, (4), 1363-1388.
123. Baumli, S.; Endicott, J. A.; Johnson, L. N., Halogen Bonds Form the Basis for Selective P-TEFb Inhibition by DRB. *Chemistry & Biology* **2010**, 17, (9), 931-936.
124. Rohde, L. A. H.; Ahring, P. K.; Jensen, M. L.; Nielsen, E. O.; Peters, D.; Helgstrand, C.; Krintel, C.; Harpsoe, K.; Gajhede, M.; Kastrop, J. S.; Balle, T., Intersubunit Bridge Formation Governs Agonist Efficacy at Nicotinic Acetylcholine alpha 4 beta 2 Receptors UNIQUE ROLE OF HALOGEN BONDING REVEALED. *J Biol Chem* **2012**, 287, (6), 4248-4259.
125. Lemke, C. T.; Goudreau, N.; Zhao, S. P.; Hucke, O.; Thibeault, D.; Llinas-Brunet, M.; White, P. W., Combined X-ray, NMR, and Kinetic Analyses Reveal Uncommon Binding Characteristics of the Hepatitis C Virus NS3-NS4A Protease Inhibitor BI 201335. *J Biol Chem* **2011**, 286, (13), 11434-11443.
126. Ramasubbu, N.; Parthasarathy, R.; Murray-Rust, P., Angular preferences of intermolecular forces around halogen centers: preferred directions of approach of electrophiles and nucleophiles around carbon-halogen bond. *Journal of the American Chemical Society* **1986**, 108, (15), 4308-4314.
127. Delekta, P. C.; Dobry, C. J.; Sindac, J. A.; Barraza, S. J.; Blakely, P. K.; Xiang, J.; Kirchoff, P. D.; Keep, R. F.; Irani, D. N.; Larsen, S. D.; Miller, D. J., Novel indole-2-carboxamide compounds are potent broad spectrum antivirals active against western equine encephalitis virus in vivo. *J Virol* **2014**.
128. Shah, P.; Westwell, A. D., The role of fluorine in medicinal chemistry. *Journal of Enzyme Inhibition and Medicinal Chemistry* **2007**, 22, (5), 527-540.
129. Böhm, H.-J.; Banner, D.; Bendels, S.; Kansy, M.; Kuhn, B.; Müller, K.; Obst-Sander, U.; Stahl, M., Fluorine in Medicinal Chemistry. *Chembiochem* **2004**, 5, (5), 637-643.
130. Kirk, K. L., Fluorine in medicinal chemistry: Recent therapeutic applications of fluorinated small molecules. *Journal of Fluorine Chemistry* **2006**, 127, (8), 1013-1029.
131. Hodgetts, K. J.; Combs, K. J.; Elder, A. M.; Harriman, G. C., Chapter 26 - The Role of Fluorine in the Discovery and Optimization of CNS Agents: Modulation of Drug-

- Like Properties. In *Annual Reports in Medicinal Chemistry*, John, E. M., Ed. Academic Press: 2010; Vol. Volume 45, pp 429-448.
132. Dorman, G.; Prestwich, G. D., Using photolabile ligands in drug discovery and development. *Trends Biotechnol* **2000**, 18, (2), 64-77.
133. Leslie, B. J.; Hergenrother, P. J., Identification of the cellular targets of bioactive small organic molecules using affinity reagents. *Chem Soc Rev* **2008**, 37, (7), 1347-1360.
134. Peters, E. C.; Gray, N. S., Chemical Proteomics Identifies Unanticipated Targets of Clinical Kinase Inhibitors. *ACS Chemical Biology* **2007**, 2, (10), 661-664.
135. Frolov, I.; Frolova, E.; Schlesinger, S., Sindbis virus replicons and Sindbis virus: assembly of chimeras and of particles deficient in virus RNA. *J Virol* **1997**, 71, (4), 2819-29.
136. Barton, D. J.; Sawicki, S. G.; Sawicki, D. L., Solubilization and immunoprecipitation of alphavirus replication complexes. *J Virol* **1991**, 65, (3), 1496-506.
137. Walsh, D.; Mohr, I., Viral subversion of the host protein synthesis machinery. *Nat Rev Micro* **2011**, 9, (12), 860-875.
138. Leslie, B. J.; Hergenrother, P. J., Identification of the cellular targets of bioactive small organic molecules using affinity reagents. *Chem Soc Rev* **2008**, 37, (7), 1347-60.
139. Fleming, S. A., Chemical Reagents in Photoaffinity-Labeling. *Tetrahedron* **1995**, 51, (46), 12479-12520.
140. Schwartz, M. A., *Photochemical probes in biochemistry*. Kluwer Academic Publishers: Dordrecht ; Boston, 1989.
141. Lamarche, N.; Gaudreau, P.; Massie, B.; Langelier, Y., Affinity of Synthetic Peptides for the HSV-2 Ribonucleotide Reductase R1 Subunit Measured with an Iodinated Photoaffinity Peptide. *Analytical Biochemistry* **1994**, 220, (2), 315-320.
142. Schuster, G. B.; Platz, M. S., Photochemistry of Phenyl Azide. In *Advances in Photochemistry*, John Wiley & Sons, Inc.: 2007; pp 69-143.
143. Evans, R. K.; Haley, B. E., Synthesis and biological properties of 5-azido-2'-deoxyuridine 5'-triphosphate, a photoactive nucleotide suitable for making light-sensitive DNA. *Biochemistry* **1987**, 26, (1), 269-276.
144. Staros, J. V.; Bayley, H.; Standing, D. N.; Knowles, J. R., Reduction of aryl azides by thiols: Implications for the use of photoaffinity reagents. *Biochem Bioph Res Co* **1978**, 80, (3), 568-572.
145. Young, M. J. T.; Platz, M. S., Polyfluorinated aryl azides as photoaffinity labelling reagents; the room temperature CH insertion reactions of singlet pentafluorophenyl nitrene with alkanes. *Tetrahedron Letters* **1989**, 30, (17), 2199-2202.
146. Pinney, K. G.; Carlson, K. E.; Katzenellenbogen, B. S.; Katzenellenbogen, J. A., Efficient and selective photoaffinity labeling of the estrogen receptor using two nonsteroidal ligands that embody aryl azide or tetrafluoroaryl azide photoreactive functions. *Biochemistry* **1991**, 30, (9), 2421-2431.
147. Galardy, R. E.; Craig, L. C.; Jamieson, J. D.; Printz, M. P., Photoaffinity Labeling of Peptide Hormone Binding Sites. *J Biol Chem* **1974**, 249, (11), 3510-3518.
148. Dorman, G.; Prestwich, G. D., Benzophenone Photophores in Biochemistry. *Biochemistry* **1994**, 33, (19), 5661-5673.

149. Lehmann, J.; Petry, S., (1→4)-β-D-Galaktosyltransferase läßt sich durch photolabile Liganden im Akzeptor-Bindebereich spezifisch kovalent modifizieren. *Liebigs Annalen der Chemie* **1993**, 1993, (10), 1111-1116.
150. Fleming, S. A., Chemical reagents in photoaffinity-labeling. *Tetrahedron* **1995**, 51, 12479-12520
151. Anilkumar, G.; Nambu, H.; Kita, Y., A Simple and Efficient Iodination of Alcohols on Polymer-Supported Triphenylphosphine. *Organic Process Research & Development* **2002**, 6, (2), 190-191.
152. Yestrepesky, B. D.; Kretz, C. A.; Xu, Y.; Holmes, A.; Sun, H.; Ginsburg, D.; Larsen, S. D., Development of tag-free photoprobes for studies aimed at identifying the target of novel Group A Streptococcus antivirulence agents. *Bioorganic & Medicinal Chemistry Letters* **2014**, 24, (6), 1538-1544.
153. Yang, H.; Li, Y.; Jiang, M.; Wang, J.; Fu, H., General Copper-Catalyzed Transformations of Functional Groups from Arylboronic Acids in Water. *Chemistry – A European Journal* **2011**, 17, (20), 5652-5660.
154. Nassal, M., 4'-(1-Azi-2,2,2-trifluoroethyl)phenylalanine, a photolabile carbene-generating analog of phenylalanine. *Journal of the American Chemical Society* **1984**, 106, (24), 7540-7545.
155. Hatanaka, Y.; Hashimoto, M.; Nakayama, H.; Kanaoka, Y., Syntheses of Nitro-Substituted Aryl Diazirines. An Entry to Chromogenic Carbene Precursors for Photoaffinity Labeling. *Chem Pharm Bull* **1994**, 42, (4), 826-831.
156. Hatanaka, Y.; Yoshida, E.; Nakayama, H.; Kanaoka, Y., Chromogenic diazirine: A new spectrophotometric approach for photoaffinity labeling. *Bioorganic Chemistry* **1989**, 17, (4), 482-485.
157. Xiong Cai, S.; Keana, J. F. W., 4-azido-2-iodo-3,5,6-trifluorophenylcarbonyl derivatives. A new class of functionalized and iodinated perfluorophenyl azide photolabels. *Tetrahedron Letters* **1989**, 30, (40), 5409-5412.
158. Zhang, M.; Mao, Y.; Ramirez, S. H.; Tuma, R. F.; Chabrashvili, T., Angiotensin II induced cerebral microvascular inflammation and increased blood–brain barrier permeability via oxidative stress. *Neuroscience* **2010**, 171, (3), 852-858.
159. Moskowitz, D. W.; Johnson, F. E., The central role of angiotensin I-converting enzyme in vertebrate pathophysiology. (1568-0266 (Print)).
160. Gubler, D. J., The global emergence/resurgence of arboviral diseases as public health problems. *Arch Med Res* **2002**, 33, (4), 330-42.
161. Sindac, J. A.; Barraza, S. J.; Dobry, C. J.; Xiang, J.; Blakely, P. K.; Irani, D. N.; Keep, R. F.; Miller, D. J.; Larsen, S. D., Optimization of Novel Indole-2-carboxamide Inhibitors of Neurotropic Alphavirus Replication. *J Med Chem* **2013**, 56, (22), 9222-9241.